Reliability Based Design of Marine Risers

by

Juan Jose Cortes Romero

A thesis submitted for the degree of
Doctor of Philosophy

Department of Marine Technology

University of Newcastle upon Tyne

March 1999

Abstract

The harsh environment in which offshore structures must operate, their intended service life and the uncertainties inherent to the load processes, have been the impulse for investigation of their reliability. The method most extensively applied for this purpose during the last two decades was the Structural Systems Reliability, which can not be coupled with the finite element method. Therefore the objectives of the present work are to investigate the applicability of a technique which allows the utilization of the reliability analysis methods with a marine riser modelled by the finite element method, FEM, and revision of the reliability levels associated with this riser, including the fatigue life. For these purposes the response surface methodology was selected, among a number of methods. A response surface approach which requires a low number of experiments with the FEM model was elected, calculations for construction of the response surface are further simplified by the assumption of statistical independence among the basic variables. It is demonstrated in the present study that the response surface is capable of producing an equivalent and explicit limit state function which is used at a second stage with the First Order Reliability Method and the Adaptive Importance Sampling simulation technique. However, it was found that the assumption of independence is not always valid. In this case, a method is proposed in which the correlated variables are implicitly considered at the level of the mechanical model. The reliability of the marine riser was reviewed with the proposed algorithms, finding that the validity of the reliability levels depend on the number of basic variables considered and their statistical properties. The significant reduction in required computing time achieved with the response surface methodology allowed parametric studies to be carried out, in order to investigate the impact of different statistical properties of the basic variables. The fatigue reliability case was also investigated with the S-N approach. The introduction of uncertainty in the fatigue life estimation proved that acceptable levels of deterministic fatigue life may render unacceptable levels of reliability. The uncertainty associated with the stress range is the most significant variable, though the present fatigue reliability formats consider it in a very simplified manner, therefore an approach is suggested with which the stress uncertainty can be considered in a more detailed fashion. However, the algorithm used here for construction of the response surface was unable to produce the required surface. Therefore it is concluded that though the response surface is capable of handling a large number of structural reliability cases, there are instances in which more research efforts are needed.

Acknowledgements

The author would like to express deep thanks to Prof. Atilla Incecik for his careful supervision, continual attention and the patience he had with this author.

In second place the author wishes to thankfully acknowledge the continual support, deep understanding and above all the extreme patience that his wife, Ivonne, has always had for him.

This work was made possible thanks to the support of the Mexican Government, through Consejo Nacional de Ciencia y Tecnologia, CONACYT, (National Council for Science and Technology), to whom the author also wishes to express his recognition.

Last but not least the author wishes to acknowledge with gratefulness the Lord God who ultimately set the things for the author to reach this stage.

LIST OF FIGURES.

LIST OF TABLES.

NOTATION.

Symbols used throughout of this thesis are defined as they are used.
Every effort has been made to apply a consistent nomenclature; however, some symbols had to be repeated, on account of the commonly accepted nomenclature for specific subjects.

Response Surface.

β	reliability index,
G,	failure function in the original space of physical variables,
$G(\mathbf{X})$	safety margin or performance function or limit state function, in the original space of physical variables,
$G(\mathbf{x})=0$	limit state equation or failure surface or limit state surface, in the original physical space,
$G(\mathbf{x})\leq 0$	failure set or failure domain in the original physical space,
$\overline{g}(\mathbf{X})$	equivalent limit state function or response function,
$\overline{g}(\mathbf{x})=0$	equivalent limit state surface or response surface,
g	failure function in the transformed space,
$g(\mathbf{U})$	safety margin or performance function or limit state function in the transformed space,
$g(\mathbf{u})=0$	limit state equation or failure surface or limit state surface, in the transformed u-space,
$g(\mathbf{u})\leq 0$	failure set or failure domain in the transformed u-space,
$h_{\mathrm{V}}(\mathbf{v})$	importance sampling function,
L	loading random variable,
P_f	probability of failure,
R	reliability,
S	resistance random variable,
$\mathbf{U}$	vector of n random basic variables in the transformed space,
$\mathbf{u}^*$	coordinates of the design point in the transformed space,
$\mathbf{u}$	vector of realisations of $\mathbf{U}$,

$\mathbf{X}$	vector of *n* random basic variables, in the original physical space,
$\mathbf{x}$	vector of realisations of $\mathbf{X}$,
$\mathbf{x}^*$	coordinates of the design point in the original physical space.

Riser Differential Equation.

A_E	external area of pipe cross section,
A_I	internal area of pipe cross section,
C_M	inertia coefficient,
C_D	drag coefficient,
E	Young's modulus of elasticity,
F_{P_E}	statically equivalent load due to external hydrostatic pressure,
F_{P_I}	statically equivalent load due to internal hydrostatic pressure,
g	acceleration of gravity,
I	second moment of inertia,
M	bending moment,
m	mass of the riser including hydrodynamic added mass,
P_E	external hydrostatic pressure,
P_I	internal hydrostatic pressure,
T_e	equivalent tension,
T_{top}	tension applied at the top of the riser,
$\mathrm{T}(y)$	tension, function of riser length,
V	volume of the riser external section,
V_S	shear force on an elemental section of the riser,
W	weight of an elemental section of the riser,
x	riser transverse displacement,
γ_I	specific weight of the internal fluid,
γ_E	specific weight of the external fluid,
γ_S	specific weight of steel,
θ	angular displacement on an elemental section of the riser,
ρ_E	density of the external fluid,

ρ_I density of the internal fluid,

Riser Finite Element Model.

A_E external area of pipe cross section,

B matrix of hydrodynamic drag coefficients,

B_{eq} equivalent linear matrix of hydrodynamic drag coefficients,

C_D drag coefficient,

C_M inertia coefficient,

$[C]$ global damping matrix,

c distance from the fibre of interest to the neutral axis,

D_E external diameter of riser pipe,

d total water depth,

$\{F\}$ global vector of nodal forces,

$\{f\}$ vector of elemental nodal forces,

g acceleration of gravity;

$g_i(y)$ *ith* interpolation function,

k wave number,

$[K]$ global stiffness matrix,

$[k]$ matrix of elemental stiffness coefficients,

l length of a riser beam element,

M_T total mass matrix, including the added mass,

M_H added mass matrix,

$[M]$ global mass matrix,

$\{Q\}$ global vector of unknown displacements,

$\{q\}$ vector of unknown displacements at the nodes of an element,

R_{TW} ratio of element weight to top tension,

T_{TOP} tension applied at the top of the riser,

t time,

U vector of horizontal components of wave particle velocity,

$\dot{U}$ vector of horizontal components of wave particle acceleration,

U'_w	complex amplitude of wave particle velocities,
V	vector of elemental volumes,
$\ddot{X}$	vector of horizontal components of riser transverse acceleration,
$\dot{X}$	vector of horizontal components of riser transverse velocity,
y	distance from sea surface to depth at which velocity or acceleration are required,
ξ	ratio of critical damping,
ζ_a	amplitude of wave height,
ρ_E	density of the external fluid,
ρ_{eq}	equivalent density,
Ω	wave circular frequency,
θ	riser angular displacement,
ω	riser circular natural frequency,
σ	bending stress.

Riser Fatigue Reliability.

a	crack length,
B	random variable to account for uncertainties in stress range determination,
C	material constant,
D	Miner's total cumulative damage,
D_i	damage accumulated at the *ith* constant stress range,
da / dN	crack growth rate,
f_i	mean zero cross frequency of the wave loading in the sea state,
f_o	average frequency of stress cycle,
Hs	significant wave height,
$\lvert H_F(\omega)\rvert^2$	transfer function,
i	number of different stress ranges, $i = 1 \ldots n$,
K	stress intensity factor,
ΔK	stress intensity factor range,
m	empirical constant defined by analysis of laboratory fatigue test data,
N	number of cycles to failure at a constant stress range,
N_{Fi}	number of cycles to failure at the *ith* constant stress range,

N_S	number of cycles at the intended service life,
N_{T_i}	number of cycles in time T, at the *ith* constant stress range,
n	number of sea states,
S	constant stress range,
S_{iav}	average stress range,
ΔS_i	regimen of stress range,
S_f	far-field stress due to applied load,
$S^{RR}(\omega)$	power spectral density of stress,
T_z	average wave period,
W^{nn}	wave power spectral density,
$Y(a)$	geometry function, which takes into account the crack geometry and specimen shape,
γ_i	fraction of time of occurrence of the ith sea state,
σ_i	root mean square of the stress process in the ith sea state,
Γ	gamma distribution,
Ω	stress parameter.

TABLE OF CONTENTS

APPENDICES.

INTRODUCTION.

Offshore structures are needed in increasingly harsh environments and are required to work in place for long service life periods. For this reason the evaluation of their safety has received significant attention. Safety assessment has been dominated until recently by the so called deterministic approach, which is characterized by the assumption that loads and stresses can be precisely predicted. In contrast, a second approach to safety is to recognise that a degree of uncertainty is present both in load prediction, materials performance and stresses predicted from mathematical models. In the early 1970's the reliability of offshore structures began to receive an important degree of attention. The methods employed at the time considered the structure as a system of elements, where the reliabilities of individual elements had to be considered, thus failure had to be specified by a path of elements failing in a given sequence. This approach was known as the Structural Systems Reliability. The limitation of this method is that state of the art structural analysis techniques, such as the finite element method cannot be used; furthermore, the determination of failure paths is not a straight forward task.

The reliability analysis of individual elements had reached a maturity with a wealth of methods available, such as the First Order Reliability Method, FORM, and Second Order Reliability Method, SORM. The main characteristic of FORM and SORM is that a function, called the *limit state function*, dividing the safety from the failure domains is required in an explicit form. On the other hand, state of the art mechanical modelling method, i.e. the finite element method, are capable of providing the stresses on any required point of the structure, while all the complex interactions occurring between the elements of the structure are completely and accurately taken into consideration. On account of the complexities of the structure behaviour the boundary separating the safety from the failure domain is complex as well and given implicitly by the finite element model. In order to overcome this limitation Monte Carlo simulation techniques had been attempted; however the large computing cost incurred when a several thousands or even hundreds of thousands of simulations with a large finite element model make this method impractical. One of the approaches proposed to overcome these limitations was the idea to provide a surrogate, but explicit, limit state function, for structures modelled by the finite element model, for which a number of methods have been proposed.

Therefore, the objective of the present work is to select a technique able to produce an equivalent limit state function for a marine riser modelled by finite elements, in order to review the reliability levels of this type of structure, including the fatigue life. A marine riser was selected for on account of the very limited attention that the reliability of this type of structure has received in the published literature. Thus, the present work is divided as follows:

Chapter 1 is devoted to a revision of the theory of structural reliability. Particular attention is given to the mathematical foundation for definition of the *reliability index*, which defines the ability of a structure to fulfil its intended purpose for a reference period. In the same fashion the theory behind the methods for determination of this reliability index are reviewed. Some of the techniques proposed for construction of a surrogate limit state are surveyed and the Response Surface Methodology is selected on account of its ease of application, as compared with the other ones.

Since a degree of error is introduced on account of the approximation of the limit state surface, required by FORM and SORM, the advanced Monte Carlo simulation techniques are reviewed. The application of the Adaptive Importance Sampling method is proposed as a means of improving the reliability index rendered by FORM, on account that this simulation technique requires very reasonable computing time and makes use of the limit state function without any approximation, other than the one required by the algorithm for construction of the response surface.

A review of the current methods for marine riser analysis is also given in Chapter 1. Of the two approaches for dynamic analysis, time and frequency domain, the frequency domain is selected on the basis that it is capable of producing fairly accurate results without a large demand of computing time. In the same fashion the current trend in fatigue reliability analysis are surveyed in this chapter. It interesting to not that at present, the approaches for fatigue reliability only make explicit consideration of the uncertainty associated with the variables associated with the material fatigue strength, while the uncertainty in stress range determination is usually considered in a very simplified fashion.

In Chapter 2 the model and algorithm employed in this work for construction of the response surface are presented in detailed. The main reason for selection of the algorithm proposed by **Bucher and Bourgund (1990)** obeys mainly to the small computer time required by it, in comparison with other approaches. Such algorithm requires only $4n + 3$ call of the finite element model, being n the number of basic variables considered in the problem. Also in this chapter the implementation of algorithm for Adaptive Importance Sampling, due to **Melchers (1990)**, is described.

In Chapter 3 the connection between the algorithms for construction of the response surface and determination of the reliability index, as applied in this work, is given. These algorithms are then validated by comparison with a number of simple examples, on account of the lack of published reliability values for the type of marine riser considered.

Chapter 4 is devoted to the description of the frequency domain finite element model implemented for the riser analysis.

Chapter 5 is dedicated to the execution of a number of parametric studies, where it is demonstrated the ability of the selected approach for construction of the surrogate limit state, or response surface. The reasonable computing time required by the algorithms selected allowed a significant number of parametric studies to be conducted, from which it was possible to identify the basic variables more important for the reliability behaviour of the riser. In the same fashion the methodology adopted permitted to review the statistical properties associated to those variable, i.e. probability distribution function, standard deviation, etc.

In chapter 6 the fatigue reliability of the riser is reviewed. As a first step the deterministic fatigue life is estimated, later the uncertainty associated with the S-N curve parameters is introduced. The reliability values obtained are compared with similar studies found in the available literature. The most interesting results appear when the uncertainty associated with stress range is introduced, in a simple form, and thanks to the response surface methodology, a number of parametric studies heighten the paramount importance of this type of uncertainty, not previously reviewed in this detailed. Hence, an approach is proposed for a more realistic consideration of the uncertainty in stress range; the algorithm selected here for construction of the response surface fails in this case. The subject of revision of different methods for construction of the response surface, in the fatigue reliability problem, is left as a recommendation for further work.

Finally Chapters 7 and 8 present respectively the conclusions and recommendations for further research.

CHAPTER 1. RELIABILITY BASED DESIGN AND MARINE RISERS.

1.0. Safety: Deterministic vs. Probabilistic Approaches.

Engineering design has been and will permanently be dominated by one concern: ***safety.*** It is this issue that has prompted different design schemes embodied in design codes. The assessment of safety has to rely on two elements: first, the mathematical models used in engineering to describe, on the one hand the loads acting on the structures and on the other the responses of the structures to such loads; and second, the data required to implement/calibrate such models.

There exist limitations in both elements.. Mathematical models contain a varying degree of simplifying assumptions, which depend on both the understanding of the physics of the problem and on the tractability of mathematics involved in the selected model itself. The physical processes of many loading environments, i.e. wind, wave, etc., are of such nature that the actual load intensity has a different value every time that is measured. Finally, quantification of load and resistance is made by measurements, which in turn are subjected to constraints on the accuracy of the equipment employed and on the amount of data that can be physically gathered. The results of all those limitations has a common name, ***uncertainty***; physical, modelling and statistical uncertainties, respectively.

The way in which uncertainties are to be handled has given place for the existing safety evaluation formats: deterministic and probabilistic. The so called deterministic design has driven engineering design for more than a hundred years. Determinism is characterised by the assumption that fixed values defining load and response can exactly be predicted from the mathematical models used. Therefore, ***deterministic design*** is based on the use of specified load intensities and specified minimum material properties as well as prescribed calculation procedures for the determination of structural responses.

There is, however, in deterministic design a strong recognition that deviations from specified values may occur and therefore bounds have been intrinsically built. Material properties used for actual design are specified as minimum expected values, whereas load intensities tend to be taken as maximum expected values. The characteristic separation between the two types of quantities leads to the central safety measure used in deterministic design: the ***safety factor***:

The safety factor is a measure of the gap between the minimum resistance and the maximum load in a specific design. This gap takes account for all the uncertainties involved in that specific design. **Figure 1.1**, which has been adopted from **Chang (1990),** shows an schematic representation of the deterministic safety problem, in which if load intensity L and material properties S could be precisely known and had fixed values a resistance slightly higher than the load would provide for an adequate safety.

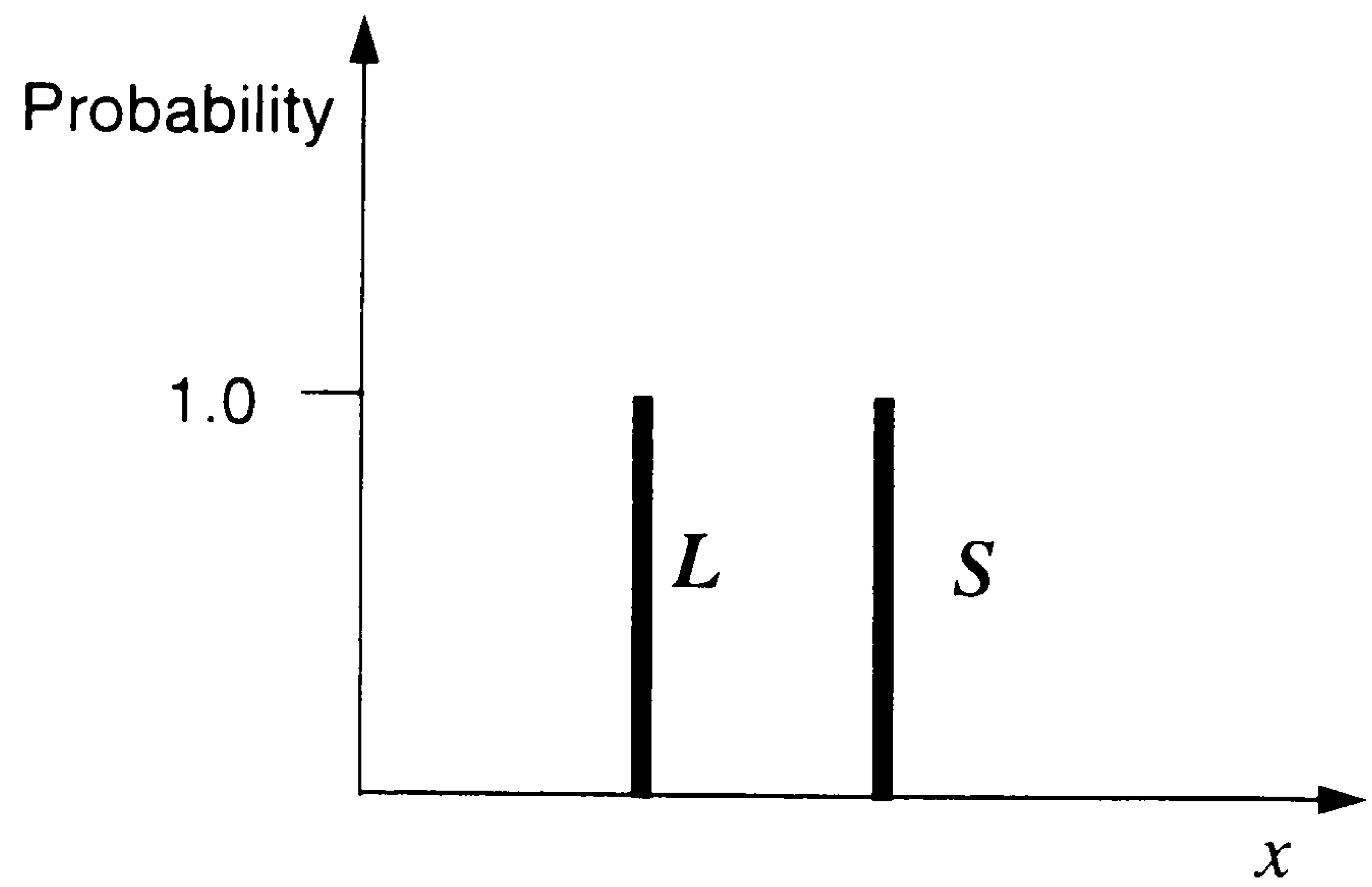

Figure 1.1. Deterministic approach to design, after **Chang (1990)**.

However, experience has demonstrated that a somewhat sufficient separation between load and resistance must be allowed in order to provide for a safe design. That gap is specified by the so called safety factors, which are usually given in codes and standard practices, as a quotient or as a comparison statement. That is, if load and resistance for a given structural component are given in terms of, say, stresses, a safe state would require that:

$$\sigma_i < \sigma_{iperm} \tag{1.1}$$

where:

σ_i , applied stress on the *ith* component

σ_{iperm}, permissible stress on the *ith* component.

Permissible stress is therefore expressed in terms of a known reference stress such as the yield stress or the ultimate resisting stress of the material, lowered through a multiplier F :

$$\sigma_{iperm} = \sigma_{iu} / F \tag{1.2}$$

where F is a safety factor. The simple format of the safety measure in deterministic design allows some consideration for uncertainties, inter-constructed in the safety factor. Hence, the main objective of deterministic design is the establishment of safety factors, which are supported by ***industry experience***.

The need for more complex structures, in severe loading environments, i.e. when wind, wave and current act from arbitrary directions in a non co-linear fashion, requires more detailed and explicit consideration of the uncertainties existing in the design variables. The uncertainties in load and resistance can be expressed by means of random variables, which allow for the explicit treatment of such uncertainty, as showed in **Figure 1.2**, adopted also from **Chang (1990)**.

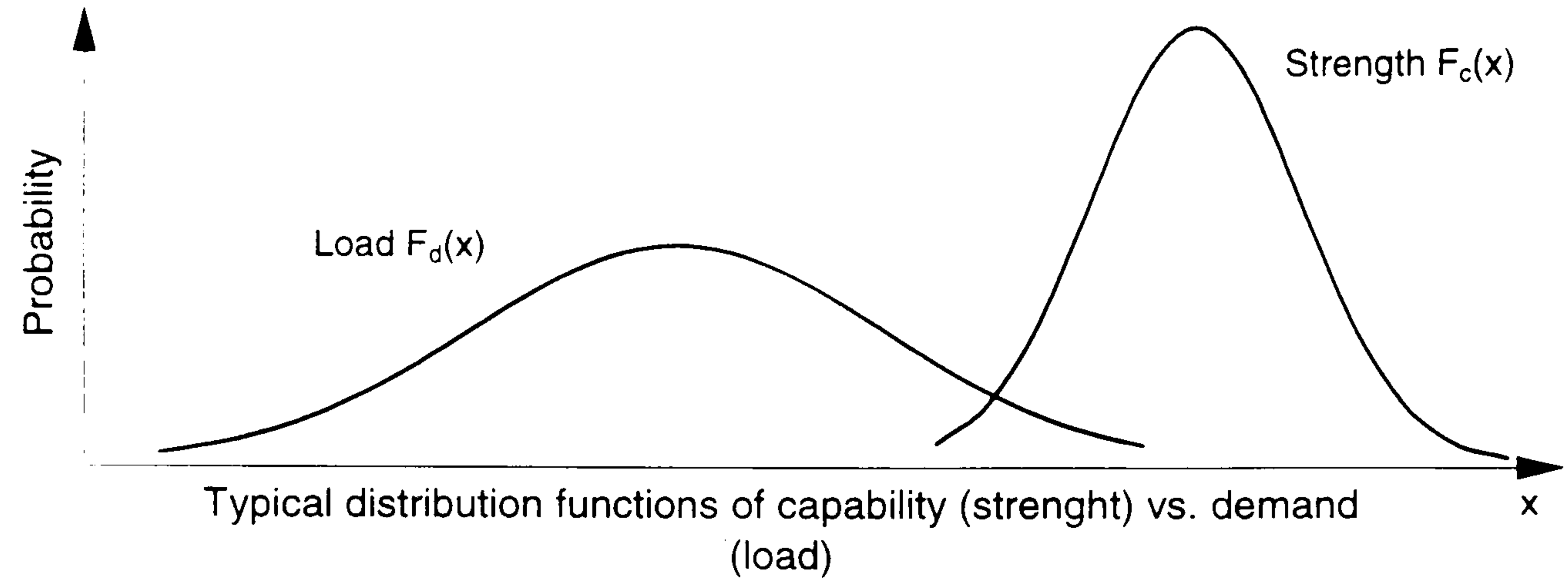

Figure 1.2. Probabilistic approach to design, after **Chang (1990)**.

This time, the establishment of a safety measure can be made under consideration of the random nature of variables and, as it can be seen from **Figure 1.2**, the range of all failure conditions is represented by the overlapping area of the two probability distribution functions, **PDF**. This area represents all events in which certain combinations of high load and low resistance would result in failure. The objective of ***probabilistic design*** is to determine the probability that any of these failure conditions is attained, such probability is termed ***probability of failure***, P_f. Following the laws of probability theory the complementary part of the probability of failure is:

$$R = 1 - P_f \tag{1.3}$$

where R is the ***reliability*** of the structure. In a general sense reliability is the probability that the structure will be able to fulfil the required design purposes for some specified period. A formal definition will be given later in **Section.1.1**. Because the primary safety measure employed in probabilistic design is the reliability, such approach is now more commonly referred to as ***reliability based design***.

1.1. The Structural Reliability Problem.

A number of approaches have been proposed and applied in structural reliability problems, exact methods and iterative ones. Consideration has been given to structural components as stand alone ones or to the whole structure as a system. In any case the main objective of structural reliability theory is the determination of the reliability, or its complement, the probability of failure. The following sections are devoted to a review of structural reliability theory and its methods.

1.1.1. Reliability, Probability of Failure and definitions.

The primary concern of reliability based design is the determination of a probabilistic measure of the safety of a given design. Therefore, the main problem of structural reliability is the determination of a probabilistic measure of safety in the case of structural problems. Referring again to **Figure 1.2**, the fundamental problem of reliability based design is the actual determination of the probability of occurrence of the events which will result in a failure condition. In order to derive an expression for the calculation of the ***probability of failure***, P_f, first, a limiting condition, called limit state, must be established. A ***limit state*** is a condition at which a structure ceases to fulfil its intended design purpose, **Laurie Kennedy (1984)**, or in other words it is a pre-established performance condition (by the designer, code requirement, project requirement, economic or social requirements, etc.) which defines a boundary between the safety domain and the failure domain. The fulfilment of a limit state defines reliability as follows:

$$R = P\{S > L\} \qquad (1.4)$$

Reliability in **Equation 1.4** is expressed as a comparison statement, that is, the resistance or strength, expressed by the random variable S must be higher than the load L, which is also a random variable. In order to facilitate the mathematical terms of such comparison, reliability can be expressed, after **Clauss, et. al (1992),** as a difference statement;

$$R = P\{S - L > 0\} \qquad (1.5)$$

or as a quotient statement:

$$R = P\{S/L \rangle 1\} \qquad (1.6)$$

A generalisation of **Equation 1.5**, allows that a function $G(\mathbf{X})$ can be established, such that:

$$R = P[G(\mathbf{X}) > 0] \qquad (1.7)$$

where G is customarily called the ***failure function***, $\mathbf{X}$ is a set of n random physical variables referred to as the ***basic variables*** and $G(\mathbf{X})$ has been defined by **Madsen, et. al. (1986),** as the ***safety margin***, $\mathbf{M}$:

$$\mathbf{M} = G(\mathbf{X}) \qquad (1.8)$$

which is a new random variable obtained by replacing the basic random variables, $\mathbf{X}$, in the failure function. $G(\mathbf{X})$ is also named by **Melchers (1987)** the ***limit state function***. On the other hand, failure is defined as the case in which particular realisations $\mathbf{x}$ of the set of basic random variables, $\mathbf{X}$, violate the established limit state, that is $G(\mathbf{X}) \leq 0$. Consequently $G(\mathbf{x}) = 0$ becomes the mathematical expression for the boundary dividing the safety from the failure domain, and it is denominated the ***limit state equation***.

Without loss of generality, two variables, at least, must be accounted for in the failure function, namely load and strength. However; any or both of the two variables might be composed by a set of other variables; for instance, the strength of a structure is a function of elastic and geometric properties of its components, including steel strength; at another level, steel strength is a function of variables such as carbon content, hardness, etc. Therefore each variable contained in the failure function is called a ***basic variable***, since it can be expressed by another set of more fundamental variables intervening in the given problem. The number of basic variables has a significant impact on the choice of reliability method and algorithms available to solve a specific problem since the efficiency or even the mathematical tractability can be affected by the number of basic variables. This subject is discussed further in **Section 1.1.3**.

Because of the laws of probability theory, once the probability of failure is known, the reliability can be easily deducted from **Equation 1.3**. Therefore, the fundamental reliability problem can be rearranged as the problem of finding the probability of failure, from **Equation 1.7**:

$$P_f = P[G(\mathbf{X}) \leq 0] \tag{1.9}$$

The variability or ***uncertainty*** of the basic variables is accounted for by means of random variables, and taking a limit state function expressed as a difference statement, as in **Equation 1.5**, then **Equation 1.9** becomes:

$$P_f = P[G(\mathbf{X}) = S - L \leq 0] = \int_{G(\mathbf{X}) \leq 0} f_{\mathbf{X}}(\mathbf{x}) d\mathbf{x} \tag{1.10}$$

where $f_{\mathbf{X}}(\mathbf{x})$ is the joint probability density function of the limit state function $G(\mathbf{X}) = \mathbf{M} = S - L$, and the domain of integration, $G(\mathbf{X}) \leq 0$, is the failure domain. The case in which there are two basic variables only, one for load and one for strength, is known as the ***fundamental case*** of structural reliability theory and if these two variables are statistically independent, then solution of **Equation 1.10** can be expressed in terms of the marginal PDF's. On the one hand PDF of the load variable and on the other the cumulative probability distribution function of the strength variable, as:

$$P_f = P[S - L \leq 0] = \int_{-\infty}^{\infty} f_L(x) F_S(x) dx \tag{1.11}$$

For a detailed deduction of this expression see **Appendix 1**. ***Reliability*** can now be defined, after **Thoft-Christensen and Baker (1982)**, as the probability that a structure or structural component will not attain any of the specified limit states during a reference period. The probability of failure has the opposite meaning.

There exist a number of approaches to solve **Equation 1.10**, they can be broadly divided in exact and approximate methods; nevertheless, because of the many developments that have occurred in the field of structural reliability since the 1950's, the Joint Committee on Structural Safety decided in 1975 that a classification of the structural reliability analysis methods was needed. Such classification, as given by **Thoft-Christensen and Baker (1982)**, is summarised here:

Level 3:

"Methods in which calculations are made to determine the "exact" probability of failure for a structure or structural component, making use of a full probabilistic description of the joint occurrence of the various quantities which affect the response of the structure and taking into account the nature of the failure domain."

Level 2:

"Methods involving certain approximative iterative calculation procedures to obtain an approximation of the failure probability of a structure or structural system, generally requiring an idealisation of the failure domain and often associated with a simplified representation of the joint probability distribution of the variables."

Level 1:

"Design methods in which appropriate degrees of structural reliability are provided on a structural element basis (occasionally on a structural basis) by the use of a number of partial safety factors, or partial coefficients, related to pre-defined characteristics of nominal values of the major structural and loading variables."

From the strict point of view of reliability analysis, **Level 1** methods are not reliability analysis methods, but safety checking methods that make use of partial safety factors. The so called ***limit-states design*** or load and resistance factor design (LRFD), as referred in certain codes, are examples of Level 1 methods, which work at the component level only.

In LRFD explicit consideration is given to a separate number of limit states, i , as:

$$\varphi_i S_i \leq \gamma_{Di} L_{Di} + \gamma_{Li} L_{Li} + \ldots \qquad (1.12)$$

Equation 1.12 defines structural failure and S_i is the strength of a member or component, φ_i is the partial strength safety factor; L_D , L_L are dead and live loads respectively and γ_D , γ_L are the corresponding safety factors. **Salmon and Johnson (1990)** stated that this approach allows for clear separation of the uncertainties in the resistance and the different types of loading effects, Additionally, the nominal values of load and strength are given by means of characteristic values.

It is important to indicate that the availability of Level 2 reliability methods has made it practical the determination of the required partial safety factors as well as code calibration for the so called LRFD design approach, **Flint, et. al. (1977)**.

The exact determination of the probability of failure, Level 3 methods, requires a full description of the joint probability density function associated with the limit state function. The evaluation of the integral of **Equation 1.10** can only be performed analytically for a few special cases involving very few basic variables. In practice multidimensional numerical integration needs to be applied and **Schueller and Stix (1987)** have reported that this approach is only efficient for problems where the number of basic variables is less than six or where the domain of integration is of a special type, i.e. hypercube, hypercircle, etc. Monte Carlo simulation methods can also be employed for determination of the probabilities of failure, **Flint, et. al. (1977)**. Furthermore, Level 3 methods can only be applied for reliability analysis of existing structures, they cannot be applied at the design stage.

Level 2 methods appeared in order to overcome the limitations inherent to Level 3 methods. Though the number of basic variables still affects the computational effort, a large number of basic variables can be successfully accommodated. Another main advantage of these methods is that they can be applied either for checking the safety of existing structures or for design at a specified reliability level of new ones. **Section 1.1.2** provides the definition of the reliability safety measure, the *reliability index*, and **Section 1.1.3** presents a more detailed description of Level 2 methods.

1.1.2. Structural Reliability Index.

Structural reliability problems are characterized by the fact that any one particular structure is usually "one-off" structure; that is, each structure is unique in the sense that no other identical structure to be working in the same specific environment usually exist, as it is the case of offshore structures. This fact places theoretical and practical constraints for the gathering of statistical data needed to build probabilistic models for load and resistance for a particular structure. In addition, offshore structures are commonly designed to provide a useful life of twenty to thirty years, this means that gathering of data should be carried out for a period of at least the same length. Consequently not enough data can be made available to fit the appropriate PDF's to load or resistance models, particularly for the sensitive ***"tails"*** of a proposed PDF. Therefore, the applicability of probability, based on the concept of relative frequencies, seems to have serious drawbacks in the case of structural reliability problems.

Structural reliability is faced with the problem that once a particular structure has been selected the reliability becomes the probability that the predictable, yet unknown, resistance, s , will not be exceeded by the extreme load effect, L , for the " un-sampled" reference period, i.e. useful life. The probabilistic measure of reliability is now dependent on the lack of knowledge about the value of the resistance, s , of the structure (s realization of S) and the physical variability of the extreme load L, **Baker and Wyatt (1979).** This second type of probability is known as ***subjective*** or ***Bayesian probability***.

The probability of failure associated with the subjective or Bayesian concept can only be considered as a nominal probability of failure, P_{f_N} because its numerical calculation lacks a number of phenomena influencing the outcome, i.e. model uncertainty, human error, etc., (which can be asserted by a relative frequency). This nominal probability of failure needs to be updated as the state of knowledge of the structure , resistance or the physical phenomenon of loading, changes.

However, in order to make a practical application of the numerical value of the probability of the failure, consistent nominal failure probabilities, expressed through a reliability index β, should be sought for different structural elements. For this purpose, the nominal probability of the failure P_{f_N} as a surrogate for the probability of failure should not be interpreted in the sense of relative frequency, but rather as a ***"formal" failure probability*** measure, interpreted as a "degree of belief", **Ditlevsen (1983).** Moreover, when the probability of failure is interpreted as a "nominal" or "formal" measure of structural failure probability, the tail sensitivity problem becomes in essence not significant, since no frequency meaning is associated to this measure, **Melchers (1987).**

Under these theoretical perceptions of nominal probability of failure, it is possible to assume that all significant uncertainties concerning the structural reliability can be expressed solely in terms of expected values and covariances of the basic variables, that is the first and second statistical moments, respectively. This representation of the parameters entering a reliability problems is known as a ***second moment*** representation. The notion of nominal probability of failure allows the establishment of an invariant measure of reliability, the ***reliability index***.

Several reliability indices have been proposed since **Freudenthal (1956)** proposed a simple reliability index and explained its geometrical properties. His work is however based on full probabilistic models, Level 3 methods, and because of the narrow interpretation of the probability concept, as well as the computational difficulties, it was not broadly accepted.

The first reliability index that made use of the second moment representation of the basic variables and which gained certain degree of acceptance was proposed by **Cornell (1969)**. He selected a failure function with a difference statement safety margin, as:

$$G(\mathbf{X}) = \mathbf{M} = \boldsymbol{S} - \boldsymbol{L} \tag{1.13}$$

and defined the ***reliability index*** (or safety index) as the distance by which $E[\mathbf{M}]$ exceeds zero. The standard deviation is used as the unit to measure this distance, in order to establish a uniform scale,

$$\beta_c = \frac{\mathrm{E}[\mathbf{M}]}{D[\mathbf{M}]} \tag{1.14}$$

furthermore, if on account of the second moment description of $\boldsymbol{S}$ and $\boldsymbol{L}$ a Normal PDF is assumed to described such variables, and if $\boldsymbol{S}$ and $\boldsymbol{L}$ are uncorrelated, then:

$$\mathrm{E}[\mathbf{M}] = \mu_S - \mu_L \tag{1.15}$$

$$D[\mathbf{M}] = \left[\sigma_S^2 + \sigma_L^2\right]^{1/2} \tag{1.16}$$

The geometrical interpretation of Cornell reliability index is presented in **Figure 1.3**.

When the failure function assumes particular realizations of the basic random variables, such that

$$G(\mathbf{s},\mathbf{l}) = \mathbf{s} - \mathbf{l} = 0\,, \tag{1.17}$$

Equation 1.17 then defines a failure boundary which is customarily called ***failure surface*** or ***limit state surface***.

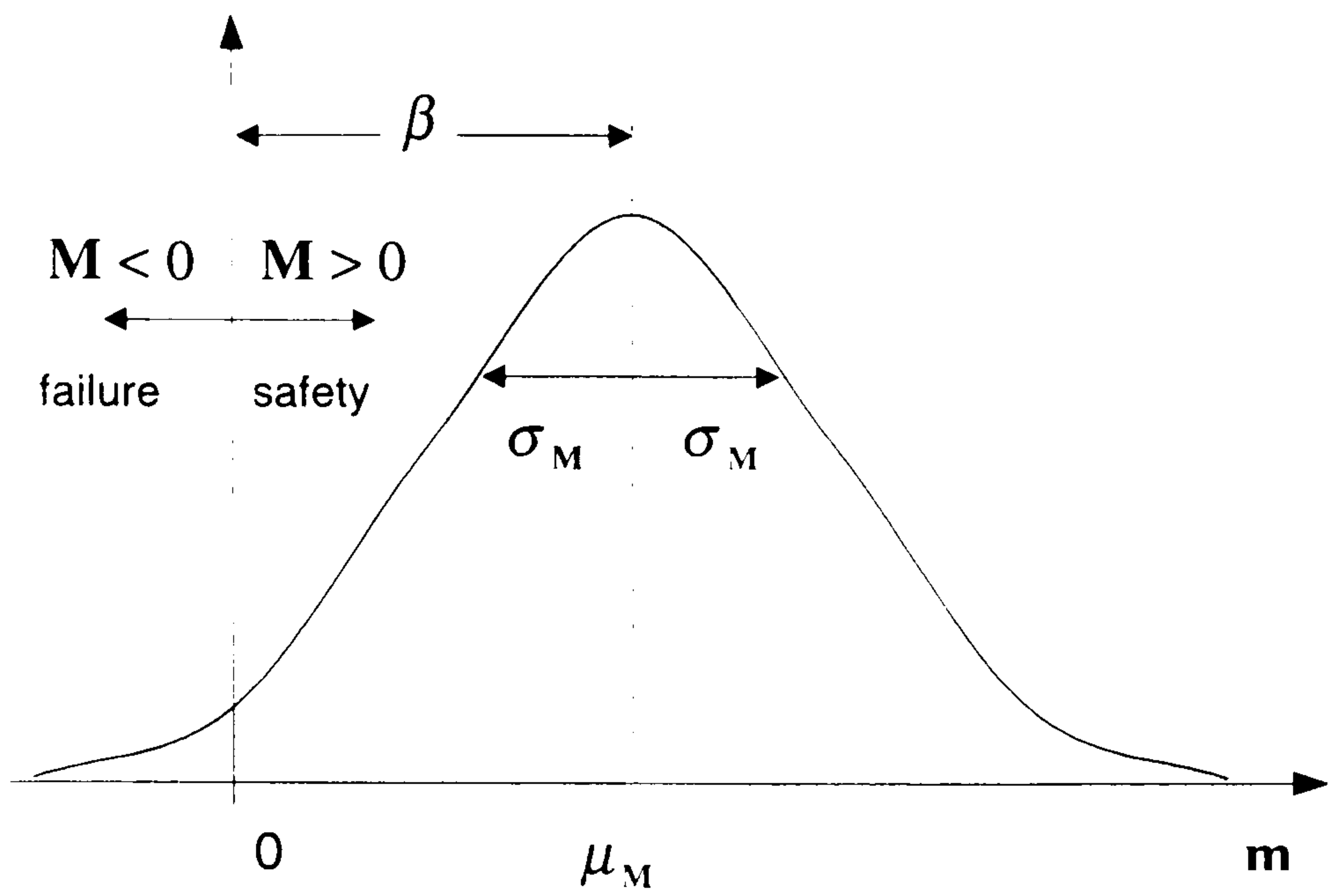

Figure 1.3. The reliability index, after **Thoft-Christensen and Baker (1982).**

Figure 1.3 shows that β is the distance from the failure surface, in this case a point, to the expected value of $\mathbf{M} = S - L$. For the general case when there are *n* basic variables and the failure function is linear, then the failure surface becomes a hyperplane and G can be written, after **Madsen, et. al. (1986)**, as:

$$G(\mathbf{x}) = \mathrm{a}_0 + \sum_{i=1}^{n} \mathrm{a}_i x_i = \mathrm{a}_0 + \mathbf{a}^T \mathbf{x} \qquad (1.18)$$

$\mathbf{a}^T$ is a row vector of constants and $\mathbf{x}$ is a column vector of realizations of the basic random variables. The safety margin associated with **Equation 1.18** is:

$$\mathbf{M} = G(\mathbf{X}) = \mathrm{a}_0 + \sum_{i=1}^{n} \mathrm{a}_i \mathrm{X}_i = \mathrm{a}_0 + \mathbf{a}^T \mathbf{X} \qquad (1.19)$$

and from **Equation 1.14** the Cornell reliability index becomes:

$$\beta_c = \frac{\mathrm{a}_0 + \mathbf{a}^T \mathrm{E}[\mathbf{X}]}{\left[\mathbf{a}^T \mathbf{C}_x \mathbf{a}\right]^{1/2}} \qquad (1.20)$$

where $\mathrm{E}[\mathbf{M}]$ is the vector of expected values and $\mathbf{C}_x$ is the matrix of covariance of $\mathbf{X}$.

In the particular case when S and L are normal random variables the safety margin, $\mathbf{M} = S - L$, is also normal and from **Figure 1.3** the nominal probability of the failure is given by:

$$\mathrm{P}_{f_N} = \Phi(-\beta) \qquad (1.21)$$

Another option for the failure function was given by **Rosenblueth and Esteva (1972)**, who suggested a logarithmic failure function, with the safety margin given by:

$$G(\mathbf{X}) = \mathbf{M} = \log(S/L), \qquad (1.22)$$

then following **Equation 1.14**:

$$\beta_{RE} = \frac{\mathrm{E}[\log(S/L)]}{D[\log(S/L)]} \tag{1.23}$$

Nevertheless, the safety margin of **Equation 1.22** is a non-linear function and its mean and standard deviation cannot be calculated solely from the second moment representation of S and L. Taylor series expansion around the point of expected values (μ_S, μ_L), can be used to linearize **Equation 1.22**, giving as a result a **first order safety margin**:

$$\mathbf{M}_{FO} = \log \mu_S - \log \mu_L + \frac{s - \mu_S}{\mu_S} - \frac{l - \mu_L}{\mu_L} \tag{1.24}$$

substitution of this linearized safety margin in **Equation 1.14** gives:

$$\beta_{FO} = \frac{\log \mu_S - \log \mu_L}{\left[V_S^2 + V_L^2\right]^{1/2}} \tag{1.25}$$

where β_{F0} is the first order reliability index, V_S and V_L are the coefficients of variation of S and L.

The values of the reliability index given by Cornell, **Equation 1.20**, and the first order reliability index of Rosenblueth and Esteva, **Equation 1.25**, are not the same, and therefore β, the reliability index, is not unique. This is due to the different choices of failure function and consequently of the different failure surfaces associated with them. The choice of linearization point, also contributes to the differences. Therefore, the reliability index, so far, is dependent on the choice of failure function and linearization point. Furthermore, determination of $\mathrm{E}[\mathbf{M}]$ and $D[\mathbf{M}]$ requires algebraic manipulation of probability density functions, which may impose additional mathematical difficulties and limitations.

This inconsistency was overcome by **Hasofer and Lind (1974)**, who proposed a transformation of the basic random variables from the original physical $\mathbf{x}$-space into a $\mathbf{u}$-space of **normalized**, **standardized** and **uncorrelated** basic variables where the vector of expected values is $\mathrm{E}[\mathbf{X}] = 0$ with unit standard derivations. If initially the basic variables are normally distributed and uncorrelated a simple transformation (standardization) can be applied, namely:

$$U_i = \frac{X_i - \mu_{X_i}}{\sigma_{X_i}} \tag{1.26}$$

The transformed $\mathbf{u}$-space of basic variables has two important properties, i) the co-ordinates of the vector of expected values coincide with the origin of system co-ordinates, and ii) the set of the U_i variables with its second moment representation is rotationally symmetric. The $\mathbf{u}$-space corresponds to a space of a multivariate normal distributions: $\Phi_n(\mathbf{u})$.

From rotational symmetry properties of the transformed $\mathbf{u}$-space it follows that the geometrical distance form the origin to any point on the limit state surface, $g(\mathbf{u})=0$, agrees with the number of standard derivations from the mean value point in the $\mathbf{x}$-space to the corresponding point $G(\mathbf{x})=0$.

Figures 1.4 and **1.5** present the original $\mathbf{x}$-space of basic variables and their transformed $\mathbf{u}$-space, respectively. The failure surface or limit state surface is showed on both cases. If the failure surface is linear, then the definition of reliability index, as originally proposed by **Cornell (1969)**, is applicable, that is, the reliability index is equal to the distance from the vector of expected values, $E[S]$ and $E[L]$, to the failure surface.

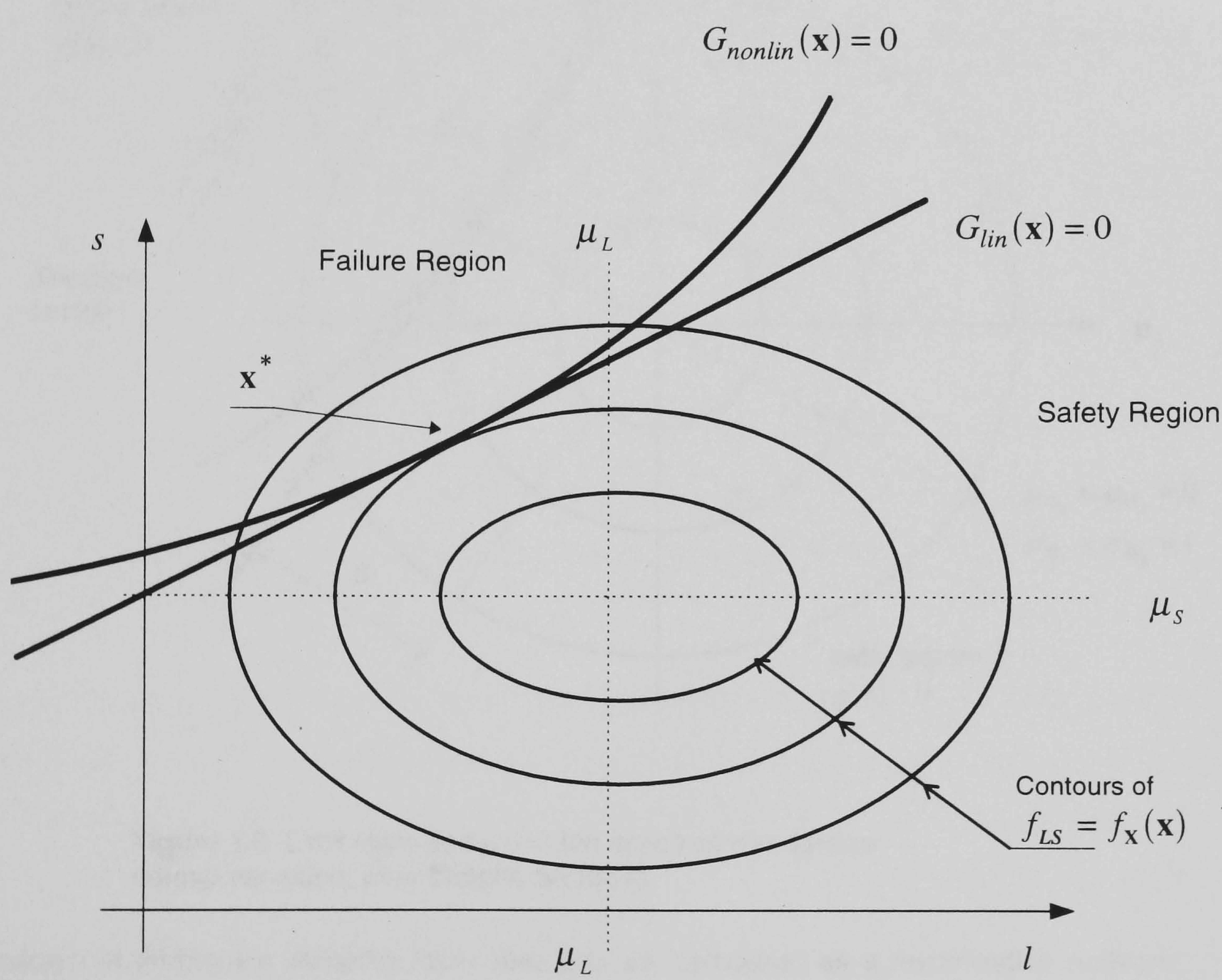

Figure 1.4. Limit state surface in the space of the basic variables, after **Melchers (1987)**.

The statistical properties of the new random variable $\mathbf{M}$, **Equations 1.15** and **1.16**, were obtained by means of the algebra of PDF's. From the geometrical interpretation of the transformed space of basic variables, **Figure 1.5**, it is observed that the marginal distribution of $\mathbf{M}$, see **Figure 1.6**, can also be obtained by integration over all the domain, from $-\infty$ to ∞, in the direction the origin to the design point, $\mathbf{u}^*$.

Furthermore, it follows from the properties of the bivariate normal distribution that the sought marginal distribution is likewise normal, therefore, **Figure 1.3** and **1.6** are fundamentally the same and the shadowed area of both figures represents the nominal probability of failure. On account of the characteristics displayed by the **u**-space, **Hasofer and Lind (1974)** defined the ***reliability index*** as the shortest distance from the origin of system coordinates to the failure surface when the space of basic variables has been transformed to the aforementioned **u**-space.

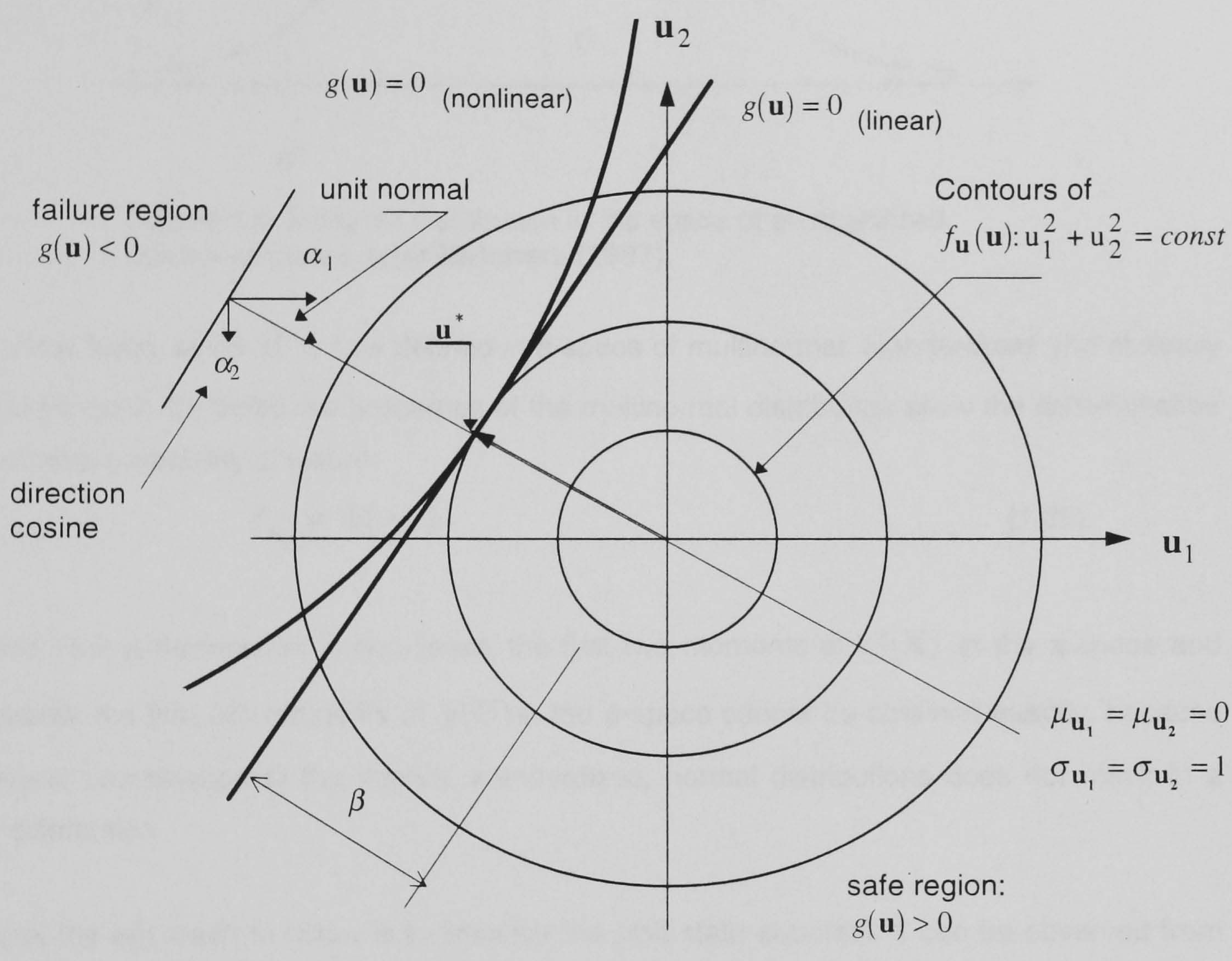

Figure 1.5. Limit state surface in the space of standardize normal variables, after **Melchers (1987)**.

The problem of finding the reliability index may now be formulated as a minimization problem: that of finding the shortest distance from the origin of coordinates to the limit state or failure surface in the transformed space of basic variables, **u**-space, that is:

$$\beta = \min\left(\sum_{i=1}^{n} u_i^2\right)^{\frac{1}{2}} = \min\left(\mathbf{u}^T, \mathbf{u}\right)^{\frac{1}{2}} \tag{1.27}$$

where $\mathbf{u}$ is a position vector from the origin to the failure surface. The point that satisfies **Equation 1.27** is usually named the ***design point***, $\mathbf{u}^*$. In the linear case this point can be found from the geometry of surfaces, as it is explained in **Appendix 2**.

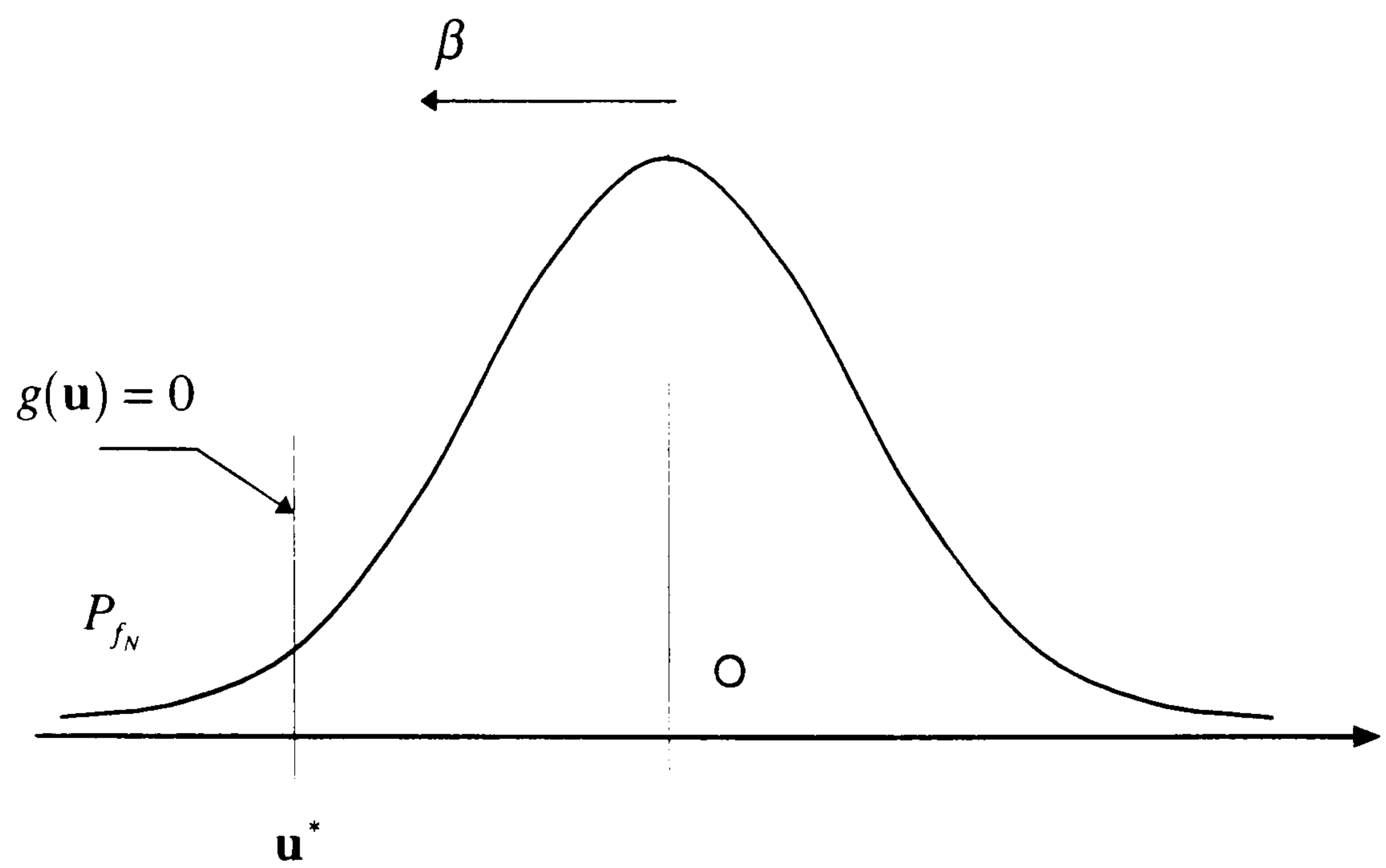

Figure 1.6. Marginal distribution in the space of standardized normal variables, after **Melchers (1987)**.

On the other hand, since β is now defined in a space of multinormal, standardized and mutually independent basic variables the properties of the multinormal distribution allow the determination of the nominal probability of failure:

$$P_{f_N} = \Phi(-\beta) \tag{1.28}$$

When the limit state function is non-linear, the first two moments of $G(\mathbf{X})$ in the $\mathbf{x}$-space and consequently the first two moments of $g(\mathbf{U})$ in the $\mathbf{u}$-space cannot be obtained exactly, because a non-linear combination of the implicit, standardized, normal distributions does not result in a normal distribution.

As before, the approach to follow is to linearize the limit state equation. It can be observed from **Figure 1.5** that the design point $\mathbf{u}^*$ represents the point of greatest probability density, that is, it makes the largest contribution to the probability of failure; therefore, it is a sensible choice to select $\mathbf{u}^*$ as the linearization point. Because of this condition it is possible to make use of the same concepts and methods used for a linear limit state equation. Then the problem of finding β for the case of a non-linear limit state can be expressed as the problem of finding the shortest distance from the origin to the linearized failure surface at the design point $\mathbf{u}^*$, as in **Equation 1.27**. In this case, since a hyperplane tangent to the design point was employed, the method becomes a ***First-Order*** one. Another approach is to approximate the non-linear limit state equation with a second order hypersurface at the design point, the method is then referred as ***Second-Order*** reliability method.

The above definition provides an invariant measure for the reliability index β, **Equation 1.27,** thanks to the rotational symmetry properties of the multivariate normal distribution. Additionally, the nominal probability of failure can be obtained from **Equation 1.21,** namely:

$$P_{f_N} = \Phi(-\beta) \tag{1.29}$$

which is consistent with the "formal" interpretation of the probabilistic measure of structural failure given by **Ditlevsen (1983).** It is also consistent with the second-moment representation of the basic variables introduced by **Cornell (1969).** That is β depends only on the first two statistical moments of the basic random variables, mean and standard deviation, quantities which completely describe the normal distribution.

There is, however, one drawback for Hasofer and Lind reliability index, which requires further discussion. The probability of failure as defined by the first order second moment reliability index of Hasofer and Lind, **Equation 1.29**, is affected by one limitation. As can be observed from **Figure 1.5**, the numerical value of the probability of failure is indeed affected by the shape of the limit state surface, linear or non-linear. With Hasofer and Lind definition for the reliability index, two different structures having one linear limit state surface and the second one non-linear limit state surface, would appear to have the same probability of failure, which is obviously inaccurate.

Ditlevsen (1979a), introduced a generalized second moment reliability index, in order to overcome the inconsistency of Hasofer and Lind reliability index. The inconsistency of the same probability of failure for different shapes of limit state functions was called by him an *ordering problem*. That is a problem associated with the order of the hypersurface which divides the failure from the safety domains. He proposed that the reliability index is to be defined as:

$$\beta_g = \Phi^{-1}(\gamma) = \Phi^{-1}\left[\int_{G(\mathbf{X})>0} \Phi(x_1)\Phi(x_2)\ldots\Phi(x_n)d\mathbf{x}\right] \tag{1.30}$$

where γ is a monotonicaly increasing function. The generalized reliability index of Ditlevsen, **Equation 1.30,** provides a consistent measure of the probability of failure for non-linear limit state hypersurfaces. However, in practice the evaluation of the integral in **Equation 1.30**, is difficult, in a similar manner as it happens with **Equation 1.10**. Therefore, **Ditlevsen (1979b)**, proposed that the non-linear limit sate surface could be approximated by a polyhedral surface, made of tangent hyperplanes fitted at selected points of the failure surface. It follows from his observations that an alternative approach is to use a second or higher order surface to approximate the failure surface, as is the case with the **Second Order Reliability Method**.

Madsen, et. al. (1986) pointed out that the numerical values of the reliability index as defined by **Hasofer and Lind (1974)** and by **Ditlevsen (1979a)** are "almost coinciding", except in few cases where the non-linearity of the limit state is significant.

Veneziano (1979) also proposed another reliability index in order to overcome the inconsistency of the **Hasofer and Lind (1974)** index. **Veneziano (1979)** proposed the use of the upper Tchebycheff bound of the probability failure. The practical use of this definition seems to be difficult, even though it can incorporate statistical information additional to the two first moments.

From the discussion above it can be observed that the applicability of a practical and universally consistent reliability index, β, seems rather difficult. However, Hasofer and Lind reliability index is likely to provide the best "practical" approach. Because of these facts, research in the field of reliability based design defined the reliability in terms of the probability of failure. The main contribution of **Hasofer and Lind (1974)** is that their reliability index approach constitutes a geometrical consistent basis for the definition of failure and safety domains, by means of a transformed normal and standardized space of uncorrelated basic variables. In the same fashion, they brought the attention to the paramount importance of the design point, $\mathbf{u}^*$, as the point of greatest contribution to the probability of failure and to the important direct relation between the design point, $\mathbf{u}^*$, and the reliability index, β, namely that the reliability index is defined as the distance from the origin of coordinates to the design point. Thanks to this definition of the reliability index, the research turned its goals to the determination of numerical procedures suitable for determination of the probability content of a region bounded by a non-linear limit state surface. This will be discussed in **Section 1.1.3**.

Therefore, it is concluded that when reliability analysis problems are reduced to the normalized $\mathbf{u}$-space of noncorrelated basic variables, the **nominal probability of failure** provides a consistent and meaningful measure to make comparisons and decisions regarding the goodness of different designs. It is also concluded that one of the most important steps for the determination of the probability of the failure is the location of the design point, $\mathbf{u}^*$.

As will be explained in **Section, 1.1.3**, different algorithms might be used for the transformation of variables and for the determination of Hasofer and Lind reliability index. Algorithms aimed to calculate the reliability index and/or the probability of failure are referred in the literature as ***First Order Reliability Methods, FORM*** or ***Second Order Reliability Methods, SORM***, depending on the order of approximation for the limit sate surface.

1.1.3. Methods of Structural Reliability.

FORM and **SORM** are a kind of Level 2 reliability analysis methods. The basic principles of these were described in the previous section. In a short manner, the main steps for the application of **FORM** and **SORM** are:

I).- **transformation**; the set of original basic variables, $\mathbf{X}$, (non independent and/or non normal) must be transformed into a set of independent, standardized and normally distributed, $\mathbf{U}$.

ii).- **location of minimum** β, the point $\mathbf{u}^*$, for which the shortest distance from the origin can be geometrically traced. It represents the point of maximum contribution to the nominal probability of failure.

iii).- **idealisation of the limit state surface at** $\mathbf{u}^*$ as a first or second order curve, for the determination of the probability of failure.

The first of the above mentioned steps is the transformation, which may be a of simple or complex nature, depending on the PDF's assigned to the variables and the independence or correlation among them. The most simple of all transformations is applicable when the variables are or may be assumed to be normally distributed and independent, in this case only a standardization is required, as given by **Equation 1.26**. **Madsen et. al. (1986)** stated that since the probability content in various sets may be reasonably approximated in a standardized normal space then it is possible to apply the idea of a one to one transformation

$$\mathbf{T}: \qquad \mathbf{X} = (X_1,\dots,X_n) \rightarrow \mathbf{U} = (U_1,\dots,U_n) \qquad (1.31)$$

The following case appears when the basic variables are mutually independent with any given distribution functions $F_{X_1},\dots,F_{X_n}$, then each variable can be transformed separately, so that

$$\Phi(u_i) = F_{X_i}(x_i), \qquad i = 1,\dots,n \qquad (1.32)$$

The transformation is then given by:

$$\mathbf{T}: \quad u_i = \Phi^{-1}\left(F_{Xi}(x_i)\right), \qquad i = 1,\dots,n \qquad (1.33)$$

with the inverse transformation:

$$\mathbf{T}^{-1}: \quad x_i = F_{Xi}^{-1}\left(\Phi(u_i)\right) \qquad i = 1,\dots,n \qquad (1.34)$$

The failure function $g(\mathbf{u})$ in $\mathbf{u}$-space is found by applying the transformation of **Equation 1.33** to the failure function in the original space:

$$g(\mathbf{u}) = G(\mathbf{T}(\mathbf{x})) \qquad (1.35)$$

In a general case, when the basic variables are not normal and not mutually independent the Rosenblatt transformation, **Rosenblatt (1952)**, which was suggested by **Hohenbichler and Rackwitz (1981)**,can be applied. The transformation is defined in a similar manner as in **Equation 1.33**:

$$\mathbf{T}: \quad \begin{aligned} u_1 &= \Phi^{-1}\left(F_1(x_1)\right) \\ u_2 &= \Phi^{-1}\left(F_2(x_2 | x_1)\right) \\ &\vdots \\ u_n &= \Phi^{-1}\left(F_n(x_n | x_1, x_2, \ldots x_{n-1})\right) \end{aligned} \tag{1.36}$$

where: $F_i(x_i, | x_1, \ldots, x_{i-1})$ is the distribution function of x_i conditional upon $(X_1 = x_1, \ldots, X_{i-1} = x_{i-1})$ so that:

$$F_i(x_i | x_1, \ldots, x_{i-1}) = \frac{\int_{-\infty}^{x_i} f_{X_1, \ldots, X_{i-1}, X_i}(x_1, \ldots, x_{i-1}, t) dt}{f_{X_1, \ldots, X_{i-1}}(x_1, \ldots, x_{i-1})} \tag{1.37}$$

Rosenblatt transformation first transforms X_1 into a standardized normal variable, after that, all conditional variables of $X_2 | X_1 = x_1$ are transformed into a standardized normal variable and so forth.

Other transformations were proposed, **Ditlevsen (1981)**, and **Der Kiureghian and Liu (1986)**, showed that the same transformation of domains given by Rosenblatt transformation can be obtained by using the matrix of correlation coefficients $\mathbf{C}_X$ and its Cholesky decomposition, $\mathbf{L}_X$. **Melchers (1987)** proposed an orthogonal transformation for a correlated vector of normally distributed basic variables. **Nakanishi and Nakayasu (1996)** suggested some improvements to the orthogonal transformation of **Melchers(1987)**, namely that it is not necessary to perform an inverse transformation of the orthogonal matrix, because **Nakanishi and Nakayasu (1996)** transformation produces first a standardized space; furthermore, they carried out a comparative study of all the above mentioned transformations and reported that the distance from the origin to the nearest point on the limit state surface in the transformed space is identical for all the transformation methods used; however, the failure and safety domains as divided by the limit state surface are not identical for all the investigated transformation methods. Furthermore, it is the opinion of the author of the present work that this problem may be overcome by using only the same type of transformation for comparison purposes in a given design or reliability assessment problem.

The second step for the application of **FORM** and **SORM** methods is concerned with the location of the design point $\mathbf{u}^*$, also known as β or reliability index and which defines the minimum distance from the origin of the system to the limit state surface.

In **Section 1.1.2** the problem of finding the design point was defined to be a minimisation problem, as stated by **Equation 1.27**. If the limit sate surface is linear, finding the design point can be easily accomplished by means of the geometry of surfaces, see **Appendix 2**.

For the case when the limit sate surface is non-linear, **Shinosuka (1983)** established that since $\mathbf{u}^*$ is not known a priory the problem of finding β still remains strictly a minimisation problem.

Several approaches have been proposed, analytical, iterative and numerical. **Shinosuka (1983)** proposed the use of Lagrangian multipliers, then the problem becomes

$$\min(\Delta) = \left(\mathbf{u}^T \cdot \mathbf{u}\right)^{1/2} + \lambda g(\mathbf{u}) \tag{1.38}$$

subject to the constraint that $g(\mathbf{u}) = 0$, the solution to this problem renders the reliability index as:

$$\beta = \frac{u_{g_L}}{\sigma_{g_L}} = \frac{-\sum_{i=1}^{n} u_i^* \left(\partial g / \partial u_i\right)}{\left[\sum_{i=1}^{n} \left(\partial g / \partial u_i\right)^2\right]^{1/2}} \tag{1.39}$$

Hasofer and Lind (1974) also proposed and iterative algorithm to find the design point as the limit of a sequence, based on a linearization by Taylor series expansion at each iteration. This algorithm, as given by **Melchers (1987)**, is adopted for the purposes of the present work, and is given in **Appendix 3**.

A geometrical interpretation of such algorithm is given by **Madsen, et al. (1986)**, see **Figure 1.7**. An initial design point, $\mathbf{u}^{(m)}$, is selected. This initial point need not to be on the failure surface, $g(\mathbf{u}) = 0$, but a trajectory $g(\mathbf{u}) = g\left(\mathbf{u}^{(m)}\right)$ is replaced by its tangent hyperplane at $\mathbf{u}^{(m)}$. Now the point $\mathbf{u}^{(m+1)}$ for the following iteration is taken as $\beta^{(m)}$, which is the shortest distance from the tangent hyperplane at $\mathbf{u}^{(m)}$ to the origin, plus an additional term added to account for the fact that $g\left(\mathbf{u}^{(m)}\right)$ may be different from zero.

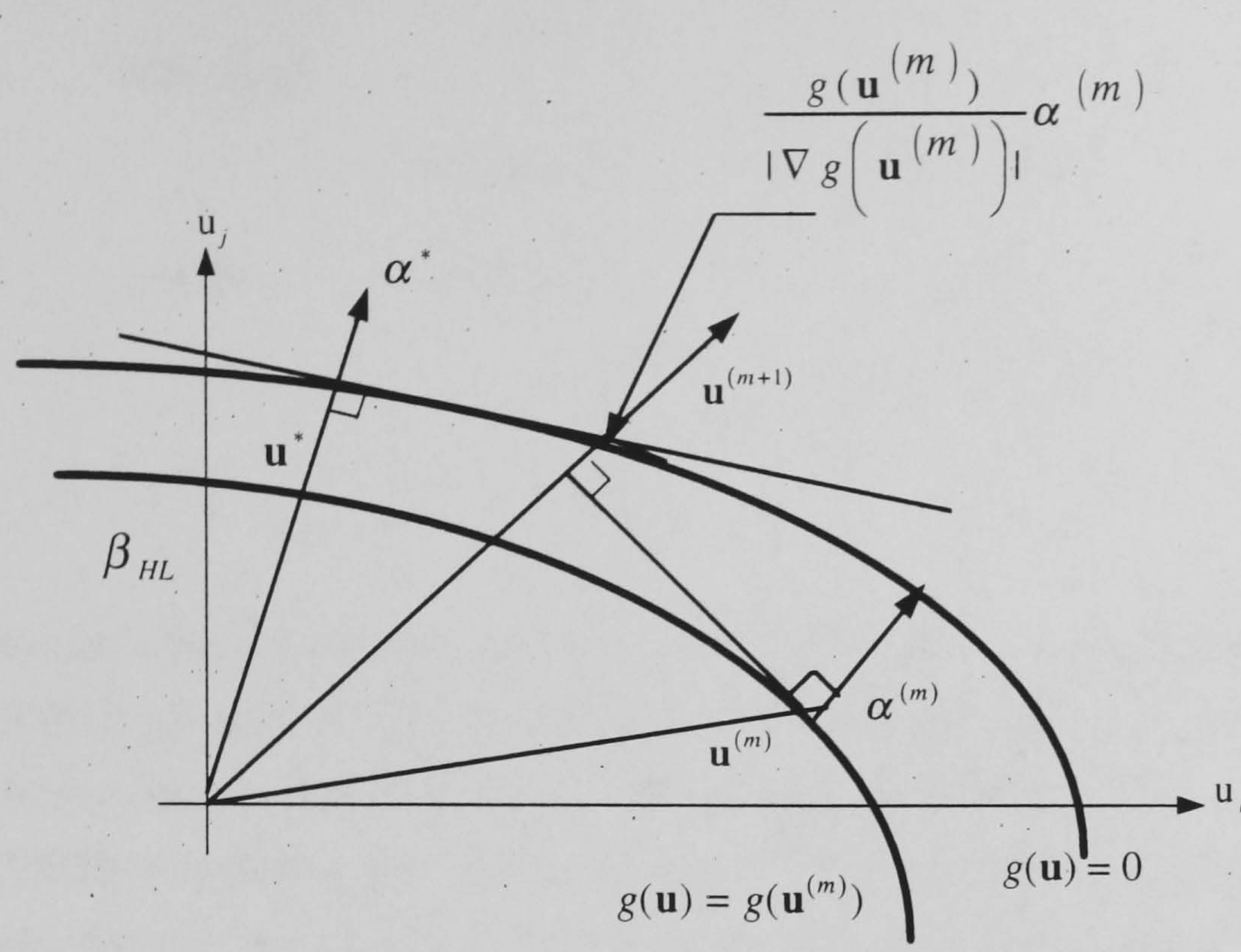

Figure 1.7. Geometrical interpretation of Hasofer and Lind algorithm, after **Madsen, et al. (1986)**.

The recurrence relationship for this algorithm, as given by **Melchers (1987)**, becomes:

$$\mathbf{u}^{(m+1)} = -\alpha^{(m)}\left[\beta^{(m)} + \frac{g\left(\mathbf{u}^{(m)}\right)}{\ell}\right] \tag{1.40}$$

This additional term comes from the relationship between $\mathbf{u}^{(m)}$ and $\mathbf{u}^{(m+1)}$, which is given by the first order Taylor series expansion of $g\left(\mathbf{u}^{(m+1)}\right) = 0$ about $\mathbf{u}^{(m)}$, that is, using index notation.

$$g_L\left(u_1^{(m+1)},\ldots,u_n^{(m+1)}\right) \approx g\left(u_1^{(m)},\ldots,u_n^{(m)}\right) + \\ + \sum_{i=1}^{n}\left(u_i^{(m+1)} - u_i^{(m)}\right)\frac{\partial g\left(u_1^{(m)},\ldots,u_n^{(m)}\right)}{\partial u_i} \tag{1.41}$$

For a detailed deduction of the recurrence formula of this algorithm, **Equation 1.40,** and a description of the steps necessary for its computer implementation, as it will be used in the present work, refer to **Appendix 3**.

Since a crucial step in **FORM** and **SORM** is precisely the location of the design point, **Bjerager (1989)** pointed out that a successful performance of these two methods depends on a "robust optimisation algorithm". Therefore, he suggested the use of the **NLPQL** algorithm, due to **Schittkowsky (1985)**. **NLPQL** is a subroutine designed to solve non-linear constrained programming problems of the kind:

$$
\begin{array}{llll}
\min f(x) & & & \\
 & g_j(x) = o, & j = 1,\dots,m_e & \\
x \in \mathrm{R}^n: & g_j(x) \geq o, & j = m_e + 1,\dots,m & \\
 & g_j(x) \geq o, & j = m_e + 1,\dots,m & \\
 & x_\ell \leq x \leq x_u & & (1.42)
\end{array}
$$

The approach followed by **NLPQL** is based on the use of sequential quadratic programming, this means that the idea of the program is to formulate a specific quadratic programming subproblem at each approximation. The algorithm of **Schittkowsky (1985)**, fulfils the terms pointed by **Bjerager (1989)** concerning the high performance requirements for the location of the design point. It was reported that **NLPQL** has been thoroughly tested with problem involving up to 100 variables and that the necessary computer time is sensibly less than that for most of the non-linear programming algorithms available.

Liu and Der Kiureghian (1988) carried out a comparison of the performance and robustness of several optimisation algorithms, robustness is understood in the sense of accuracy. Their study included algorithms on the gradient projection, augmented Lagrangian, Hasofer and Lind, a modification of Hasofer and Lind, and sequential quadratic programming methods, **SQP**. Their conclusions presented **SQP**, gradient projection method and modified Hasofer and Lind method as suitable algorithms for the optimisation objectives of the reliability analysis. From the results that those authors provided it seems to be feasible to say that **SQP** methods are the ones that provide better performance.

The third step in the application of **FORM** and **SORM** methods is the actual determination of the probability of failure, following the assumption that the limit state surface may be idealized as a first order hyperplane, **FORM**, or a second order hypersurface, **SORM**.

When the limit sate surface is linear or when the level of non-linearity of this surface is such that the assumption of linearity will not lead to excessive loss of accuracy, the probability of failure may be obtained as:

$$P_f = \Phi(-\beta) \qquad (1.43)$$

where Φ represents the cumulative normal distribution function. In this case, a first-order hyperplane was used to approximate the limit state surface. The method is known as a **FORM**, (First-Order Reliability Method).

If the degree of non-linearity of the limit state surface has to be considered, the approach followed in the reliability analysis is to fit a second order hypersurface on the limit state surface at the design point. **Fiessler, et al. (1979)** proposed the use of a quadratic approximation by means of a second order Taylor series expansion about $\mathbf{u}^*$. The problem, however, continues to be the estimation of the probability content outside of a region bounded by a second-order approximation of the failure surface, as showed in **Figure 1.8**.

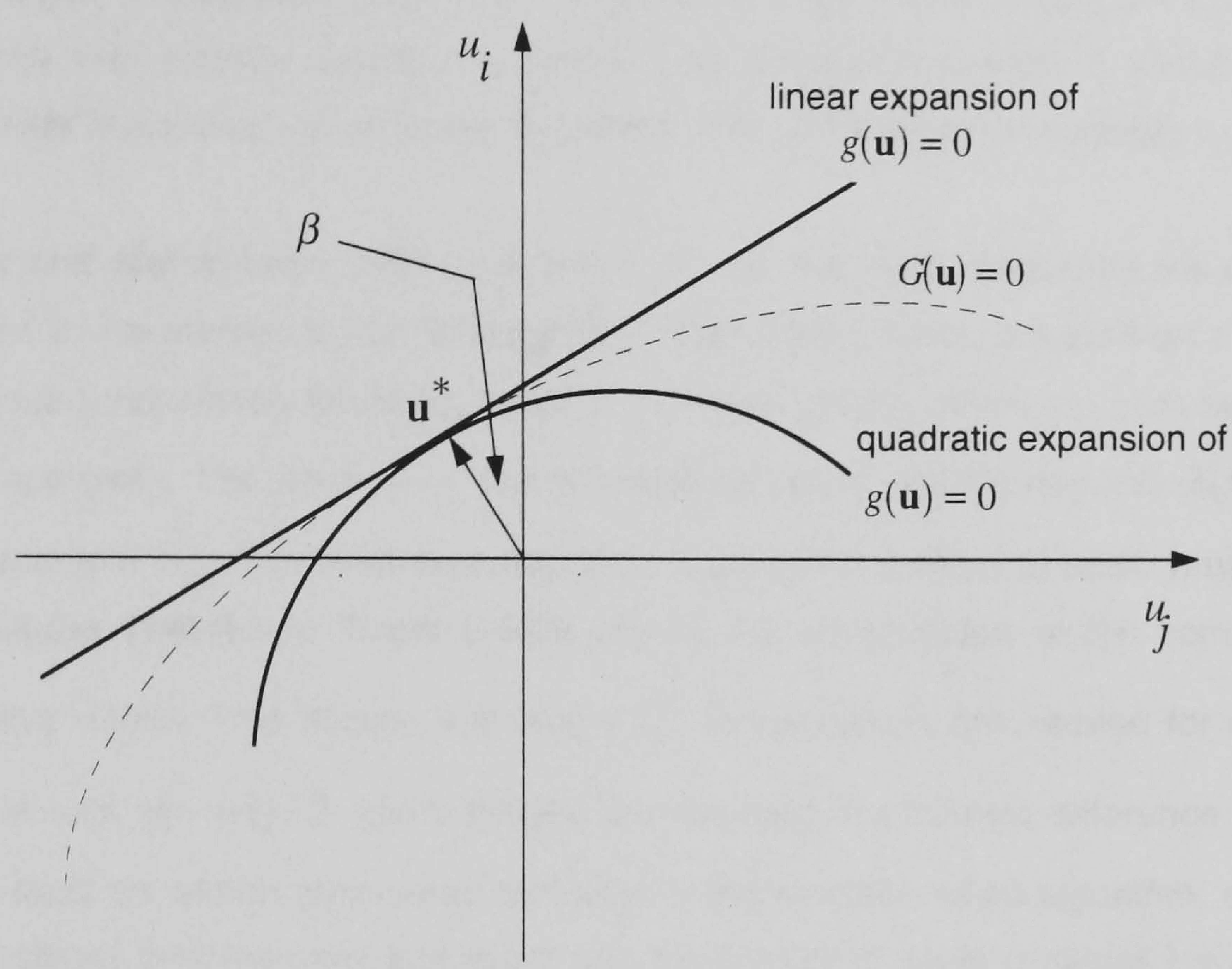

Figure 1.8. Error in estimation of the probability of failure induced by linear and quadratic approximations of the limit state surface.

Breitung (1984) found a closed form solution to estimate the probability of failure by applying a correction factor to the probability of failure as determined by the **FORM** method. Such correction factor is the result of considering the *kth* number of main curvatures of the failure surface at the design point, that is:

$$P_f \approx \Phi(-\beta)\prod_{i=1}^{n-1}\left(1+\beta_{k_i}\right)^{-1/2} \tag{1.44}$$

Der Kiureghian, et al. (1987), proposed a paraboloid approximation of the failure surface by means of a point fitting method in orthogonal directions only, instead of a curvature fitting in either the principal or main curvatures, as was done in all the previous approaches. **Tvedt (1988)** reported that all the aforementioned procedures suggested for the application of **SORM** produced some degree of inaccuracy with respect to the probability failure. He then proposed an exact expression derived for a parabola, here presented as reported by **Bjerager (1989)**:

$$P_f = \phi(\beta)\,\mathrm{Re}\left[i\left(\frac{2}{\pi}\right)^{1/2} \int_{t=o}^{i\infty} \frac{\exp\left\{\dfrac{(t+\beta)^2}{2}\right\}}{t} \prod_{j=1}^{q-1}(1-tk_j)^{-1/2}\,dt \right] \tag{1.45}$$

where:

i , the imaginary unit,

k_j , are the $q-1$ principal curvatures in u^* .

The integral of **Equation 1.45** is one dimensional and **Tvedt (1988)** pointed out that it can be efficiently evaluated by means of a saddle point integration method. It should also be noted that the **SORM** formula of this equation, **Equation 1.45**, is based on a parabolic curve fitting method.

Haldar and Mahadevan (1995) presented a brief discussion regarding the computational effort required by the method of **Der Kiureghian, et al. (1987)**, which is based on a point fitting method and those proposed by **Breitung (1984)** and **Tvedt (1988)**, which are both based on a curvature fitting approach. The method of **Der Kiureghian, et al. (1987)** requires $8(n-1)$ deterministic calculations in order to define the probability, *n* being the number of basic variables. The formulas of **Breitung (1984)** and **Tvedt (1988)** require the computation of the complete second order derivative matrix. This implies that $n(n+1)^2$ computations are needed for a central difference scheme and $n(n+1)/2$ computations are required if a forward difference scheme is applied. These facts should be considered carefully for the selection of an algorithm, since the number of computations become more significant with the number of basic variables involved.

In order to reduce the computational efforts inherent in the curvature and point fitting methods. **Der Kiureghian, et al. (1991)** proposed an iterative method which avoids the actual determination of the second derivative matrix or the solution of the Eigen value problem. The approach of this algorithm is to determine the curvature in a decreasing order of their magnitudes, which is the same order of their importance in the reliability analysis. The computation can, therefore, be stopped when the curvature computed is considered sufficiently small. **Der Kiureghian et al. (1991)** stated that this method is very efficient in problems involving a large number of basic variables, 99, in which case the CPU time required for this algorithm is less than 2 percent of that required for the "conventional" **SORM**.

It might be worth to note that a number of algorithms joining two or more of the three above mentioned stages were proposed at different steps during the development of the reliability analysis techniques.

Rackwits and Fiessler (1978) proposed an algorithm in which they combined the iterative method of **Hasofer and Lind (1974)** to find the design point and considered that since the basic variables may not be normally distributed, some statistical information, other than the mean and standard deviation might be available, and should not be discarded. In this fashion they suggested that non normal variables could be transformed into equivalent normal ones.

Later, **Hohenbichler and Rackwitz (1981)** combined the **Hasofer and Lind (1974)** iterative algorithm and the **Rosenblatt (1952)** transformation.

Parkinson (1980) proposed an algorithm in which the transformation of **Equation 1.26** is directly applied to the recurrence relationship of **Equation 1.44**, with the advantage that transformation to the **u**-space and backward transformation to $\mathbf{x}$ -space are not required.

These methods acquired the denomination of First-Order Reliability Methods, **FORM**, or the **transformation methods**. At some point during the history of developments of the reliability analysis methods they were also known as advanced **First-Order Second-Moment** methods, **AFOSM**, because the approach of transforming the basic variables into a space of normalized and standardized variables was regarded as an extension of the First-Order Second-Moment approach introduced by **Cornell (1969)**.

1.1.4. Structural Systems Reliability.

A large number of structures are composed by a number of structural elements or components, such arrangement of **components** becomes a system, or more properly a **structural system**. The reliability analysis problem now consists of the determination of the global probability of failure of a structural system, taking into consideration the different failure modes or failure paths that may occur. That is, a structural system, i.e. an offshore jacket, usually reaches collapse only after the failure of several components. Each of the many different combinations of failure of the components or the sequence in which failure of individual components evolve constitutes a **failure path** or **failure mode**. The branch of reliability analysis devoted to the analysis of structural systems is customarily called **Structural Systems Reliability**.

Reliability analysis methods as described in **Sections 1.1.2** and **1.1.3** were conceived for the analysis of single components, and therefore they are not applicable to structural systems in a direct manner, but different modelling techniques for the structural systems have to be applied first, in order to provide a suitable model for the subsequent reliability analysis.

There are two basic types of models for the reliability analysis of structural systems: series systems and parallel systems. Combinations of series and parallel systems are possible. A **series system**, as described by **Thoft-Christensen and Baker (1982)**, is showed in **Figure 1.9b**. Series systems are also known as "weakest link" systems, because when one of the elements of the system fails, then the whole system collapses. This is the case of isostatic structures, since there is no redundancy the failure of one element means the failure of the whole structural system. Therefore, the isostatic truss structure of **Figure 1.9a** can be represented by the model of **Figure 1.9b**.

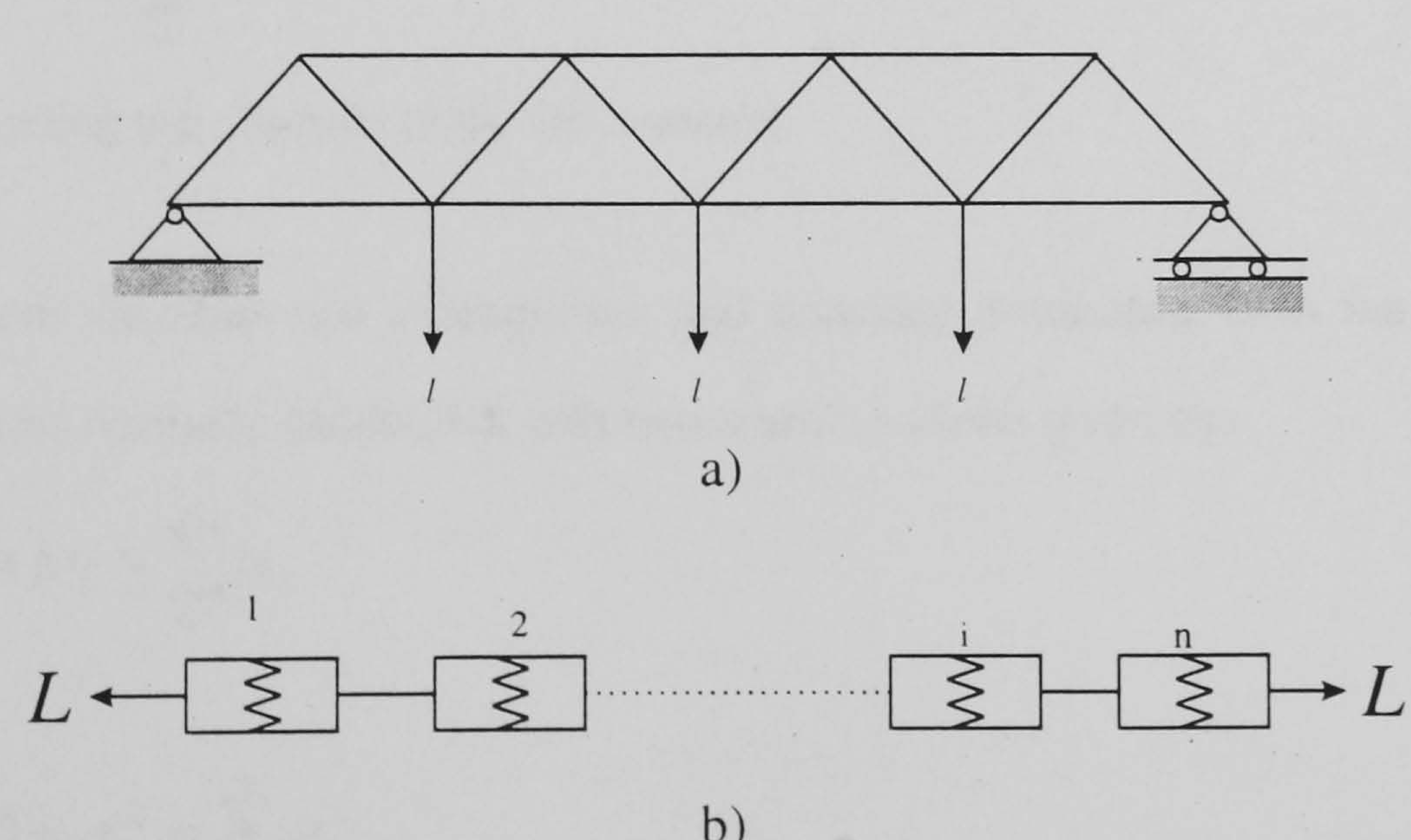

Figure 1.9 a) and **b)**. Statically determined structure and its series system model, after **Thoft-Christensen and Baker (1982)**.

The structural systems reliability model does not represent the mechanical behaviour of the structure, neither the loads applied to such model necessarily represent the actual load distribution on the real structure, such simplifications are needed in order to facilitate the establishment and analysis of failure paths. These models are intended to reflect the **failure interactions**, rather than the specific mechanical behaviour, i.e. stress distribution, of the structure or its particular components.

In order to deduce an expression to calculate the probability of failure of a series system the probability density function of the strength of each component needs to be considered. Individual strengths of each element are assumed to be statistically independent from each other. Then the cumulative PDF of the strength of the system as given by **Thoft-Christensen and Baker (1982)**, becomes:

$$F_S(\mathbf{x}) = 1 - \prod_{i=1}^{n}(1 - F_{S_i}(x_i)) \tag{1.46}$$

Now, the probability of failure can be obtained by substituting **Equation 1.46** in **Equation 1.11**:

$$P_f = 1 - \int_{-\infty}^{\infty} \prod_{i=1}^{n}\left(1 - F_{S_i}(x_i)\right)(f_L(x))dx \tag{1.47}$$

Equation 1.47 is applicable to series systems composed by brittle or ductile materials since the failure of any single element implies the failure of the system.

Parallel systems, as the one showed in **Figure 1.10**, are also known as "**fail safe**" systems, because a number of elements in the system must fail for the whole system to fail. The determination of P_f in parallel systems depends on whether the behaviour of the material is brittle or ductile. The strength of a system of *n* parallel ductile elements is expressible in the form:

$$S = \sum_{i=1}^{n} S_i \ , \tag{1.48}$$

with S_i representing the strength of the *ith*. element.

If the S_i random variables are independent and normally distributed, then the strength of the system, S, is also normally distributed, with mean and variance given by:

$$E[S] = \mu_S = \sum_{i=1}^{n} \mu_i \tag{1.49}$$

and

$$Var[S] = \sigma_S^2 = \sum_{i=1}^{n} \sigma_i^2 \ . \tag{1.50}$$

When μ_S and σ_S are known, it is then possible to apply **FORM** or **SORM**.

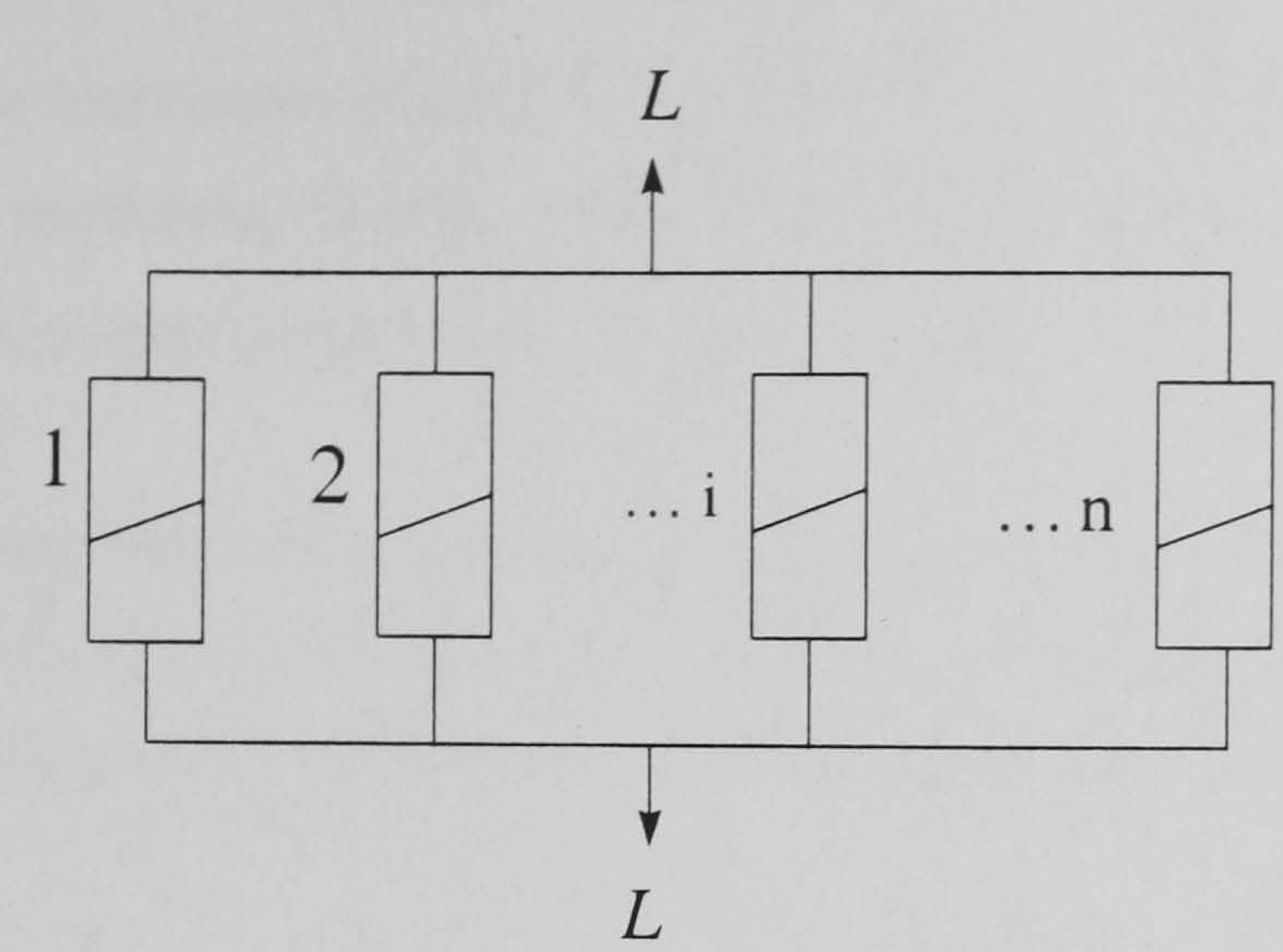

Figure 1.10. Parallel system, failure interaction model, after **Thoft-Christensen and Baker (1982)**.

More complex structures may be modelled by a combination of series and parallel systems, usually each mode of failure is modelled by a parallel system and different failure modes are linked in a series system, thus forming a series system of parallel systems, as showed in **Figure 1.11**.

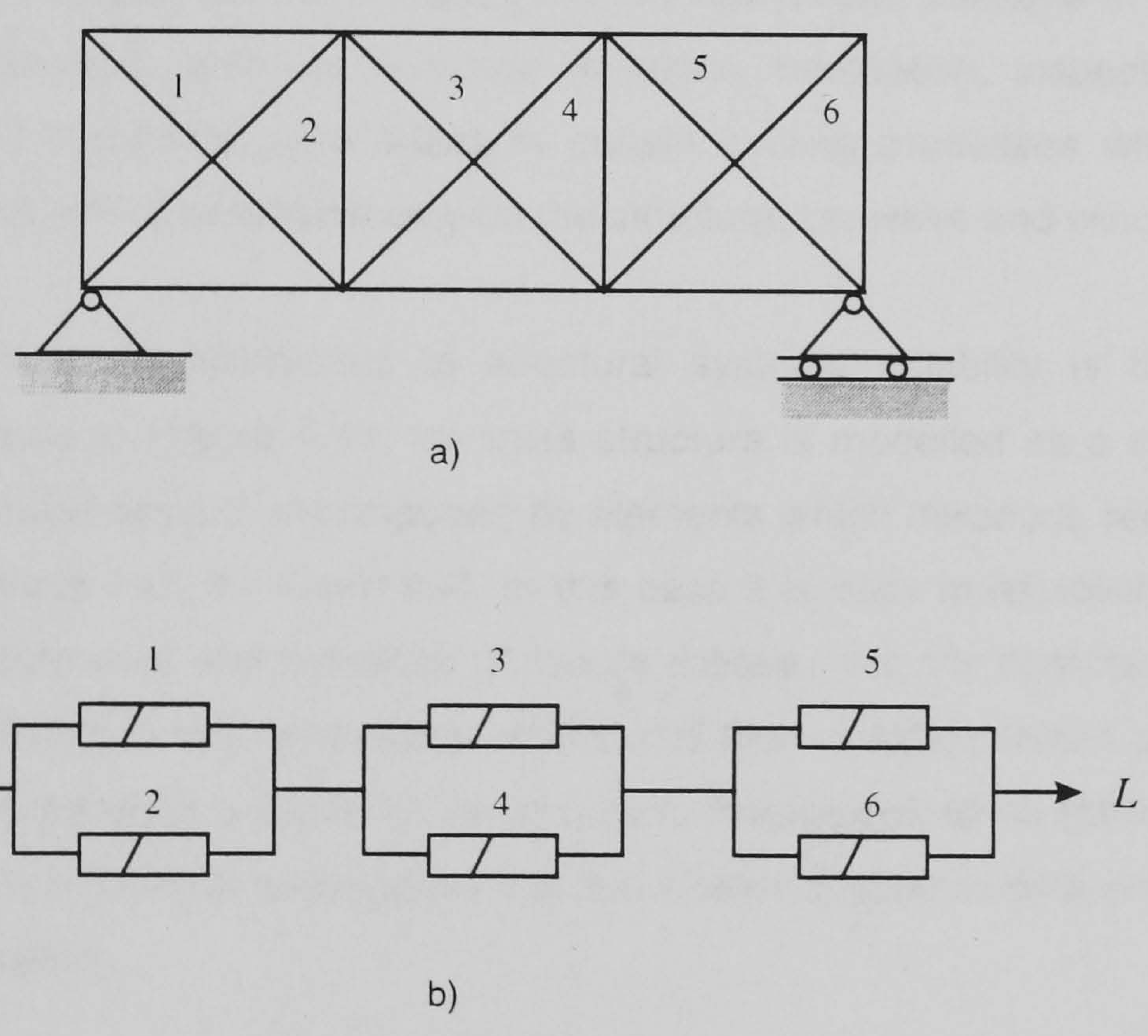

Figure 1.11 a) and **b)**. Series system of parallel systems, **Thoft-Christensen and Baker (1982)**.

Equations 1.47 to **1.50** are applicable only to very simple structures, therefore, in order to extend the concepts of structural systems reliability to more realistic structures, i.e. structures with a high degree of redundancy, like an offshore jacket structure, it has been necessary to circumscribe the determination of the probability of failure to the calculation of "bounds", as described by **Thoft-Christensen and Baker (1982)**. In the same fashion only the dominant failure modes are searched for. Among the techniques suggested for these purposes are the **branch and bound** and the β **-unzipping methods**. **Shetty (1993)** proposed the use of a selective enumeration method to identify the dominant failure modes of large structures.

The construction of failure interaction models, as those presented in **Figures 1.9b** and **1.10**, requires the consideration of several variables, geometry of the structure, which many times directly affects the redundancy of the system, material performance, statistical correlation and redundancy.

With respect to material performance, the influence of brittle or ductile material behaviour has already been mentioned, but other material behaviours, i.e. plastic behaviour have also been investigated. **Beyko and Bernitsas (1992)** presented the application of elastic/plastic material behaviour in relation to a reliability analysis method based on perturbation techniques. Reliability analysis by perturbation methods is described in **Section 1.1.6**. **Murotsu, et al. (1992)** developed a computer program for the analysis of semisubmersible platforms, considering the use of portal frame structures whose material behaviour is modelled by plastic nodes.

Statistical correlation is usually difficult to determine, **Moses (1995)**, because of the influence of several different parameters, such as common materials, fabrication, inspection and testing procedures, etc. Load correlation also arises in certain loading processes which are directly affected by another one acting simultaneously on the structure, i.e. wave and wind loads.

One of the most critical considerations in structural systems reliability is the definition of redundancy. As exhibited in **Figure 1.11**, the truss structure is modelled as a series of parallel systems and each parallel system is composed by elements which introduce redundancy in the system, namely diagonals 1+2, 3+ 4 and 5+6. In this case it is easy to establish the number of redundant structural elements and therefore of failure modes. Yet, for complex structures the identification of redundancy is not necessarily simple and then complex failure patterns have to be analysed in order to produce a model of the structure. **Frangopol, et al. (1991)** presented an evaluation of several definitions of redundancy that have been applied in different approaches of structural systems reliability.

The reliability analysis methodology based on failure interaction models, also known as **failure mode analysis**, requires an important degree of idealisation that usually does not directly represent the mechanical behaviour of the structure. Because of such degree of idealisation it is not possible to use the state of the art modelling techniques, i.e. finite element method, in conjunction with failure mode analysis.

Direct methods for reliability analysis, such as Monte Carlo simulation and methods devised for **implicit performance functions**, described in **Sections 1.1.5** and **1.1.6**, respectively, have the advantage that there is usually no limitation with respect to the mechanical modelling technique employed, either simple or sophisticated, i.e. finite element method, boundary element method, etc. However, the failure modes can only be devised in an implicit way, and therefore the insight on the failure process that failure mode analysis provides might not be usually obtained.

On the other hand, recent safety requirements have prompted the use of techniques such as **risk analysis** and **risk management**, which are based on the analysis of possible malfunctions and accident scenarios, including the effects of human error. **Moses (1995)** pointed out that **Structural Systems Reliability** has a large potential for the analysis of such accident scenarios. The reliability of a structure after the event of an accident has been named by **Liu and Moses (1991)** residual reliability.

1.1.5. Reliability Analysis by Monte Carlo Methods.

Another branch of the reliability analysis methods relies on the Monte Carlo simulation techniques. Since the main objective of the reliability analysis is the actual determination of probabilities, either of success, safety, or failure, and the objective of the Monte Carlo methods is to determine probabilities, therefore, its applicability to structural reliability seems very appropriate.

The basic principle of **Monte Carlo simulation** is the random generation of a "large" number of samples, N, from the universe of possible outcomes of a specific process, i.e. the failure or safety state of a bar subjected to tension loads. Then the samples are statistically analysed and estimation of the probabilities related to a given event, failure, N_f or safety, N_s, are drawn, as:

$$P_f = \frac{N_f}{N} \tag{1.51}$$

The approach of **Equation 1.51** is known as direct or crude Monte Carlo simulation.

Monte Carlo techniques can also be regarded as methods aimed at the estimation of the value of a multiple integral, **Hamersley and Handscomb (1964)**, of the type

$$\int_0^1 \cdots \int_0^1 \mathbf{R}(x_1,\ldots,x_n)dx_1,\ldots,dx_n \tag{1.52}$$

where $\mathbf{R}$ is a vector valued random function. **Equation 1.52** can be expressed, without loss of generality, as:

$$\int \mathbf{R}(\mathbf{x})d\mathbf{x} \tag{1.53}$$

Equation 1.53 is an equivalent expression for determination of the probability of failure as given by **Equation 1.10**. Comparison of these two expressions reinforce the concept that Monte Carlo methods are applicable to reliability analysis methods. However, one drawback has, until recently, largely constrained the applicability of Monte Carlo techniques. That is, the number of simulations has to be large. The number of simulations can be determined as a function of the accuracy required to estimate the probability of interest. Such accuracy is given in terms of bounds called **confidence intervals**, given by **Kreyszig, (1993)**, as:

$$P(\theta_1 \leq \theta \leq \theta_2) = \gamma \tag{1.54}$$

where P, the probability that an amount of interest, θ, lies between the boundaries θ_1 and θ_2 is equal to γ.

For the case of a normal distribution the boundaries are given by:

$$\theta_{1,2} = \overline{\theta} \pm z_{\alpha/2}\sigma\sqrt{N} \tag{1.55}$$

where $z_{\alpha/2}$ is equal to 1.96 for a 95% confidence interval, θ, is the required probability of failure, N, the number of simulations and σ the standard deviation of the sample. However, σ, cannot be known before performing the actual simulations. Furthermore, θ, the probability of failure is also unknown, therefore it seems more convenient to construct a confidence interval based on a level of error between the actual probability of failure and the estimated one, $\xi = P_f - \overline{P}_f$, then **Equation 1.54** becomes:

$$P\left(-z_{\alpha/2}\sigma < \xi < +z_{\alpha/2}\sigma\right) = 0.95 \tag{1.56}$$

But, σ still remains unknown and different approaches have been suggested to approximate it. Since proper confidence intervals can only be constructed after the actual simulations have been performed, other approaches have been proposed to estimate the initial number of simulations.

Harbitz (1986), suggested that an initial estimate of the number of simulations is:

$$N = 10/P_f \tag{1.57}$$

based on the consideration that N and P_f follow a binomial distribution. If the order of magnitude of the probability of failure is 10^{-5}, then N is equal to 100 000. Previous authors, **Mann, et al. (1974)**, suggested that the number of simulations required for a 95% confidence interval need to be of the order of 10 000 to 20 000. Nevertheless, direct Monte Carlo simulation requires several thousand of repetitions of the experiment. If the experiment requires the analysis of a structure modelled by finite elements, then the cost of the Monte Carlo simulation becomes prohibitively expensive.

Different variance reduction techniques have been proposed in order to concentrate the simulation on the domain of interest, i.e. the failure domain. Several techniques have been investigated. One of such techniques is called **importance sampling**, **Harbitz (1986)** demonstrated that "reasonable" results can be obtained by only 100 simulation. Other approaches include stratified sampling, Latin hypercube sampling, and antithetic variates. A summary of the basic principles and a comparison of their accuracy and efficiency was given by **Schueller, et al. (1989)**.

From the above mentioned techniques, importance sampling is the approach that has received broader consideration. One of the first researchers to propose the method was **Harbitz (1986)**, since then, several applications and variations have also been suggested. **Schueller and Stix (1987)** gave an overview of the method and indicated that it provided new stimulation in the reliability analysis field. **Bucher (1988)** and **Melchers (1989)**, independently, reported that the potential of importance sampling to solve structural system reliability problems is very good. Later **Melchers (1990)** proposed an **adaptive importance sampling** algorithm which increases the efficiency of the importance sampling approach.

The objective of importance sampling is to concentrate the sampling process in the area of interest, close to the design point, $\mathbf{u}^*$. Near this boundary the probability of a given sample point to lay on the failure or safety domain is close to 0.50, if the selected sampling function, $h_V(\mathbf{v})$, is normally distributed and centred at the design point. This characteristic greatly reduces the total number of sample points necessary to obtain an adequate estimation of the probability of failure. However, the dispersion of $h_V(\mathbf{v})$ has to be proposed by the analyst. The mathematical expression of the adaptive importance sampling approach is given by **Melchers (1990)**, as:

$$P_f = \frac{1}{N}\sum_{j=1}^{N}\left\{ I\left[D\colon G\left(\mathbf{v}_j\right) \leq 0\right] \frac{F_X\left(\mathbf{v}_j\right)}{h_V\left(\mathbf{v}_j\right)} \right\} \tag{1.58}$$

Where $I[\cdot]$ is an indicator function $I[\cdot]=1$ if x is in the failure domain, $I[\cdot]=0$ other wise $G[\cdot]$ is the limit state function, $F_X[\cdot]$ is the probability density function of the particular reliability problem and $h_V[\cdot]$ is the importance sampling probability density function.

Since usually the location of the design point is not known *a priori*, this one must be searched for. The objective of the adaptive importance sampling approach is to improve the efficiency of the importance function as information about the failure domain is gathered, by making it possible to position the importance sampling function close to the design point. Also the dispersion of the importance sampling function is reduced as its mean value approaches the design point $\mathbf{u}^*$. A more detailed description of the adaptive importance sampling approach and an algorithm for its application are given in **Section 2.5**.

1.1.6. Implicit Limit States.

In **Sections 1.1.2** and **1.1.3** the principles and basic methods of structural reliability analysis were described. One basic assumption was made for such descriptions, that the limit state function, $G(\mathbf{X})$, is explicitly available in a closed form. However, for many structural engineering problems this function is not easily obtainable. Moreover, many times the response of the structure, failure or safe state, has to be obtained by means of state of the art mechanical modelling methods, such as the finite element method. In these cases the limit state function is available only implicitly. One possible method to deal with these cases is the Monte Carlo simulation, described in the last section. Other approaches available include **sensitivity analysis** and **response surface methodology**.

Haldar and Mahadevan (1995) provided a description of the basic principles of sensitivity analysis. This technique makes use of the different magnitudes of impact that the uncertainty of each basic random variable entering a problem has in the structural response. Variables with small significance, that is the structural response has a small sensitiveness to changes in that particular variable, may be ignored in subsequent deterministic analysis, thus saving computational effort. Three main variations of sensitivity analysis were referred by those authors. The first is based on finite differences, perturbations are applied to each variable and then the corresponding change in structural response is determined by repeated deterministic structural analysis. In the second, classic perturbation methods, which can be based on the chain rule of differentiation, are applied to the to the finite element model elements, stiffness matrix, load vector, displacements vector, etc. In the third method application is based on the iterative perturbation techniques.

Sensitivity analysis can be used in two ways, one is to construct an approximate closed form of the limit state function and the second is to determine the response gradient for direct use in the reliability analysis.

Cruse, et al. (1988) applied sensitivity analysis to produce a computer program, NESSUS, whose main objective is to construct a closed form relationship between the input and output variables, that is the limit state function is approximated in the original space by applying perturbation analysis about the mean values of the basic variables, for later application of reliability analysis methods, i.e. **FORM**, **SORM** methods.

Another approach that makes use of the perturbation theory was suggested by **Beyko and Bernitsas (1992)**. It was called **large admissible perturbations**. It also produces a closed form approximation of the limit state function, in order to solve the reliability analysis problem by means of **FORM** and **SORM** methods.

The second kind of the approaches to implicit limit states, mentioned at the beginning of this section, is the one denominated response surface methodology. The response surface methodology was originally proposed by **Box (1954)**, its application to structural reliability analysis, has been developed over the last ten years.

Among the first applications of response surface methodology to reliability analysis is the one proposed by **Bucher and Bourgund (1990)**. The application of the method as suggested by them consists of the use of a polynomial approximation to produce an equivalent function, $\overline{g}(\mathbf{X})$, which will approach the true limit state surface, $G(\mathbf{x}) = 0$. A polynomial function of the type was proposed:

$$\overline{g}(\mathbf{X}) = a + \sum_{i=1}^{n} b_i X_i + \sum_{i=1}^{n} c_i X_i^2 \tag{1.59}$$

where $i = 1,\ldots,n$ is the number of basic variables.

In order to construct the polynomial of **Equation 1.59** the repeated deterministic analyses of the structùre with the finite element model are necessary. Therefore, one of the main concerns of the response surface methodology as suggested by them is to maintain the number of deterministic analyses as low as possible, without compromising the accuracy of the equivalent function, $\overline{g}(\mathbf{X})$. In such fashion, different approaches have been suggested to construct the response function. These are briefly described in **Section 1.1.7**.

1.1.7. Response Surface Methodology.

The response surface methodology as applied to structural reliability analysis has as its objective the construction of an equivalent closed form polynomial function, $\bar{g}(\mathbf{X})$, in order to approximate the true limit state function, $G(\mathbf{X})$, for cases in which such limit state function is implicit, i.e. the response of the structure can only be obtained by finite element analysis or other sophisticated mechanical modelling methods.

In order to be applicable to the reliability analysis methods, like FORM, SORM, Monte Carlo, simulation, etc., the equivalent function, $\bar{g}(\mathbf{X})$, has to comply with a number of requisites, it:

- must be of a simple mathematical form, in order to maintain a reasonable computational effort in subsequent calculations,
- must be of an explicit closed form,
- should maintain the number of free parameters as low as possible, so as to reduce the number of experiments with the full finite element model, and
- has to be able to approximate the different forms of limit state functions encountered in structural mechanics.

Therefore, a suitable choice for the equivalent function, $\bar{g}(\mathbf{X})$, is a second order polynomial type function, as indicated by **Equation 1.59**. In order to determine the unknown coefficients in this equation, a number of experiments with the mechanical model, i.e. finite element model, are required. The number of terms in the polynomial may be varied, mixed terms may be included or not; however, it should be born in mind that the overall computational effort will be directly affected by any of these choices. Several approaches have been proposed in order to maintain the number of experiments as low as possible, in a systematic fashion. **Bucher and Bourgund (1990)** suggested an interpolation procedure in order to determine $\bar{g}(\mathbf{X})$, which is explained in detail in **Sections 2.3** and **2.4**. The total number of deterministic analyses required to determine the unknown coefficients of **Equation 1.59**, namely:

$$\bar{g}(\mathbf{X}) = a + \sum_{i=1}^{n} b_i X_i + \sum_{i=1}^{n} c_i X_i^2 \qquad (1.60)$$

is $4n+3$, being n the number of basic variables. The accuracy of the equivalent function around the design point is warranted by means of an *adaptive* procedure, which quickly approaches the true design point.

Muzeau, et al. (1993) proposed the use of the **least square method** for the approximation of the response surface. The minimum required number of true values of $G(\mathbf{X})$ is:

$$L = \frac{(n+1)\cdot(n+2)}{2} \qquad (1.61)$$

for the equivalent function:

$$\overline{g}(\mathbf{X}) = a + \sum_{i=1}^{n} b_i X_i + \sum_{i=1}^{n} c_i X_i^2 + \sum_{i=1}^{n-1} \sum_{j=i+1}^{n} d_{ij} X_i X_j \qquad (1.62)$$

On the other hand, the choice of realisations of the basic variables, necessary to determine the unknown coefficients of **Equation 1.62**, has to be a *judicious choice.* Though, the accuracy of the later approach is somehow better than that of **Equation 1.60**, the actual number of experiments with the finite element model cannot be easily known. Indeed, the stability of the solution for $\overline{g}(\mathbf{X})$ depends upon the minimisation of:

$$\sum_{r=1}^{N} \left| Q^{(k)}(X_l^r) - G(X_l^r) \right|^2 \qquad (1.63)$$

where $Q^{(k)}(X_l^r)$ is the *kth* approximation of the actual value of the structural response $G(X_l^r)$, and N is the total number of experiments required.

It is important to recall that the response surface, $\overline{g}(\mathbf{x}) = 0$, is a surrogate of the limit state surface, $G(\mathbf{x}) = 0$, in other words, it is an approximation of the boundary dividing the failure from the safety domain and therefore it defines the limits of integration over the failure domain, **Equation 1.10**. Hence, the particular stochastic properties of the random basic variables, i.e. probability density function, correlation, etc., may be disregarded in the selection of points for interpolation, points at which the actual value of $G(\mathbf{X})$ is required, only second moment information may be utilised. Once the response surface is obtained the influence of different distribution functions and/or correlation effects can be studied, with reduced computational effort, **Bucher and Bourgund (1990)**.

When the required coefficients in **Equation 1.60** are available it is possible to apply well established reliability analysis methods, like **FORM** and **SORM**. **Bucher and Bourgund (1990)**, suggested that the application of the importance sampling technique is feasible. However, the recent developments in advanced Monte Carlo methods, make it feasible the application of adaptive importance sampling. A detailed description of the response surface methodology and the required computer algorithms, including the required ones for adaptive importance sampling, as applied in the present work, are given in **Chapter 2**.

Since the actual limit state function is replaced by an equivalent polynomial approximation some degree of error is introduced in subsequent calculations made with the equivalent function, $\overline{g}(\mathbf{X})$. **Schueller, et al. (1991)** suggested a statistical procedure to quantitatively evaluate the amount of error. On the other hand, they report that response surface methodology is suitable for problems covering **serviceability** and **collapse** failure modes.

The research on the applicability of response surface methodology to structural reliability problems is on progress. **Kim and Na (1997)** proposed the use of vector projection sampling points for construction of the response surface. **Lee, et al. (1993)** reported on the performance of different polynomial approximations used to increase the accuracy of the response surface. Two approaches were proposed and compared, first the number of terms in a polynomial equation of the type of **Equation 1.60** was increased, in the second approach all feasible domain of the basic variables was divided into several sections. Their results seem to confirm that the last approach is the most accurate and efficient.

Muzeau, et al. (1993) reported on the use of least squares method to construct the response function. Their methodology is then applied to the evaluation of standard codes of steel design. However, no comparison or reference to other approaches of response surface methodology was made.

The use of response surface methodology to solve reliability analysis problems of complex structures or structural systems is gaining acceptability. In the field of offshore structures **Lebas, et al. (1992)** reported the application of the response surface methodology to the design of a jacket type structure for the Gulf of Guinea. The reliability analysis of flexible type risers have been covered by **Hanson and Nielsen (1994)** and **Nielsen and Hanson (1995)**, who constructed the response surfaces by means of linear regression and applied this methodology to the determination and study of important basic variables.

1.1.8 .Target Reliability.

The application of structural reliability theory can be performed in two ways; indirectly, through codes, or directly through the structural reliability analysis of special structures such as those having large consequences of failure, i.e. the failure of offshore structures could have a large impact on loss of human life, environmental damage and economic loss. In the first case the results of reliability analysis are implicitly embodied in design codes following the Load and Resistance Factor Design, LRFD, approach. The partial safety factors required in that kind of codes are derived by means of the reliability theory and its methods. In the second case methods such as FORM, SORM and Monte Carlo simulation, as described in **Sections 1.1.3** and **1.1.5** to **1.1.7** have to be applied directly at the design stage or for revision of existing structures. In this instance it is then necessary to count with a predefined reference value of the reliability index or **target reliability index**, which will preserve a desired or an adequate level of safety.

In general terms the definition of target values for the reliability index requires considerations of social and economical character, for many industries, including the offshore oil industry, this is still an ongoing process. This situation is confirmed by the chronology of efforts to introduce reliability based codes in this industry. Det Norske Veritas introduced the use of partial safety factors in its Rules for the Design, Construction and Inspection of Offshore Structures, **DNV (1977)**, and more recently the American Petroleum Institute introduced the LRFD version of the Recommended Practice for Planning, Designing and Constructing Fixed Offshore Platforms, **API RP2A - LRFD, API (1993)**, for optional use.

The literature review carried out for the purposes of this work was not able to find recommended target reliability index values for the particular case of marine risers. However, as a guidance, a resume of some of the suggested or required values for other types of structures is presented here.

One of the earliest recommendations for target reliability levels was given by **Ravindra and Galambos (1978)**, in the context of code calibration for the LRFD approach. They recommended a default value of $\beta = 3.0$ as a general requirement. They pointed out that this value is applicable to components of highly redundant structures, therefore it should not be applied if the consequences of failure are considered to be serious.

Subsequent studies included the influences of failure mode, load combination and consequences of failure.

Madsen, et al. (1986) presented a discussion of the reliability index levels required by the National Building Code of Canada, 1975. These are summarized in **Table 1.1**.

Failure mode	β_0
Yielding in Tension and Flexure	4.0
Compression and Buckling Failure	4.75
Shear Failure	4.25

Table 1.1. Target reliability values required by the National Building Code of Canada, 1975. Data taken from **Madsen, et al. (1986)**.

In the same fashion, **Madsen, et al. (1986)** also presented the requirements of the Nordic Committee on Building Regulations, 1978. These target reliability values are given in **Table 1.2**.

Failure consequences	β_0
Less serious failures consequences	3.1
Common cases	4.265
Very serious failure	5.2

Table 1.2. Target reliability values required by the Nordic Committee on Building Regulations, 1978. Data taken from **Madsen, et al. (1986)**.

Mansour and Wirsching (1996) presented target reliability values provided by an study carried out by **Ellingwood, et al. (1980)**, which included metal, reinforced and pre-stressed concrete and masonry structures. These values, presented in **Table 1.3** were used to developed the American National Standard A-58. Furthermore, such target reliability levels were prescribed for structural members with an expected service life of 50 years.

Member, Limit State	Target Reliability Level (β_0)
Structural steel	
Tension member, yield	3.0
Beams in flexure	3.0
Column, intermediates slenderness	3.5
Reinforced Concrete	
Beam in flexure	3.0
Beam in shear	3.0
Tied column, compressive failure	3.5
Masonry, unreinforced	
Wall in a compression, uninspected	5.0
Wall in a compression, inspected	7.5

Table 1.3. Target reliability levels proposed by **Ellingwood, et al. (1980)**, as presented by **Mansour and Wirsching (1996)**.

Reed and Brown (1992) prepared a summary of the target reliability index values required by the American Institute of Steel Construction LRFD specifications for structural members with an intended service life of 50 years. These values are presented in **Tables 1.4**.

Structural Type	Target Reliability Level (β_0)
Metal structures for buildings (dead, live, and wind loads)	2.5
Metal structures for buildings (dead, live, and snow, and earthquake)	1.75
Metal structures for buildings (dead, live, and snow loads)	4 to 4.5
Reinforced concrete for buildings (dead, live, and snow loads)	
* ductile failure	3
* brittle failure	3.5

Table 1.4. Target reliability levels for steel structures, after **Reed and Brown (1992)**.

The design rules of the **Eurocode No. 3, (1989)**, Design Steel Structures, require the target reliability levels indicated in the **Table 1.5**, for structures with a reference period of 50 years.

Reference period 50 years Safety class	Ultimate limit states P_f	β_f	Serviceability limit states P_f	β_f
reduced safety	-5.10^{-4}	3.3	-16.10^{-2}	1.0
normal safety	-7.10^{-5}	3.8	-7.10^{-2}	1.5
increased safety	-8.10^{-6}	4.3	$-2.3\cdot 10^{-2}$	2.0

Table 1.5. Target reliability values required by the **Eurocode No. 3, (1989)**.

!n order to covert the values of β_f for a reference period of $T_f = 50$ years to another reference period T_2 the following formula is indicated by the **Eurocode No. 3, (1989)**:

$$\beta_2 = \Phi^{-1}\left[\Phi(\beta_f)^{T_2/T_f}\right] \tag{1.64}$$

were Φ the standardized normal distribution and $\Phi(\beta_f)$ is the safety probability for the period T_f.

Concerning the marine and offshore industries **Thayamballi, et al. (1987)** reviewed the suggested target reliability levels for Tension Leg Platforms, TLP, and other offshore structures and compared them with values found for other types of structures. These values are presented in **Figure 1.12**.

Mansour and Wirsching (1996) presented a thorough revision of the target reliability index with the aim to make recommendations for floating structures. Among the target reliability levels summarized by them are the recommendations of A.S. Veritas Research, branch of Det Norske Veritas, these are presented here in **Table 1.6**.

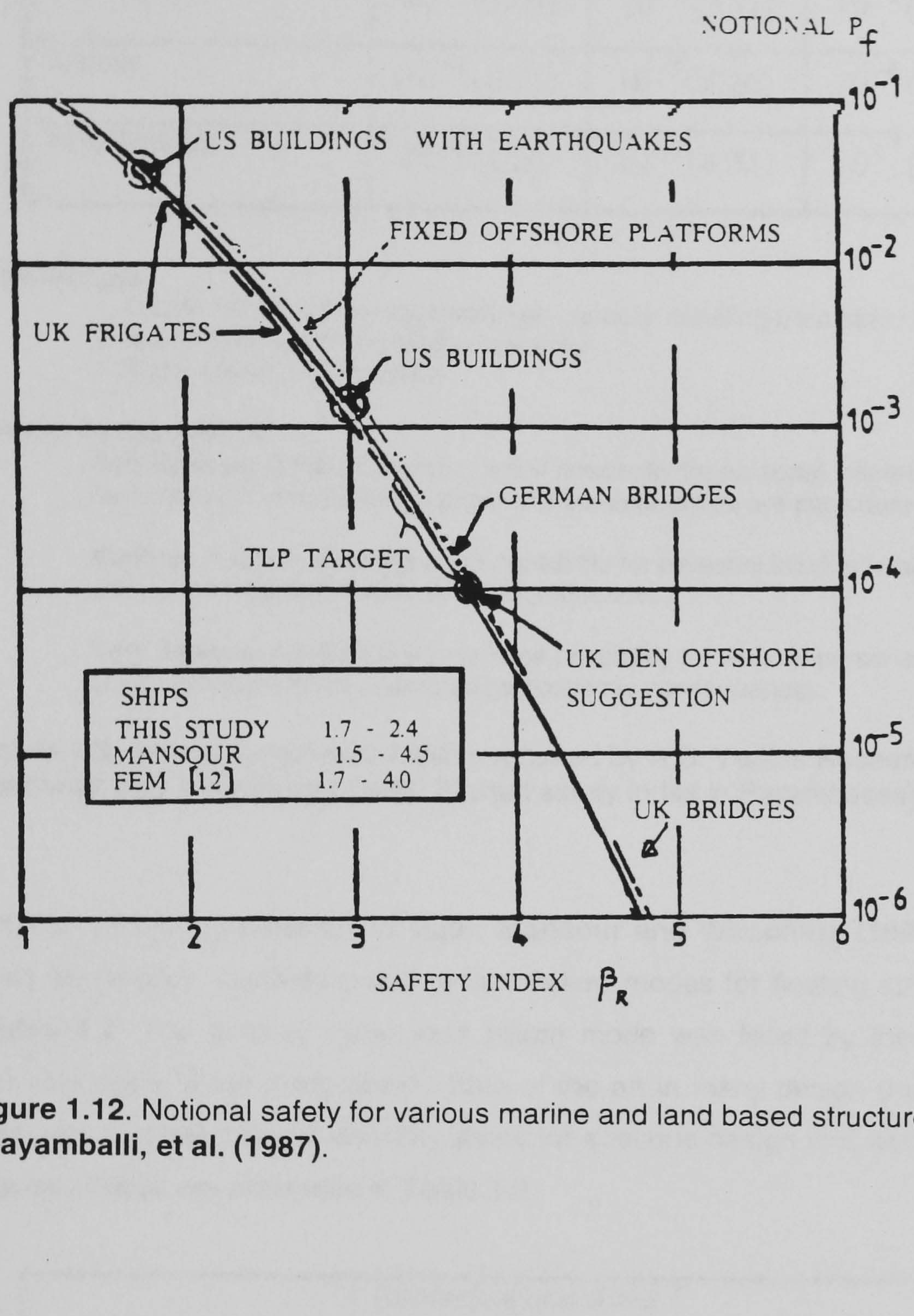

Figure 1.12. Notional safety for various marine and land based structures after **Thayamballi, et al. (1987)**.

	Failure Type		
Failure Consequences	1	2	3
Non Serious	$10^{-3}(3.09)$	$10^{-4}(3.71)$	$10^{-5}(4.26)$
Serious	$10^{-4}(3.71)$	$10^{-5}(4.26)$	$10^{-6}(4.75)$
Very Serious	$10^{-5}(4.26)$	$10^{-6}(4.75)$	$10^{-7}(5.20)$

Failure Type

1. Ductile failure with reserve strength capacity resulting from strain hardening.
2. Ductile failure with no reserve capacity
3. Brittle failure and instability

Failure Consequences:

Non Serious. A failure implying small possibility for personal injuries; the possibility for pollution is small and the economic consequences are considered to be small.

Serious. A failure implying small possibility for personal injuries/fatalities or pollution or significant economic consequences.

Very Serious. A failure implying large possibility for several personal injuries/fatalities or significant pollution or very large economic consequences.

Table 1.6. Annual Target probabilities required by A.S. Veritas Research, as resumed by **Mansour and Wirsching (1996)**, (Target safety index in Parentheses).

As a conclusion of the aforementioned study, **Mansour and Wirsching (1996)** proposed target safety levels for primary, secondary and tertiary failure modes for floating structures, presented here in **Table 1.7**. The primary initial yield failure mode was listed by them because it was considered necessary, since it represents state of the art in many design practice. In the same fashion they also proposed target reliability levels for a fatigue design and were considered to be life time values. These are presented in **Table 1.9**.

Failure mode	Consequences of the Failure	β_0
Primary (initial yield)		5.0
Primary (ultimate)	Very serious	4.0
Secondary	Serious	3.0
Tertiary	Not serious	2.5

Table 1.7. recommended target reliability levels for floating structures, after **Mansour and Wirsching (1996)**.

Category	Description	β_0
1	A significant fatigue crack is not considered to be dangerous to the crew, will compromise the integrity of the structure, will not result in pollution; repairs should be relatively inexpensive	1.5
2	A significant fatigue crack is not considered to be immediately dangerous to the crew , will not immediately compromise the integrity of the structure, and will not result in pollution; repairs will be relatively expensive	3.0
3	a significant fatigue is considered to compromise the integrity of the structure and put the crew at risk and/or will result in pollution. Severe economic and political consequences will result from significant growth of the crack	3.5

Table 8. Recommended target reliability index for fatigue design, after **Mansour and Wirsching (1996)**.

On the other hand, for the case of structures with large economic consequences of failure i.e. offshore structures, it has been proposed that the target reliability levels can be established on the basis of economic value analysis or social considerations, or a combination of both.

Concerning the approach based on economic considerations only, **Bea (1990)** proposed the following criteria:

$$\beta_m = \left[-\ln \frac{1.83}{(PVF)(CR)} \right]^{0.625} \qquad (1.65)$$

where β_m is the target reliability index value, PVF is the present value of unit annual cost uniformly distributed in time and discounted over T years (design life). CR is the ratio of expected cost of the platform loss of serviceability (cost of failure CF) to the cost needed to decrease the likelihood of the platform loss of serviceability by a factor of 10, $CR = CF/\Delta C$.

Mansour and Wirsching (1996), pointed out that in theory, the economic value analysis approach would be the preferred method, it is however impractical because of the data requirements of the model.

Flint, et al. (1977) proposed the following formula as a "rational target total risk of failure", based on a social criteria:

$$P_{f_t} = \frac{10^{-4} K_S T}{n_r} \qquad (1.66)$$

where P_{f_t} is the probability of failure due to any cause during the design life T. The average number of people within or near the structure during the period of risk is n_r. The social factor, K_S, given in **Table 1.9**, represents the level of risk which the society would be unprepared to pay for increasing the safety.

Nature of Structure	K_S
Places of public assembly, dams	0.005
Domestic, office, trade and industry	0.05
Bridges	0.5
Towers, masts, offshore structures	5

Table 1.9. Social criterion factor, K_S, after **Flint et al. (1977)**.

Stahl (1986) extended the above cited criteria of **Flint, et al. (1977)** in order to include more detailed economic considerations:

$$P_a = \frac{C}{[EQCF + (\nu\eta_r^2/K_S)]PVF} \qquad (1.67)$$

For a detailed explanation of the terms in this expression refer to **Appendix 4**.

Basically the terms of **Equation 1.67** relate economical and social aspects with the target probability of failure. On the economical area the total cost of failure and effects of devaluation are accounted for. The social issues are considered in the same fashion as in the criteria established in **Equation 1.66**.

1.2. Marine Riser Analysis.

1.2.0 .Generalities.

Exploitation of offshore oil and gas fields requires a large variety of facilities. A platform or deck above the sea surface where drilling or production equipment is installed and operated, raw materials stored and services for crew allowed. On the sea bed, a subsea wellhead and a blow out prevention stack or a production tree are placed. The link or communication between the sea bed equipment and above sea surface facilities is the ***riser***. In the particular case of drilling operations the riser provides a passage for the drill string as well as drilling fluids.

Drilling may proceed from a fixed or a floating platform. If a fixed platform is used the riser is attached to its structural elements. Because of this kind of support the sea loads on the riser are minimized and in every case transferred to the subsea structure of the platform. In these conditions the functions of the riser are reduced mainly to those of a conduit and therefore this type of riser is customarily called the ***conductor***. Other type of drilling or production operations demand the use of a floating platform. In this case the loads which the riser must withstand become of a different nature. On its ends the riser is fixed to the sea bed equipment and to the floating platform, without any possible provision for support in mid water, thus, the sea hydrodynamic loads must be entirely resisted by the riser. Furthermore, the sea surface motion and currents also induce horizontal displacements or excursions of the floating vessel, which must be followed by the upper end of the riser This second class of riser is known as a ***marine riser***.

A marine riser is comprised of a number of elements which are aimed to provide stability and to reduce the amount of stresses imposed to it by sea surface and floating vessel motions. **Sheffield (1980)** provided a description of the physical elements of a typical marine riser, as shown in **Figure 1.13**. The ***riser joints*** are pipe sections connected one after another to form the main riser body, the kill and the choke lines are usually integrally attached to the riser joints. A riser ***tensioner*** is required to provide stiffness to the riser which otherwise would be unstable since the bending stiffness provided by the steel pipe alone is insufficient to prevent excessive deflection and buckling. Tension demands increase proportionally with depth, hence in deep water the tensioning equipment is subjected to high loads that may lead to elevated stresses and excessive wear at the upper sections of the riser. For these reasons ***buoyancy modules*** are some times attached to the riser at different depths, they provide additional buoyancy and reduce the requirements of applied top tension. Syntactic foam elements or steel cans are the most common type. A ***telescopic*** or ***slip joint*** is installed at the top of the riser. Its purpose is to compensate for the heave of the vessel, by allowing physical extension of the riser body and thus helping to minimize tension variations. The ***lower ball joint*** permits the riser to rotate about the equipment fixed on the seabed and thus compensates for vessel static offset as well as surge and sway without imposing significant stress to the riser body.

An ***upper ball joint*** is optionally installed to allow for rotation, in order to decrease the stress caused by riser motion at the transition of stiffness that occurs between the telescopic joint and the riser body.

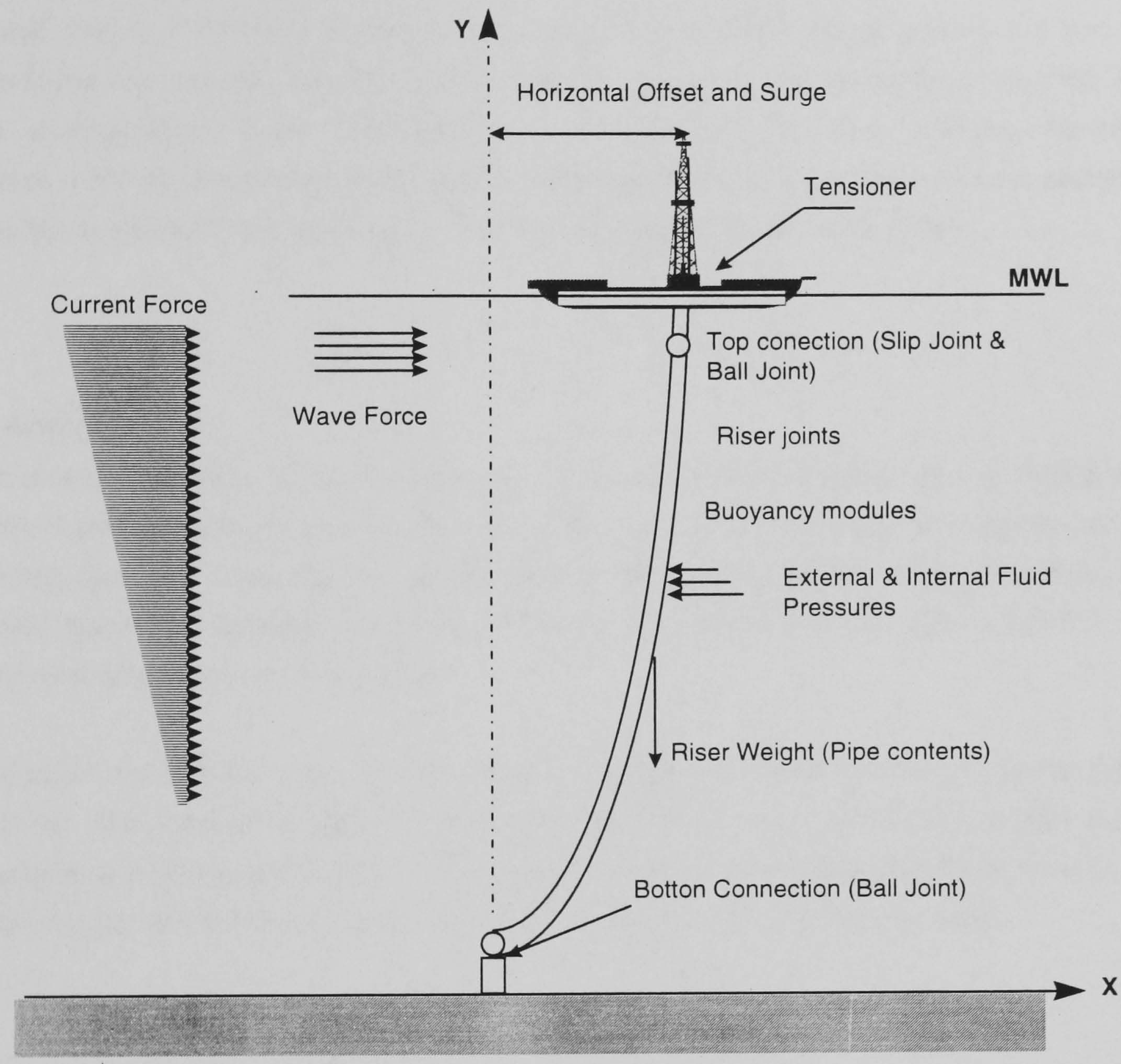

Figure 1.13. Elements of a typical marine riser, after **Sheffield (1980)**.

1.2.1. Methods of Marine Riser Analysis.

Marine risers similar to the one described in the previous section have been in use since the introduction of floating drilling. The analysis procedures have evolved from the static to the dynamic analysis, according to the needs of water depth and environmental conditions. The characteristic slenderness of the riser makes it highly dependent on externally applied tension in order to avoid excessive bending stresses or buckling collapse. In spite of its apparently simple shape the riser is a nonlinear hydroelastic analysis problem. **Chiu (1992)** pointed out that the severity of the nonlinearities depend on the structural and motion characteristics of the riser and on the considerations made regarding the fluid surrounding it. Riser analysis, therefore possesses a variety of important problems. This situation is confirmed by the numerous analytical approaches published in the literature, as it will be portrayed in the following review.

Static Analysis:

A static analysis by means of power series was carried out by **Fischer and Ludwing (1966)**, who demonstrated the importance of externally applied tension in order to provide an adequate control of bending stresses. They also recognized the importance of possible dynamic effects, but suggested that if riser diameter was kept to a minimum at water depths of 1000 ft. (304.8 m.) or less, dynamic effects would not be critical.

Current loads and floating platform offset constitute a static load in a number of riser analyses procedures. The dynamic analysis is sometimes performed on a particular statically stable configuration and others are carried out in conjunction with the static case. Therefore, most of the research dealing with the static analysis is treated in conjution with the dynamic case.

Dynamic Analysis:

As exploration and production of oil moved into deeper waters, concerns for the dynamic behavior of marine risers became more important. Many Different approaches have been introduced to study the dynamic behavior of the rigid marine riser, the literature is extensive and the present review will concentrate in some of the representative work.

The natural frequencies of the marine drilling riser were investigated by **Daering and Huang (1976)** with the aim to study the effects of various parameters on such frequencies such as the fluid surrounding the riser, internal fluid (drilling mud) and variations of top tension along the riser due to gravity. The differential equations of motion were solved by a method of power series. It was concluded that riser tension was one of the main parameters defining the natural frequencies.

Daering and Huang (1979) applied modal analysis to the problem of riser vibration. The nonlinear hydrodynamic load term was linearized, based on the principle of energy equivalence. The main conclusion was that the first five modes of vibration are enough to determine riser stresses for engineering purposes.

A time domain finite element method capable of consideration of surface vessel motion, nonlinear stiffness of intermediate ball joints and hydrodynamic excitation of a periodic wave was presented by **Gardner and Kotch (1976)**.

Time domain is the most flexible of the dynamic analysis techniques. It can accommodate nonlinear effects of material and hydrodynamic load nature. Random excitation can also be studied with time domain methods. The response needs to be calculated at different time steps, therefore a long computer time is usually required. Considerations about the particular technique to define the necessary time step are of fundamental importance in terms of cost of the analysis. Many other works treating the time domain analysis of marine risers have been reported. Since they deal mainly with nonlinear aspects and introduction of random excitation a number of typical works are mentioned in this section.

On other hand, the frequency domain approach to dynamic analysis results in great decrement of computational time. In frequency domain analysis the steady state response of the system can be usually found in a close form. It has been recently demonstrated that in some cases accuracy comparable to time domain solutions can be achieved with frequency domain analysis, **Basu (1995)**. For this reason, since the early studies of marine riser dynamic behavior important research efforts have been dedicated to the formulation and application of the frequency domain analysis techniques.

One of the first published works on riser dynamic analysis is due to **Burke (1974)**, in which the fourth order differential equation of motion is reduced to a series of first order differential equations and then integrated numerically by a fourth order Runge Kuta method. The analysis presented in the frequency domain for a steady state response, included linearization of the drag term by equating the work done by the non-linear form and the one of a proposed linear expression, or the *principle of energy equivalence*.

Young, et al. (1978) used a “variable increment” finite difference formulation in the frequency domain to find the steady state response of the riser. Random and regular waves were included. Vortex shedding effects were claimed to be introduced, (though, no details of such effects on the riser behavior were given). A particular characteristic of this model is that no scheme for Morison’s load linearization was applied. One of the most important definitions given by them is, perhaps, the ***effective tension*** on the riser, that is the effects of internal and external pressures on the total tension acting along the riser.

One of the main concerns in the frequency domain analysis is the effects of the linearization technique applied on both accuracy of the results and computational effort. **Spanos and Chen (1980)**, employed the *equivalent linearization* technique to linearize Morison's drag term, including also current effects. Their model is based on the finite element method and they also produced a geometric stiffness matrix which takes into consideration the effective tension as well as the weight effects. The proposed equations of motion were solved iteratively for the steady state response. Later, **Spanos, et al.(1990)** presented an extension of the above mentioned work in order to account for a harmonic variation of the applied top tension by means of time averaging.

A linearization procedure based on the *describing function technique*, from the Theory of Control, was given by **Krolikowski and Gay (1980)**. The differential equation of motion was linearized and the forcing function expanded in a Fourier series in order to derive a closed form algebraic solution. This approach were applied to the cases of regular wave and wave plus current. The *statistical linearization* technique was used for the cases of random wave only and random wave plus current. The input was considered as a sum of sinusoidal waves so that the Fourier expansion technique was applicable. It was not specified which technique was used for the spatial discretization of the system. The results obtained for the frequency domain analysis were compared to the time domain ones. The authors stated that their method is nearly as accurate as the time domain.

In the same direction of efforts devoted to improve the linearization procedures applied in the frequency domain analysis, **McIver and Lunn (1983)** presented an approach based on the one due to **Krolikowski and Gay (1980)**; however, in addition to the linearization of the drag term, **McIver and Lunn (1983)**, introduced the linearization of wave forces which are calculated at the displaced position of the riser and also considered the variation of the riser wet surface at the surface of the wave. The results obtained with the later technique were compared with those from the time domain and the ones due to **Krollikowski and Gay (1980)**. **McIver and Lunn (1983)** stated that the new linearization technique renders results closer to the ones of time domain than those obtained with the method of **Krollikowski and Gay (1980)**. A limitation in the technique of **McIver and Lunn (1983)** is that only regular wave cases can be analyzed.

Patel and Sarohia (1984) presented a finite element frequency domain approach, consistent with the schemes proposed by **Burke (1974)** and **Young, et al. (1978)** in the sense that the current effects together with the horizontal offset of the floater are considered mainly a static effect. Furthermore, the non-linear effects due to large deflections were introduced at the stage of the static analysis, which was performed by applying incrementally an "effective lateral load" The boundary displacement due to platform offset was also applied incrementally until a stable static configuration was reached, the stiffness matrix was updated at each of the increments. The dynamic analysis was then applied at a second and separated stage using the final configuration from the static analysis and considering loads from the harmonic oscillations of top boundary and the wave particle motion. The total response of the riser was found by the superposition of the static and dynamic effects. The linearization scheme employed for the drag term is the same as the one given by **Burke (1974)**. The results of this approach were compared against time domain results and other commercial riser analysis programs.

The most common approach to frequency domain analysis is to linearize the drag term. One solution was offered by **Basu (1995)** in the frequency domain that fully takes into account the non-linearity of the relative velocity drag term in Morison's equation. His approach was based on a finite difference model and by means of a Fast Fourier transforming algorithm interactively found an "effective load" for a chosen number of harmonics from a periodic wave. The riser response was sought for each of those harmonic loads, which were finally added in order to determine the total response. The approach includes dynamic response of risers under current, regular waves, boundary motion and variations of wetted surface at the sea level. It was stated by **Basu (1995)** that this approach is capable of matching the accuracy of "the best time domain solution".

Random Analysis:

Tucker and Murtha (1973) performed a frequency domain non-deterministic analysis of a riser subjected to random wave spectrum loading. The model was based on finite differences and the modal superposition method was used, therefore the drag term had to be linerized. However, difficulties associated with the inclusion of vessel motion and the non-linear drag limited the applicability of this method.

Another approach to the random dynamic analysis was presented by **Westing (1983)**, who determined the riser response by numerical time domain simulations. A unidirectional Pierson-Moskowitz spectrum was discretized into a finite number of randomly phased components in order to generate correlated time series of wave particle kinematics and riser top motion. With this procedure the wave surface elevation, riser top motion and wave particle kinematics were simulated as random Gaussian processes. Expressions for the normalized cumulative probability distribution function of Morison's load were given for the special case of narrow band Gaussian sea state. Then, short term extreme peak predictions were made and the structural integrity against first excursion failure was assessed for a northern North Sea riser.

Kirk (1984), applied a linearized spectral analysis method and a single wave linearized frequency domain analysis in order to compare peak values of riser bending moment against peak values estimated from the root mean square (**rms**) values rendered by the spectral analysis. The linearization procedure was based on the principle of energy equivalence. The solution method was based on the Galerkin/modal method in which the differential equation of motion was solved by assuming that the total response was given by the superposition of a number of shape functions or normal modes. As a result values for the ratio of mean peak value to rms were proposed for risers with non-resonant modes and for deep water risers with one or two resonant or near resonant modes.

Nonlinear Analysis:

A number of schemes have been reported dealing with different aspects of marine riser non-linearities. **Huang and Chucheepsakul (1985)**, presented a method for the static analysis of a riser experiencing large displacements. Their method utilized the stationary condition of the functional representing the energy and work of the riser system.

Kokarakis and Bernitsas (1987) applied a time-incremental algorithm on a riser discretized by finite elements, the proposed model used Morison's equation to compute hydrodynamic loads and Newmark method was used for the time domain analysis. The three dimensional non-linear behavior due to hydrodynamic load, torsion and distributed couples, inertia forces and varying axial tension was investigated on a riser initially vertical with a circular cross section

Boubenider (1992) developed a three noded cylindrical beam finite element, an axial hybrid finite element and an axial-torsional hybrid element, in order to account for large displacements and rotations, as well as axial-torsion-bending coupling. The non-linear hydrodynamic loads were evaluated on the current configuration of the riser and the dynamic analysis was performed in the time domain. Results and performance from other commercial programs were used to compare his results.

A three dimensional time domain dynamic analysis of marine risers was presented by **Modi, et al. (1994)**. Large deflections and rotation of the riser were included. Shear effects are considered in the analysis by means of Timoshenko beam theory. Internal flow was also taken into account. Geometric non-linearities caused by rotation and non-linear terms in the strain-displacement relations were taken into account. A Lagrangian formulation approach were used to derive the differential equations of motion which were solved by a "predictor-corrector" algorithm. The conclusions stated by **Modi, et al (1994)**, are that according to their study the ocean current loading is a static force and forces exerted by ocean waves are the main external excitation source to the marine riser, though it was not mentioned how this last effect compared with boundary imposed displacements.

In view of the above discussion it is judged convenient, at this stage, to adopt the frequency domain approach for the finite element model of the marine riser, since it can provide a mechanical model with a reasonable computational effort, yet accurate enough to provide dependable results.

1.2.2. Comparative Studies and Riser Analysis Validation.

As showed in **Section 1.2.1** the number of approaches used to analyze the marine riser problem is significant. In fact, it is so numerous that comparative studies have been required in order to assess their applicability and accuracy.

Comparative studies:

Chakrabarti and Frampton (1982) reviewed the main formulations of twenty six riser analysis computer programs and pointed out differences of them in respect to non-linear drag terms, effective tension, buoyant weight and riser contents. However, no numerical comparison among them was performed.

Validation of riser analysis schemes:

Despite the considerable number of riser analysis approaches, validation of these is most commonly performed against other analytical approaches, i.e. frequency domain vs. time domain. A limited amount of work appears to have been published in relation tothe validation against experimental or full scale test of risers.

Egeland and Solli (1980) compared the results of six different computer programs against a set of full scale data. Both time domain and frequency domain schemes were included with either regular or irregular sea waves and varying degrees of nonlinearities considered. The authors provided information on the sensitivity of these schemes relative to each other. However, they stated that they found it difficult to compare absolute values of measured and computed responses due to high sensitivity of riser response to current and platform motion.

Patel and Sarohia (1982) compared the results of a two dimensional finite element model of a riser against results from scale tests. A riser to a scale of 1:23 in a 7.6 m. deep tank was used and measurements of wave elevation, platform surge, and in-line and transverse displacements as well as bending stresses at several locations along the riser length were collected. The experimental data showed that significant transverse displacement and bending stresses were introduced by vortex shedding. Therefore, recommendations were given in order to introduce these effects in the theoretical riser model.

Verbeek (1983) performed a measurement campaign on several risers located in different North Sea fields. The measured stress at the wave active zone were compared against theoretical predictions based on both analytical solution methods and numerical time domain simulation techniques. It was concluded that the measurements were "in-line" with results based on the generally accepted model of **Nordgren (1982)**, which does not take into consideration longitudinal dynamic response, torsional response or large angular motions. He noted that the approach followed in the measurements campaign does not permit detailed verification.

Results of another campaign of field measurements were presented by **Cook and Gardner (1985)**. Though their objective was not to validate or calibrate any particular riser analysis model it was mentioned that the model of **Krollikowski and Gay (1980)** was considered for comparison with experimental data. The main conclusion from this work is that the riser tension system is able to induce bending excitation due to angular deviation between the riser longitudinal axis and the applied top tension.

1.2.3. Marine Riser Reliability Analysis.

Reliability analysis of a kind of marine risers, namely flexible risers, have been recently published. This tendency appears to have been driven by the need of long term operation of floating production systems in increasing water depths.

At present, reliability analysis appears to be concentrated on the flexible riser type. Flexible risers are made of a composite pipe section which allows for significant bending radius. Some of the characteristic configurations of flexible risers include free hanging, lazy and steep S as well as lazy and steep wave. **Jiao (1992)**, carried out a research on a limit state design criteria applied to flexible risers and concluded that the present safety factor format rendered "very different" safety levels.

Hanson and Nielsen (1994) made extensive use of the response surface approach for the reliability based design of flexible risers. The response surfaces were constructed by means of linear regression. Their studies indicated that the important parameters with respect to probability of failure are the stiffness of the bending stiffener, wave height and accuracy of the vessel positioning system.

Nielsen and Hanson(1995) applied the same response surface approach to an specific riser design, and concluded that the basic variables defining the riser capacity accounted for more than 90% of the probability of failure in certain cases.

These publications highlight the significance of reliability based design applied to a kind of marine risers as a means of improved safety assessment. An important subject regarding rigid marine risers, the safety assessment by recent techniques of reliability based design, seems to have received scarce or possibly no attention in the published literature.

1.3. Fatigue Reliability Analysis.

1.3.0. Generalities.

One of the most important failure models in structural design is fatigue. This failure mode has been the subject of numerous research works, mainly because fatigue is characterised by failure at an stress level below the maximum working one specified by design and usually with little or no warning, therefore with possible catastrophic consequences, as it has unfortunately happened, i.e. Alexander Kieland disaster.

The principal mechanism leading to fatigue failure is the initiation and propagation of cracks in the structure, as a consequence of fluctuating stress levels. Such stress oscillations are due to the cyclic nature of the load processes, such as wind and wave, which in turn induce a dynamic response of the structure. Therefore, offshore structures are sensitive to fatigue failure, specially if the structural behaviour is predominantly dynamic, as in the case of slender or deep water structures. The basic fatigue mechanism is aggravated by a number of factors, the presence of surface manufacturing defects, particularly at welds, stress concentrations due to poor design or fabrication details, significant residual stress, corrosive environment, etc.

Prediction of fatigue life can be made by a number of techniques. The probabilistic description of the sea surface by spectral methods is now a days the most frequently adopted method. In relatively recent years the reliability approach has gained major acceptability and its implementation for the fatigue analysis has been suggested for code safety checks, **Wirsching (1984)**. In the following sections description a of the basic principles defining the most accepted approaches is presented.

1.3.1. The S-N Approach to Fatigue Analysis.

The analysis of fatigue has been dominated by two main techniques, the S-N curves and the fracture mechanics approach.

The S-N curves is the classic approach to fatigue. It is characterised by the use of the so called S-N diagrams, which relate the fatigue life, in number of cycles to failure, N, to the constant cyclic stress range, S, at which such failure is attained. The S-N diagram is obtained by subjecting a number of smooth specimens up to fatigue failure at different levels of stress range. The results are plotted in a log-log format and a curve is fitted by the least squares or linear regression methods. Commonly the S-N curve presents a linear trend which is expressed by:

$$NS^m = K \tag{1.68}$$

where:

N, number of cycles to failure at a constant stress range,

S, stress range,

m, and K, empirical constants defined by the least square analysis of laboratory data.

One of the main characteristics of the S-N diagram is that they are subjected to a very significant statistical scatter, as depicted in **Figure 1.14**, thus reflecting the large uncertainty in the parameters involved and the difficulties associated with its modelling. **Wirsching (1995)** indicated that typical coefficients of variation for laboratory test to define the cycles to failure, N, ranges from 30 to 150%.

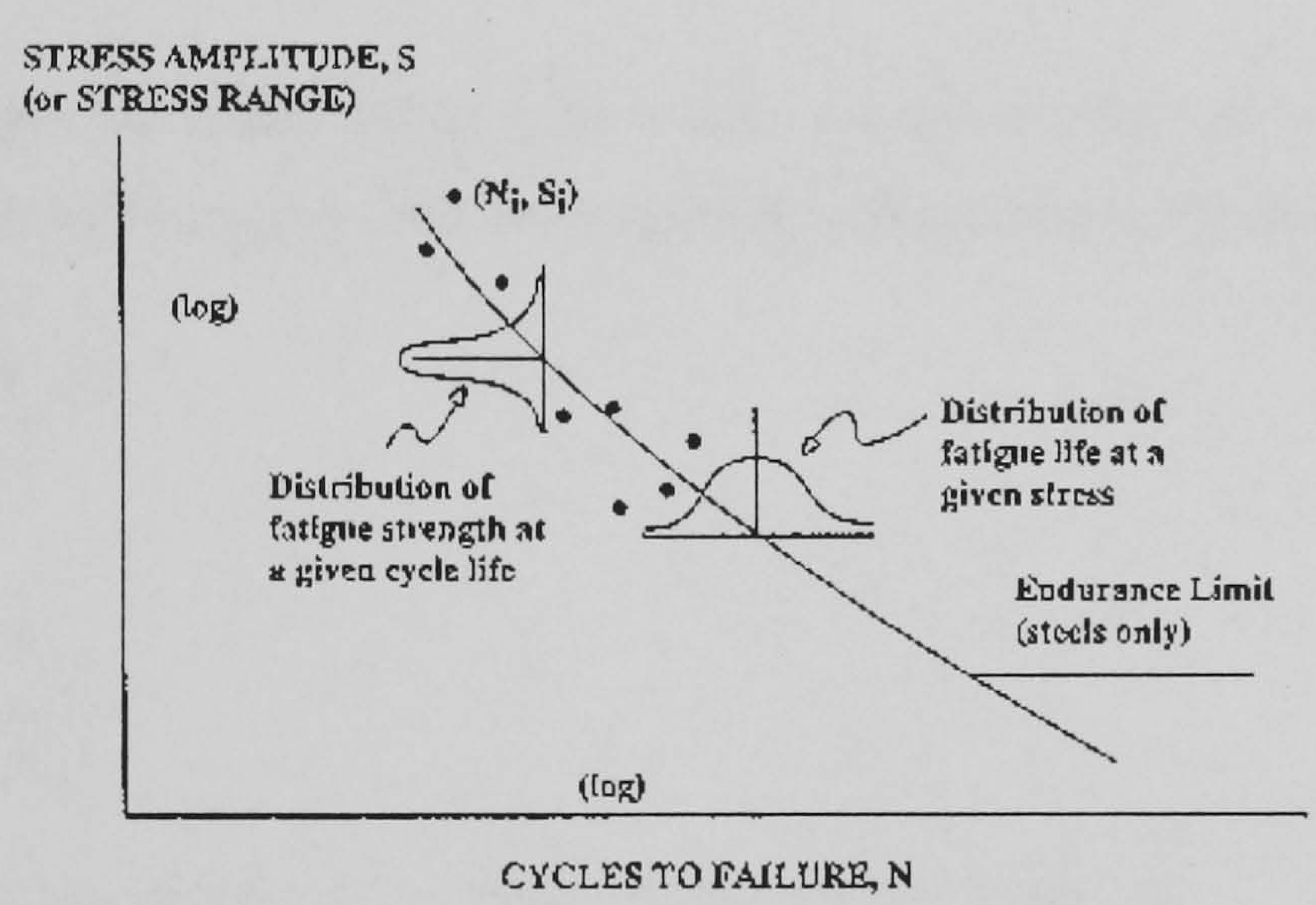

Figure 1.14. A typical S-N curve and characteristic uncertainty, after **Wirsching (1995)**.

Nevertheless, the S-N diagram have been the basic tool for fatigue life prediction. Since “failure” is generically defined, the S-N diagrams can by used to relate stress to either crack initiation or total fatigue failure. The Department of Energy, **DOE (1984)**, indicated that when selecting an S-N curve a definition of failure is implicitly considered, customarily the through the wall crack used in the laboratory for the fatigue experiments.

The S-N diagram is used to predict the structure’s life by comparison of the intended service life, N_S, with the number of cycles, N, at which failure occurs for the constant stress range at which the component is operating. Structures are more commonly subjected to a variable amplitude of stress range, due to the random nature of load, therefore the response of the system, the stress range, will also be random. The problem of random fatigue is complex since the sequence of stress variation or stress history may be of importance, specially when the difference between adjacent cycles is large. On the other, hand fatigue data is given in the form of S-N diagrams for constant amplitude stress range, **Miner (1945)**, neglecting the effects of load sequence, proposed a model in which the damage sustained by the component over a period of time for a given constant stress range is accumulated and added to the damage incurred at other stress ranges, mathematically:

$$D = \sum_{i=1}^{n} \frac{N}{N_{F_i}} \tag{1.69}$$

where:

D, total cumulative damage,

i, number of different stress ranges, $i = 1 \ldots n$,

N, number of cycles sustained at ith stress range,

N_{F_i}, number of cycles to failure at ith stress range.

The cumulative damage rule of **Equation 1.69** is also known as Palmgren-Miner, since a similar rule was propose before by Palmgren, **Wirsching (1995)**. **Equation 1.69** can be expressed as:

$$D = \sum_{i=1}^{N} Di \tag{1.70}$$

where:

$$D_i = \frac{N_{T_i}}{N_{Fi}} \tag{1.71}$$

N_{T_i}, total number of cycles in time T, at the constant stress range, S_i,

N_{Fi}, number of cycles to failure at constant stress range, S_i,

Furthermore, Miner's rule states that at failure when $N_T = N_F$ and $D = \Delta = 1$.

Therefore, the cumulative damage can be expressed as:

$$D = \sum_{i=1}^{n} Di = \Delta = 1 \tag{1.72}$$

By introduction of **Equation 1.68** into **Equation 1.70**, damage can be expressed now as:

$$D_i = \frac{N_T}{K} S_i^m \tag{1.73}$$

Furthermore, if the average frequency of stress cycle is defined as:

$$f_\circ = \frac{N_T}{T} \tag{1.74}$$

where:

N_T, number of stress cycles in period T.

Then the expression for fatigue damage, **Equation 1.71** can be written as:

$$D_i = \frac{f_o T}{K} S^m = \frac{T}{K}\Omega \tag{1.75}$$

where:

$$\Omega = f_o S^m \tag{1.76}$$

is defined as the stress parameter.

Two main methods are currently in use to determine the value of the stress parameter, the first is the deterministic and the second is the so called probabilistic or spectral method. Before describing these methods, it is convenient to indicate that the sea surface variation is more realistically described by a wide band random process; however, it is widely accepted that the assumption of a narrow band process or transformation of it into a narrow band process, is considered valid for engineering purposes.

The sea state surface is a long term non stationary process and it is well accepted that for short periods of the time, between three to six hours, the sea surface remains as a stationary process, with stationary statistical properties, therefore a long term non stationary sea surface can be described as a set short term stationary processes with a Gaussian probability distribution.

It is now possible to return to the description of the methods employed for determination of the stress parameter, **Equation 1.76**.

In the deterministic approach, the data from the time history is used to define a significant wave height, Hs, and average wave period, Tz, for each of the stationary processes describing the long term sea state. Then each set of Hs and Tz can be used in a deterministic fashion to determine the stress at the fatigue sensitive points of the structure. Another common procedure, **Cronin, et al. (1978)**, is to construct a curve of stress range versus wave height and divide it into regimens of stress range ΔS_i:

$$\Delta S_i = S_i - S_{i-1} \tag{1.77}$$

represented by the average stress range:

$$S_{iav} = \frac{S_i + S_{i-1}}{2} \tag{1.78}$$

is used to represent the constant stress range required for a comparison with the S-N diagram. On the other hand, from the wave exceedence diagram the number of wave occurrences for each selected stress range S_{iav} are obtained. Finally Miner's rule can be applied in order to assess the fatigue life of the structure.

In the probabilistic or spectral method the stress parameter is determined using the statistical information contained in each of the short term sea states defining the environmental condition.

Using Fourier analysis techniques, the time series corresponding to a given short term sea state is represented by superposition of a number of sinusoidal components, and presented as a frequency spectrum in which the ordinate at a particular frequency is the variance of the component sinusoidal wave. The units of the ordinate are (quantity)^2 per unit frequency and since power is directly related to the variance such frequency spectrum is customarily referred to as power spectral density function, W^{nn}. The response of a structure to a spectral load is also an spectral quantity and the response is related to the input load by the so called transfer function:

$$S^{RR}(\omega) = \left|H_F(\omega)\right|^2 W^{nn}(\omega) \tag{1.79}$$

where:

$\left|H_F(\omega)\right|^2$, transfer function, and

$S^{RR}(\omega)$, power spectral density of stress.

The transfer function is found by analyses carried out in the frequency domain, and applying the stochastic linearization technique to the non-linear terms. If the transfer function of **Equation 1.79** is linear the stress peaks will conform to a probability distribution that can be derived theoretically from the spectral bandwidth, a parameter which defines the type of process as narrow or wide band. Furthermore, for a narrow band Gaussian process, as can be assumed in most cases, the response will confirm to a Raleigh probability distribution function, **Cronin, et al. (1978)**, which is defined by the root mean square value of such process, σ, equivalent to the standard deviation of a distribution function. Therefore, with the response quantity given by a Raleigh distribution the stress parameter is given by:

$$\Omega = \left(2\sqrt{2}\right)^m \Gamma\left(\frac{m}{2}+1\right)\sum_{i=1}^{n}\gamma_i f_i \sigma_i^m \tag{1.80}$$

f_i, mean zero cross frequency of the wave loading in the sea state,

γ_i, fraction of time of occurrence of the ith sea state,

σ_i, root mean square of the stress process in the ith sea state,

Γ, the gamma distribution

m, material constant

n, number of sea states

1.3.2. The Fracture Mechanics Approach to Fatigue Analysis.

The fracture mechanics approach has become one of the most accepted methods to estimate the fatigue life. This method takes into consideration the fact that structures unavoidably posses flaws, such as a cracks, at the time that they start their service life. Defects are many times due the characteristics of the fabrication process, i.e. welding, rolling, etc. Usually such small surface defects lead to cracks at the earliest application of the load. Therefore the fracture mechanics developed expressions that relate the crack growth rate per cycle of load applied, da / dN, to changes in the stress intensity factor, ΔK. The relationship developed by **Paris and Erdogan (1963)** is the most frequently adopted one:

$$\frac{da}{dN} = C(\Delta K)^m \tag{1.81}$$

where:

a, crack length,

N, number of cycles,

ΔK, stress intensity factor range,

m, C, are material constants.

The m and C constants are obtained from laboratory data in a similar manner as for the S-N curves.

The stress intensity factor range, ΔK n is plotted as a function of crack growth rate, da / dN; therefore this data is subjected to an important degree of variability or statistical scatter, due to material properties and experimental techniques used. **ASCE (1982)** reports that coefficients of variation in da / dN may approach 50% due to laboratory techniques while the scatter due to material properties is represented by coefficients of variation in da / dN of 0.15 to 0.25%.

The stress intensity factor is computed by linear elastic fracture mechanics and is usually expressed as a function of the crack geometry:

$$K = Y(a)S_f\sqrt{\pi a} \tag{1.82}$$

where:

$Y(a)$, geometry function, which takes into account the crack geometry and specimen shape,

S_f, far-field stress due to applied load,

therefore:

$$\Delta K = Y(a)\Delta S_f\sqrt{\pi a} \tag{1.83}$$

Substitution of **Equation 1.83** in the Paris-Erdogan law, **Equation 1.81**, then separation of the variables and integration results in:

$$\frac{1}{C}\int_{a_o}^{a}\frac{dz}{Y(z)^m\left(\sqrt{\pi a}\right)^m}=N_T\Delta S^m \qquad (1.84)$$

where:

a_o, initial crack size,

a, crack size at the end of period T under the stress range ΔS,

N_T, number of cycles in period T.

Introducing **Equation 1.74** in **Equation 1.84** then becomes,

$$\frac{1}{C}\int_{a_o}^{a}\frac{dz}{Y(z)^m\left(\sqrt{\pi a}\right)^m}=Tf_oS^m = T\Omega \qquad (1.85)$$

Equation 1.85 was derived for the variable amplitude stress range where the final size of the crack, at time T, is compared against a critical size, if the failure criterion corresponds to the most common S-N failure criteria, the through the wall crack.

The stress parameter, $\Omega = f_oS_i^m$, corresponds to the deterministic case of the fracture mechanics approach to fatigue and it is the same as in **Equation 1.76**. Similarly as in the S-N approach Ω can be found by probabilistic spectral analysis, namely **Equation 1.80**.

1.3.3. Fatigue Reliability Analysis.

As mentioned before, the characteristic S-N data is subjected to a large degree of uncertainty. Similarly, the required data in the fracture mechanics approach, $da\,/\,dN$ - ΔK, is subjected to an important degree of variability.

On the other hand the spectral approach to sea surface description makes evident the probabilistic properties of the sea environment. Therefore, the application of the structural reliability methods, seems appropriate to treat the fatigue phenomenon.

The structural reliability problem, determination of the probability of failure or associated reliability index, β, requires the determination of a limit state function, given by **Equation 1.13**, namely:

$$G(X) = M = S - L = S(X_A) - L(X_B) \qquad (1.86)$$

where S and L represent the strength and load variables respectively. X is a vector of random variables, S and L may also depend on a number of basic variables.

For the S-N approach the above limit state can be expressed as:

$$G(U,V) = R(U) - S(V) \qquad (1.87)$$

where R is the fatigue strength at life N_S and S is the stress range. This approach is used for the constant amplitude stress range high cycle fatigue, **Wirsching (1995)**.

If Miner's rule is introduced, **Equation 1.87** becomes:

$$G(X) = \Delta - \sum_{i\in(H_Z,T_Z)} D_i \le 0 \qquad (1.88)$$

where failure occurs when the accumulated damage sustained by the structure, D, is larger than the total damage at failure, Δ. If Miner's rule is applied to the problem of finding the fatigue reliability, at a required service life, N_S, of a structure subjected to a random load, the limit state proposed by **Wirsching (1995)** is:

$$G(X) = N(X) - N_S \qquad (1.89)$$

With the limit state given by any of three previous expressions it is possible to apply any of the reliability analysis methods, FORM, SORM, etc., in order to determine the reliability coefficient. However, in this case it is possible to derive a closed form expression for the limit state depending on two variables only. Considering that both variables conform to a Normal distribution the Cornell reliability index, **Equation 1.14**, is applicable. If the random variables are considered to be longnormally distributed then the format proposed by **Rosenblueth and Esteva (1972), Equation 1.25** is pertinent.

Wirsching (1984) developed a closed form solution for the reliability index, following the S-N approach and Miner's rule. He adopted the longnormal format on account of his experimental data suggesting that the number of cycles to failure, N, confirms to such distribution. Departing from **Equation 1.75**, namely:

$$D = \frac{T}{K} = \Omega \tag{1.90}$$

and expressing it in terms of the time to fatigue failure, when $D = \Delta$, then:

$$T = \frac{\Delta K}{B^m \Omega} \tag{1.91}$$

The random variable B was introduced in order to account for the inaccuracies and uncertainties in the fatigue stress parameter. Therefore, T is also a random variable and the probability of fatigue failure is:

$$P_f = P(T \leq T_S) \tag{1.92}$$

where T_S is the intended service period. Then the applicable limit is:

$$G(X) = T(X) - T_S$$

Following the lognormal format **Wirsching (1984)** found that:

$$\beta = \frac{\ln\left(\tilde{T}/T_S\right)}{\sigma_{\ln T}} \tag{1.93}$$

where: $\tilde{T}$, the median value of T is given by:

$$\tilde{T} = \frac{\tilde{\Delta}\tilde{K}}{\tilde{B}^m \Omega} \tag{1.94}$$

and the standard deviation of T is:

$$\sigma_{\ln T} = \ln\left[\left(1 + C_{\Delta}^2\right)\left(1 + C_K^2\right)\left(1 + C_B\right)^2\right]^{1/2} \tag{1.95}$$

As indicated before the stress parameter, Ω, can be evaluated by the deterministic approach, **Equation 1.76** or spectral method, **Equation 1.80**.

The most significant contribution of **Wirsching (1984)** is perhaps the introduction of a random variable to account for all the inaccuracies in the fatigue stress range estimation. He suggested that the variable random variable B can be divided as follows

$$B = B_M \cdot B_S \cdot B_F \cdot B_N \cdot B_H \tag{1.96}$$

where the subindices stand as follows: M, fabrication an assembly operations, S, sea state description, F, wave load predictions, N, nominal loads, H, estimation of hot spot stress concentration factors. However, it is of paramount importance to mention that the uncertainty variable, B, is a surrogate for estimation of the uncertainty, it does not explicitly account for uncertainty in variables entering the mechanical model of the structure, i.e. the finite element model, such as stiffness, hydrodynamic coefficients, etc. In other words, the mechanical model is considered deterministic, with the exception of the environmental variables. Moreover, this characteristic can be clearly observed in the spectral relationship between load and stress, **Equation 1.79**, namely:

$$S^{RR}(\omega) = \left|H_F(\omega)\right|^2 W^{nn}(\omega), \tag{1.97}$$

where the response to a spectral load becomes also spectral, but the transfer function remains deterministic. A comparison with the reliability method presents an important difference, while the reliability approach intends to consider the random nature of all the variables involved in the structural model, $G(X)$, the fatigue reliability approaches, up to the moment, have only taken into consideration the random nature of the sea surface, load, and the fatigue model variables.

The approach to fatigue reliability suggested by **Wirsching (1984)**, has also been followed for derivation of the limit state and closed form solutions for the reliability index in the connection with the fracture mechanics approach. **Skjong (1995)** proposed the following limit state,

$$G(X) = \int_{a_o}^{a_i} \frac{dz}{Y(z,\mathbf{Y})^m \left(\sqrt{\pi a}\right)^m} - CT\Omega \tag{1.98}$$

with terms already defined in **Equation 1.85** The random variable $\mathbf{Y}$ is a vector of random parameters to account for uncertainties in the calculations of ΔK, in the same fashion as B in the **Equation 1.94**.

The approach suggested by **Wirsching (1984)**, namely, the introduction of one random variable to account for uncertainties in the variables rendering the stress, has been largely adopted during the last decade and used amply in the published literature, for instance: **Ximenes (1991)**, **Jiao and Moan (1992)**, **Hu and Chen (1993)**, **Zimmerman and Banon (1994)**, **Fang and Xu (1995)**.

1.3.4. Riser Fatigue Reliability Analysis.

The fatigue reliability analysis of a rigid steel drilling riser was reviewed by **Souza and Goncalves (1997)**, proposing the following limit state function:

$$G_S(X) = \Delta - \frac{1}{K} \cdot \sum_{j=1}^{h} P_j \cdot \left[\sum S_{a_i}^m\right]_j$$

where:

Δ, critical cumulative damage at which failure occurs, Miner's rule,

K, material constant from the S-N diagram,

$\left[\sum_i S_{a_i}^m\right]_j$ sum of stress amplitudes, for each load condition j during riser's life,

P_j, probability of occurrence of an environmental load during the structure's life,

with Δ, K_S and $\left[\sum_i S_{a_i}^m\right]_j$ considered random variables.

The sum of stress amplitudes $\sum_i S_{a_i}^m$ was found from the time domain analysis, in contrast with the more common assumption that if the sum is sufficiently large the uncertainty associated with it is small and could be written as $E\left[N_{T_i}\right]E\left[S_{a_i}^m\right]$,with $E[\cdot]$ standing for expected value. Furthermore, they considered the sum of stress amplitude to conform to a generalised gamma probability distribution function, with a mean value given by:

$$E\left[S_{a_i}^m\right] = \frac{1}{\lambda^m} \cdot \frac{\Gamma\left(b + \frac{m}{c}\right)}{\Gamma(b)}$$

where b, c and λ are generalised gamma parameters, and standard derivation given by **Crandall (1958)**:

$$\frac{\sigma\left[\sum S_{a_i}^m\right]_j}{E\left[\sum S_{a_i}^m\right]_j} = \left[\frac{f_1(m)}{\xi\left(\frac{n_S}{T_S}\right)T}\right]^{1/2}$$

where:

$f_1(m)$, function tabulated by **Crandall (1958)**,

ξ, damping coefficient.

The reliability index was then found by means of FORM.

Souza and Goncalves (1997) indicated that their approach is more complex that the one suggested by **Wirsching (1984)**; however, it is not clear how the first authors accounted for the uncertainty in stress range estimation, other than the uncertainty related with the environment.

They concluded that their procedure is more complex and complete than the one proposed by **Wirsching (1984)** on account that the stress distribution is modelled as a wide band process, the non-linearities of the riser dynamic behaviour are included through time domain analysis and the sum of stress amplitude is modelled as a random variable, giving, therefore, "more conservative results about the fatigue life".

It is important to notice that in the same way as in all of the approaches found in the literature review performed by this author, the approach of **Souza and Goncalves (1997)** does not consider uncertainty in the variables involved in the mechanical model itself; that is, randomness is accounted for in environment and S - N curve model only.

SUMMARY, Chapter 1.

The basis underlying the structural reliability analysis were summarized. Particularly, the mathematical foundations for the definition of the reliability index were given and a number of techniques for its determination reviewed, including analytical, iterative and simulation. The main limitation of the present reliability analysis methods is that an explicit and closed form function defining the limit state surface is required. Usually, for the case of structures that demand modeling by sophisticated techniques, such as finite elements, the limit state surface is given only in an implicit form. There exists, however, a few approximation techniques that can provide a surrogate of such surface, one of them is the Response Surface Methodology.

A literature review on the subject of marine riser analysis was presented. A number of frequency domain dynamic analysis approaches have been published because they can offer reasonably good accuracy at a low computational cost, as compared to the time domain approaches. Results from non-linear analysis models demonstrate that there exist a number of areas in which research is necessary, namely vortex shedding and its interaction with in-line dynamic displacements, the degree of sensitivity of riser response to current and platform motion and the relative significance of wave particle or floater motion as sources of dynamic excitation. Few experimental studies exist to compared or validate the analytical approaches. Validation of theoretical models against experimental or full scale test is very limited in the publicly available literature. However, those few studies confirm the need for research and extension of the present theoretical models in order to cover the already mentioned areas.

Concerning the reliability analysis of offshore structures by means of Response Surface techniques, this is very limited, in the particular case of the marine riser it also appears that very few studies have been published, all of them treating the reliability of the flexible riser. The linear regression approach to response surface methodology was the technique used.

In view of the above and with the objective of performing the reliability analysis of a steel marine riser, the Response Surface Methodology is selected for the approximation of the limit state surface. The subsequent reliability analysis will be performed by means of advanced Monte Carlo techniques. Concerning the finite element model of the riser it is judged convenient at this stage to adopt the frequency domain approach because it can provide a mechanical model with a balance between accuracy and computational effort appropriate for the purposes of investigating the applicability of the selected response surface technique to the reliability analysis.

The current methods for fatigue life estimation were found to be the S-N curves and the Fracture Mechanics approach; the S-N curves method in conjunction with the spectral description of the sea surface are the one most commonly used methods. The reliability approach to fatigue was also reviewed. The limit states for this type of failure have been developed considering that only the variables related to the fatigue model contain uncertainty. The uncertainty associated with the stress range determination is concentrated, somehow artificially, in one variable that accounts for uncertainties in fabrication and assembly operations, sea state description, wave load predictions and nominal loads. The fatigue reliability of a rigid type marine riser was found published. The main characteristic of this approach is that the uncertainty in stress is assumed to be accounted for by means of a time domain analysis; however as in all the approaches to fatigue reliability found in the literature review, the system variables, variables entering the finite element model, i.e. stiffness, are considered deterministic.

CHAPTER 2. RESPONSE SURFACE MODEL.

2.0. Generalities.

As was outlined in **Section 1.1.7.** the objective of response surface methodology is to produce an equivalent and explicit closed form expression, $\overline{g}(\mathbf{X})$, that approximates the true, but unknown, limit state function, $G(\mathbf{X})$. The equivalent function will enable us to proceed with the reliability analysis by means of any of its methods. Therefore, this section is devoted to the description of the model utilised in this work to construct the response surface.

2.1. Link Between the Response Surface and the Finite Element Model.

One of the constraints of structural systems reliability is the difficulty in obtaining a *failure interaction model* capable of taking into consideration all the mechanical interactions and effects of redundancy that exist in a complex structural system. The effects of such overall interactions upon any particular component or on the whole structure can presently be modelled with a very good degree of accuracy by techniques such as the finite element method. The actual impact of all the structural interactions on the reliability analysis methods is that the limit state function usually exists in an implicit and non closed form, which is not suitable for application of the reliability analysis methods.

The link between the reliability analysis requirements and the state of the art mechanical modelling techniques can be obtained through the response surface methodology. The aim of the response surface methodology is to provide systematic methods to obtain a closed form equivalent transfer function, $\overline{g}(\mathbf{X})$, able to relate in a simple mathematical form the response of the system with its input variables, while taking into consideration the complex interactions that occur in it.

2.2. Response Surface Methodology.

When the value of the response depends upon a number of variables, X_i, i.e. the basic variables, then, there exist some function, g, which relates those variables with the response, and can be expressed as:

$$g(X_1, X_2, \dots X_k) = \eta \qquad (2.1)$$

where η is the response of the system and the transfer function g is called the true **response function, Khuri and Cornell (1987).** If the response function is continuous and smooth, then it can be represented by a polynomial of degree n. Furthermore, such polynomial expression can be represented by a hypersurface, when $\eta = 0$, **Equation 2.1** is called the **response surface.**

On the other hand, in **Section 1.1.1** it was defined that the limit state equation is found when the limit state function reaches values of zero for particular realisations of the basic variables, that is:

$$G(\mathbf{x}) = 0 \qquad (2.2)$$

Equation 2.2 is a transfer function that relates the loading and system variables, $\mathbf{X}$, to the response of the system. and establishes a boundary between the failure and safety domains, as exhibited in **Figures 1.4** and **1.5**. By comparison of **Equation 2.1** and **2.2** it can be observed that it is possible to represent the mechanical behaviour of a structural system by means of a response surface.

Therefore, the objective of the response surface methodology applied to the structural reliability analysis problem is to produce an equivalent or transfer function, $\overline{g}(\mathbf{X})$, that will permit the determination of the failure or safety state of the structure, upon input of a set of values of the basic variables, $\mathbf{X}$.

2.3. Construction of the Response Function.

The construction of the response or equivalent function, $\overline{g}(\mathbf{X})$, is accomplished by means of experimentation with the structural system. The determination of the response by means of the deterministic finite element model to a given set of values of the basic variables is considered as one experiment. The objective of any response surface methodology scheme is to control or minimise the number of experiments required for determination of the response function to a desired level of accuracy. A brief description and comparison of a number of approaches aimed at this objective was presented in **Section 1.1.7**. The approach to be utilised in the present work is the one suggested by **Bucher and Bourgund (1990)**.

The response function must be expressed by a simple mathematical form, yet it has to be able to describe with enough accuracy the behaviour of the structure. Such mathematical simplicity is required for keeping the computational efforts needed within reasonable bounds, at two stages, first for construction of the response function itself, and second to maintain applicability of reliability analysis techniques, such as Monte Carlo simulation. An adequate choice is a polynomial expression, which is simple in mathematical terms and capable of representing the different forms of limit states usually encountered in structural reliability analysis. The particular polynomial adopted for the present work is the one suggested by **Bucher and Bourgund (1990)**:

$$\bar{g}(\mathbf{X}) = a + \sum_{i=1}^{n} b_i X_i + \sum_{i=1}^{n} c_i X_i^2 \qquad (2.3)$$

It should also be noted that **Equation 2.3** is a second order approximation of the safety margin, $G(\mathbf{X})$, as expressed by **Equation 1.13**.

The equivalent function, $\bar{g}(\mathbf{X})$, is to be constructed by adaptive interpolation. An experimental region is set by establishing a hypercuboidal region, centred at the point of mean values, $\mathbf{x} = \bar{x}_i$, and bounded by "centroids" at the medians of the hypercurbe. **Figure 2.1** shows this definition of the experimental region for the case of two basic variables.

The distance from the centre of the hypercurbe to the centroids is given as:

$$x_i = \bar{x}_i \pm f_i \sigma_i \qquad (2.4)$$

where σ is the standard deviation of the *ith* variable and $\bar{x}_i$ the corresponding mean value and f_i is an arbitrary factor. The choice of numerical value for f_i will depend on the shape of the limit state surface, if it is not smooth different values of f_i might be needed. A second factor affecting the selection of f_i is that this must be chosen so as to provide input values compatible with the limits of the particular load and mechanical finite element models, i.e. no negative wave periods or natural frequencies may be allowed.

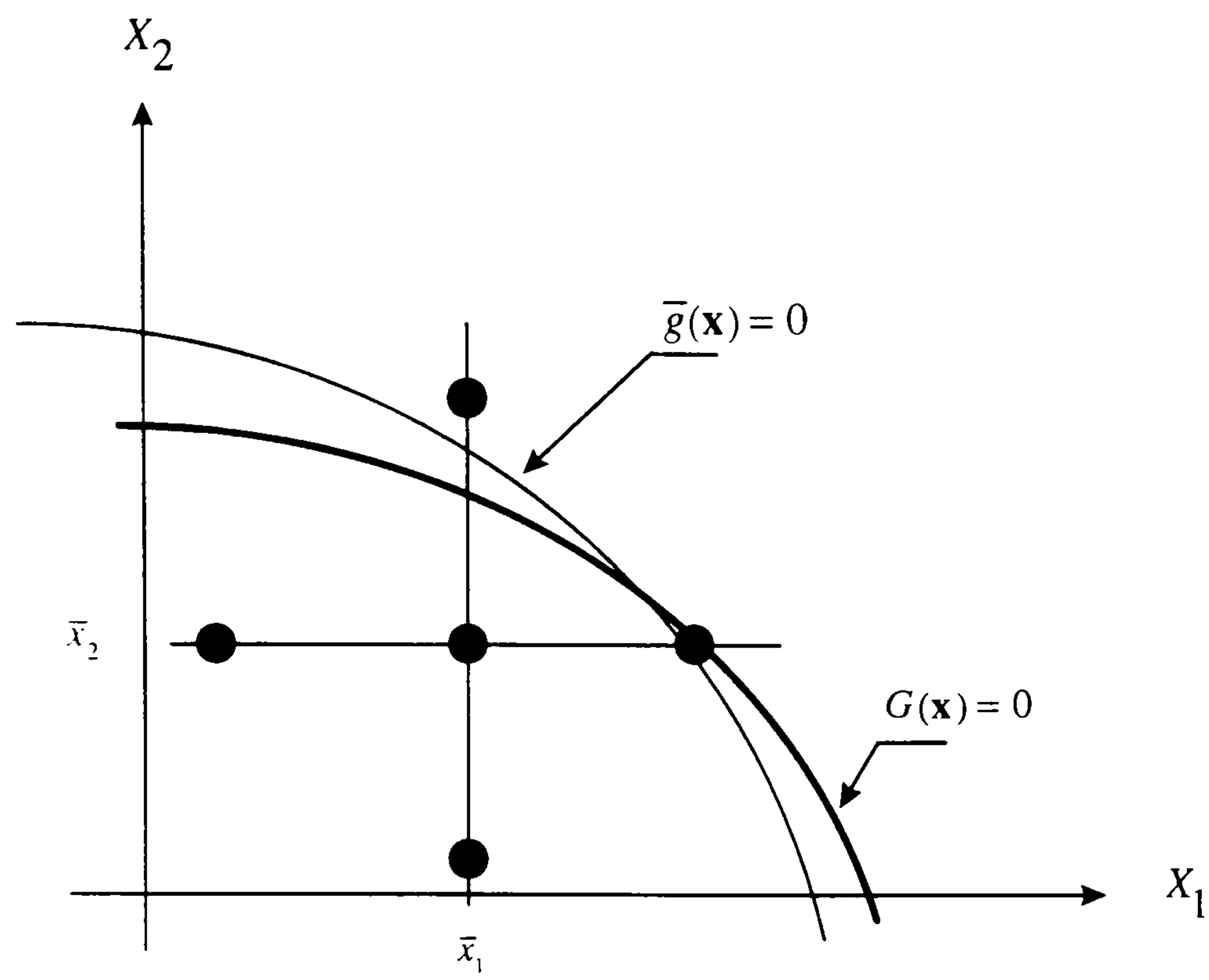

Figure 2.1. First approximation of the response surface centred on the mean values, after **Bucher and Bourgund (1990)**.

The objective of the interpolation process is to determine the coefficients a_i, b_i and c_i in **Equation 2.3.** With this aim it is necessary to establish a linear system:

$$[x_{ii}]\begin{Bmatrix} a_i \\ b_i \\ c_i \end{Bmatrix} = \{G(\mathbf{x})\} \qquad (2.5)$$

The vector $\{a_i, b_i, c_i\}^T$ is the vector of unknown coefficients. Each centroid in **Figure 2.1** represents an actual value of the response of the system, $G(\mathbf{x})$, for the particular realisations of the basic variables at those points. The matrix x_{ii} contains the sets of realisations of the basic variables at the selected centroids in the experimental region. Solution of **Equation 2.5** yields the unknown coefficients.

The number of experiments required to construct the transfer function, i.e. the response function as displayed in **Figure 2.1**, is equal to:

$$2n+1 \qquad (2.6)$$

where n is the number of basic variables. **Equation 2.6** represents the number of points at which the actual response, $G(\mathbf{x})$, given by the finite element model has to be provided.

2.4. The Role of the Design Point.

Equation 2.3 is an approximation of the true, but unknown limit state function, $G(\mathbf{X})$, and it is the main interest of the reliability analysis methods to count with an accurate expression of the equivalent limit state surface, $\bar{g}(\mathbf{x}) = 0$. Therefore, some means are required by which the accuracy of the response surface can be enhanced.

Since the design point defines the region of maximum contribution to the probability of failure, see **Section 1.1.2**, it is appropriate thus that one improves the accuracy of the response surface locally, at the design point. **Bucher and Bourgund (1990)** proposed a simple yet very efficient adaptive approach to improve the accuracy of the response function at this location.

First, the response surface is determined following the procedure given in **Section 2.3**. However, at the end of this stage it is not known how well the obtained equivalent function represents the true limit state function. Therefore, this first approximation of the response function will be denoted $\bar{g}_1(\mathbf{X})$. Now, in order to increase the accuracy of $\bar{g}_1(\mathbf{X})$, a new centre point, closer to the limit state surface than the point of mean values will be obtained in the following manner. With the assumption that all basic variables are uncorrelated and with the second moment information available it is possible to obtain an estimation of the design point, $\mathbf{x}_1^*$, using $\bar{g}_1(\mathbf{X})$. The required estimation of the design point can be accomplished by means of FORM, SORM, Monte Carlo simulation or any of the reliability analysis algorithms available, which were described in **Section 1.1.3**. The iterative FORM algorithm of **Hasofer and Lind (1974)**, as presented in **Appendix 4**, will be applied here for that purpose, when convergence of this method is not attained, the Adaptive Importance Sampling method, to be described in **Section 2.5**, will be used.

This first estimation of the design point will be used only with the purpose of finding a new centre point in the experimental region. This new centre point, which will cover regions in the failure domain that could not be reached before, will be used for a second application of the interpolation procedure already described in **Section 2.3**, see **Figure 2.2**. Therefore, a refined approximation of the response function, $\bar{g}(\mathbf{X})$, is to be found in this way. The required new centre point is determined by interpolation on a straight line running from the vector of mean values, $\bar{\mathbf{x}}$, to the first estimation of the design point, $\mathbf{x}_1^*$, that is:

$$\mathbf{x}_{\mathrm{M}} = \bar{\mathbf{x}} + \left(\mathbf{x}_1^* - \bar{\mathbf{x}}\right)\frac{G(\bar{\mathbf{x}})}{G(\bar{\mathbf{x}}) - G\left(\mathbf{x}_1^*\right)} \tag{2.7}$$

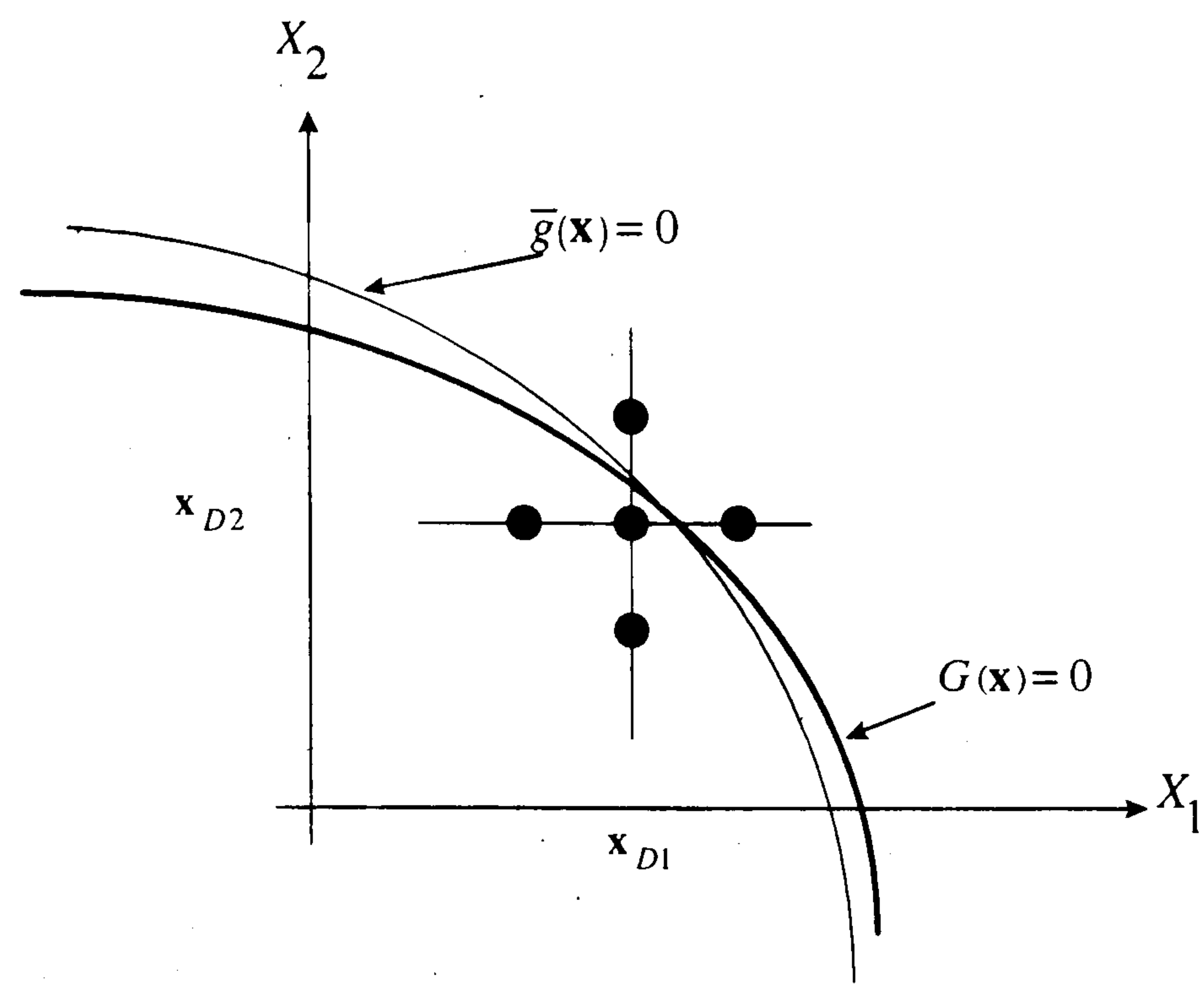

Figure 2.2. Second approximation of the response surface centred on the estimated design point, after **Bucher and Bourgund (1990)**.

Since the interpolation procedure is applied two times and additionally one more true response of the structure is required in order to satisfy **Equation 2.7**, the total number of experiments required by the adaptive response surface procedure is:

$$4n+3 \tag{2.8}$$

The algorithm used for the computer implementation of the above described procedure is presented in **Appendix 5**.

Now that the response function, $\bar{g}(\mathbf{X})$, has been obtained it is possible to proceed with the reliability analysis, i.e. the determination of the probability of failure, by means of any of the methods described in **Sections 1.1.3** and **1.1.5**, that is FORM, SORM or Monte Carlo methods. **Bucher and Bourgund (1990)** suggested the use of the advanced Monte Carlo technique called **Importance Sampling**. However, the progress recently achieved in this area make it possible to apply the **Adaptive Importance Sampling** method, which will be described in the following section.

It most be noted, however, that the approach adopted here for construction of the response function, **Bucher and Bourgund (1990)**, is not always guaranteed to produce the required result, on account that on some instances the system of equations generated may be nearly singular, as it occurs in one of the cases attempted in the riser fatigue reliability, see **Section 6.3**. Though it is recognised by **Bucher and Bourgund (1990)** that the values of f_i, **Equation 2.4**, are arbitrary and may be significant if the limit state surface is not smooth, no guidelines so as its selection were provided.

2.5. Determination of the Probability of Failure.

With the limit state surface given in an approximate but explicit closed form by the response surface, $\overline{g}(\mathbf{x})=0$, it is possible to apply the reliability analysis, i.e. determination of the probability of failure, by any of the reliability analysis methods, FORM, SORM, Monte Carlo simulation , etc.

Some degree of error is introduced by FORM and SORM methods, because the actual curvature of the limit state surface is approximated by these methods as a first or second order hypersurface. The accuracy can be improved by the use of advanced Monte Carlo simulation techniques, and since simulations are made with the response function, $\overline{g}(\mathbf{X})$, the required computational effort is not excessive. Furthermore, **Harbitz (1986)** concluded that the technique called **importance sampling** is able to produce adequate results with "a few hundreds of simulations". More recent advances produced the **adaptive importance sampling** method, **Melchers (1990)**. The later technique is applied here to determine the probability of failure.

Importance sampling is one of the Monte Carlo simulation techniques aimed to reduce the variance of the sample by concentrating the sampling points in the domain of interest, i.e. the failure domain. This is accomplished by introducing an *importance sampling* probability density function, $h_{\mathrm{V}}(v)$, placed over the region of importance, v.

The probability of failure is given by **Equation 1.10**, namely:

$$P_f = \int_{G(\mathbf{X})\le 0} f_{\mathbf{X}}(\mathbf{x})d\mathbf{x} \tag{2.9}$$

Now, an *indicator function* will be introduced:

$$I\left[D\colon G_i(\mathbf{x}\le \mathbf{0})\right]=1 \tag{2.10}$$

where $G_i(\mathbf{x})$ is the *ith* realisation of the limit state function. The indicator function , I, discriminates if a value of $G_i(\mathbf{x})$ belongs to the domain of failure, D, for which $I=1$, or to the safety domain, for which $I=0$. Introducing **Equation 2.10** in **2.9**, the later becomes:

$$P_f = \int \cdot\cdot_x \cdot\cdot \int I[\cdot] f_{\mathbf{X}}(\mathbf{x})d\mathbf{x} \tag{2.11}$$

At this time the importance sampling function, $h_{\mathrm{V}}(v)$, is introduced in **Equation 2.11**:

$$P_f = \int \cdot\cdot_x \cdot\cdot \int I[\cdot]\frac{f_{\mathbf{X}}(\mathbf{v})}{h_{\mathrm{V}}(\mathbf{v})} h_{\mathrm{V}}(\mathbf{v})d\mathbf{v} \tag{2.12}$$

The approach of the importance sampling technique is graphically presented in **Figure 2.3**.

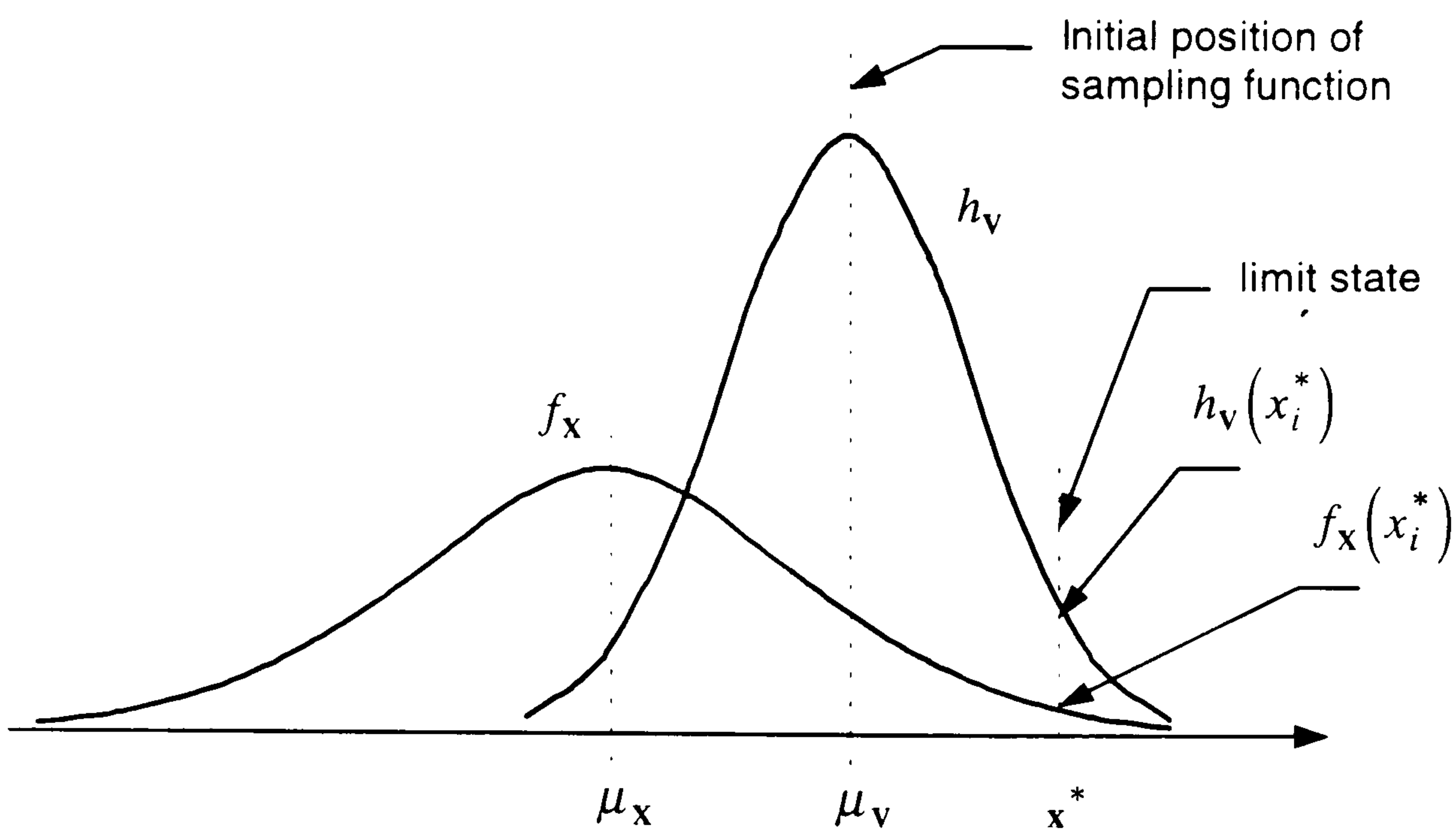

Figure 2.3. Positioning of the importance sampling function in the adaptive importance sampling approach, after **Melchers (1990)**.

An unbiased estimator of **Equation 2.12** is:

$$P_f = \frac{1}{N}\sum_{j=1}^{N}\left\{ I[D\!: G(\mathbf{v}_j)]\frac{f_X(\mathbf{v}_j)}{h_V(\mathbf{v}_j)} \right\} \tag{2.13}$$

where $\mathbf{v}_j$ is the vector of sample points, taken from the domain of the importance sampling function, $h_V(\mathbf{v})$.

Recalling from **Section 1.1.2** that the region with largest contribution to the probability of failure is known to be located around the design point, the applicability of the importance sampling technique to the reliability analysis problem appears very convenient. It follows that the ideal location for the importance sampling function is the design point or its surroundings. However, the true location of the design point might not be known in advance, in this case it has to be searched for. This search can be performed by placing the importance sampling function at a given location, say the point of mean values, with an appropriately large variance, in order to find the values of $f_X(\mathbf{x})$ for a given set of values taken from the domain of $h_V(\mathbf{v})$. A new centre for location of the importance sampling function is found by applying the following criterion: the best point in any given set of sample points falling in the failure domain is the one for which $f_X(\mathbf{x})$ is maximum. The criterion is based on the assumption that the design point exists and is unique, this requires that the local curvature of the $f_X(\mathbf{x})$ hypersurface is of the same sign and grater in value than the local curvature of the limit state hypersurface, $G(\mathbf{x}) = 0$. This condition is called the convexity condition.

On the other hand, the probability density function of the importance sampling function as well as its variance, have to be selected by the analyst. It can be observed that the variance of the sampling function directly affects the variance of **Equation 2.13**, therefore, it is desirable to reduce it every time that a new and more accurate location of the design point is achieved, so as to reduce the variance in the unbiased estimator of the probability of failure.

Then if the location of the importance sampling functions changed from ${}_1h_{\mathbf{V}}({}_1\mathbf{v})$ to ${}_2h_{\mathbf{V}}({}_2\mathbf{v})$, **Equation 2.13**. is modified as follows:

$$P_f = \sum_{j=1}^{N_1} \left\{ \frac{I\left[{}_1\mathbf{v}_j\right] f_{\mathbf{X}}\left({}_1\mathbf{v}_j\right)}{N \cdot {}_1h_{\mathbf{V}}({}_1\mathbf{v}_j)} \right\} + \sum_{j=N_1+1}^{N_2} \left\{ \frac{I\left[{}_2\mathbf{v}_j\right] f_{\mathbf{X}}\left({}_2\mathbf{v}_j\right)}{N \cdot {}_2h_{\mathbf{V}}({}_2\mathbf{v}_j)} \right\} \tag{2.14}$$

where $I\left[{}_k\mathbf{v}_j\right]$ is an abbreviation of $I\left[\cup_{k=1}^{n} G\left({}_k\mathbf{v}_j\right) \le 0\right]$. A generalisation of **Equation 2.14** is:

$$P_f = \frac{1}{N} \sum_{k=1}^{n} \sum_{j=N_{k-1}-1}^{N_k} I\left[{}_k\mathbf{v}_j\right] \frac{f_{\mathbf{X}}\left({}_k\mathbf{v}_j\right)}{{}_kh_{\mathbf{V}}({}_k\mathbf{v}_j)} \tag{2.15}$$

where *j* is the index of the number of samples $N_k - N_{k-1}$ taken from ${}_kh_{\mathbf{V}}({}_k\mathbf{v})$, and *k* is the index of the number *n* of importance sampling functions employed up to that stage.

Since the response surface provides an approximation of the limit state surface, a very close approximation of the design point can be established and used as a fixed point to locate the sampling function, $h_{\mathbf{V}}(\mathbf{v})$. However, the variance of this function has still to be proposed by the analyst. It was found in this work that more accurate results for the probability of failure can be achieved if a starting point in the surroundings of the actual design point is used as the initial point of the importance sampling procedure and the adaptive selection of the point of maximum likelihood is allowed to proceed.

The algorithm used to implement a computer code for the adaptive importance sampling method, as described above, is presented in **Appendix 6**.

2.6. Errors in the Response Surface and its Measurement.

The accuracy of the reliability analysis depends of two factors:

a).- accuracy of the mechanical model, this refers to both the accuracy of the mathematical model and the precision of the computer algorithm used to determine the response of the structure to load effects. For the case of marine risers, this will be discussed in **Chapter 5.0**.

b).- accuracy of the reliability analysis model, additionally to the accuracy of the reliability analysis methods, already discussed **Chapter 1**, the application of the response surface methods causes further concerns about the accuracy. These will be discussed in the following.

The response surface is an approximate polynomial function of the true but unknown limit state surface. This approximation carries an implicit error due to lack of fitness, showed graphically in **Figure 2.4**, and mathematically expressed as:

$$\xi(\mathbf{x}) = G(\mathbf{x}) - \bar{g}(\mathbf{x}) \tag{2.16}$$

where $G(\mathbf{x})$ represents the true limit state surface, $\bar{g}(\mathbf{x})$ is the equivalent response function, and ξ is the quantitative measure of the lack of fit.

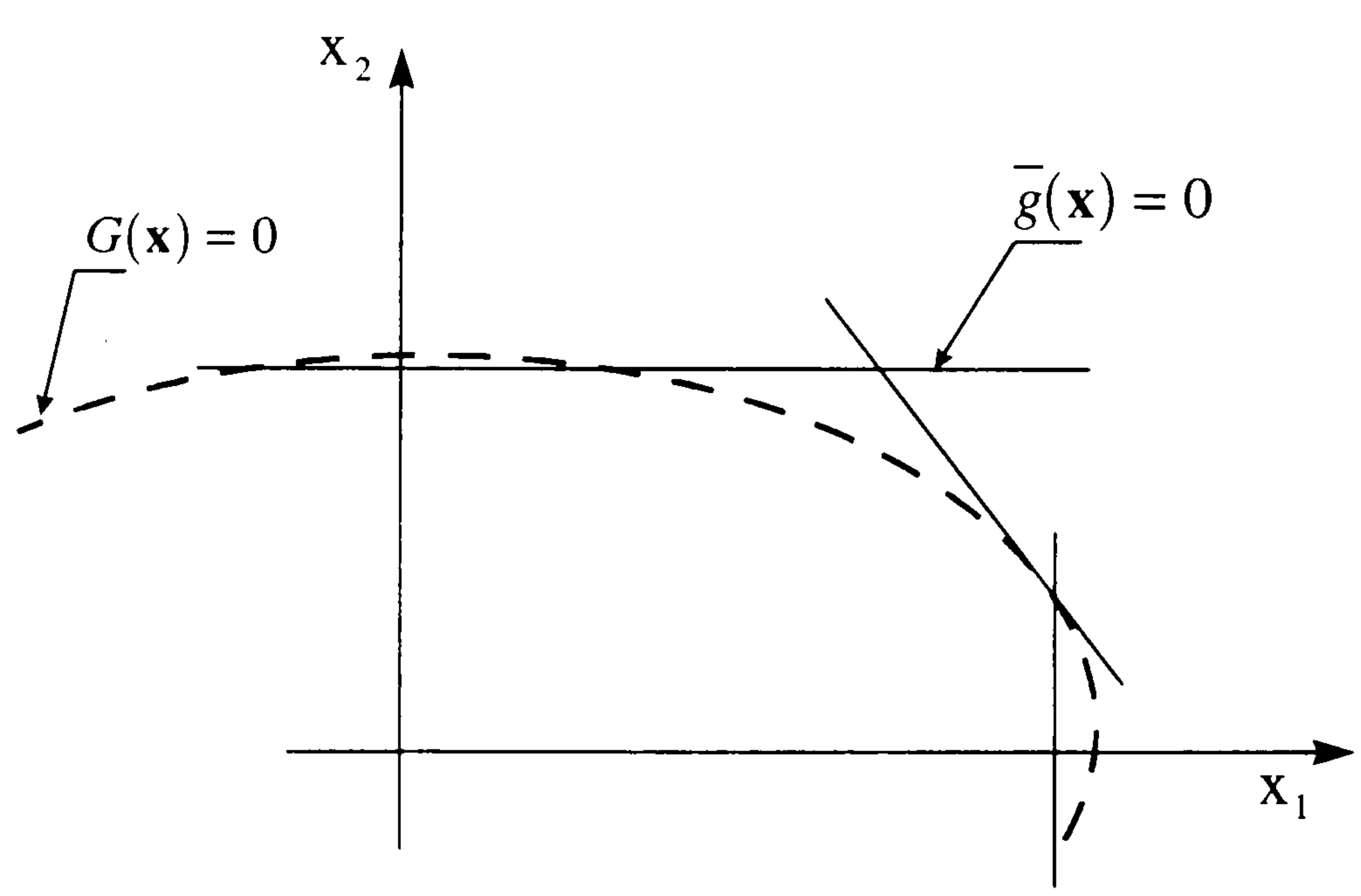

Figure 2.4. Lack of fit or error between the limit state surface and the response surface.

This error can be reduced by increasing the order of the polynomials. **Lee et al. (1993)** provided a study of different degrees of polynomials. However, the larger the complexity of the polynomial the larger of the number of experiments required with the complete finite element model and consequently the cost.

A number of the techniques have been proposed in order to solve this accuracy problem in two possible ways:

i) construction of the response surface at the important regions.

ii) estimation of error due to lack of fit.

The first criterion applied in order to secure an appropriate fitness of the response surface is to identify the important regions of the problem. It was discussed in the **Section 1.1.2** that the region with more significant contribution to the probability of failure is the area around the design point. Therefore a number of approaches have been suggested to improve the fitness of the response surface at this location. **Bucher and Bourgund (1990)**, proposed an adaptive approach, which is followed in this work and was described in **Sections 2.3** to **2.5**.

Briefly this approach relies in the acquisition of knowledge of the experimental region and therefore of the failure domain by finding the design point corresponding to a first approximation of the response surface. Then the first approximation of the important region is used as the center of a second and improved approximation.

In a similar fashion for cases when the determination of the Cumulative Distribution Function, CDF, of a response quantity, such as stress, strain, natural frequency, etc., is necessary, **Thacker and Wu (1992)** proposed to find a number of response surfaces following the locus of realizations of the basic variables satisfying the given limit states, (important regions), covering the entire domain of the CDF's of the basic variables.

The above mentioned approaches are oriented to the construction of the response surface at the important region, thus providing a sensible level of accuracy. However, errors due to lack for fit are still present. The problem of lack / goodness of fit has been recognized by a number of authors.

Turk, et al (1994) applied the least squares method for construction of the response surface. They noted that the accuracy of the response surface depends on the technique applied for the design of experiments. **Labeyrie and Schoefs (1996)** pointed that the goodness of the fit depends on two subjects, first on the selection of the basic variables and secondly on the errors associated with the regression techniques. Concerning this last type of error, **Böhm and Brückner-Foit (1992)** proposed a criteria for acceptance or rejection of a response surface model. For this purpose they proposed the following expression:

$$\lambda_{\text{exp}} = \left[\frac{E[SS_L]\nu_\xi}{\nu_L E[SS_E]} \right]^{1/2} \tag{2.17}$$

where λ_{exp} is the definition of the lack of fit, the closer this value is to 1.0 the better the fit of the response surface. $E[SS_L]$ is the expected value of the lack of fit sum of squares. $E[SS_E]$ is the expected value of the pure error sum of squares and their relative degrees of freedom are ν_L and ν_ξ. These values are to be obtained by an analysis of variance, ANOVA. The application of this well known statistical technique is described by **Böhm and Brückner-Foit (1992)** in connection with their suggested acceptance / rejection criterion and it depends on error values obtained from the regression model by the least squares method. However; no numerical threshold for acceptance or rejection of a response surface is suggested.

In another approach towards error estimation **Schüeller, et al. (1991)** suggested the application of conditional sampling as a means to generate sets of realizations of the basic variables close to the limit state surface, in order to calculate $\bar{g}(\mathbf{x})$ and compare this value with $G(\mathbf{x})$. Nevertheless, no guidelines are given as to an acceptable level of error or as to how this error could be used to improve the calculated probability of failure.

From the above discussion it is concluded that for the purposes of parametric studies of reliability it may be assumed that if a systematic approach for response surface construction is applied, like the one proposed by **Bucher and Bourgund (1990)** and adopted here, the level of error present is relatively consistent and therefore the conclusions drawn from such studies are valid within the same level of error. However; for construction of the response surface for a final analysis of a given design, it is necessary to determining the level of error.

SUMMARY, Chapter 2.

The algorithm to be applied for construction of the response surface in this work is described in this Chapter. This algorithm was selected for two reasons: i) the number of required experiments is relatively low and constant with respect to the number of basic variables; ii) it provides a very systematic approach and refines the response surface at the important region; therefore the level of lack of fit error can be assumed to be small and relatively consistent. These characteristics represent an advantage when parametric studies are required since the conclusions drawn are compatible with respect to the implicit level of error. Furthermore, this is an important consideration since despite methods are proposed in the literature towards acceptance / rejection of a response surface and error measurement, no indications as to numerical values for acceptability are suggested. On the other hand, however, the algorithm selected and described in this chapter may fail to rendered the required response function in some instances.

CHAPTER 3. VALIDATION OF THE RESPONSE SURFACE AND RELIABILITY ANALYSIS METHODOLOGIES.

3.0. Generalities.

The approach adopted for the present work is a combination of two separated techniques. First, the Response Surface Methodology provides a surrogate for the actual limit state function, which may be given in an implicit manner, i.e. by a finite element model. Then, in a second stage, any of the existing methods for determining the reliability index, β, can be employed. Therefore, this methodology will be called: Reliability Analysis Based on Response Surfaces or **RABRS**.

3.1. Algorithm for RABRS.

The detailed application of the RABRS methodology consist of the following steps:

1.- Definition of a failure criteria or limit state, such as bending stress, deflection, buckling, fatigue, etc.

2.- Selection of those variables to be treated as random, as well as their representative Probability Distribution Functions (PDF's), e.g. wave height, top tension, material strength, etc.

3.- Selection of mechanical model, the definition of this model is the main principle which leads to the application of the Response Surface Methodology, RSM. If the failure criteria and degree of complexity of the mechanical model allow for an explicit limit state function to be built, then RSM is not strictly necessary. However, if a complex mechanical model is required, for instance based on the finite element method, then RSM is one of the options available to construct an equivalent, yet explicit, limit state function.

4.-Application of RSM to derive an explicit function or response surface, equivalent to the implicit limit state function.

5.- Determination of the design point by FORM, if this methods does not converge then use Adaptive Importance Sampling, AIS.

6.- Refinement of the response surface by a second application of RSM, but this time centering the interpolation at a location between the mean values and the design point found in step 4.

7.- Determination of the reliability index by any of the reliability analysis methods. In this work the methods to be applied are: FORM, simple Monte Carlo simulation and AIS.

This methodology can be observed in a graphical manner in **Figure 3.1**.

METHODOGY FOR RELIABILITY ANALYSIS BASED ON RESPONSE SURFACES

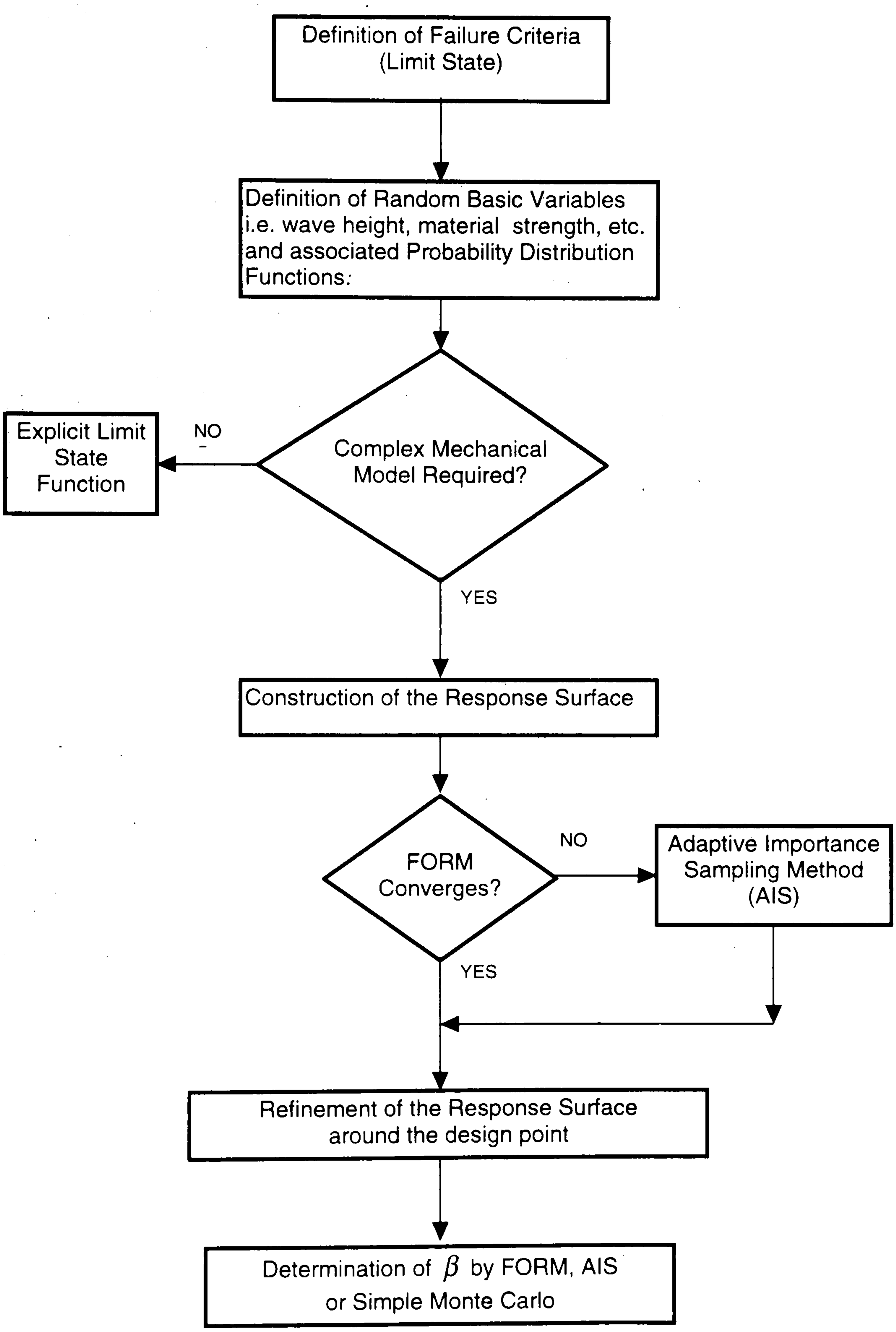

Figure 3.1. Flow diagram for RABRS.

3.2. Studies to Validate the Algorithm for RABRS.

In order to test the accuracy of the RABRS algorithm a number of simple cases for which results are easily available and published were selected and then this methodology applied for comparison purposes.

The cases selected for this comparative study are:

Case 1.-Example 5.3, **Thoft-Christensen and Baker (1982)**.

Consider the statically indeterminate beam showed in **Figure 3.2**, loaded by a concentrated force p and assume that the beam fails when $|m| \geq m_F$, where m_F is a critical limit moment and m is the maximum moment in the beam. Further assume that p, l and m_F are realizations of uncorrelated random variables P, L and M_F with:

$\mu_P = 4kN$, $\sigma_P = 1kN$

$\mu_L = 5m$, $\sigma_L \sim 0m$

$\mu_{M_F} = 20kNm$, $\sigma_{M_F} = 2kNm$

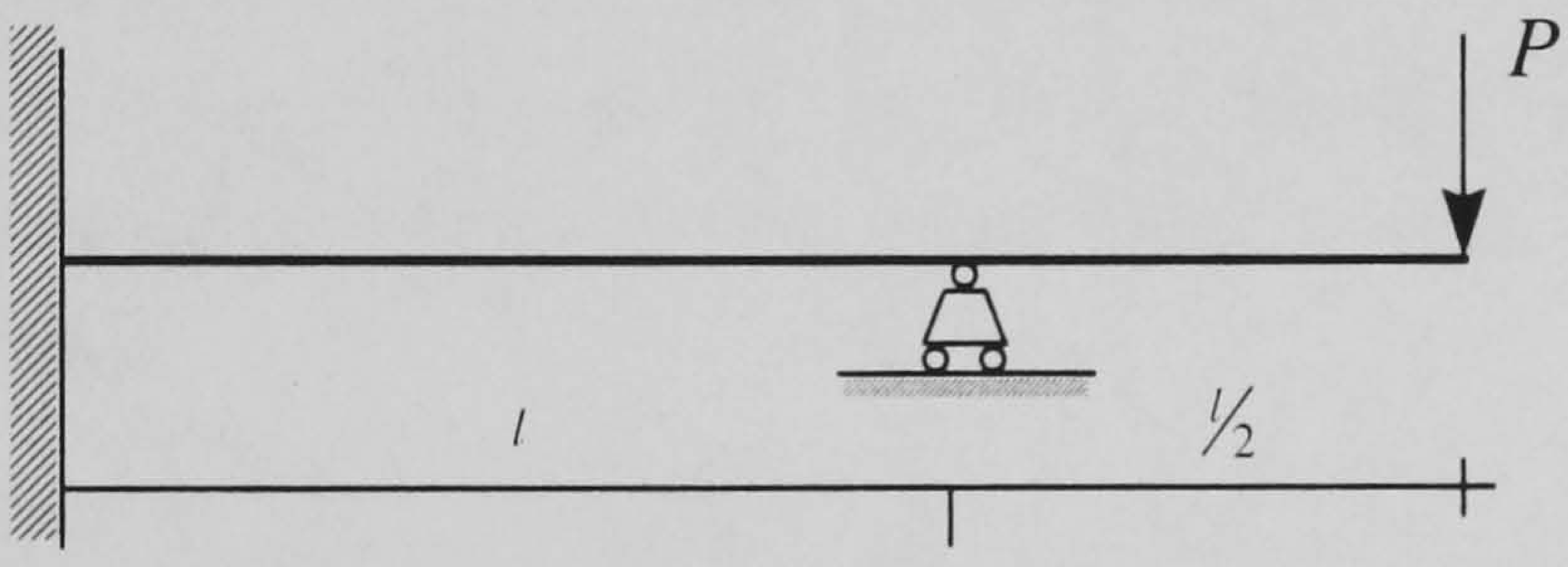

Figure 3.2. Beam for Case 1.

Case 2.- Exercise 5.3, **Thoft-Christensen and Baker (1982)**.

Consider the elastic beam showed on **Figure 3.3** with a uniform load p, length l and critical limit moment m_F. Assume that p, l and m_F are realizations of the uncorrelated random variables P, L and M_F with:

$\mu_P = 2M_P/m$, $\mu_P = 0.4M_P/m$

$\mu_L = 4m$, $\sigma_L = 0.4m$

$\mu_{M_F} = 5Mpm$, $\sigma_{M_F} = 0.4Mpm$

The maximum bending moment is $m_{\max} = \frac{9}{128} pl^2$. Calculate the reliability index β for the following failure mode $m_{\max} \geq m_F$.

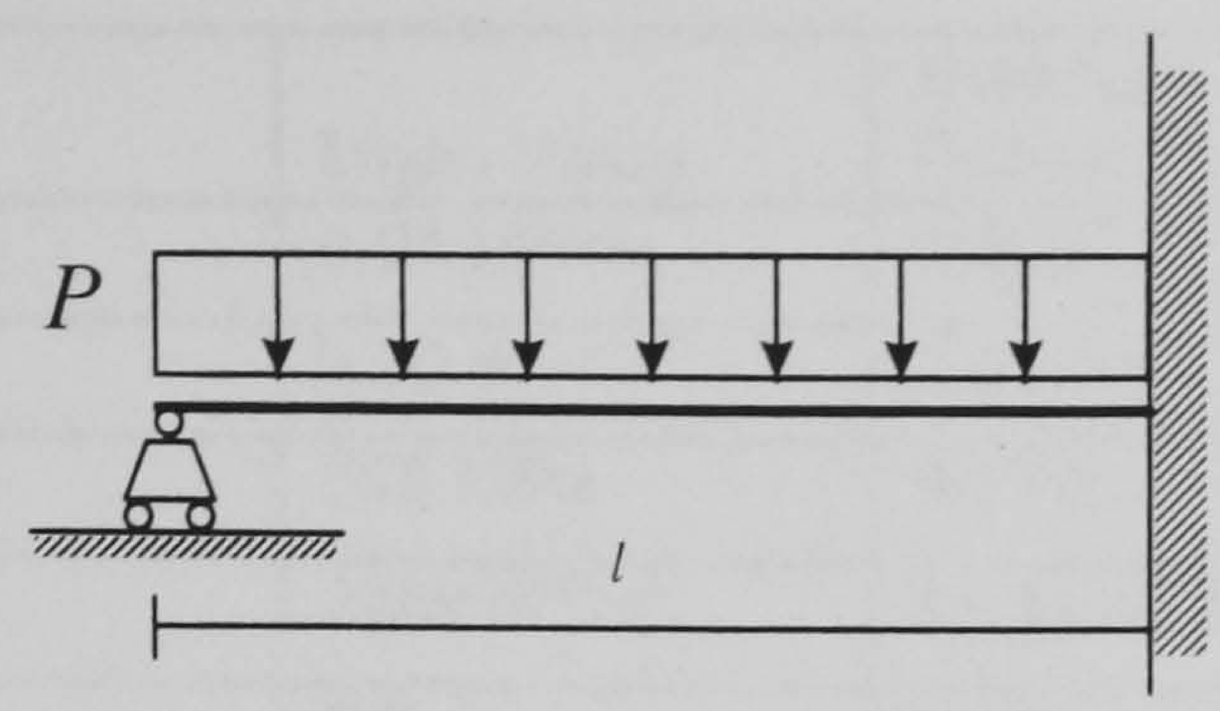

Figure 3.3. Beam for Case 2.

Case 3.- Example 4.3, **Madsen, et al. (1986)**.

The cross section of a reinforced concrete beam is showed in **Figure 3.4**. The sectional bending moment is M_B. The ultimate bending moment is:

$$M_U = \left|1 - K\frac{A_S T_S}{BDT_C}\right| A_S D T_S$$

Where A_s is the area of reinforcement, T_B the yield stress of the reinforcement, T_C the maximum compressive strength of the concrete, B the width of the beam, D the effective depth of the reinforcement, and K is a factor related to the stress-strain relation of concrete. For an ideal plastic stress-strain curve, K equals 0.5, and for a linear elastic stress-strain curve, K equals 2/3. The mean values and standard deviations for each variable are given in **Table 3.1**. The set of basic variables is:

$$Z = (M_B, D, T_S, A_S, K, B, T_C)$$

and a safety margin is the difference between M_U and M_B:

$$M = Z_2 Z_3 Z_4 - \frac{Z_5 Z_3^2 Z_4^2}{Z_6 Z_7} - Z_1$$

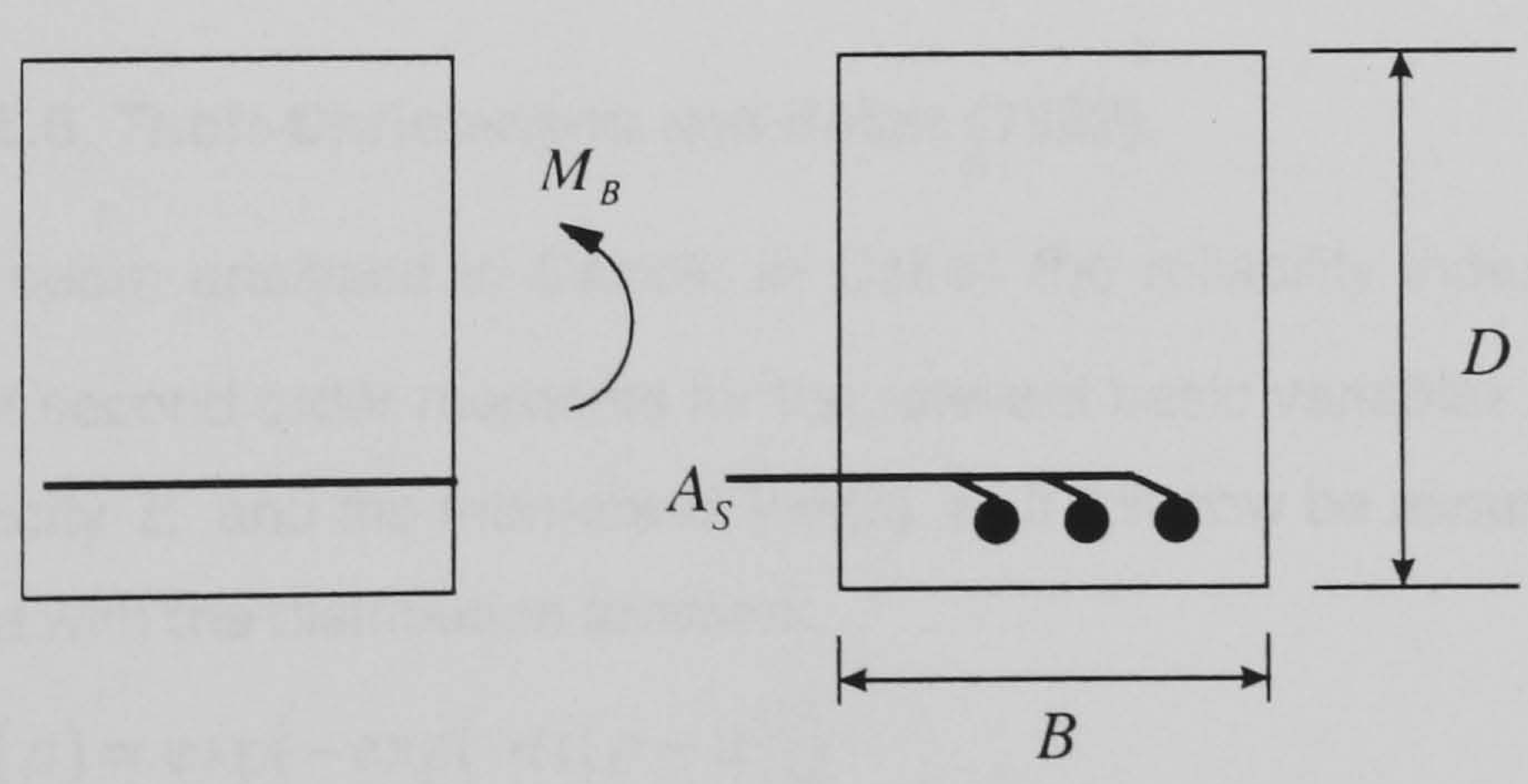

Figure 3.4. Reinforced concrete cross section subjected to pure bending, Case 3.

Variable	Symbol	Mean Value	Standard Derivation	Coefficient of Variation
M_B	Z_1	0.01 MNm	0.003 MNm	0.30
D	Z_2	0.30 m	0.015 m	0.05
T_S	Z_3	360 MPa	36 MPa	0.10
A_S	Z_4	226x10^{-6}m^2	11.3x10^{-6}m^2	0.05
K	Z_5	0.5	0.05	0.10
B	Z_6	0.12 m	0.006 m	0.05
T_C	Z_7	40 MPa	6 MPa	0.15

Table 3.1. Basic Variables for Case 3.

Case 4.- Example 5.5, **Thoft-Christensen and Baker (1982)**.

Consider the same beam as in **Case1**, but now with the following deflection failure criterion:

$$U_{\max} = \frac{5}{48}\frac{p\ell^3}{ei} \geq \frac{1}{30}\ell$$

where $u_{\max}$ is the maximum deflection, e the modulus of elasticity and i the relevant moment of inertia. Further, let $u_{\max}$, p, l, e, and i be realizations of uncorrelated random variables $U_{\max}$, P, L, E and I with:

$$\mu_P = 4kN \quad , \quad \sigma_P = 1kN$$
$$\mu_L = 5m \quad , \quad \sigma_L \cong 0m$$
$$\mu_E = 2.10^7\ kN/m^2 \quad , \quad \sigma_E = 0.5\cdot 10^7\ kN/m^2$$
$$\mu_I = 10^{-4}m^4 \quad , \quad \sigma_I = 0.2\cdot 10^{-4}m^4$$

Case 4a.- Example 6.8, **Thoft-Christensen and Baker (1982)**.

Consider again the beam analyzed in **Case4**. In Case4 the reliability index β was calculated solely on the basis of second order moments for the relevant basic variables, namely the load P, the modulus of elasticity E and the moment of inertia I. It will now be assumed that the load P is Gumbel distributed with the distribution function:

$$F_P(p) = \exp\left(-\exp\left(-\alpha(p-u)\right)\right)$$

and the density function:

$$f_P(p) = \exp\left(-\exp\left(-\alpha(p-u)\right) - \alpha(p-u)\right)\alpha$$

The two parameters α and u can be calculated from the following expressions for the mean μ_P and the standard deviation σ_P:

$$\mu_P = u + 0.5772/\alpha \qquad \sigma_P = \frac{\pi}{\sqrt{6}}\cdot\frac{1}{\alpha}$$

3.3. Results and Discussion.

The reliability indices, β, were calculated for the five cases described in the previous section, using the response surface as expressed by **Equation 2.3**, with the corresponding coefficients presented in **Table 3.2**, where the subindices indicate the first of second approximation of the response surface.

CASE 1

	$a_1 =$ 0.000		$a_2 =$ 0.000	
P	$b_1 =$ 1.000	$c_1 = 0.000$	$b_2 =$ 1.000	$c_2 = 0.000$
M_F	$b_1 = -2.500$	$c_1 = 0.000$	$b_2 = -2.500$	$c_2 = 0.000$

CASE 2

	$a_1 =$ 2.250		$a_2 =$ 4.336	
P	$b_1 = -1.125$	$c_1 =$ 0.000	$b_2 = -1.631$	$c_2 =$ 0.000
L	$b_1 =$ 0.000	$c_1 = -0.141$	$b_2 =$ 0.000	$c_2 = -0.187$
M_F	$b_1 =$ 1.000	$c_1 =$ 0.000	$b_2 =$ 1.000	$c_2 =$ 0.000

CASE 3

	$a_1 = -0.051$		$a_2 = -0.037$	
Z_1	$b_1 =$ 0.081	$c_1 =$ 0.000	$b_2 =$ 0.062	$c_2 =$ 0.000
Z_2	$b_1 =$ 0.00007	$c_1 =$ 0.000	$b_2 =$ 0.000	$c_2 =$ 0.000
Z_3	$b_1 =$ 108.000	$c_1 = -13500.000$	$b_2 =$ 84.156	$c_2 = -8891.411$
Z_4	$b_1 = -0.001$	$c_1 =$ 0.000	$b_2 = -0.001$	$c_2 =$ 0.000
Z_5	$b_1 =$ 0.018	$c_1 = -0.049$	$b_2 =$ 0.011	$c_2 = -0.029$
Z_6	$b_1 =$ 0.00006	$c_1 =$ 0.000	$b_2 =$ 0.000	$c_2 =$ 0.000
Z_7	$b_1 = -1.000$	$c_1 =$ 0.000	$b_2 = -1.000$	$c_2 =$ 0.000

CASES 4 and 4a

	$a_1 = -2.000$ E+03		$a_2 = 4.442$ E+02	
E	$b_1 =$ 0.000	$c_1 = 0.000$	$b_2 = 0.000$	$c_2 = 0.000$
I	$b_1 =$ 5.604 E+06	$c_1 = 0.000$	$b_2 =$ 7.406 E+06	$c_2 = 0.000$
P	$b_1 = -7.812$ E+01	$c_1 = 0.000$	$b_2 = -7.812$ E+01	$c_2 = 0.000$

Table 3.2. Coefficients of the response surfaces.

In order to compare the accuracy of the reliability index as rendered by the RABRS methodology **Table 3.3** presents the values of β given by a number of approaches. In the first instance, the β values were calculated using the original limit state equations by means of FORM method and simple Monte Carlo simulation with five (MCS I) and fifteen (MCS II) millions of simulations, respectively. Therefore, the second and more extensive simulation can be considered as the "exact" value, for comparison purposes. Also the FORM reliability indices, presented in the second column of **Table 3.3**, are the ones provided by the authors cited for each case.

Cases	ORIGINAL LSF			RESPONSE SURFACE				
	Published Result	This Study		This Study				
	FORM	MCS I	MCS II **"Exact"**	FORM	MCS I	MCS II	AIS I Original Space	AIS II Universal Space
case 1	3.1234752	3.1287	3.1252	3.1234752	3.126196	3.117932	3.11736	3.11736
case 2	3.05075	3.072333	3.071380	3.05236	3.039810	3.036800	3.04051	3.04051
case 3	3.41	3.39333	3.39853	3.41241	3.41018	3.40403	3.39093	3.39093
case 4	3.29	3.224966	3.220138	3.44759	3.459593	3.445522	3.44518	3.44518
case 4a	3.32	3.20325	3.20538		3.40921	3.40958	3.42738	3.41284

MSC I 5 000 000 sample points,
MCS II 15 000 000 sample points,
AIS I Original space (12 000 sample points over 120 locations of the sampling function, initial standard deviation of the sampling function: 1.5),
AIS II Universal space (12 000 sample points over 120 locations of the sampling function, initial standard deviation of the sampling function: 1.5), seeds in all AIS cases are same.

Table 3.3. Validation table for the RABRS algorithm.

Secondly the RABRS methodology was applied and using the equivalent limit state equation or response surface the reliability indices were calculated for each case. The methods employed for this purpose were FORM, simple Monte Carlo simulation, using the same simulation lengths as before, and finally the Adaptive Importance Sampling, AIS, method.

Using the "exact" reliability index as a reference it can be observed that for the first three cases the reliability indices compare well with the exact ones. It is worth remembering that the sources of deviation are two, in the first place the approximation error due to lack of fit of the response surface, and in the second instance the statistical error inherent to Monte Carlo simulation. This fact is highlighted in **Case 1**, where the original limit state surface is linear and therefore the reliability index given by FORM is also exact. It can be observed that when the reliability index is found with the response surface and using FORM the result is exactly the same as with the original limit state equation. Hence, it can be concluded that the response surface represents without error the original limit state equation. The deviations observed in the values of β when the simulation techniques are used for this case appear solely as a result of the statistical error.

Cases 2 and **3** are slightly nonlinear, however, the values of the reliability index found with the response surface are consistent with those found with the original limit state equation.

For **Cases 4** and **4a** the differences in β between the original limit state equation and the response surface are slightly higher. It can be assumed that the lack of fit is more important here because the degree of nonlinearity is also higher. It is important to mention that the level of statistical error appears to be consistent with the values from the original limit state equation. That is, the values of β given by the second simple Monte Carlo simulation, MCS II, with the original limit state equation, differ from **Case 4** to **Case 4a** by 0.02 to 0.025 units of standard deviation, which is about the same level for the values given by AIS II with the response surface. This is an important characteristic for parametric studies; though there may be a slight deviation from the exact value of β, the numerical differences in the reliability index for variations of the same case is consistent with the differences found when the original limit state equations are used.

Consequently, the conclusions drawn from a parametric study based on RABRS can be considered valid. **Cases 4** and **4a** also denote that the concerns about lack of fit should grow as the degree of non-linearity of the original limit state equation increases.

On the other hand, since one of the characteristic of the AIS method is that an "adequate" standard deviation for the sampling function has to be selected by the analyst, it was considered convenient to attempt to find which particular ratio of sampling function standard deviation to basic variable standard deviation, σ_V / σ_X, could be considered appropriate. **Melchers (1989)** pointed that good results can be obtained for σ_V / σ_X in the range of 1 to 2. He found through empirical studies that values of this ratio of less than 1 produced overestimates of the reliability index and that larger values resulted in slower rates of convergence. It is important to note that he used the mechanical model, not a surrogate of it, such as the response surface used in this work.

One of the advantages of the RABRS methodology is that long Monte Carlo simulations, particularly when variance reduction techniques are applied, can be achieved with a small computational effort, therefore, it was decided to empirically review if the ratios σ_V/σ_X recommended by **Melchers (1989)** were influenced if the calculations are carried out in the original or in the standardized space of basic variables. For this purpose, the reliability indices for **Cases 1** and **4a** were determined in both the original and standardized spaces of basic variables, using the AIS method with the same starting seeds for all cases and with ratios of standard deviations σ_V/σ_X running from 0.5 to 4.5. **Figures 3.5** and **3.6** present the β values for **Case 1**. It can be observed that for the case of a linear limit state equation the results of the simulations rendered the same results regardless of the working space. For the non-linear case, **Case 4a**, presented in **Figure 3.7** there are small differences in the results of each simulation, but they tend to converge to each other as the ratio σ_V/σ_X increases. These differences are attributed to the characteristics of each working space. In the standardized space the shapes of the PDF's are more smooth, with hypercircles in every case, this is thought to facilitate the process by avoiding sharp regions, however, the numerical precision may be diminished by the larger number of transformations required, also the non-linear response surface becomes more non-linear, possibly with sharp regions. The opposite situation occurs when the calculations are performed in the original space, usually a more smooth response surface with perhaps sharp regions, depending on the types of PDF's, but less loos of accuracy due to a lower number of transformations.

On the other hand, for the linear case, **Figures 3.5** and **3.6**, the reliability index appears to approach better the exact values with larger values of the σ_V/σ_X ratio, but this is not the case for the non-linear case, **Figure 3.7**. Furthermore, if the limit state surface is linear FORM renders an accurate value of the reliability index.

It can therefore be concluded that the recommendation of **Melchers (1989)** concerning the values for the σ_V/σ_X ratio are not sensibly affected by the use of the original or the standardized space.

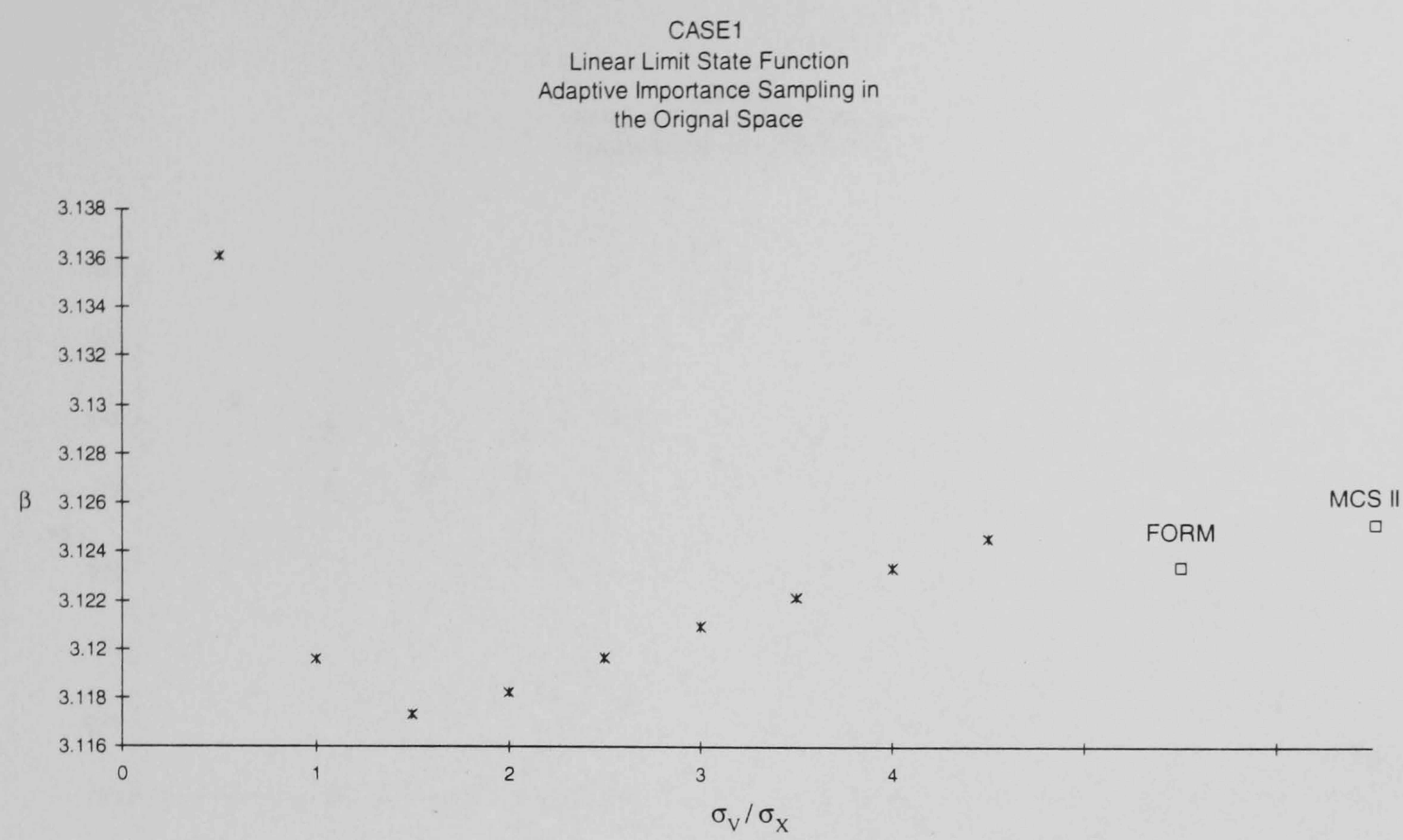

Figure 3.5. Reliability index vs. ratio of standard deviation between sampling and basic variables PDF's. Original space, linear limit state equation.

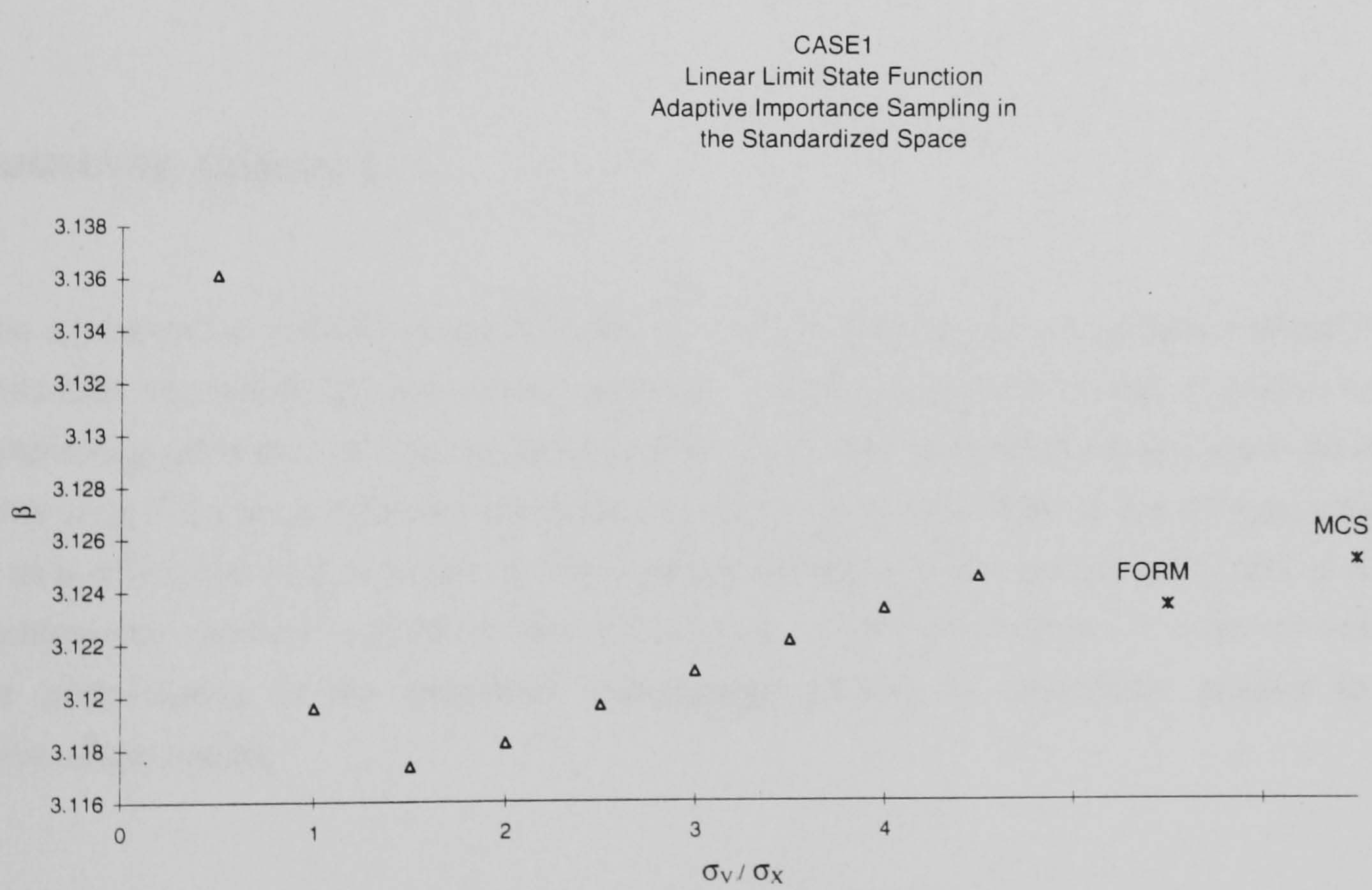

Figure 3.6. Reliability index vs. ratio of standard deviation between sampling and basic variables PDF's. Standardized space, linear limit state equation.

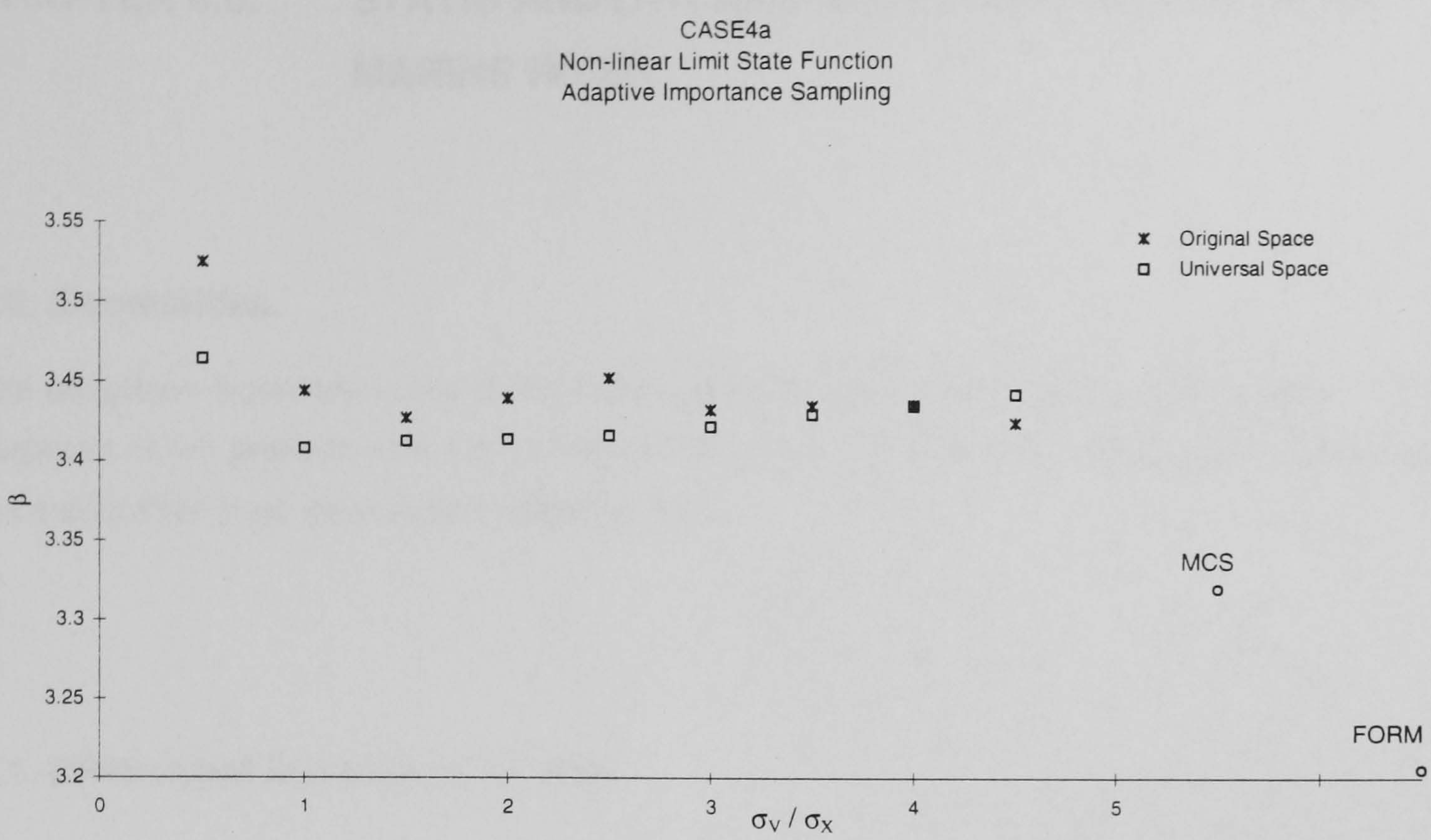

Figure 3.7. Reliability index vs. ratio of standard deviation between sampling and basic variables PDF's. Comparison of values from original and standardized spaces, non-linear limit state equation.

SUMMARY, Chapter 3.

The algorithm for reliability analysis based on the use of the response surface methodology was described and tested against simple examples. The results show that such algorithm exhibits a satisfactory performance. The empirical studies conducted demonstrate that there is no apparent advantage if the work is carried out in the original or the standardized space of basic variables. It is also concluded that selection of the standard deviation of the sampling function is a difficult problem that requires judgement from the analyst. In the same fashion, it is demonstrated that the performance of the proposed methodology allows for parametric studies to render dependable results.

CHAPTER 4.0. STATIC AND DYNAMIC ANALYSES MODELS FOR A MARINE RISER.

4.0. Generalities.

The equations representing the static and dynamic behavior of the marine riser selected for the purposes of the present work are derived in this section. The reasons for selection of the model to be described here were given in **Section 1.2.1**.

4.1. Differential Equation of Motion.

Following developments from **Daering and Huang (1976)** and **Chakrabarti (1990)**, the differential equation of motion applicable to a marine riser is derived in the following. The riser is modeled as a beam-column under the assumptions that:

1) the length of segment is small, so that

$$\cos d\theta \approx 1 \quad ; \quad \sin d\theta \approx d\theta \tag{4.1a}$$

2) small deflection beam theory is valid,

$$\cos\theta \approx \frac{dy}{ds} \quad ; \quad \sin\theta \approx \frac{dx}{ds} \tag{4.1b}$$

3) the angle of deflection θ is small

$$ds \approx dy \quad ; \quad \cos\theta \approx 1 \quad ; \quad \sin\theta \approx \frac{dx}{dy} \quad \text{and} \quad \frac{d\theta}{dy} = \frac{d^2x}{dy^2} \tag{4.1c}$$

For the riser showed in **Figure 4.1** the equation of motion for the free vibration problem will be derived first. The equilibrium of vertical forces in a section of the riser, as presented in **Figure 4.2** gives:

$$\frac{\partial \mathrm{T}}{\partial y} = W \tag{4.2}$$

where T is the tension along the riser and W is its weight.

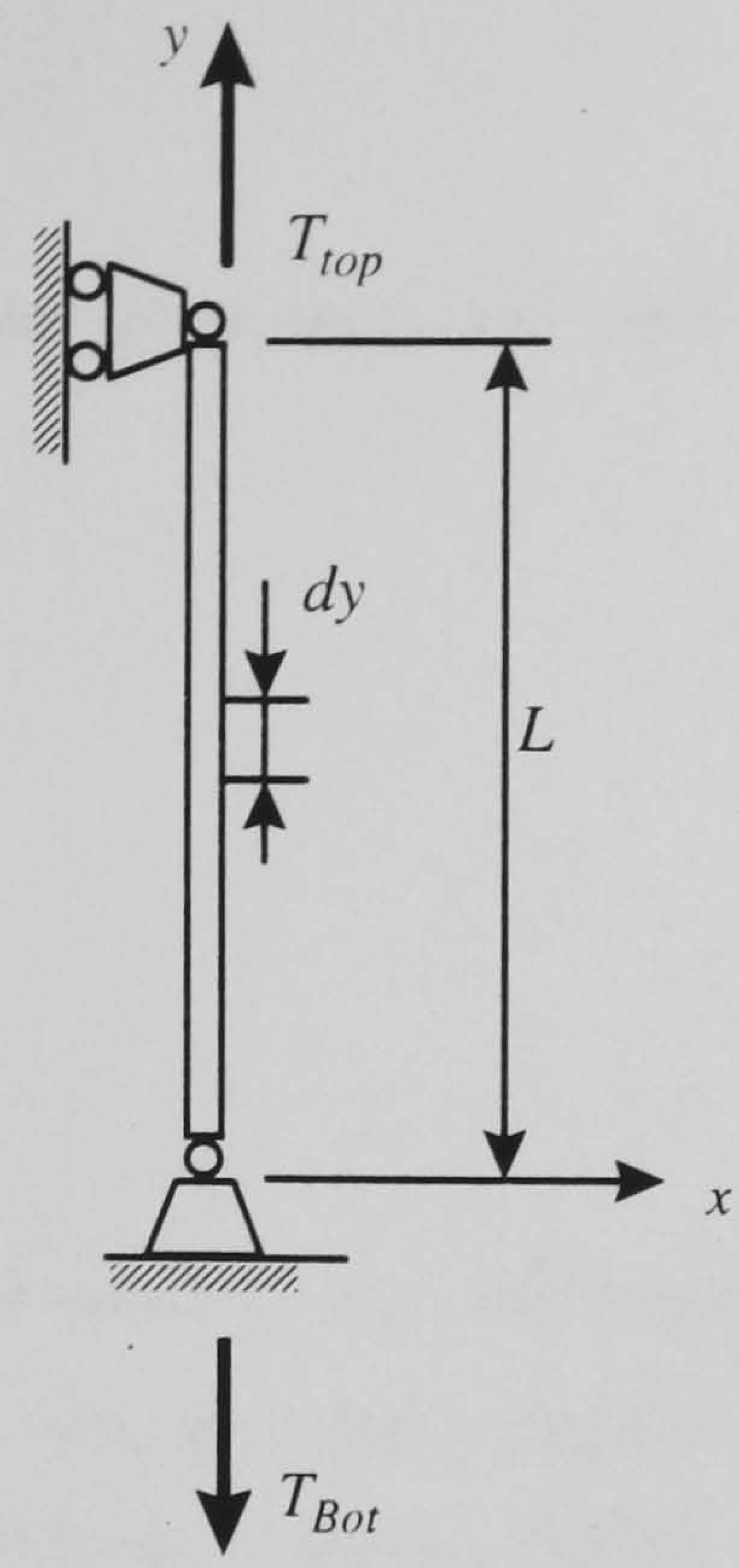

Figure 4.1. Coordinate system for the riser, after **Daering and Huang (1976)**.

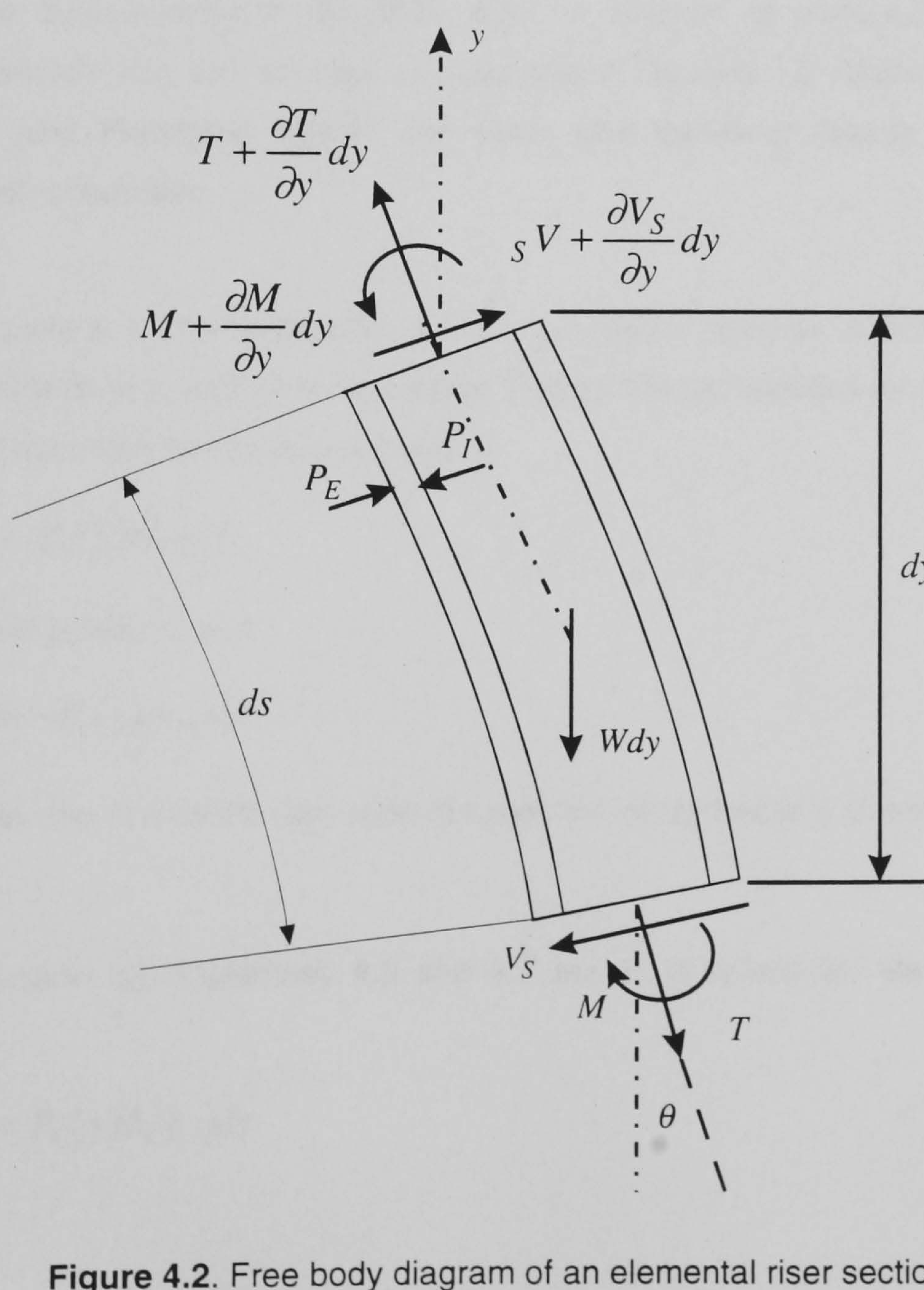

Figure 4.2. Free body diagram of an elemental riser section, after **Daering and Huang (1976)**.

The summation of moments gives:

$$\frac{\partial \mathrm{M}}{\partial y} = V_S \tag{4.3}$$

where V_S is the shear force on an elemental section of riser, as showed in **Figure 4.2**, and the Bernoulli-Euler equation is:

$$\mathrm{EI}\frac{\partial^2 x}{\partial y^2} = \mathrm{M} \tag{4.4}$$

therefore:

$$\frac{\partial}{\partial y}\left[\mathrm{EI}\frac{\partial^2 x}{\partial y^2}\right] = V_S \tag{4.5}$$

The marine riser is also subjected to external, P_E, and internal hydrostatic pressures, P_I, due to sea water and drilling mud, respectively, and these must be taken into consideration in order to calculate the bending effects. **Daering and Huang (1976)** transformed such hydrostatic forces into statically equivalent ones. After performing the summation for the static equilibrium, tension and the statically equivalent hydrostatic forces remained collected in one term, as it will be demonstrated subsequently in **Equation 4.11**. A number of authors, later, generalized the previous approach into the concept of ***equivalent tension***, i.e. **McIver and Olson (1981)**, **Chakrabarti and Frampton (1982)** and **Patel and Geoffrey (1990)**, all of whom besides presented mathematically

rigorous derivations of the expression for the equivalent tension. Another scheme, based on physical considerations, was given by **Sparks (1984)**, the expressions for the statically equivalent hydrostatic loads given by this last author are:

$$F_{P_E} = P_E(y)A_E(y) \tag{4.6}$$

for the external pressure, and

$$F_{P_I} = -P_I(y)A_I(y) \tag{4.7}$$

for the internal one. A detailed derivation of these two expressions is given in **Appendix 7**.

If the forces given by **Equations 4.6** and **4.7** act on a differential element of the riser they become:

$$F_{P_E} = P_E(y)A_E(y)dy \tag{4.8}$$

and

$$F_{P_I} = -P_I(y)A_I(y)dy \tag{4.9}$$

where:

A_E, external area of pipe cross section,

A_I, internal area of pipe cross section,

P_E, external hydrostatic pressure, and

P_I, internal hydrostatic pressure,

given at depth y.

The next step is to add all the horizontal components of tension, riser weight and statically equivalent external and internal pressures, including the time dependent inertial effect and hydrodynamic added mass:

$$m\frac{\partial^2 x}{\partial t^2}dy = \frac{\partial}{\partial y}\left\{\mathrm{T}(y)\sin\theta dy + \left(\mathrm{P}_E(y)A_E(y)\sin\theta dy - \mathrm{P}_I(y)A_I(y)\sin\theta dy\right)\right\} - \frac{\partial V}{\partial y}dy\cos\theta \tag{4.10}$$

On account of the small deflection assumptions expressed by **Equations 4.1**, then, **Equation 4.10** becomes:

$$m\frac{\partial^2 x}{\partial t^2} = \frac{\partial}{\partial y}\left\{[\mathrm{T}(y) + (\mathrm{P}_E(y)A_E(y) - \mathrm{P}_I(y)A_I(y))]\frac{\partial x}{\partial y}\right\} - \frac{\partial V}{\partial y} \tag{4.11}$$

where:

$$\mathrm{T}(y) = \mathrm{T}_C + \int \gamma_S\left(A_E(y) - A_I(y)\right)dy \tag{4.12}$$

and:

T_C, constant tension,

γ_S, specific weight of steel.

T_C is a constant tension specified at some point on the riser, which is modified by the effect of gravity, that is, the weight of the steel pipe. The constant tension is usually specified at the top or bottom end of the riser. If the top tension is specified **Equation 4.12** takes the form:

$$\mathrm{T}(y) = \mathrm{T}_{top} - \int_y^{top} \gamma_S\left(A_E(y) + A_I(y)\right)dy \tag{4.13}$$

Now, substituting **Equation 4.5** into **Equation 4.11** and assuming that the riser cross sectional area is constant along its length:

$$\frac{\partial^2}{\partial y^2}\left[\mathrm{EI}\frac{\partial^2 x}{\partial y^2}\right]-\frac{\partial}{\partial y}\left\{\left[\mathrm{T}(y)+\left(\mathrm{P}_E(y)A_E-\mathrm{P}_I(y)A_I\right)\right]\frac{\partial x}{\partial y}\right\}+m\frac{\partial^2 x}{\partial t^2}=0 \qquad (4.14)$$

Equation 4.14 is the equation of motion for the free vibration case and its second term is referred in the literature as the ***effective tension***, i.e. **Chakrabarti and Frampton (1982)**. This equation of motion has the same form as the equation derived by **Daering and Huang (1976)**.

On the other hand, **Equation 4.14** can be written as:

$$\frac{\partial^2}{\partial y^2}\left[\mathrm{EI}\frac{\partial^2 x}{\partial y^2}\right]-\frac{\partial}{\partial y}\left[\mathrm{T}_e(y)\frac{\partial x}{\partial y}\right]+m\frac{\partial^2 x}{\partial t^2}=0 \qquad (4.15)$$

where the effective tension is:

$$\mathrm{T}_e=\mathrm{T}(y)+\mathrm{P}_E(y)A_E-\mathrm{P}_I(y)A_I \qquad (4.16)$$

An alternative form of **Equation 4.15** can be obtained by substituting explicitly the derivative of its second term:

$$\frac{\partial}{\partial y}\left[\mathrm{T}_e(y)\frac{\partial x}{\partial y}\right]=\mathrm{T}_e(y)\frac{\partial^2 x}{\partial y^2}+\frac{\partial \mathrm{T}_e(y)}{\partial y}\frac{\partial x}{\partial y} \qquad (4.17)$$

where:

$$\frac{\partial \mathrm{T}_e(y)}{\partial y}=\frac{\partial}{\partial y}\left[\mathrm{T}(y)+\left(\mathrm{P}_E(y)A_E-\mathrm{P}_I(y)A_I\right)\right] \qquad (4.18)$$

with $\mathrm{T}(y)$ given by **Equation 4.13**

$$\frac{\partial}{\partial y}\mathrm{T}(y)=\frac{\partial}{\partial y}\left[\mathrm{T}_{top}+\int\gamma_S\left(A_E-A_I\right)dy\right] \qquad (4.19)$$

$$\frac{\partial}{\partial y}\mathrm{T}(y)=\gamma_S\left(A_E-A_I\right) \qquad (4.20)$$

if $A_S=A_E-A_I$ is the cross section area of the pipe wall thickness, then:

$$\frac{\partial}{\partial y}\mathrm{T}(y)=\gamma_S A_S \qquad (4.21)$$

Now, the hydrostatic pressure is given by

$$\mathrm{P}(y)=-g\rho y \qquad (4.22)$$

where g is the acceleration of gravity and ρ is the density, therefore:

$$\frac{\partial}{\partial y}\left[\mathrm{P}_E(y)A_E - \mathrm{P}_I(y)A_I\right] = -g\left(\rho_E A_E - \rho_I A_I\right) \tag{4.23}$$

If the specific weight is given by gravity times the density, that is :

$$\gamma = g\rho \tag{4.24}$$

then **Equation 4.23** becomes:

$$\frac{\partial}{\partial y}\left[\mathrm{P}_E(y)A_E - \mathrm{P}_I(y)A_I\right] = \gamma_I A_I - \gamma_E A_E \tag{4.25}$$

Substituting **Equation 4.21** and **4.25** in **Equation 4.18**:

$$\frac{\partial}{\partial y}\mathrm{T}_e(y) = \gamma_S A_S - \gamma_E A_E + \gamma_I A_I \tag{4.26}$$

Equation 4.26 is usually called ***buoyant weight***, **Chakrabarti and Frampton (1982).**

Substituting **Equation 4.16** and **4.26** in **Equation 4.17**,

$$\frac{\partial}{\partial y}\left[\mathrm{T}_e(y)\frac{\partial x}{\partial y}\right] = \left(\mathrm{T}(y) + \mathrm{P}_E(y)A_E + \mathrm{P}_I(y)A_I\right)\frac{\partial^2 x}{\partial y^2} + \left(\gamma_S A_S - \gamma_E A_E + \gamma_I A_I\right)\frac{\partial x}{\partial y} \tag{4.27}$$

Therefore, substituting **Equation 4.27** in **Equation 4.15** and considering that the riser undergoes horizontal displacements in the $x - y$ plane only, the final form of the equation of motion for free vibration becomes:

$$m\frac{d^2 x}{dt^2} + \frac{d^2}{dy^2}\left[\mathrm{EI}\frac{d^2 x}{dy^2}\right] - \left(\mathrm{T}(y) + \mathrm{P}_E(y)A_E - \mathrm{P}_I(y)A_I\right)\frac{d^2 x}{dy^2} - \left(\gamma_S A_S - \gamma_E A_E + \gamma_I A_I\right)\frac{dx}{dy} = 0 \tag{4.28}$$

A marine riser is usually exposed to the effects of wave particle kinematics, namely velocity and acceleration. Load due to wave particle motion is considered by a modified form of Morrison's equation. **Clauss, et al. (1992)** indicated that when a structural element, i.e. the riser, moves itself, the Froude-Krylov force depends only on the wave particle acceleration, while the inertia and drag forces depend on the relative accelerations and velocities respectively, that is:

$$F(t) = \rho_E V\dot{U} + \rho_E V\left(C_M - 1\right)\left(\dot{U} - \ddot{X}\right) + \frac{1}{2}\rho_E C_D A_E\left|U - \dot{X}\right|\left(U - \dot{X}\right) \tag{4.29}$$

where:

A_E area of the riser external cross section.

C_D drag coefficient,

C_M inertia coefficient,

$\dot{U}$, horizontal component of wave particle acceleration,

U, horizontal component of wave particle velocity,

V volume of the riser external section,

$\ddot{X}$, horizontal component of riser transverse acceleration, and

$\dot{X}$, horizontal component of riser transverse velocity.

Thus, for the forced vibration case, **Equation 4.28** is subjected to a forcing function given by **Equation 4.29** and becomes:

$$m\frac{d^2x}{dt^2}+\frac{d^2}{dy^2}\left[\mathrm{EI}\frac{d^2x}{dy}\right]-\left(\mathrm{T}(y)+\mathrm{P}_E(y)A_E-\mathrm{P}_I(y)A_I\right)\frac{d^2x}{dy^2}-\left(\gamma_S A_S-\gamma_E A_E+\gamma_I A_I\right)\frac{dx}{dy}=F(t) \tag{4.30}$$

with $F(t)$ given by **Equation 4.29**. **Equation 4.30** possesses the same form as the equation derived by **Chakrabarti (1990)**.

Since the riser is attached to the platform, the motion that the platform undergoes results in a displacement of the riser top boundary. Such boundary displacement becomes a force that has to be added to the forcing function of **Equation 4.29**.

4.2. Differential Equation for Static Analysis.

Considering that in the static analysis case the effect of inertial forces is null and that the load does not vary with time, **Equation 4.30** is reduced to:

$$\frac{d^2}{dy^2}\left[\mathrm{EI}\frac{d^2x}{dy^2}\right]-\left(\mathrm{T}_e(y)+\mathrm{P}_E(y)A_E-\mathrm{P}_I(y)A_I\right)\frac{d^2x}{dy^2}-\left(\gamma_S A_S-\gamma_E A_E+\gamma_I A_I\right)\frac{dx}{dy}=F \tag{4.31}$$

It is considered in the static analysis case that the load on the riser is the horizontal steady current profile, given as a drag load as:

$$F=\frac{1}{2}\rho_E C_D D_E U_c(y)|U_c(y)| \tag{4.32}$$

where:

C_D, drag coefficient,

D_E, external diameter of the riser pipe,

U_c, steady current velocity, and

ρ_E the density of external fluid, that is, the sea water.

In the same fashion as in the dynamic case, the top node of the riser is also subjected to a static displacement of the floater and the boundary displacement must be added to force already stated by **Equation 4.32**.

On the other side, it is important to mention that **Equation 4.31** has the same form as the one given by **Patel and Sarohia (1982)**.

4.3. Finite Element Equations of Motion.

The differential equation of motion, **Equation 4.30**, for the riser problem can be expressed in an alternative form by a system of algebraic linear matrix equations. This transformation is possible after a discretization process in which the riser is idealized as an assemblage of small beam elements, i.e. finite elements.

The advantage of the discretization of a structure is that the differential equation describing its behaviour can be reduced to a series of algebraic equations in which solutions for the physical variable of concern, i.e. displacement, are given at the nodes of the element and the behavior in its interior is modeled through selected *interpolation* or *shape* functions. Therefore, a finite element, i.e. a beam element, holds, for instance, stiffness properties, that is force-displacement coefficients, which can be arranged in matrix form, so that the displacements at the nodes of the beam can be known from:

$$[k]\{q\} = \{f\} \tag{4.33}$$

where:

$[k]$, elemental stiffness coefficients matrix,

$\{q\}$, vector of unknown displacements at the nodes, and

$\{f\}$, vector of nodal forces.

There exists a number of methods to derive these coefficients. The early approach made use of the concept of *generalized coordinates* to express the polynomials defining the behavior in the interior of the element, other concepts such as energy principles and the principle of virtual displacements were needed as well. Two subsequent approaches which make use of the *interpolation* function concept are, the *energy methods*, which involve variational principles of solid mechanics, i.e. minimum potential energy, and, secondly, the method of weighted residuals, which is based on the minimization of the residual left after an approximate or trial solution is substituted into the differential equation representing the system.

In general terms the derivation of the properties of a particular finite element by application of virtual displacements consist in the application of unit virtual displacements at the boundary nodes of such element, thus resulting in a deflected shape. The deflections within the element can be modeled by polynomial functions that satisfy the nodal and internal continuity requirements. Then the work done by the external forces is equated to that of the internal forces, and the new equation solved for the required coefficients of the element.

Once the coefficients of the finite element are known, the global matrix representing the total system, i.e. the global stiffness matrix, can be assembled by noting that the displacements of adjacent nodes of the structure must be equal, the *direct method*, resulting in a total system of the following form:

$$[K]\{Q\}=\{F\} \tag{4.34}$$

where:

$[K]$, global stiffness matrix,

$\{Q\}$, global vector of unknown displacement and,

$\{F\}$, global vector of nodal forces.

The finite element equation given by **Equation 4.34** represents the static case, where the deflections depend on the stiffness coefficients only. Furthermore, the discretization process reduced the system to a one with a limited or finite number of degrees of freedom. In the dynamic case, however, the inertial and dissipative forces intervene in the equilibrium of the system. In order to derive the general finite element equation of motion for a multiple degree of freedom, **MDOF**, system **Petyt (1990)** indicated that Hamilton's principle states that the sum of time variations of the difference between kinetic and potential (strain) energies and the work done by the non-conservative forces (i.e. damping) equals zero. Furthermore, he showed that application of Hamilton's principle leads to the Lagrangian form of the equations of motion for any system that can be described in terms of *n* independent displacements, or in other words a system that can be discretized. Substitution in Lagrange's equations of expressions for the kinetic and strain energies and for the work of damping forces in terms of *n* independent velocities and displacements yields the general form of the equation of motion for a MDOF system:

$$M\ddot{X}+C\dot{X}+KX=F(t) \tag{4.35}$$

where:

$[M]$, global mass matrix,

$[C]$, global damping matrix, and

$[K]$, global stiffness matrix.

Therefore, the marine riser discretized by a number of beam elements, as showed in **Figure 4.3**, becomes a system with many, but finite degrees of freedom, and then the equation of motion as given by **Equation 4.35** is applicable. The next step is therefore to find the coefficients of the mass, damping and stiffness matrices in such equation. The vertical displacements of the riser are considered to be zero and thus are eliminated from the corresponding mass, damping and stiffness matrices, this is because vertical waves forces for the riser are not significant, see Morrison's equation, **Equation 4.29**.

The bending stiffness matrix for a beam element of constant cross section was given by **Clough and Penzien (1993)**:

$$K_B = \frac{2EI}{l^3}\begin{bmatrix} 6 & 3l & -6 & 3l \\ 3l & 2l^2 & -3l & l^2 \\ -6 & -3l & 6 & -3l \\ 3l & l^2 & -3l & 2l^2 \end{bmatrix} \tag{4.36}$$

where:

E, Young's modulus,

I, second moment of inertia, and,

l, length of the beam element.

The stiffness matrix of **Equation 4.36** was derived by application of the procedure outlined at the beginning of this section and the following Hermitian interpolation functions, also adopted from **Clough and Penzien (1993)**:

$$g_1(y) = 1 - 3\left(\frac{y}{l}\right)^2 + 2\left(\frac{y}{l}\right)^3 \tag{4.37a}$$

$$g_2(y) = 3\left(\frac{y}{l}\right)^2 - 2\left(\frac{y}{l}\right)^3 \tag{4.37b}$$

$$g_3(y) = y\left(1 - \frac{y}{l}\right)^2 \tag{4.37c}$$

$$g_4(y) = \frac{y^2}{l}\left(\frac{y}{l} - 1\right) \tag{4.37d}$$

The polynomials g_1 and g_2 define tranlational displacements and the polynomials g_3 and g_4 describe rotational displacements.

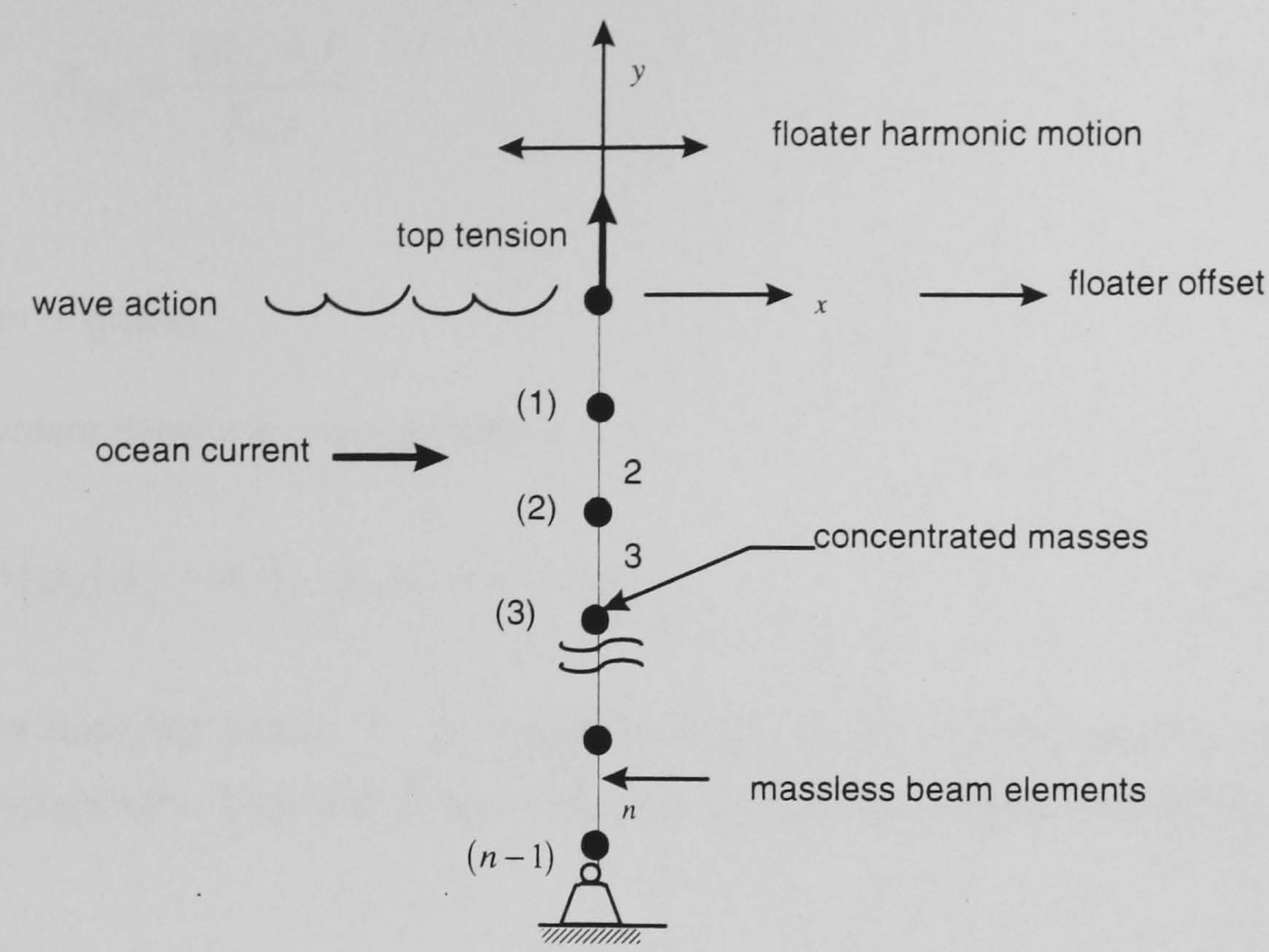

Figure 4.3. Riser finite element discretization and actions.

Inspection of **Equation 4.15** shows that there are two sources of stiffness on the riser, one due to the elastic and geometric properties of riser cross section, EI; and the second, arises from the applied tension at the top of the riser, which is turn affected by the external and internal pressures. Consequently, a second stiffness matrix that accounts for the effects of the externally applied tension is needed, this is called the *geometric stiffness* matrix. The form of the geometric stiffness matrix that was proposed by **Spanos and Chen (1980)** is adopted for the present work.

$$\frac{T_{TOP}}{l}\begin{bmatrix} \frac{3}{5}[(1-2i)R_{TW}+2] & \frac{l}{10}[1-iR_{TW}] & -\frac{3}{5}[(1-2i)R_{TW}+2] & \frac{l}{10}[1-(i-1)R_{TW}] \\ & \frac{l^2}{30}[(3-4i)R_{TW}+4] & -\frac{l}{10}[1-iR_{TW}] & \frac{l^2}{60}[(2i-1)R_{TW}-2] \\ & & \frac{3}{5}[(1-2i)R_{TW}+2] & -\frac{l}{10}[1-(i-1)R_{TW}] \\ SYMMETRIC & & & \frac{l^2}{30}[(1-4i)R_{TW}+4] \end{bmatrix}$$

(4.38)

where:

T_{TOP}, tension applied at the top of the riser, and

R_{TW}, ratio of element weight to top tension; given by:

$$R_{TW} = \frac{g\rho_{eq}A_e l}{T_{TOP}} \tag{4.39}$$

and:

g, acceleration of gravity;

ρ_{eq}, the equivalent density is given as follows:

$$\rho_{eq} = \left[\rho_S\left(A_E - A_I\right) - \rho_E A_E + \rho_I A_I\right]\frac{1}{A_E} \tag{4.40}$$

Concerning the damping matrix, C, in **Equation 4.35**, a form of damping proportional to the stiffness is adopted here. This kind of damping accounts for the material internal damping, **Petyt (1990)**.

$$C = a_0 K \tag{4.41}$$

where:

$$a_0 = \frac{2\xi_1}{\omega_1} \tag{4.42}$$

where:

ω_1, first natural circular frequency,

ξ, ratio of critical damping.

This particular form of damping heavily damps the higher modes of vibration, this effect is in agreement with **Daering and Huang (1979)**, who found by modal analysis that the first five modes of vibration are the ones with larger contribution to the total response.

A lumped mass approach is introduced for the present riser model. The masses of adjacent finite elements are concentrated at the intersection of adjacent nodes, thus the elemental mass matrix is:

$$m = \rho_{eq} A_E l \begin{bmatrix} \frac{1}{2} & 0 \\ 0 & \frac{1}{2} \end{bmatrix} \tag{4.43}$$

The advantage of this type of mass model is that no coupling effects are present and then the computational effort is reduced. Furthermore, the rotational displacement coefficients included in the stiffness and damping matrices can be expressed in terms of the translations by means of the ***static condensation*** technique, which is applied at a later stage.

The riser system represented by **Equation 4.35** is subjected to a forcing function given by Morison's load, **Equation 4.29**, namely:

$$F(t) = \rho_E V\dot{U} + \rho_E V(C_M - 1)(\dot{U} - \ddot{X}) + B|U - \dot{X}|(U - \dot{X}) \tag{4.44}$$

where:

V, the vector of elemental volumes is given by $V = (v_1, v_2, \ldots v_i)$ with, $v_i = \frac{\pi D_E^2}{4} l$, and

B, the matrix of hydrodynamic drag coefficients is assembled from the following elemental submatrices:

$$b_i = \begin{bmatrix} \frac{1}{4}\rho_E C_D l D_E & 0 \\ 0 & \frac{1}{4}\rho_E C_D l D_E \end{bmatrix} \tag{4.45}$$

The form of the submatrix of **Equation 4.45** indicates that drag coefficient C_D may vary from one element to another, according to depth. In this work, however, C_D is assumed constant along the riser length.

At this stage, the Morison's load, **Equation 4.29**, is to be explicitly introduced in the equation of motion, **Equation 4.35**, as follows:

$$M\ddot{X} + C\dot{X} + KX = \rho_E V\dot{U} + \rho_E V(C_M - 1)(\dot{U} - \ddot{X}) + B|U - \dot{X}|(U - \dot{X}) \tag{4.46}$$

Collecting riser displacement related terms on the left hand side and water kinematics related terms on the other:

$$\mathrm{M}\ddot{X} + \rho_E(C_M - 1)V + C\dot{X} + \mathrm{K}X = \rho_E C_M V\dot{U} + \mathrm{B}|U - \dot{X}|(U - \dot{X}) \tag{4.47}$$

and replacing

$$M + \rho_E(C_M - 1)V = M_T \tag{4.48}$$

and

$$\rho_E C_M V = M_H \tag{4.49}$$

Equation 4.46 becomes:

$$M_T\ddot{X} + C\dot{X} + KX = M_H\dot{U} + B|U - \dot{X}|(U - \dot{X}) \tag{4.50}$$

The top node of the riser, or boundary, is subjected to a harmonic displacement, due to surge of the floater to which it is attached. In order to account for these imposed displacements, the vector of displacements is separated into unknown internal displacements and prescribed boundary displacements, as follows:

$$X = \begin{bmatrix} X_I \\ X_B \end{bmatrix} \tag{4.51}$$

In the same fashion, the equation of motion, **Equation 4.50**, can be partition, **Patel and Sarohia (1984)**:

$$\begin{bmatrix} M_{T_{II}} & M_{T_{IB}} \\ M_{T_{BI}} & M_{T_{BB}} \end{bmatrix} \begin{bmatrix} \ddot{X}_I \\ \ddot{X}_B \end{bmatrix} + \begin{bmatrix} C_{II} & C_{IB} \\ C_{BI} & C_{BB} \end{bmatrix} \begin{bmatrix} \dot{X}_I \\ \dot{X}_B \end{bmatrix} + \begin{bmatrix} K_{II} & K_{IB} \\ K_{BI} & K_{BB} \end{bmatrix} \begin{bmatrix} X_I \\ X_B \end{bmatrix} =$$

$$\begin{bmatrix} M_{H_{II}} & M_{H_{IB}} \\ M_{H_{BI}} & M_{H_{BB}} \end{bmatrix} \begin{bmatrix} \dot{U}_I \\ \dot{U}_B \end{bmatrix} + \begin{bmatrix} B_{II} & B_{IB} \\ B_{BI} & B_{BB} \end{bmatrix} \begin{bmatrix} |U_I - \dot{X}_I|(V_I - \dot{X}_I) \\ |U_B - \dot{X}_B|(V_B - X_B) \end{bmatrix} + \begin{bmatrix} 0 \\ F_B \end{bmatrix} \tag{4.52}$$

where F_B is the force required to cause the prescribed surge of the surface platform. The dynamic response of the riser for the internal degrees of freedom can be obtained from the upper set of equations in **Equation 4.52**, and noting also that because of the lumped mass formulation adopted, the off-diagonal terms of M_T, M_H and B are zero, the following equations are obtained:

$$M_{TII}\ddot{X}_I + C_{II}\dot{X}_I + K_{II}X_I = M_{HII}\dot{U}_I + B_{II}|U_I - \dot{X}_I|(U_I - \dot{X}_I) - C_{IB}\dot{X}_B - K_{IB}X_B \tag{4.53}$$

For convenience, the procedure for the treatment of the prescribed boundary displacements was described first, **Equation 4.53**; however, it should be noted that submatrices for the internal and boundary nodes in the damping and stiffness matrices in **Equation 4.52**, contain both translational as well as rotational degrees of freedom. Since the lump mass model was adopted, the stiffness and damping matrices must be further compacted, so that the order of these two matrices is consistent with the order of mass and hydrodynamic drag matrices, both of which depend on the translational displacements only. The procedure required to achieve a reduction of the degrees of freedom consists in expressing the rotational displacements in terms of the translations, this process is known as *static condensation*, which is adopted here from **Clough and Penzien (1993)** and is described in the following.

The stiffness matrix K given by **Equation 4.46**, can be partitioned by separating the translational from the rotational degrees of freedom:

$$\begin{bmatrix} K_{tt} & K_{tr} \\ K_{rt} & K_{rr} \end{bmatrix} \begin{bmatrix} X_t \\ X_r \end{bmatrix} = \begin{bmatrix} f_t \\ 0 \end{bmatrix} \tag{4.54}$$

where the subindices t and r stand for translation and rotation, respectively. Now, from the second set of equations in **Equation 4.54**,

$$X_r = \theta - K_{rr}^{-1} K_{rt} X_t \qquad (4.55)$$

Substituting **Equation 4.55** in first subset of equations in **Equation 4.54**:

$$K_{tt} X_t + K_{tr}\left(-K_{rr}^{-1} K_{tr} X_t\right) = f_t \qquad (4.56)$$

$$\left(K_{tt} - K_{tr} K_{rr}^{-1} K_{tr}\right) X_t = f_t \qquad (4.57)$$

or,

$$[K]\{x\} = F \qquad (4.58)$$

where:

$$K = K_{tt} - K_{tr} K_{rr}^{-1} K_{rt} \qquad (4.59)$$

Equation 4.59 is the system stiffness matrix, in which the number of degrees of freedom has been reduced by a factor of two, and is now consistent with the mass matrix. Once the finite element solution for the displacements X is available it is possible to find the rotational displacements by means of **Equation 4.55**.

The reduced order stiffness matrix from **Equation 4.59** has to be further partitioned in order separate the boundary node from the internal horizontal degrees of freedom:

$$K = \begin{bmatrix} K_{II} & K_{IB} \\ K_{BI} & K_{BB} \end{bmatrix} \qquad (4.60)$$

Equation 4.60 is the stiffness matrix introduced in **Equation 4.52**. Since the damping of the system is stiffness proportional, the damping proportionality coefficient, a_0, **Equation 4.41** can be applied directly to **Equation 4.60**.

4.4. Finite Element Static Analysis.

In the same manner as the differential equation for static analysis was derived as a particular case from the differential equation of motion, the finite element equation for static analysis is a particular case of the finite element equation of motion.

In the case of static analysis the inertial forces do not participate, neither dissipative forces, and the external load is assumed to be time invariant. Therefore, **Equation 4.53** becomes;

$$K_{II}X_I = \frac{1}{2}\rho_E C_D D_E U_C(y)|U_C(y)| - K_{IB}X_B \qquad (4.61)$$

The first right hand side term of **Equation 4.61** corresponds to the steady ocean current, the second one belongs to the imposed boundary displacement, X_B , due to floating platform offset.

4.5. Method of Solution.

It was established in **Section 1.2.1** that a frequency domain approach is to be followed for the dynamic analysis. Nevertheless, because of the possible interaction of steady ocean current velocity and wave particle velocity there are two alternatives to perform the static and dynamic analyses. One is to carry out the static and dynamic analysis simultaneously by combining the current velocity and the relative velocity of wave and structure in the expression for Morison's load, that is:

$$F(t) = \rho_E V\dot{U} + \rho_E V(C_M - 1)(\dot{U} - \ddot{X}) + B|U_C + U - \dot{X}|(U_C + U - \dot{X}) \qquad (4.62)$$

where:

U_C, ocean current.

Such approach is followed by **Spanos and Chen (1980)** and **Daering and Huang (1979)**. The second alternative is to perform separated static and dynamic analyses. In the static case the load considered is ocean current only and the imposed boundary displacement is the one due to floating platform static offset; the dynamic analysis includes wave actions and harmonic displacements of platform as well. Static and dynamic effects are finally superimposed. This scheme is used by **Patel and Sarohia (1984)**, **Burke (1974)** and **Young, et al (1978)**. The later approach is adopted here for the solution of the finite element model.

4.5.1. Static Solution.

The static solution is accomplished by solving the system of equations given in **Equation 4.61** for the internal displacements, X_I. It should be noted that non-linear effects are not considered, see **Figure 4.4a**

4.5.2. Dynamic Solution.

The solution for the dynamic case is performed in the frequency domain, the external loads considered are illustrated in **Figure 4.4b**. The application of the frequency domain approach requires linearization of the drag related term, **Equation 4.53**, such drag term is:

$$B_{II}\left|U_I - \dot{X}_I\right|\left(U_{II} - \dot{X}_I\right) \qquad (4.63)$$

The following linear form is proposed by **Patel and Sarohia (1984)** and adopted here:

$$B_{eq}\left(U_I - \dot{X}_I\right) = B_{II}\left|U_I - \dot{X}_I\right|\left(U_I - \dot{X}_I\right) \qquad (4.64)$$

Therefore, substituting **Equation 4.64** in the equation of motion, **Equation 4.53**, and collecting riser displacement terms on the left hand side and wave kinematics terms and the terms related to the imposed boundary motion on the right hand side, the linearized equation of motion is:

$$M_{TII}\ddot{X}_I + \left(C_{II} + B_{eq}\right)\dot{X}_I + K_{II}X_I = M_{HII}\dot{U} + B_{eq}U - C_{IB}\dot{X} - K_{IB}X \qquad (4.65)$$

Before the explicit form of the linearized equivalent drag term, B_{eq}, can be derived, it is necessary to adopt a particular wave theory for determination of the wave particle kinematics. The linear theory, Airy, is assumed for the present work. The horizontal wave partied velocities and acceleration, adopted from **Clauss, et. al. (1992)**, are given respectively by:

$$U = \zeta_a \omega \frac{\cosh(y+d)}{\sinh kd}\cos(\theta) \qquad (4.66)$$

and

$$\dot{U} = \zeta_a \omega^2 \frac{\cosh(y+d)}{\sinh kd}\sin(\theta) \qquad (4.67)$$

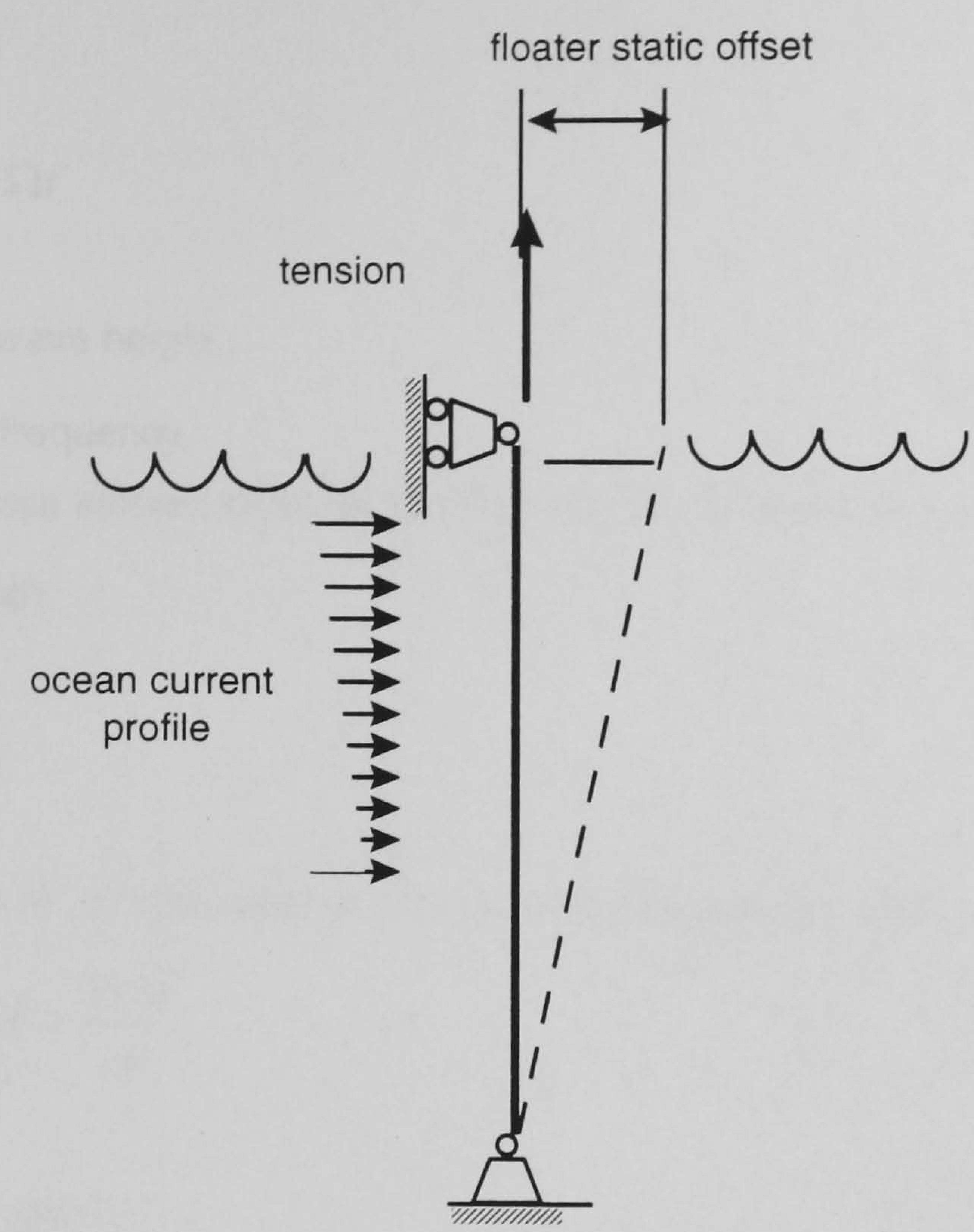

Figure 4.4a. Loads for riser static analysis.

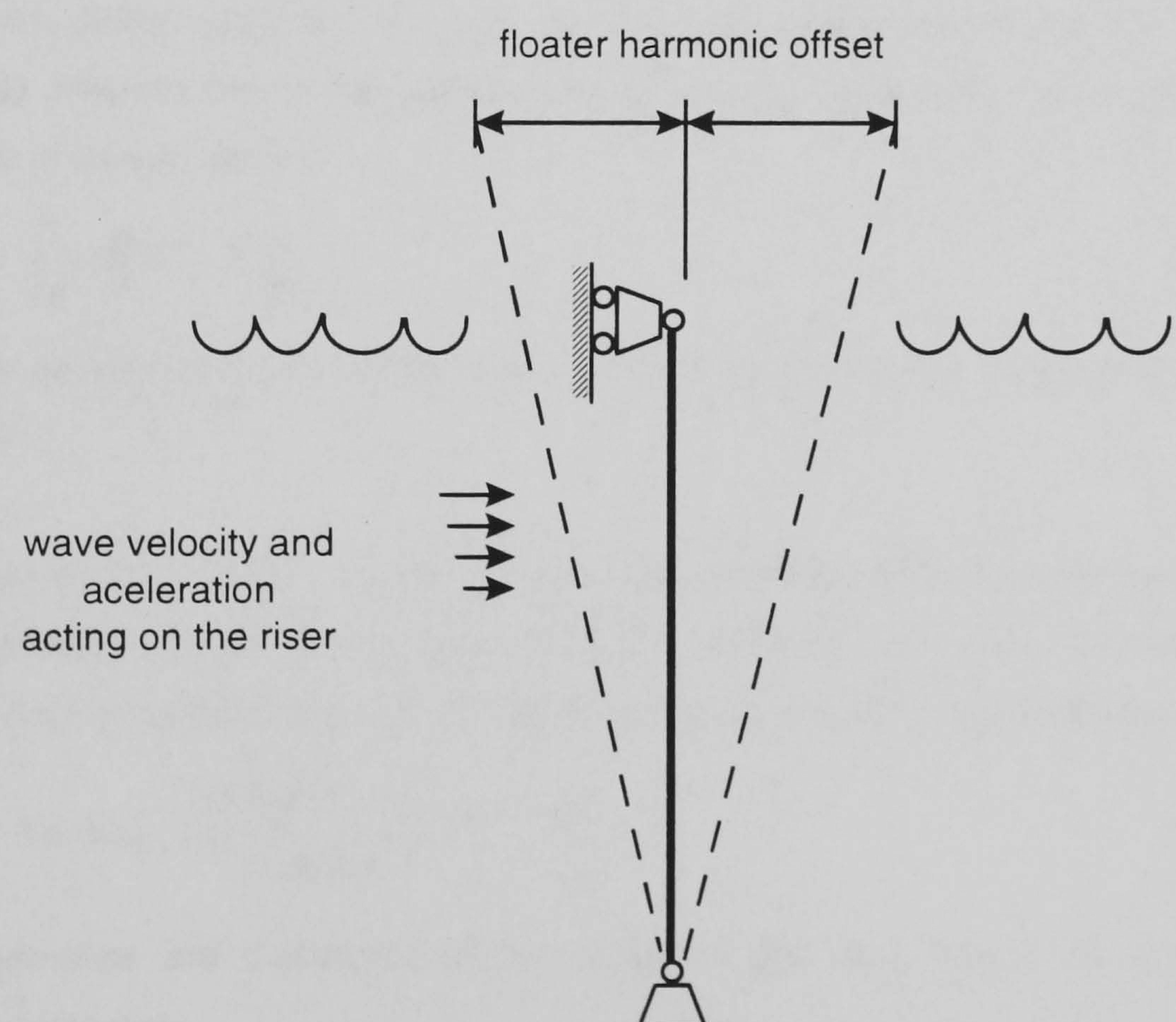

Figure 4.4b. Loads for riser dynamic analysis.

with:

$$\theta = kx - \Omega t \tag{4.68}$$

where:

ζ_a , amplitude of wave height,

Ω , wave circular frequency,

y , distance from sea surface to depth at which velocity or acceleration are required,

d , total water depth,

t , time, and

k , wave number.

The wave number, k , is obtained from the so called dispersion relation:

$$kd \tanh kd = \frac{\Omega^2 d}{g} \tag{4.69}$$

where:

g , acceleration of gravity.

The wave number, given by **Equation 4.69**, can be found by an iterative scheme.

The linearized form of the drag term, B_{eq}, in **Equation 4.65** can be obtained by equating the work done by the non-linear drag and the one done by the proposed linearized form. **Patel and Sarohia (1984)** obtained one of the expressions for the linearized drag, which will be used here for the dynamic analysis, namely:

$$B_{eq} = \frac{8}{3\pi} B \left| \left(U - \dot{X} \right)_{\max} \right| \tag{4.70}$$

with B already defined by the assembling of elemental hydrodynamic drag submatrices, given by **Equation 4.45**.

In order to solve the equations of motion, as given by **Equation 4.65**, the approach suggested by **Patel and Sarohia (1984)** is adopted here. For convenience, the complex form of the expressions for wave particle kinematics, **Equation 4.66** and **4.67**, are introduced, as follows:

$$U_w = \mathrm{Re}\left[\Omega \zeta_a \frac{\cosh k(y+d)}{\sinh kd} e^{i(kx - \Omega t)} \right] \tag{4.71}$$

The wave kinematics are calculated at the center of the pipe, that is at $x = 0$, therefore, **Equation 4.71** becomes:

$$U_w = \mathrm{Re}\left[\Omega \zeta_a \frac{\cosh k(y+d)}{\sinh kd} e^{-i\Omega t} \right] \tag{4.72}$$

or,

$$U_w = \mathrm{Re}\left(U_w' e^{-i\Omega t}\right) \tag{4.73}$$

where U_w' is the complex amplitude.

Therefore the wave particle acceleration becomes:

$$\dot{U}_w = \mathrm{Re}\left(-i\Omega U_w' e^{-i\Omega t}\right) \tag{4.74}$$

The steady state response of the riser governed by **Equation 4.65** to a sinusoidal excitation will also be proportional to $e^{-i\Omega t}$. Then the riser displacements, velocities and accelerations are given by:

$$X = \mathrm{Re}\left(X' e^{-i\Omega t}\right) \tag{4.75a}$$

$$\dot{X} = \mathrm{Re}\left(-i\Omega X' e^{-i\Omega t}\right) \tag{4.75b}$$

$$\ddot{X} = \mathrm{Re}\left(-\Omega^2 X' e^{-i\Omega t}\right) \tag{4.75c}$$

In the same manner, the complex form of the imposed displacements and velocities at the boundary are:

$$X_B = \mathrm{Re}\left(X_B' e^{-i\Omega t}\right) \tag{4.76a}$$

$$\dot{X}_B = \mathrm{Re}\left(-i\Omega X_B' e^{-i\Omega t}\right) \tag{4.76b}$$

By substitution of **Equations 4.73, 4.74, 4.75** and **4.76** in **Equation 4.65** the equation of motion becomes:

$$-\Omega^2 M_{TII} X' e^{-i\Omega t} - i\Omega\left(C_{II} + B_{eq\,II}\right) X' e^{-i\Omega t} + K_{II} X' e^{-i\Omega t} =$$

$$-i\Omega M_{HII} U_W' e^{-i\Omega t} + B_{eqII} U_W' e^{-i\Omega t} + i\Omega C_{IB} X_B' e^{-i\Omega t} - K_{IB} X_B' e^{-i\Omega t} \tag{4.77}$$

Simplifying **Equation 4.77**:

$$\left\{K_{II} - \Omega^2 M_{TII} - i\Omega\left(C_{II} + B_{eqII}\right)\right\} X' = -i\Omega M_{HII} U_w' + i\Omega C_{IB} X_B' - K_{IB} X_B' = F' \tag{4.78}$$

Equation 4.78 is the complex equation of motion governing the riser dynamics. However, because the equivalent drag term depends on the still unknown riser horizontal velocity, **Equation 4.78** has to be solved iteratively, **Patel and Sarohia (1984)** proposed the following approximation of the equivalent damping term as initial iteration:

$$B_{eq} = 0.20 \begin{bmatrix} \left(M_{TII} K_{II}\right)_{11}^{1/2} & & \\ & \left(M_{TII} K_{II}\right)_{22}^{1/2} & \\ & & \left(M_{TII} K_{II}\right)_{nn}^{1/2} \end{bmatrix} \tag{4.79}$$

which is adopted here.

There is a number of methods available to solve **Equation 4.78**. In order to describe the approach to be employed here, from **Petyt (1990)**, the equation of motion, **Equation 4.78**, can be rewritten in the following way:

$$\{A_R + A_I\} \cdot (X_R + X_I) = (F_R + F_I) \tag{4.80}$$

where the real and imaginary parts of the resisting and excitation forces have been conveniently grouped, as follows:

$$A_R = \left(K_{II} - \Omega^2 M_T\right)_R \tag{4.81a}$$

$$A_I = -\Omega\left(C_{II} - Beq_{II}\right)_I \tag{4.81b}$$

$$F_R = \left(Beq_{II} U_w'\right)_R - \left(K_{IB} X_B'\right)_R \tag{4.82a}$$

$$F_I = \left(\Omega C_{IB} X_B'\right)_I - \left(\Omega M_H U_w'\right)_I \tag{4.82b}$$

Performing explicitly the multiplication indicated by **Equation 4.80** and recalling that $i \cdot i = -1$, and $i \cdot n_R = in = n_I$ and collecting real and imaginary parts,

$$\left.\begin{array}{lll} A_R \cdot X_R & -A_I \cdot X_I & = F_R \\ A_I X_R & +A_R X_I & = F_I \end{array}\right\} \tag{4.83}$$

Now, expressing **Equation 4.83** in matrix form and substituting **Equations 4.81** and **4.82**, the following expression is obtained:

$$\begin{bmatrix} K_{II} - \Omega^2 M_T & \Omega\left(C_{II} + Beq_{II}\right) \\ -\Omega\left(C_{II} + Beq_{II}\right) & K_{II} - \Omega^2 M_T \end{bmatrix} \begin{bmatrix} X_R \\ X_I \end{bmatrix} = \begin{bmatrix} Beq_{II} U_w' - K_{IB} X_B' \\ \Omega\left(C_{IB} X_B' - M_H U_w'\right) \end{bmatrix} \tag{4.84}$$

The submatrix $\left[K_{II} - \Omega^2 M_T\right]$ becomes singular or near singular when the excitation frequency becomes equal or nearly equal to the natural frequency of vibration. However, with the equation of motion as given by **Equation 4.84** there are two possible directions to proceed for its solution. Gauss elimination with row interchange can be applied. Alternatively it is possible to apply Crout factorization, in which the matrix of coefficients on the left hand side of the system is expressed as the LU product. The second method of solution is adopted here. On the other hand, the disadvantage of expanding the equations of motion in the form showed in **Equation 4.84** is that the system of equations to be solved is twice as large as in the original system of equations. Though, as already mentioned, the later approach provides an option to deal with the singularity incurred when the frequency of excitation is equal or near equal to the natural frequency.

4.5.3. Total Solution.

The displacements obtained from the static and dynamic analyses of the riser, as described in **Sections 4.5.1** and **4.5.2** respectively, are superposed, in order to obtain the total displacements. The bending stresses are calculated subsequently, as explained in **Section 4.5.5**. The axial stresses due to the externally applied top tension are obtained separately, as described in **Section 4.5.4**.

4.5.4. Determination of the Axial Stresses.

Spanos and Chen (1980) provided the following expression for determination of axial stress on the riser at node i :

$$\sigma_{ai} = \frac{T_{TOP}}{A_S}\left[1-(i-l)R_{TW}\right] \tag{4.85}$$

where:

T_{TOP} , tension applied at the top of the riser,

R_{TW} , ratio of top tension to weight, as given by **Equation 4.39**,

A_S , cross section area of riser pipe.

4.5.5. Determination of Bending Stresses.

The bending stresses are determined from the theory of beam deflections, **Buchanan (1988)**:

$$\frac{d^2 x^*}{dy^2} = \frac{M}{EI} \tag{4.86}$$

where x^* is the transverse deflection from the undeflected position. The foregoing deflection is the combined result of tranlational and rotational displacements at the nodes, as the result from the static condensation procedure applied, **Equation 4.58**. Furthermore, as indicated by **Spanos and Chen (1980)**, the deflection can be expressed in terms of the nodal displacements and the interpolation functions, **Equations 4.37**, used for construction of the bending stiffness matrix, namely:

$$x^*_{(i)}(y) = x^*_i g_1(\bar{y}) + x^*_{i-1} g_2(\bar{y}) + \theta^*_i g_3(\bar{y}) + \theta^*_{i-1} g_4(\bar{y}); \qquad 0 \le \bar{y} \le l \tag{4.87}$$

where:

g_i, interpolation functions given by **Equations 4.37**,

x^*_i, tranlational displacements,

θ^*_i, rotational displacements.

The asterisks, again, are used to denote that the displacements are referred to the undeflected position. The values of the rotational displacements are obtained from the expressions of static condensation, **Equation 4.55**.

In order to obtain the bending moments, the second derivative of **Equation 4.87** is introduced in **Equation 4.86** and subsequently with the value of the moment found in this way the well known flexural formula can be applied:

$$\sigma = \frac{Mc}{I} \tag{4.88}$$

where:

σ, bending stress,

c, distance from the fibre of interest to the neutral axis.

4.6. Riser Analysis Results and Validation.

In order to obtain the necessary information concerning the accuracy and dependability of the riser model to be used in the present work, and described in the previous sections, a number of riser cases were taken from the published literature and their results compared with the ones obtained with this model.

4.6.1. Natural Frequencies.

The natural frequencies of the riser are the first comparison case. For this purpose riser data is presented in **Table 4.1**, taken from **Daering and Huang (1976)**, who solved the differential equations of motion by means of a method of power series. The natural frequencies obtained by them for a 152.4 m. (500 ft.) riser are presented in the last column of **Table 4.2**.

Weight of riser, including 554.57 N/m (38 lb/ft) for choke and kill lines.	w	3123.09 N/m (214 lb/ft)
External cross section area	A_E	0.292 m^2 (3.14 ft^2)
Internal cross section area	A_I	0.278 m^2 (2.99 ft^2)
Sea water density	ρ_w	1037.99 kg/m^3 (64.8 lb/ft^3)
Drilling mud density	ρ_m	1361.16 kg/m^3 (85 lb/ft^3)
Second moment of inertia	I	1.3056×10^3 (3136.9 in^4)
Modulus of elasticity	E	2.07×10^{11}Pa (4.32×10^6 lb/ft^2)
Tension at bottom	T_B	1272128 N (286 000 lb)
Mass, including hydrodynamic added mass	m	995.91 kg/m (20.8 slugs/ft)

Table 4.1. Data for riser natural frequencies, after **Daering and Huang (1976)**.

Spanos and Chen (1980) derived the natural frequencies for the same riser analyzed by **Daering and Huang (1976)**, this time using a finite element approach, these results are given in **Table 4.2** and are compared with the frequencies derived with the computer program written for the purposes of this work. As can be observed from this table the natural frequencies accomplished here compare well with the results from the researchers already mentioned.

Mode	Number	of	Elements				Ref. 1
	6	6	10	10	20	20	
	Ref. 2	This work	Ref. 2	This work	Ref. 2	This work	
1	0.831	0.8305	0.831	0.8306	0.831	0.8307	0.815
2	1.827	1.8267	1.831	1.8307	1.831	1.8311	1.804
3	3.083	3.0825	3.120	3.1196	3.123	3.1231	3.088
4	4.555	4.5541	4.761	4.7603	4.778	4.7775	4.737
5	5.925	5.9246	6.767	6.7658	6.832	6.8308	6.789
6			9.093	9.0922	9.301	9.3001	
7			11.604	11.6031	12.193	12.1917	
8			14.008	14.0067	15.506	15.5044	
9			15.826	15.8241	19.232	19.2295	
10					23.352	23.3492	
11					27.835	27.8321	
12					32.630	32.6270	
13					37.658	37.6540	
14					42.798	42.7939	
15					47.881	47.8763	
16					52.678	52.6724	
17					56.904	56.8981	
18					60.243	60.2372	
19					62.397	62.3912	

Ref. 1: **Daering and Huang (1976).**
Ref. 2: **Spanos and Chen (1980).**

Table 4.2. Comparison of natural frequencies for a 500 ft long riser. Frequencies in radians per second.

In order to verify more completely the performance of this code, one more case was analyzed. The riser used by **Spanos and Chen (1980)** for their parametric study was also used here for comparison of the natural frequencies. The data for this case is available in **Table 4.3**. In the same fashion, the values of the natural frequencies obtained in here are compared with the ones provided by the above mentioned authors and are presented in **Table 4.4**. As in the case before, it can be noticed that the values in both cases compare adequately.

Length, m. (ft.)	182.88 (600)	365.76 (1200)	609.60 (2000)
Diameter, m. (in)	0.4064 (16)	0.4064 (16)	0.4064 (16)
Modulus of elasticity, Pa (lb/ft^2)	2.001×10^{11} (4.18×10^9)	2.001×10^{11} (4.18×10^9)	2.001×10^{11} (4.18×10^9)
Second moment of inertia, m^4 (ft^4)	4.35×10^{-4} 0.0504	4.35×10^{-4} 0.0504	4.35×10^{-4} 0.0504
weight, including added mass, N/m (lb/ft)	3939.77 (269.96)	3939.77 (269.96)	3939.77 (269.96)
C_I	0.5	0.5	0.5
C_D	0.7	0.7	0.7
Top tension, N (lb)	1.2 × weight	1.2 × weight	1.2 × weight

Table 4.3. Data for riser natural frequencies, after **Spanos and Chen (1980)**.

Length / Mode	600 ft Ref. 3	600 ft This work	1200 ft Ref. 3	1200 ft This work	2000 ft Ref. 3	2000 ft This work
1	0.541	0.5415	0.363	0.3633	0.279	0.2789
2	1.207	1.2068	0.746	0.7463	0.564	0.5645
3	2.047	2.0476	1.152	1.1518	0.854	0.8542
4	3.096	3.0959	1.582	1.5822	1.149	1.1496
5	4.359	4.3597	2.031	2.0312	1.450	1.4501
6	5.812	5.8128	2.418	2.4823	1.753	1.7537
7	7.370	7.3707	2.911	2.9117	2.056	2.0562
8	8.853	8.8536	3.313	3.3150	2.352	2.3518
9	10.006	10.0069	3.757	3.7570	2.634	2.6339
10					2.901	2.9011
11					3.164	3.1647
12					3.442	3.4425
13					3.751	3.7510
14					4.121	4.1211

Ref. 3: **Spanos and Chen (1980).**

Table 4.4. Comparison of natural frequencies (radians / sec.).

It is worth to observe at this stage that though **Spanos and Chen (1980)** do not submit an explicit derivation of the differential equation on which their finite element model is based, a good degree of approximation of their natural frequencies with those contributed by **Daering and Huang (1976)**, see **Table 4.2**, demonstrates that the geometric matrix proposed by the first authors accurately models the characteristic influence of tension and weight on the riser stiffness, i.e. the effective tension and buoyant weight. Indeed, recalling that the natural frequencies depend only on the stiffness and mass properties of the system, $\left[K-\varpi^{2}M\right]$, the correlation of natural frequencies confirms that the stiffness and mass are correctly modeled.

4.6.2. Bending Stresses.

In a second step for assessment of the riser analysis approach followed in this work, the bending stresses rendered by the present model were compared against those available in the literature. The first case corresponds to **Burke (1974)** who presented the distribution of the bending stresses along the depth of a 365.76 m. (1200 ft) drilling riser. The characteristics of such riser were provided in **Table 4.5**, and the motion characteristics of the floating platform to which it is supported are showed in **Figure 4.5**. The bending stress distributions for three different combinations of wave height and period, as given by **Burke (1974)**, are illustrated in **Figure 4.6**.

The stress distributions obtained in this work can be observed in **Figures 4.7a**, **4.7b** and **4.7c**. It can be noticed that in the three cases the maximum stresses obtained in this work are somehow larger than those stated by the aforementioned author; however, the distributions possess a reasonable degree of similarity. It is important to notice that the distributions displayed in **Figure 4.6** do not seem to indicate clearly the values of the stresses at the top of the riser.

Length	1200 ft	1600ft.
$E \times I$, lb/ft^2	1.62×10^8	1.62×10^8
Weight, lb/ft	92 (in water)	92 (in water)
External Diameter, ft	1.67	1.67
Internal Diameter, ft	1.25	1.25
C_I	0.5	0.5
C_D	0.7	0.7
Static Top Tension, Kips	257	322

Table 4.5. Data for riser bending stresses, after **Burke (1974)**.

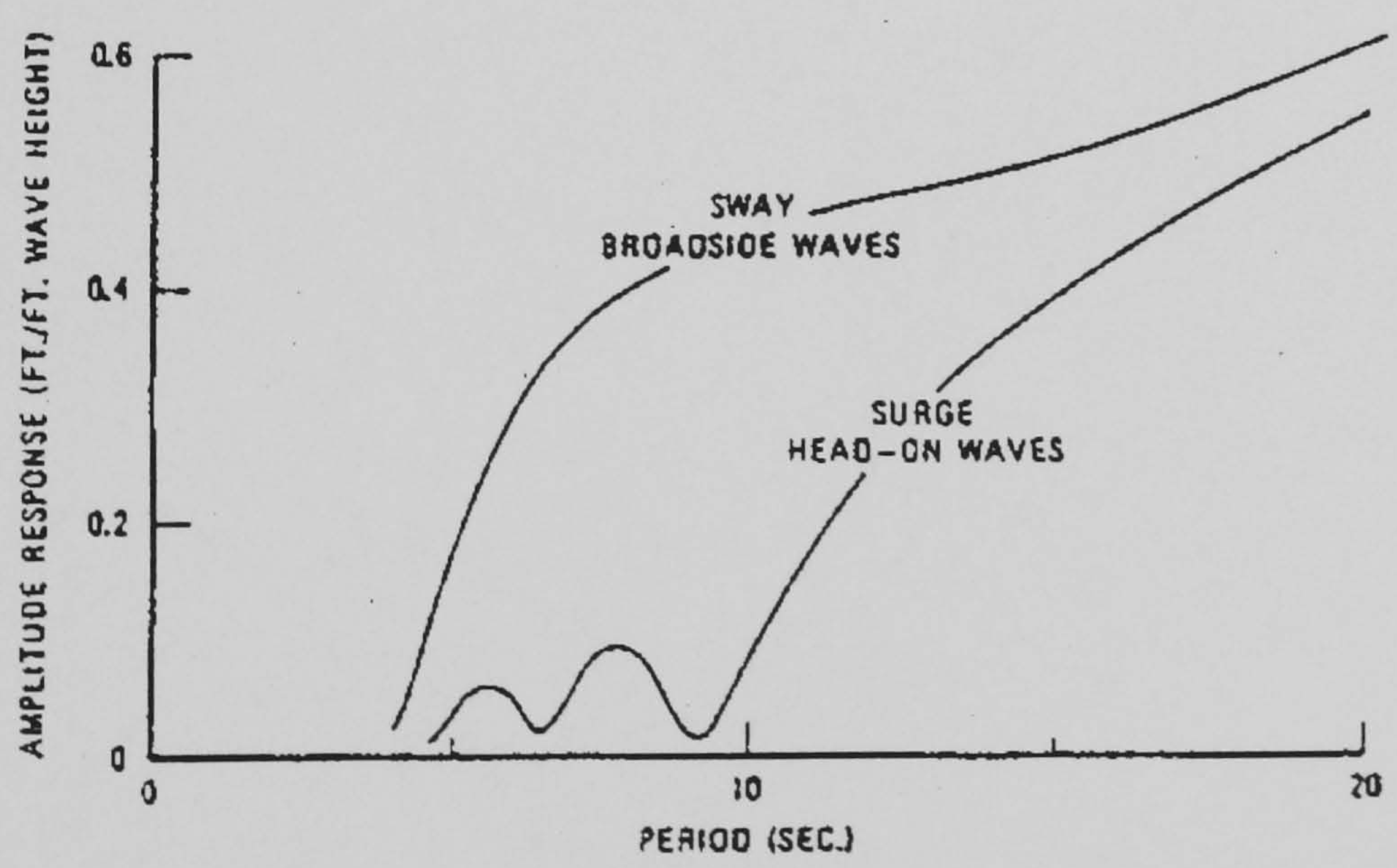

Figure 4.5. Surge and sway response for a drilling barge, after **Burke (1974)**.

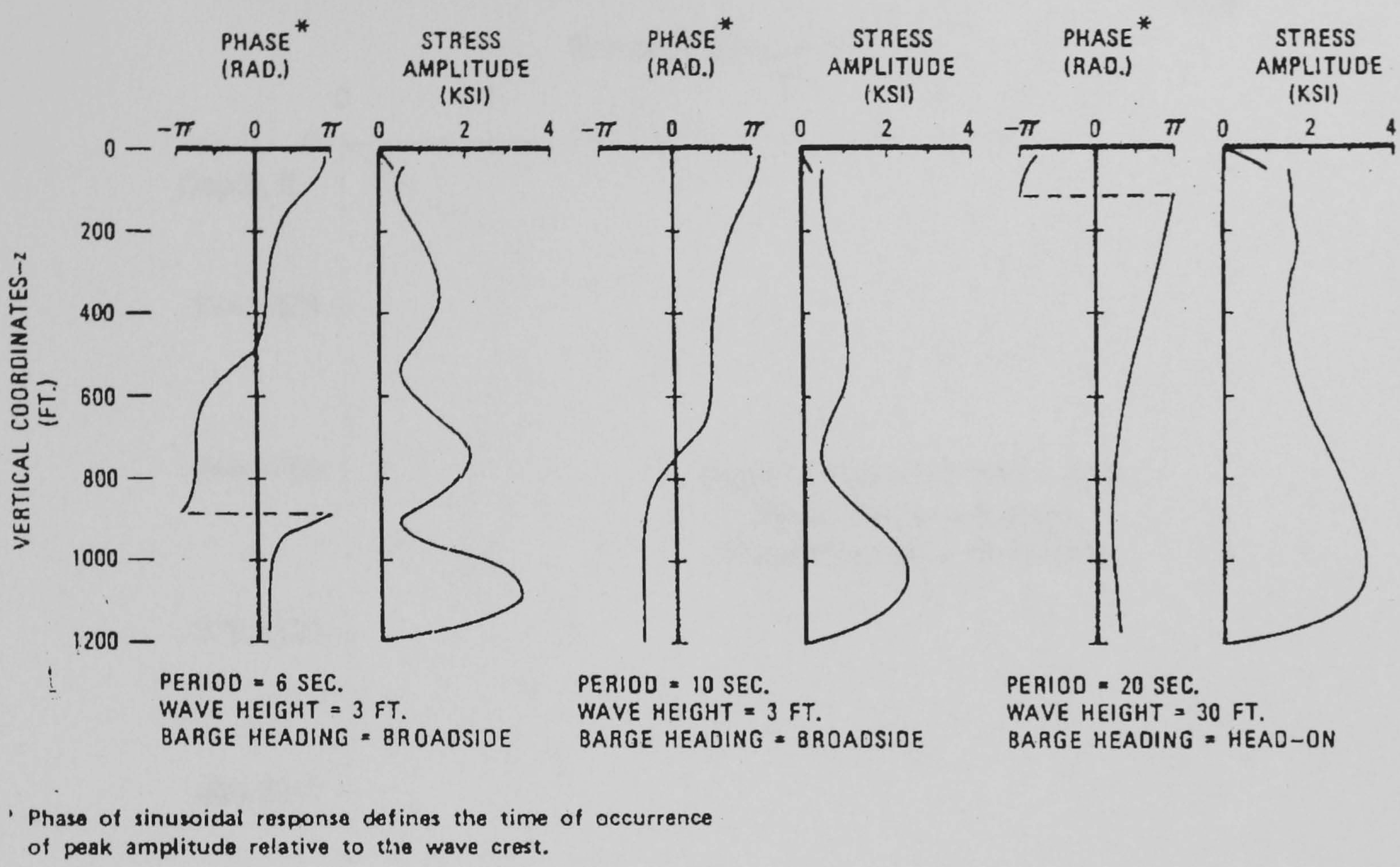

Figure 4.6. Distribution of bending stress with riser depth, after **Burke (1974)**.

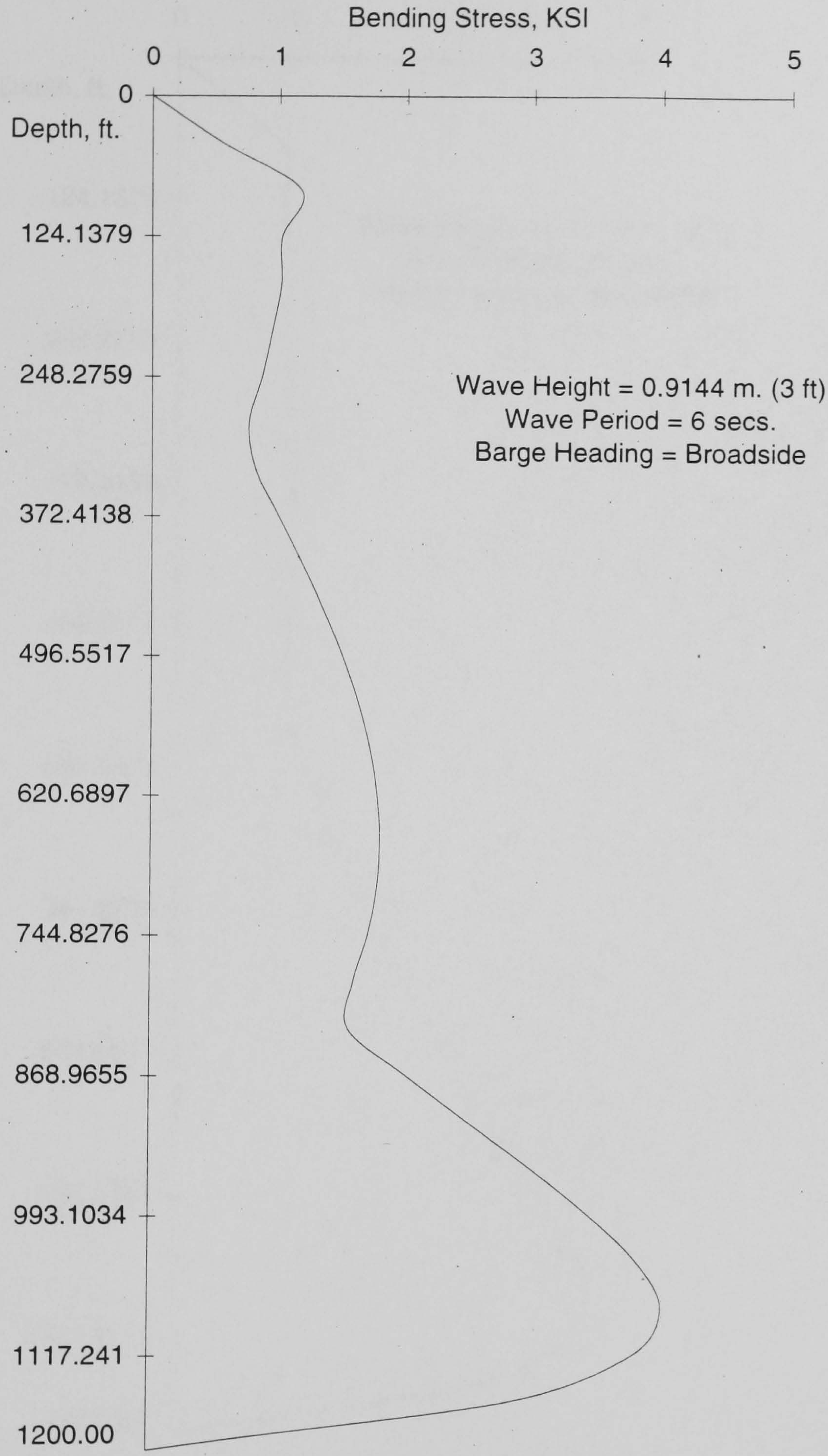

Figure 4.7a. Bending stress distribution. 365.76 m. (1200 ft) 0.4064 m. (16 in) riser.

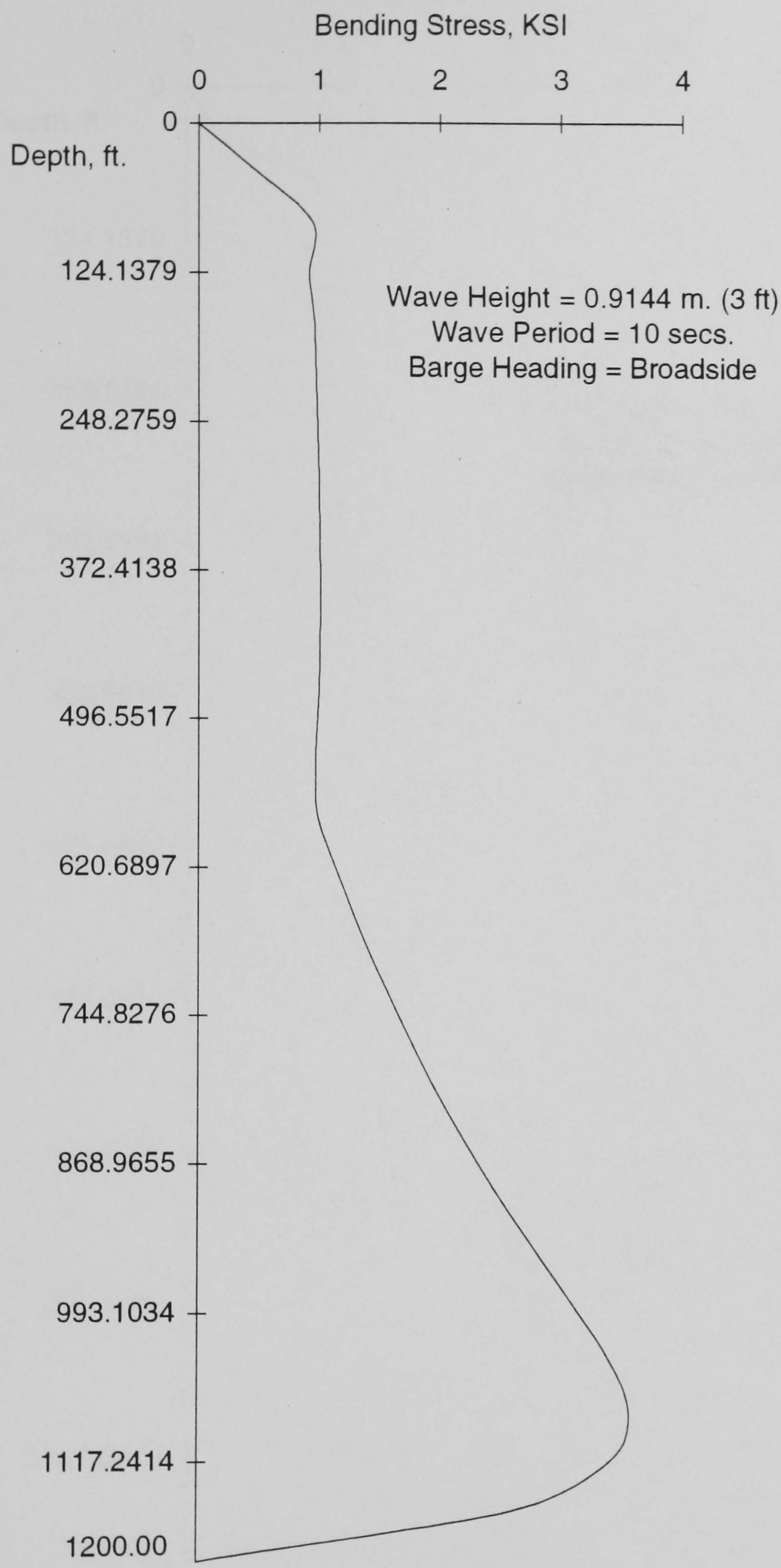

Figure 4.7b. Bending stress distribution. 365.76 m. (1200 ft) 0.4064 m. (16 in) riser.

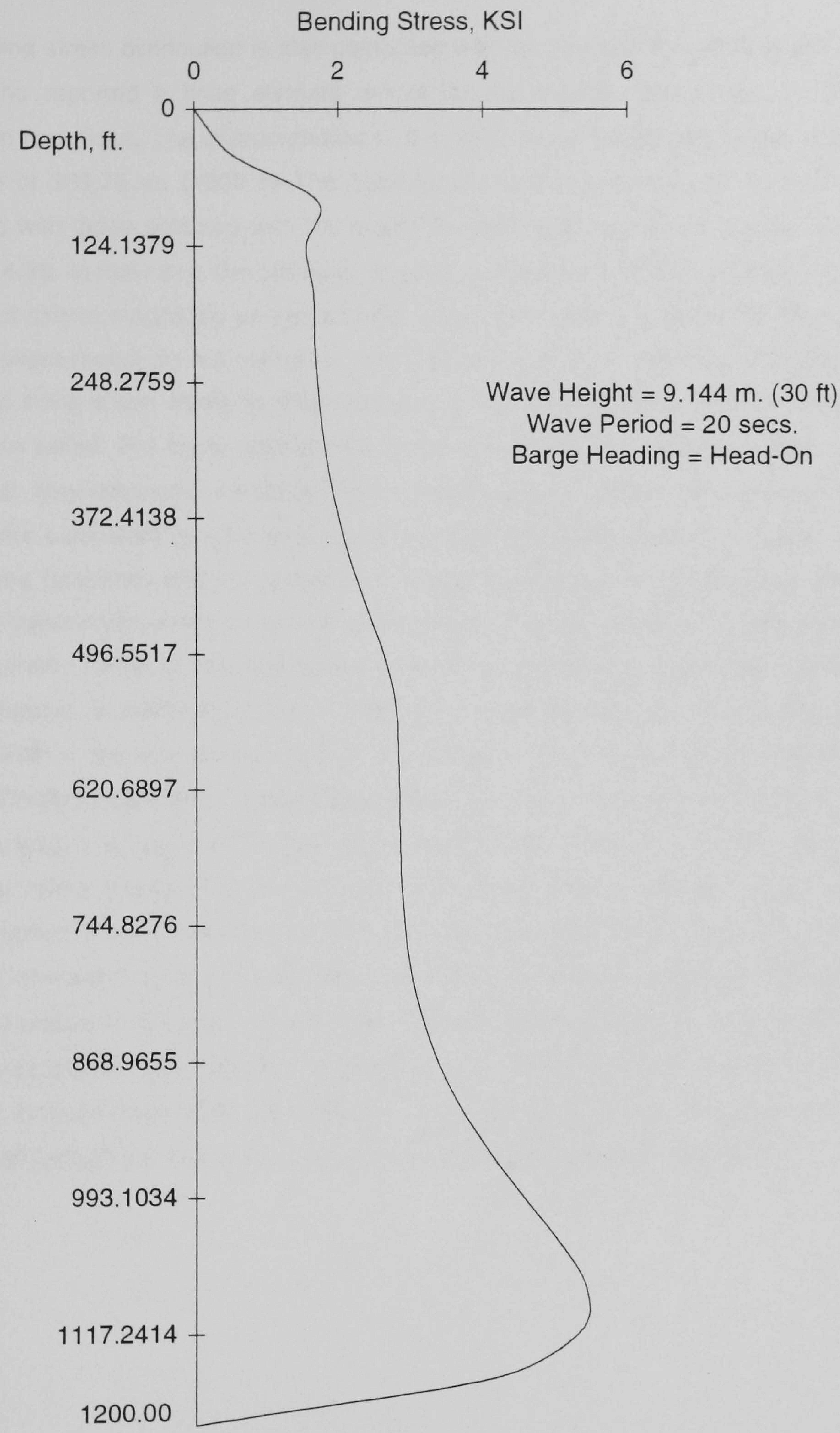

Figure 4.7c. Bending stress distribution. 365.76 m. (1200 ft) 0.4064 m. (16 in) riser.

The bending stress distribution is also compared with the one contributed by **Spanos and Chen (1980)** who reported a finite element model for the marine riser based on the equivalent linarization technique. The characteristics of that riser were already introduced in **Table 4.3**, for the depth of 365.76 m. (1200 ft) The bending stress distributions given by such authors are compared with those obtained with the model for the present work and are showed in **Figures 4.8a** and **4.8b**. In this case, the stresses reported by **Spanos and Chen (1980)** at the top of the riser are of similar magnitude as those found at the lower part of it, whilst the stresses predicted by the present model do not contain a prominence as large at that section of the riser. As an attempt to bring some clarity to this discrepancy, the stress distributions contributed by other authors are called. The stress distributions featured by **Patel and Sarohia (1982)** are showed in **Figure 4.9**, they employed a finite element model based on a differential equation that explicitly features the equivalent tension and buoyant weight, **Equation 4.30**, and presented both time domain and frequency domain analysis for a 500 ft long riser. It can be seen that a common feature of these distributions is that the larger values of stress are found at both ends of the riser, but the general forms of the distributions are not strictly similar to the ones presented in the previous figures. In a similar fashion, a 1371.60 m. (4500 ft) riser was analyzed by **Gardner and Kotch (1976)** in the time domain with a finite element model, based on the differential equation given by **Chakrabarti (1990)**, namely **Equation 4.30**. Such riser is presented here for reference in **Figure 4.10**. It is observed that the stress distribution in this case is rather different than the ones cited before, however the characteristic of the maximum stresses being at either ends of the riser is retained. It must be borne in mind, of course, that all the risers presented in **Figures 4.6** to **4.10** hold different lengths and this factor does influence the stress distribution; furthermore, the dynamic analysis of the riser of **Patel and Sarohia (1982)** was made on a non-linear statically stable configuration, and the riser of **Gardner and Kotch (1976)** accounts for the non-linear effects of Morison's equation. Nevertheless, the main objective of this comparison is to exhibit that different analytical approaches reported yield different stress distributions.

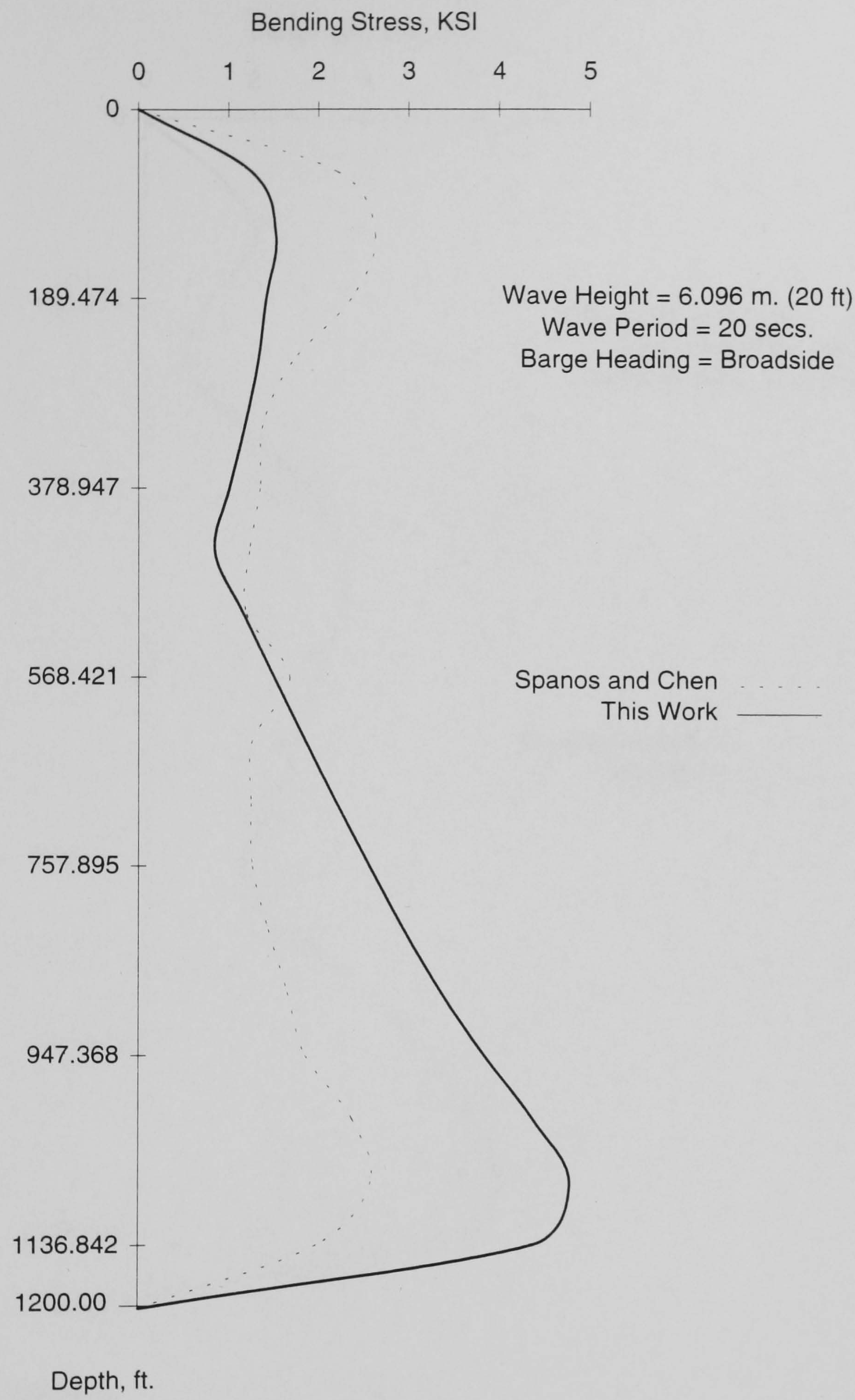

Figure 4.8a. Bending stress distribution. 365.76 m. (1200 ft) 0.4064 m. (16 in) riser.

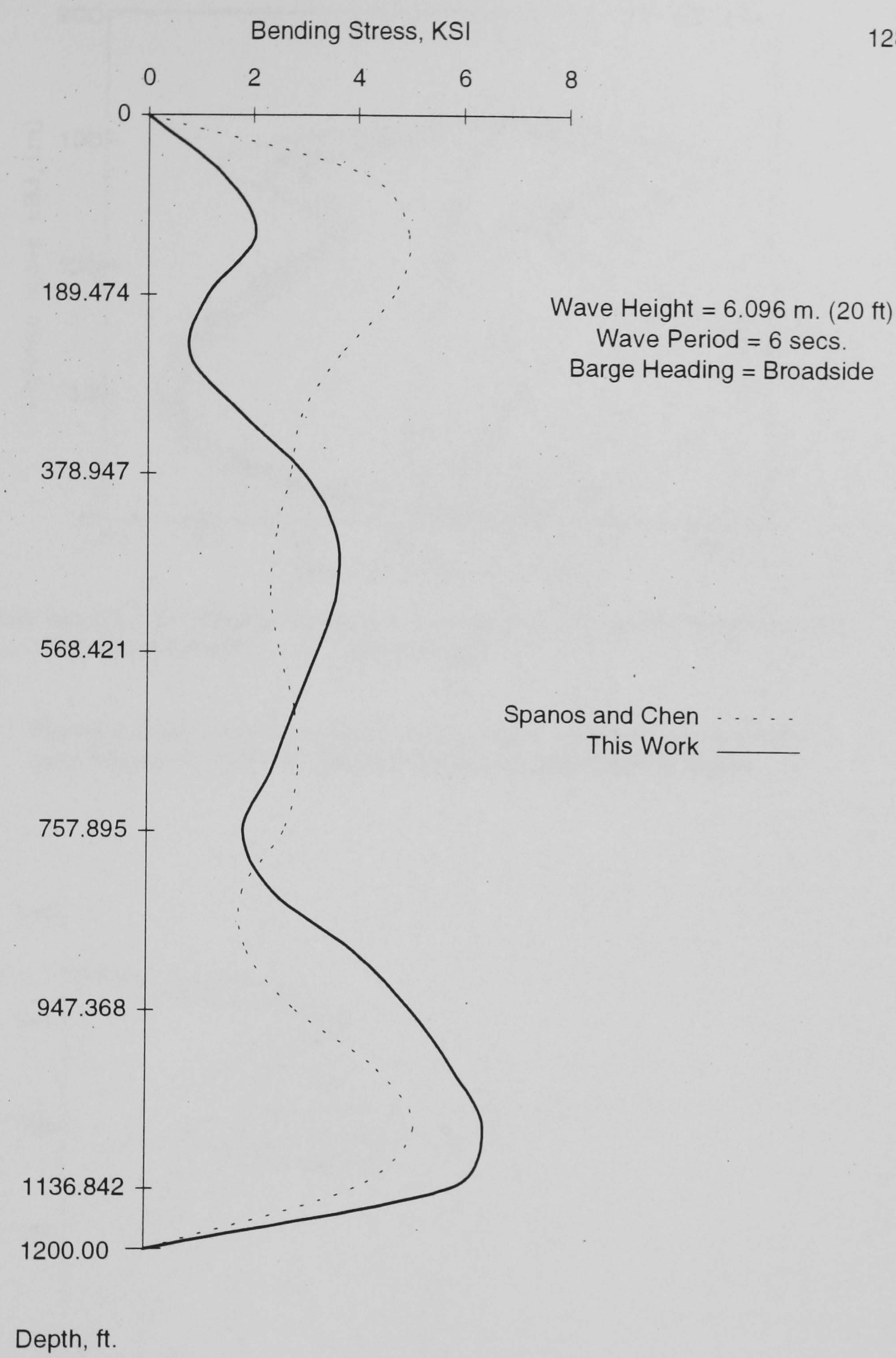

Figure 4.8b. Bending stress distribution. 365.76 m. (1200 ft) 0.4064 m. (16 in) riser.

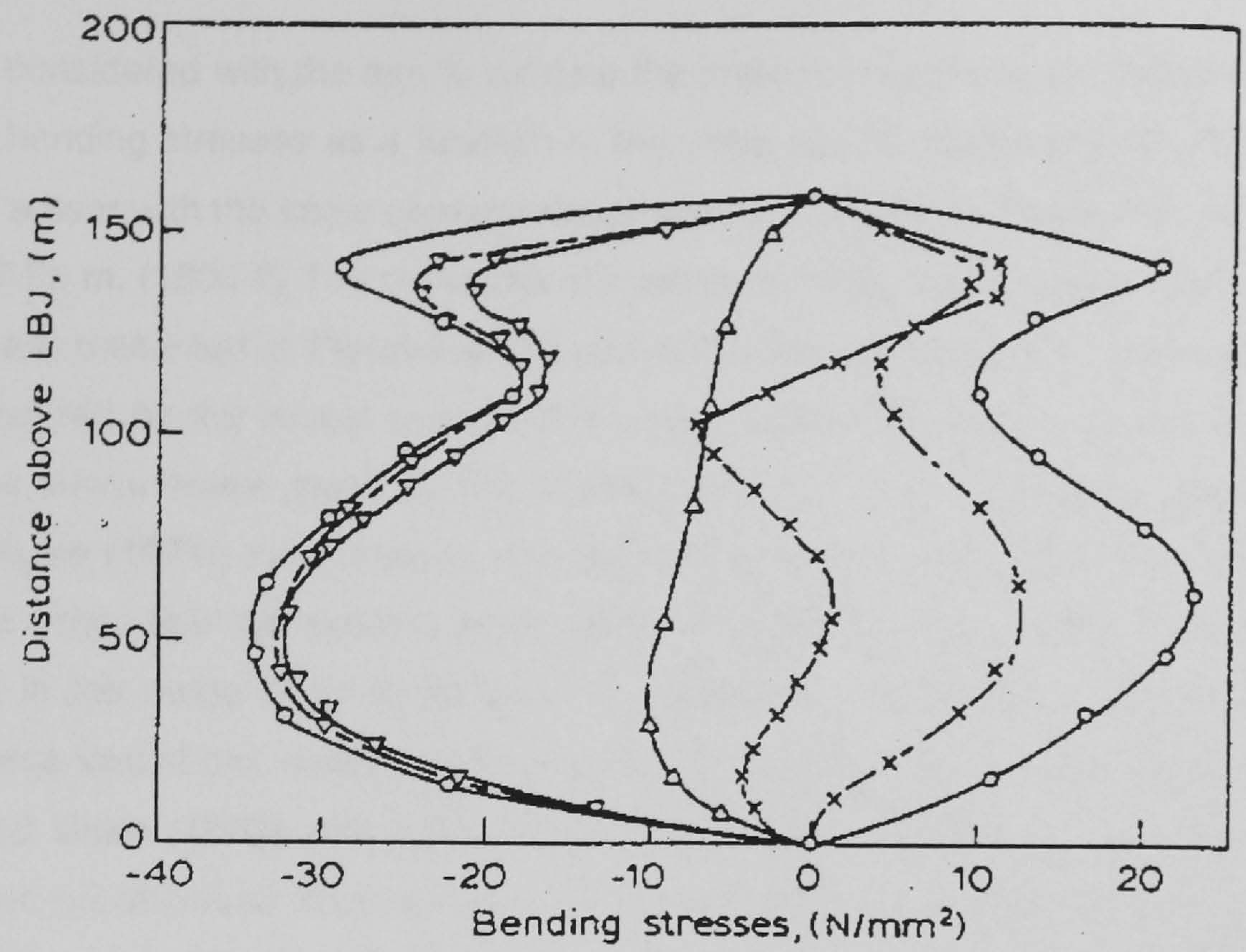

△, static value; ○, API results; △, static + dynamic (min): ×, static + dynamic (max); ——— frequency domain; ....time domain.

Figure 4.9. Bending stress distribution for American Petroleum Institute case 500-20-1D 152.4 m. (500 ft.), after **Patel and Sarohia (1984)**.

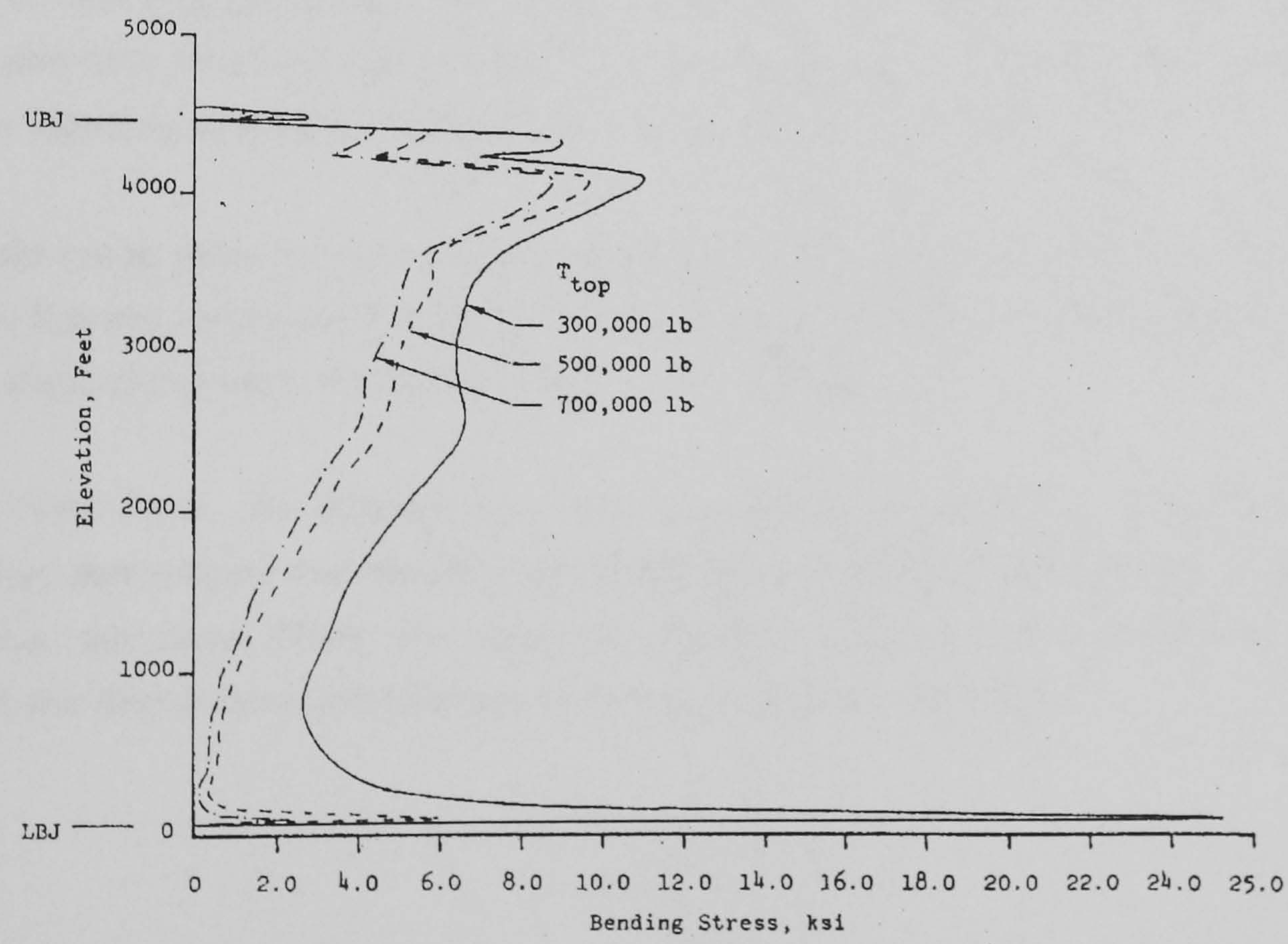

Figure 4.10. Envelope of maximum bending stresses for a 1371.6 m. (4500 ft) long riser, time domain, after **Gardner and Kotch (1976)**.

The next step considered with the aim to validate the present model was to compare the values of the maximum bending stresses as a function of the wave period. **Burke (1974)** presented such a distribution for a riser with the same characteristics already indicated in **Table 4.5**, but this time with a length of 487.68 m. (1600 ft) The variations of maximum stress with wave periods contributed by **Burke (1974)** are presented in **Figures 4.11a** and **4.11b** and are compared at the same time with the results rendered by the model used in this work. A visual inspection of the last two figures shows that the stress levels given by the model used here are consistently larger than those reported by **Burke (1974)**; nevertheless, the general shape of the curves present a degree of similarity in the sense that the maxima and minima of stress lay in the same regions of the wave period, except in the range of 14 to 20 seconds, which was not covered by the work of **Burke (1974)**. The same kind of plot, maximum bending stress as a function of wave period, was supplied by **Spanos and Chen (1980)**, and it is showed here in **Figure 4.12a** and **4.12b** for comparison purposes. It can be observed that this type of curves appear to be relatively insensitive to wave period, that is, they are smooth non-linear functions of the wave period, whilst the curves reported by **Burke (1974)** are strong non-linear functions of the same variable. Unfortunately, during literature review made for the purposes of the present work the author was unable to find other published reports providing similar plots

The results discussed in the above paragraphs appear to be according to the facts already identified in the literature review, **Section 1.9**, in the direction that the results from a significant number of riser analysis approaches render responses within acceptable bounds; however, the authors who have tried to correlate responses of a number of models among themselves and with field data ,**Egeland and Solli (1980)**, reported to have found this task difficult.

The results rendered by the riser analysis model built for the purposes of this work are found to be within the bounds encountered in the published literature. Therefore, it is considered adequate for the next stage of this work, the marine riser reliability analysis.

On the other hand, the differences in the riser stresses reported in the different analysis approaches demonstrate that ***model uncertainty***, already defined in **Section 1.0**, is significant for the marine riser case. There are methods proposed to account for such type of uncertainty, therefore, the discussion in the following section is considered convenient.

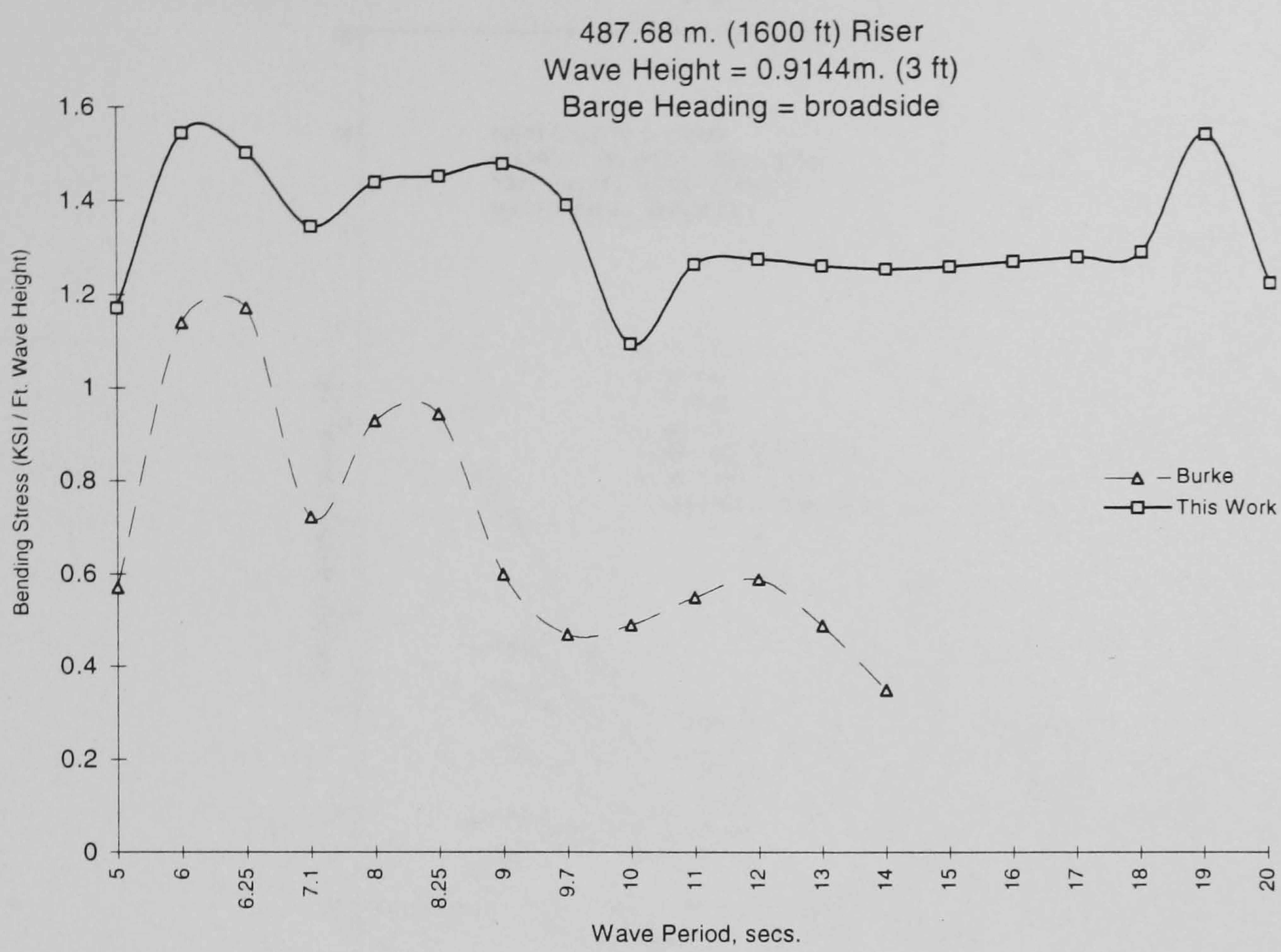

Figure 4.11a. Comparison of maximum bending stress vs. wave period.

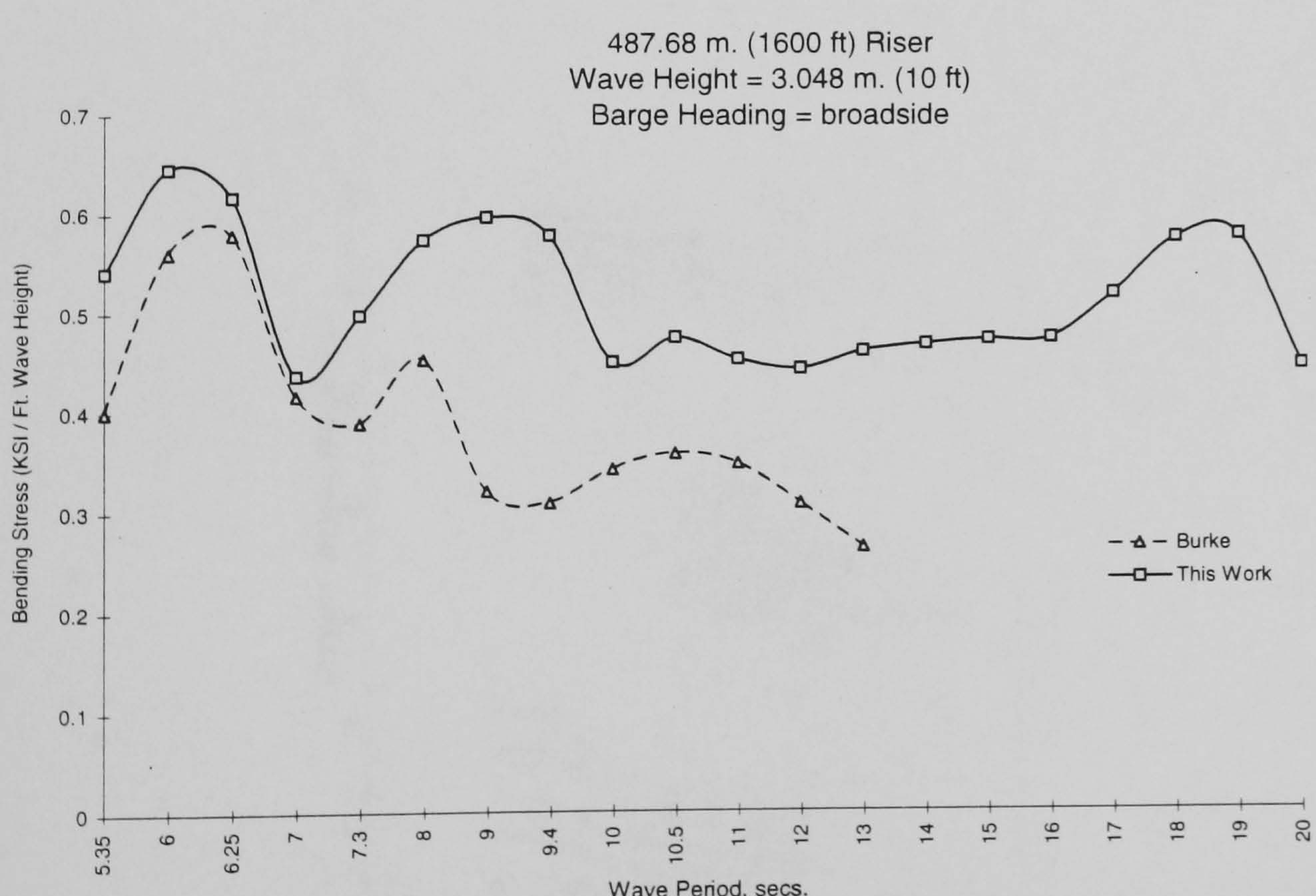

Figure 4.11b. Comparison of maximum bending stress vs. wave period.

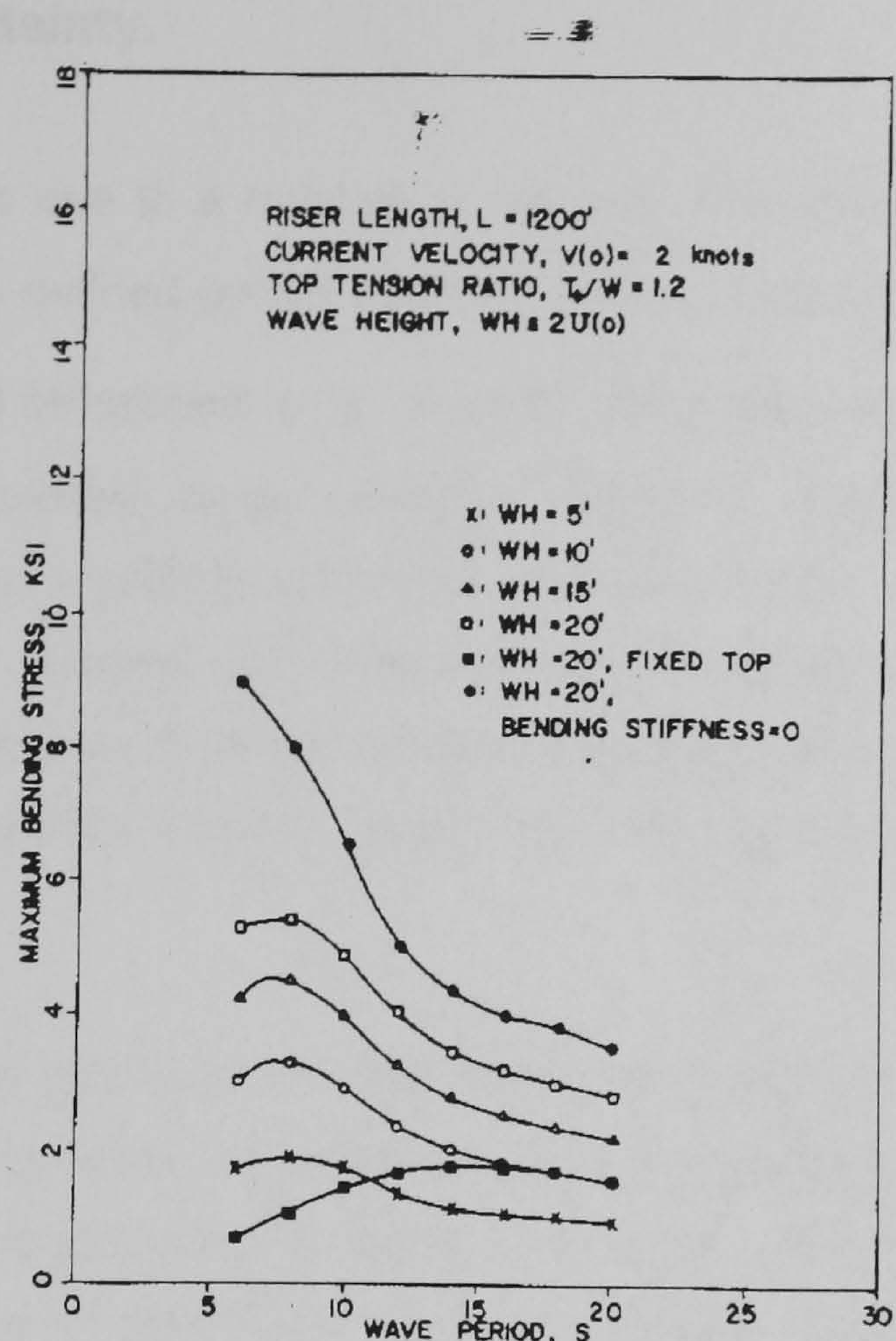

Figure 4.12a. Maximum bending stress vs. wave period, for different wave heights, riser length 365.76 m. (1200 ft), after **Spanos and Chen (1980)**.

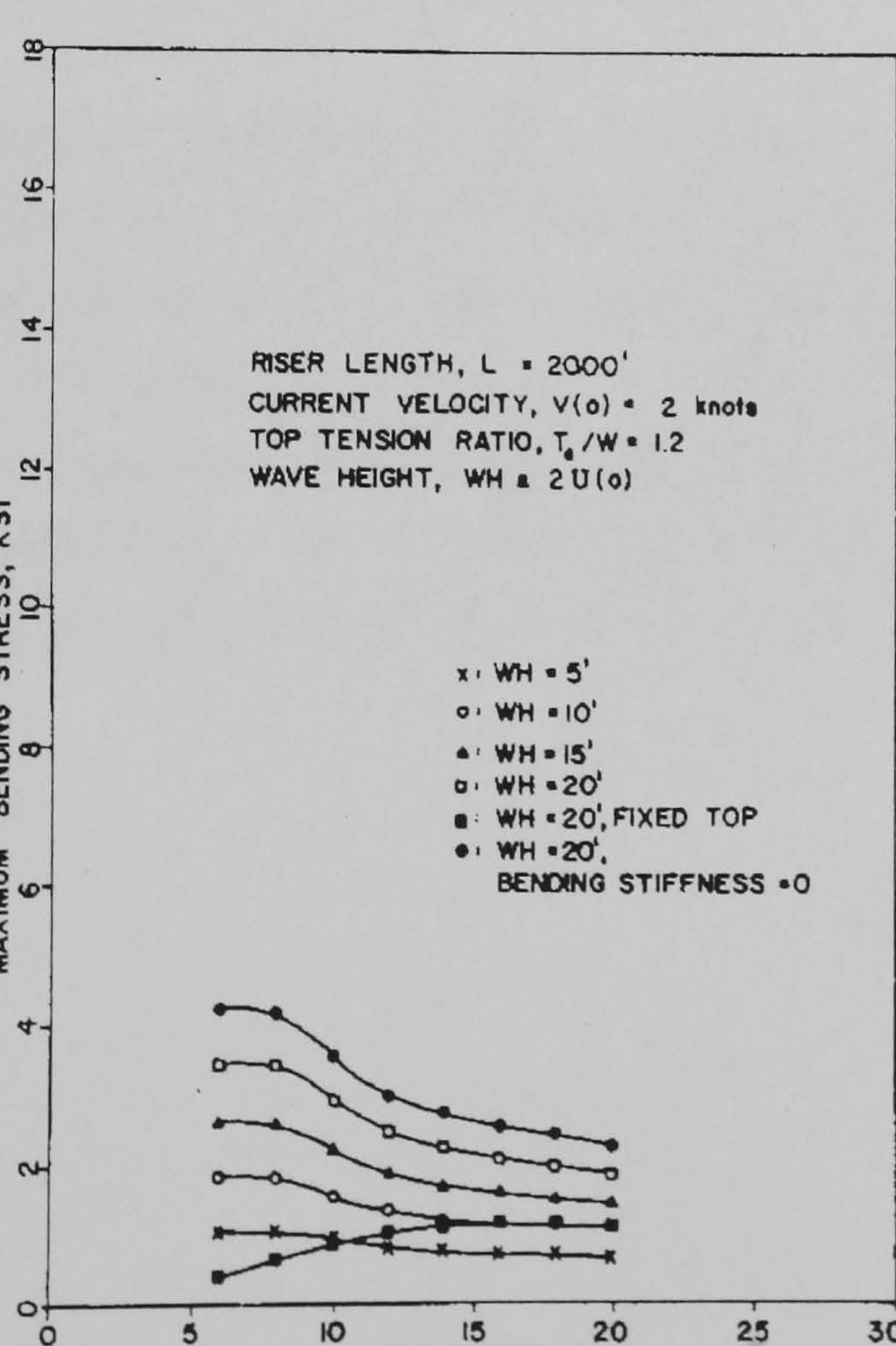

Figure 4.12b. Maximum bending stress vs. wave period, for different wave heights, riser length 609.60m. (2000 ft), after **Spanos and Chen (1980)**.

4.7. Model Uncertainty.

Model uncertainty is due to a number of reasons. The boundary between the safety and failure domains is uniquely defined by the selected failure criteria and the mechanical model, $g(\mathbf{x}) = 0$; however, the choice of function g is no unique. The response of the structure, as given by $g(\mathbf{x})$, depends on the selected basic variables; therefore, neglected basic variables may have a fluctuating degree of significance on the accuracy of the response. In cases where a simple analytical model is adopted and later corrected through factors obtained by experimentation, uncertainty arises as a result of the number of experiments available and the statistical techniques used to fit the correction values. Hence, the limit state surface can be realised as a random surface.

In the instance of the marine riser, it has been demonstrated in **Section 4.6** that model uncertainty arises on account of several important assumptions and simplifications applied to the mechanical model in each of the proposed analytical approaches, this fact demonstrates that some lack of knowledge about the interrelation of physical variables defining the behaviour of the riser is still present. The best form to overcome this limitation, in this case, would be to improve the riser analysis model; nevertheless, this has proved not to be a straight forward matter, i.e. scale test results from **Patel and Sarohia (1982)** indicated that vortex shedding induced significant transverse displacement, which is not considered in the riser analysis approaches found reported.

A number of methods have been proposed for the treatment of model uncertainty and its further introduction in the reliability analysis. In the case of the marine riser, where a significant number of analytical approaches are available, it could be possible to select a number of such riser analytical models and use their results in order to produce statistics and define an applicable probability density function, then one of the methods available for introduction of model uncertainty could be fitted. However, it is judged that without statistical information of the riser responses from other analytical approaches any attempt to introduce model uncertainty would be difficult, if not arbitrary.

SUMMARY, Chapter 4.

Following the procedures available in the published literature, a finite element, static and frequency domain dynamic analyses models for a marine riser were established for the purposes of carrying out a riser reliability analysis. In order to validate such model, the results rendered by it were compared with those from other published works. It was found that the results of this work's model are within the bounds of other riser analysis models; therefore, it is considered adequate for the purposes of performing a riser reliability analysis.

CHAPTER 5.0. RELIABILITY ANALYSIS OF THE MARINE RISER.

5.0. Generalities.

The objectives of this chapter are to:

i).- Demonstrate the applicability of the response surface methodology and adaptive importance sampling technique to the prediction of the reliability index of structures modeled by the finite element method, in this case a marine riser.

ii).- Illustrate how this methodology makes it possible to conduct a large number of studies that provide information to support the selection of adequate probability density functions and its parameters for the basic variables considered. This studies can also help to assess the relative importance of each basic variable in the overall behavior of the riser.

iii) Show that the assumption of independence between the basic variables for construction of the response surface may not always lead to accurate surfaces.

5.1. Description of the Model for Sensitivity Studies.

The riser to be used for the following sensitivities studies is the one employed by **Spanos and Chen (1980)**, which was already described in the previous chapter, the corresponding details were provided in **Table 4.3**.

Concerning the basic variables to be included in this study it must born in mind that the accuracy of the response surface depends on the number of significant basic variables included, as mentioned in **Section 4.6.3**. Therefore, with the information provided by the riser finite element model it was judged that the significant basic variables for this kind of riser are:

1).- Wave Height,

2).- Wave Period,

3).- Harmonic Offset, that is the platform sway, as it affects the riser response,

4).- Top Tension, externally applied tension at the top of the riser,

5).- Static offset,

6).- Inertia Coefficient,

7).- Drag Coefficient,

8).- Strength of the riser pipe.

Since the intention of this study is to demonstrate the applicability of the RABRS methodology, it was decided to use a number of combinations of these variables for different studies. As it will be seen in the following, this approach was also useful to observe the impact of each one of the variables in the total behavior of the riser.

In order to make comparisons possible the response surface construction and adaptive importance sampling simulation were carried out by keeping the key parameters constant, these are presented in **Table 5.1**. Although, the selection of the standardized or the original space of the basic variables is not significantly different, as was demonstrated in **Section 3.3**, the calculations were made in the standardized space of the basic variables, using the second approximation of the design point as the centre for initiation of the AIS procedure, with the same seeds, whenever possible.

Multiplication factor for construction of the response surface.	f_i = 3.3 ,see **Equation 2.4**.
Method for determination of the reliability index.	Adaptive Importance Sampling
Initial ratio between variance of sampling PDF and basic variable PDF.	$\dfrac{\sigma[h_{\mathbf{v}}(\mathbf{v})]}{\sigma[f_{\mathbf{v}}(\mathbf{v})]} = 2.0$
Space selected for determination of the reliability index.	Standardized
Starting point for AIS	2nd approximation of the design point given by FORM
Seeds for initiation of simulation	constant
Limit state criterion	**Equation 5.1**
PDF and standard deviation of material strength	Lognormal, $\sigma = 0.1(\mu)$

Table 5.1. Parameters for construction of the response surface and Adaptive Importance Sampling simulation.

The failure criterion selected for all the studies included in this chapter is based on the maximum bending stress that the riser pipe is able to withstand:

$$\text{maximum bending stress - steel strength} \leq 0 \tag{5.1}$$

The strength considered is the yield stress of the material.

Another point of great significance is the choice of Probability Density Function, PDF, associated with each of the basic variables. The ideal approach would be to conduct measurements of the values of each basic variable in their actual environments and by means of statistics theory to find the PDF that best fits such data. This point has been one of the most difficult to resolve in reliability based design, since usually it is difficult and expensive to obtain sufficient data to fit correctly a PDF. Some authors have proposed and used PDF's and standard deviations for reliability studies carried out for other types of structures. The PDF's and standard deviations suggested by **Baker and Wyatt (1979)** have been used as a guidance for this work; however, it is intended to present in the following sensitivity studies how the RABRS method allows to review the effects of different choices of PDF and associated standard deviations. In order to do so, the steel pipe strength will always be assumed to be lognormally distributed, with a coefficients of variation of 10 % and nominal strength value of 172 N/mm^2 (25000 psi.). This assumption may be justified on the basis that the strength can never accept negative values. Concerning the choice of standard deviation, 10% is possibly higher than what can be achieved by industry; nevertheless, this value was selected on the basis that it provides values of the reliability index that facilitate the identification of trends more easily.

5.2. Deterministic Stresses.

Before proceeding with the reliability studies it is considered convenient to present the deterministic bending stresses of the riser as a function of wave period and for one wave height, 6.096 m. (20 ft.), see **Figure 5.1a**, for a 182.88 m. (600ft) long riser. This will help to assess tendencies observed in the reliability analysis case. It is important to observe the influence of platform sway. Referring to the same figure, the stresses for the riser without static or harmonic offsets, the ***vertical riser*** case, are the lowest ones. In the static case only ocean current is considered and the bending stresses are therefore constant with respect to wave period. When the only source of dynamic excitation is the direct action of waves on the riser wall, it is important to observe that the bending stresses are very similar to the static ones, except around the first and second natural periods, where a small bulge is present. For the riser with static offset and wave actions as the only source of dynamic excitation, the case with ***platform static offset*** only, it is observed that the stresses hold similar tendencies as before but with slightly higher values, due to the static effect of the imposed top boundary displacement. In the third case the platform sway or harmonic offset is introduced, it can be noticed that the platform motion, or harmonic offset, is the main source of dynamic stresses; furthermore such dynamic stresses are largely influenced by the wave period. The effect of the relative velocities is also very noticeable at the first natural mode, this important stress reduction effect can be explained by the high relative velocities imposed by the platform motion, which in turn provide a large hydrodynamic damping. Finally the maximum stresses observed in **Figure 5.1a** are the total stresses, resulting from the addition of the stresses due to the externally applied top tension, the axial stress

Figure 5.1b presents the total stresses for the same riser as **Figure 5.1a**, this time for three different wave heights. It is possible to observe how the stresses present a steep slope at periods around the first natural one. This behaviour is the effect of the of the relative riser velocities, which are significantly increased at such periods due to resonance effects, therefore the hydrodynamic damping plays a very significant role.

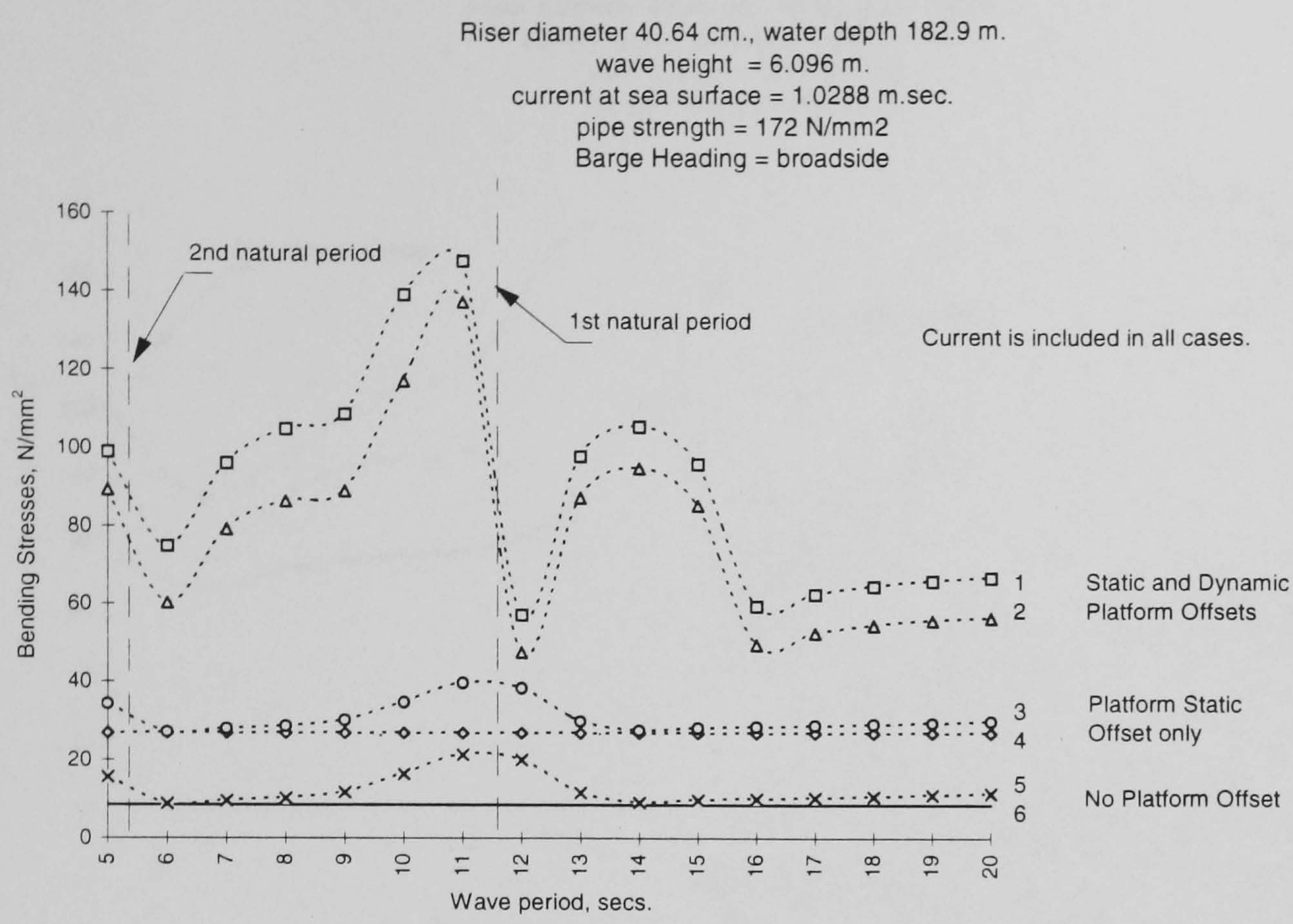

The loads on the riser are the following:

- 1 Total stress, due to Static and Dynamic Platform Offsets + wave kinematics + ocean current + axial stress.
- 2 Maximum bending stress, due to Static and Dynamic Platform Offsets + wave kinematics + ocean current.

- 3 Maximum bending stress, due to Static Platform Offset + wave kinematics + ocean current.
- 4 Maximum bending stress, due to Static Platform Offset + ocean current.

- 5 Maximum bending stress, due to wave kinematics + ocean current.
- 6 Maximum bending stress, due to ocean current.

Figure 5.1a. Deterministic bending stresses for different loading conditions

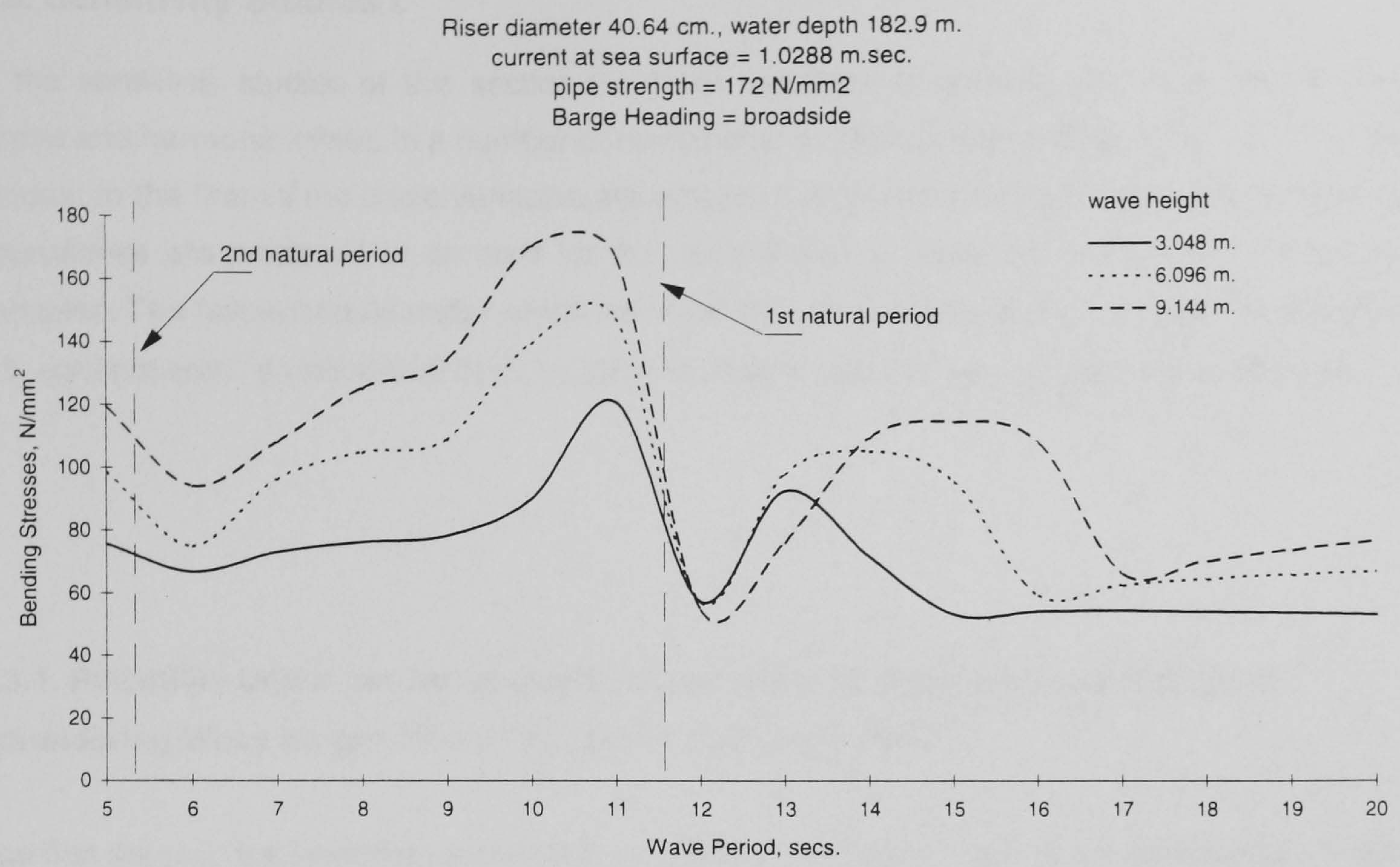

Figure 5.1b. Deterministic total stresses due to Static and Dynamic Platform Offsets + wave kinematics + ocean current, for different wave heights.

5.3. Sensitivity Studies I.

In the sensitivity studies of this section the basic variables considered are wave height, wave period and harmonic offset, in a number of combinations. These studies are divided into two main groups, in the first all the basic variables are assumed to be independent and in the second two approaches are proposed to account for the dependence of harmonic offset on the other two variables. The failure criteria under which the reliability index is to be studied is given by **Equation 5.1**, consequently, an additional basic variable is always present, the material or pipe strength.

5.3.1. Reliability Under the Assumption of Independence Between Basic Variables, Considering Wave Height, Wave Period and Harmonic Offset.

The first stage in the investigation of the behavior of the reliability index is to assume that all basic variables are mutually independent, in the statistical sense. **Bucher and Bourgund (1990)** suggested this assumption in order to facilitate the construction of the response surface, indicating that the correlation between the basic variables could be considered later, using the response surface and not the original mechanical model. Although, three basic variables, wave height, wave period and harmonic offset, are considered in this section, some cases involving these variables separately are going to be reviewed initially, so as to ease appreciation of their individual significance. Before presenting the results of the sensitivity studies performed in this section, it is convenient to summarize the characteristics of the cases to be discussed, see **Table 5.2**.

All basic variables independent

	Basic variables	PDF type	Mean value	cov.
Case 1	wave height	several	6.096 m.	several
Case 2	wave period	several	6 to 20 secs.	several
Case 3	wave height, harmonic offset	several Lognormal	6.096 m. as in **Fig.4.5**.	several 10%
Case 4	wave height wave period harmonic offset	several Lognormal Lognormal	6.096 m. 6 - 20 secs. as in **Fig.4.5**.	several 10% 10%

cov., coefficient of variation.

Table 5.2 Cases for sensitivity analysis, independent basic variables.

Case 1.

The first case to be reviewed is for two basic variables: wave height and material strength. The values of the reliability index are plotted as a function of wave period, since, as demonstrated in **Figures 5.1a** and **5.1b**, the maximum bending stress is highly dependent on the wave period. **Figure 5.2a** shows the reliability index considering three different types of PDF's for wave height, while the steel strength is kept as lognormally distributed, with a fix coefficient of variation of 10%. The standard deviation associated with the wave height is varied so as to observe the impact on the reliability index. Since large values of standard deviation anticipate large levels of uncertainty, it is expected to see a rate of decrement of the reliability index as the standard deviation is increased. It can be observed how the reliability index presents noticeable changes in connection with the wave period. However, it is also perceived that the different types of PDF's, normal, lognormal and extreme type I ,ET-I, associated to wave height and variations in their standard deviations seem to have little or no effect in the values of β. This fact can be more clearly appreciated in **Figures 5.2b** and **5.2c**, where β is plotted against changes in the standard deviation of wave height and assuming three different types of PDF's. In the case of a wave period of 16 second, there seems to be some decrement of β as the standard deviation increases, but for the case of 6 seconds β is kept constant, despite variations on PDF type and standard deviation. This behavior is unexpected.

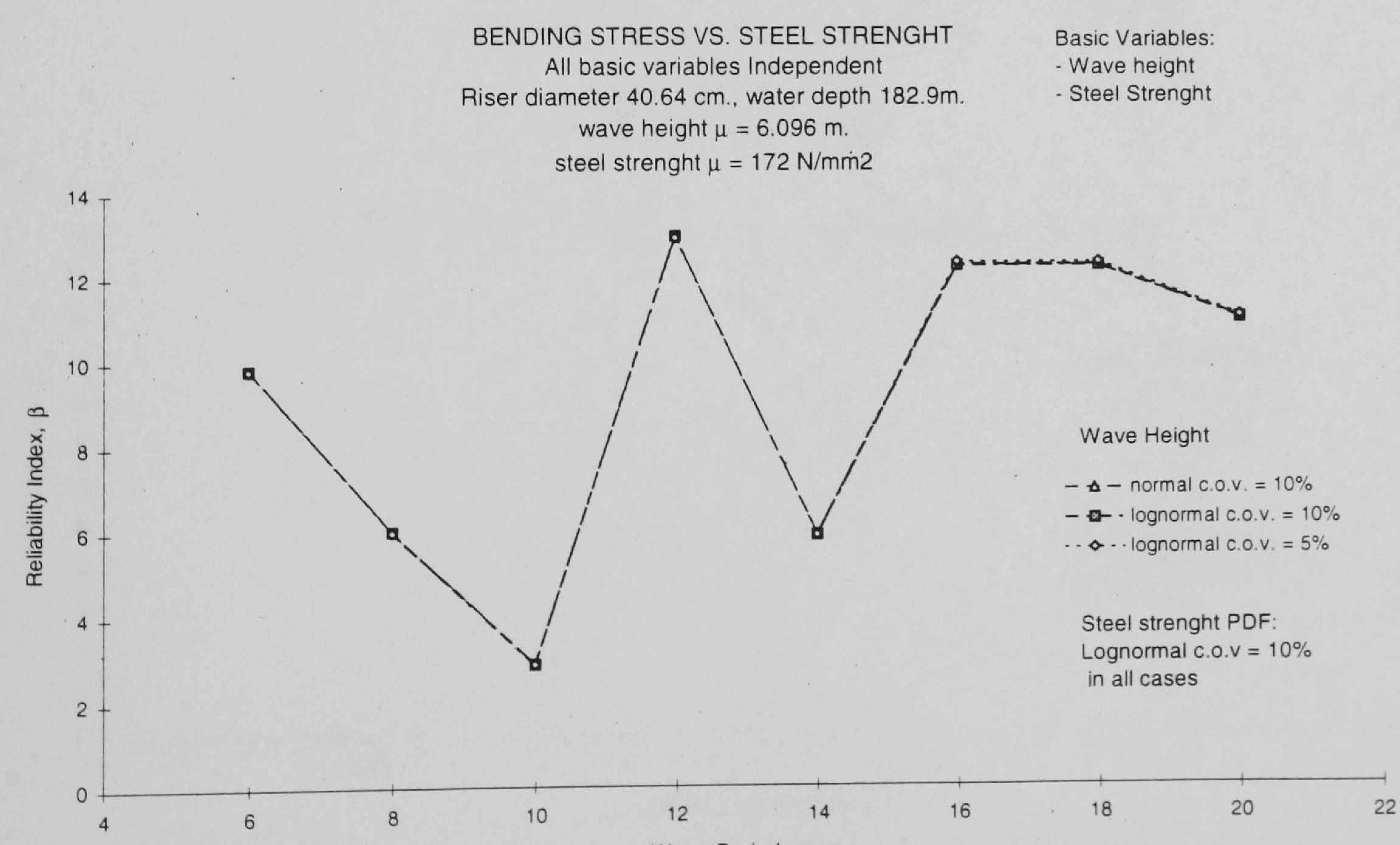

Figure 5.2a. Variations of reliability index with wave height, **Case1**.

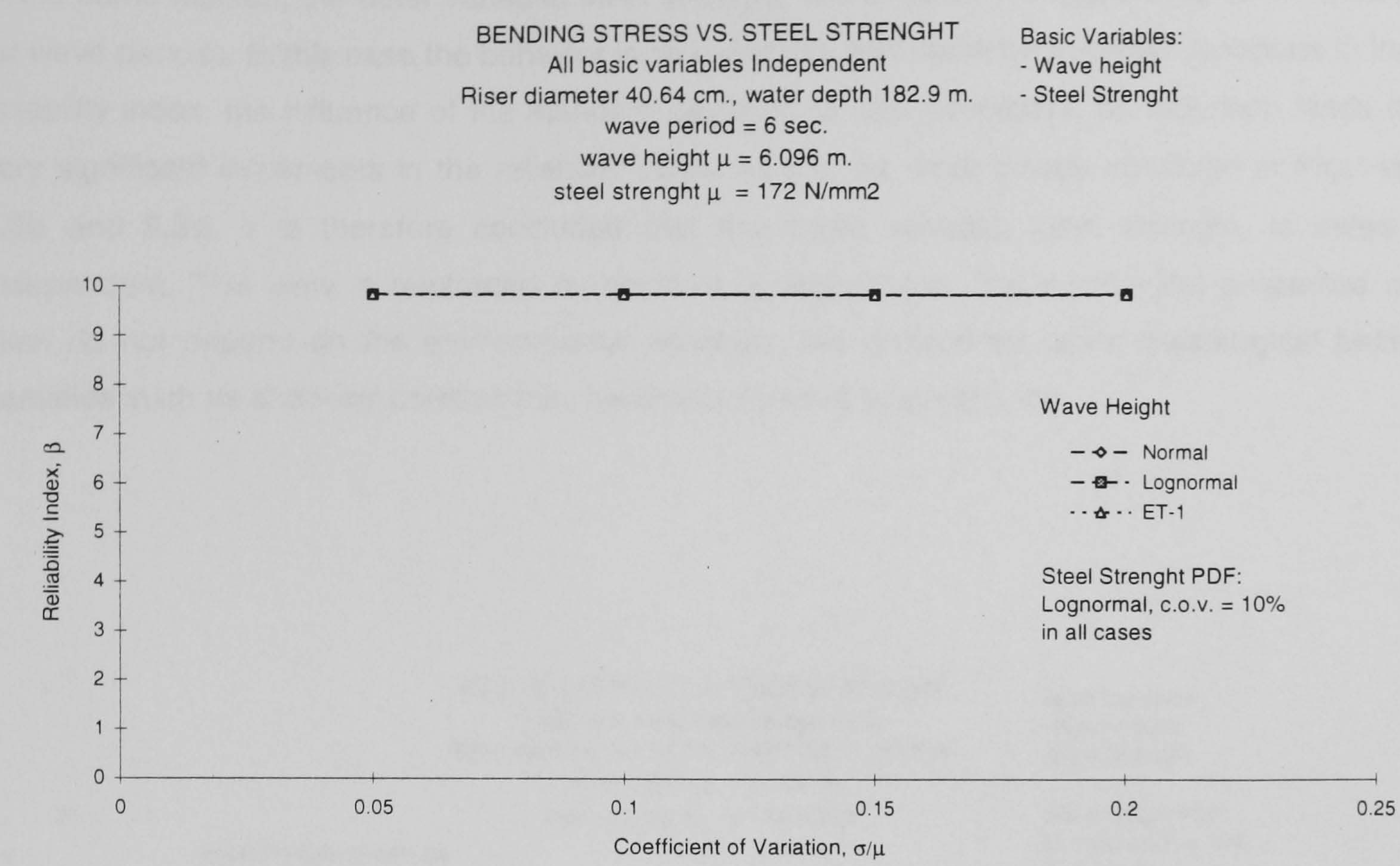

Figure 5.2b. Variation of the reliability index with wave height standard deviation, **Case 1**, for a wave period of 6 seconds.

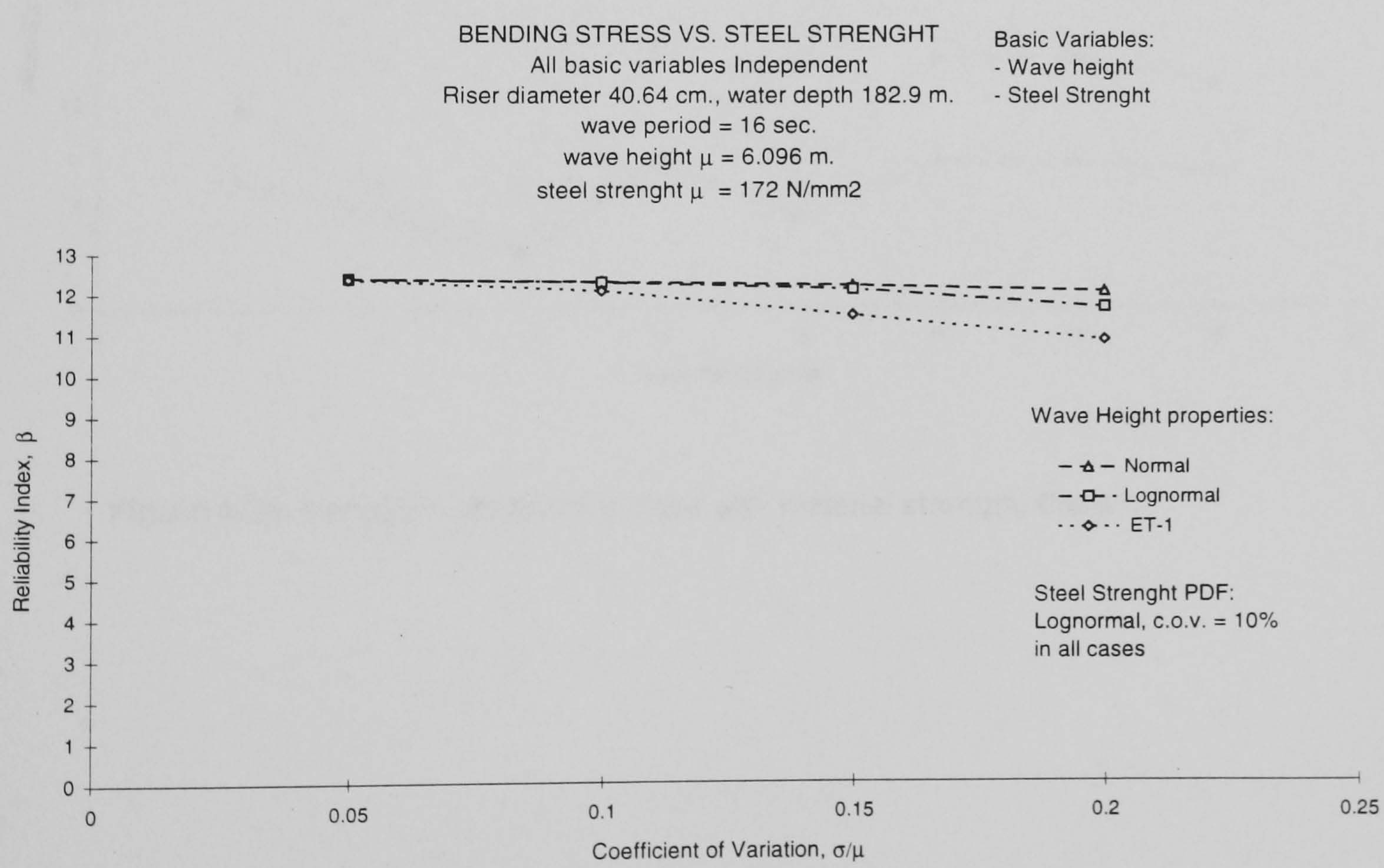

Figure 5.2c. Variation of the reliability index with wave height standard deviation, **Case 1**, for a wave period of 16 seconds.

In the same fashion, the other variable, steel strength, is compared in **Figure 5.3a** for a number for wave periods. In this case the behavior is as expected, different PDF's render variations in the reliability index, the influence of the standard deviation is also noticeable, its reduction leads to very significant increments in the reliability index, as can be more clearly observed in **Figures 5.3b** and **5.3c**. It is therefore concluded that this basic variable, steel strength, is indeed independent. This view is reinforced by physical considerations, the mechanical properties of steel do not depend on the environmental variables, but depend on other metallurgical basic variables such as chemical composition, hardness, thermal treatment, etc.

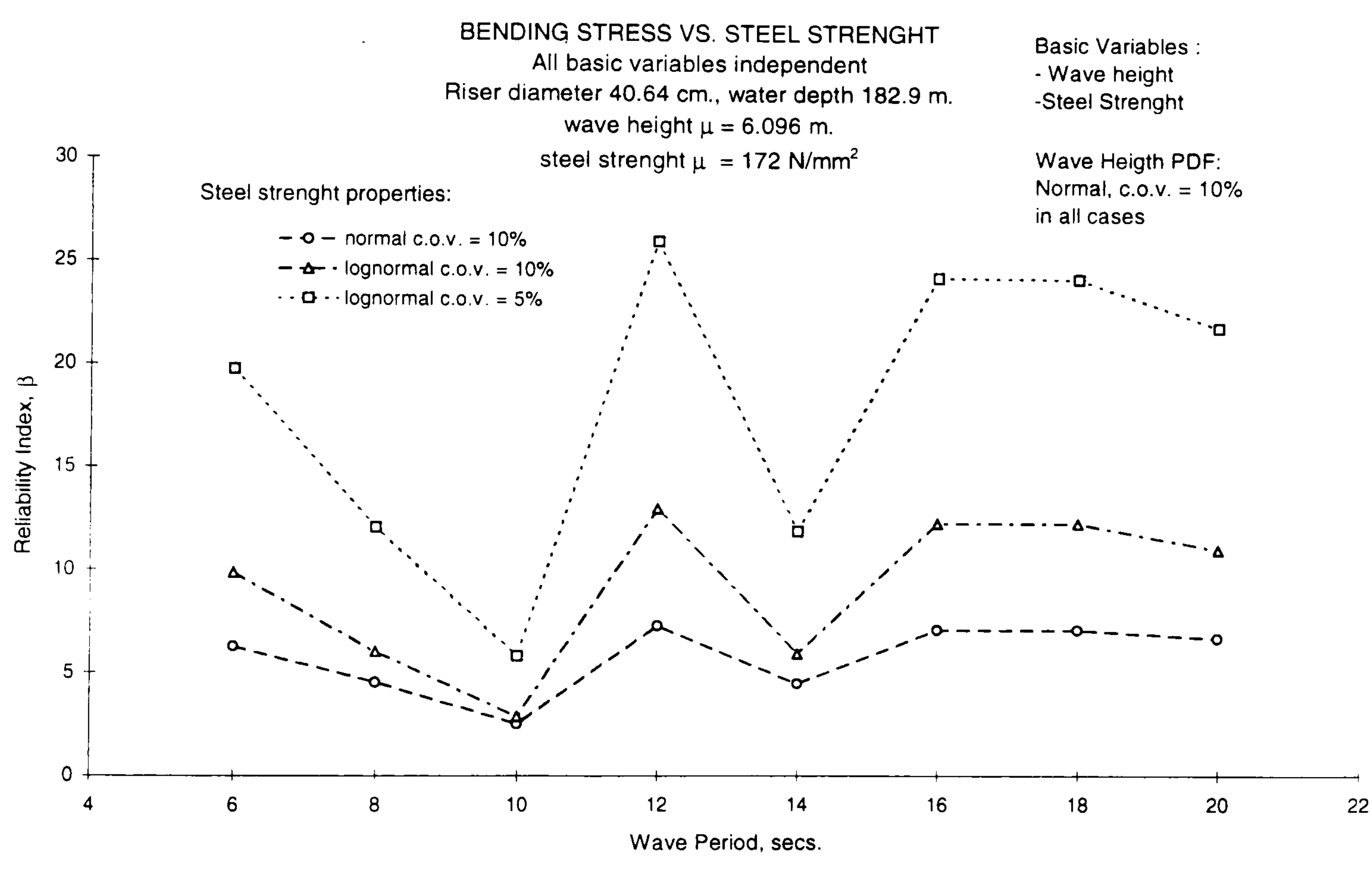

Figure 5.3a. Variations of reliability index with material strength, **Case1**.

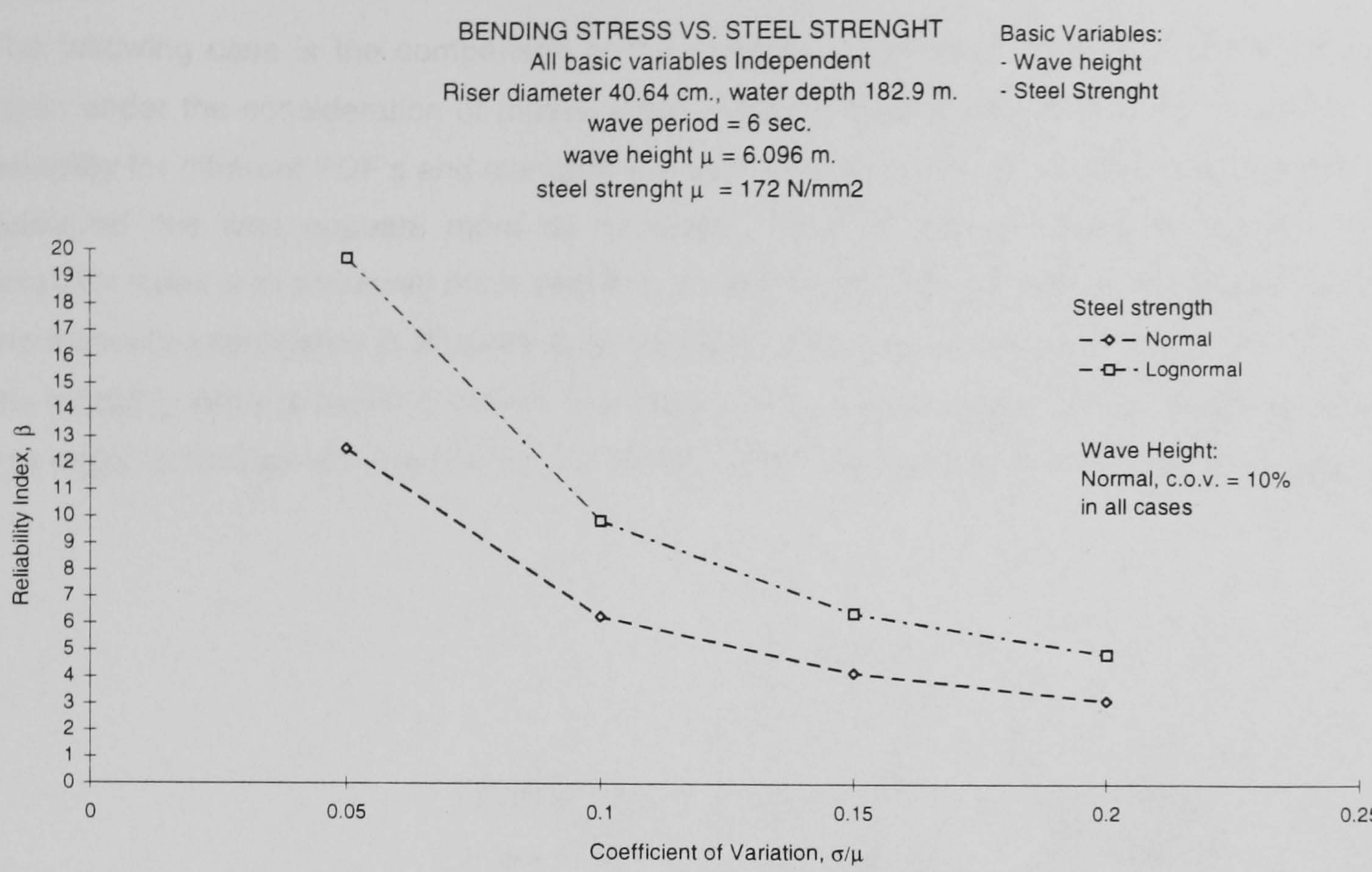

Figure 5.3b. Variation of reliability index with material strength standard deviation. **Case1**.

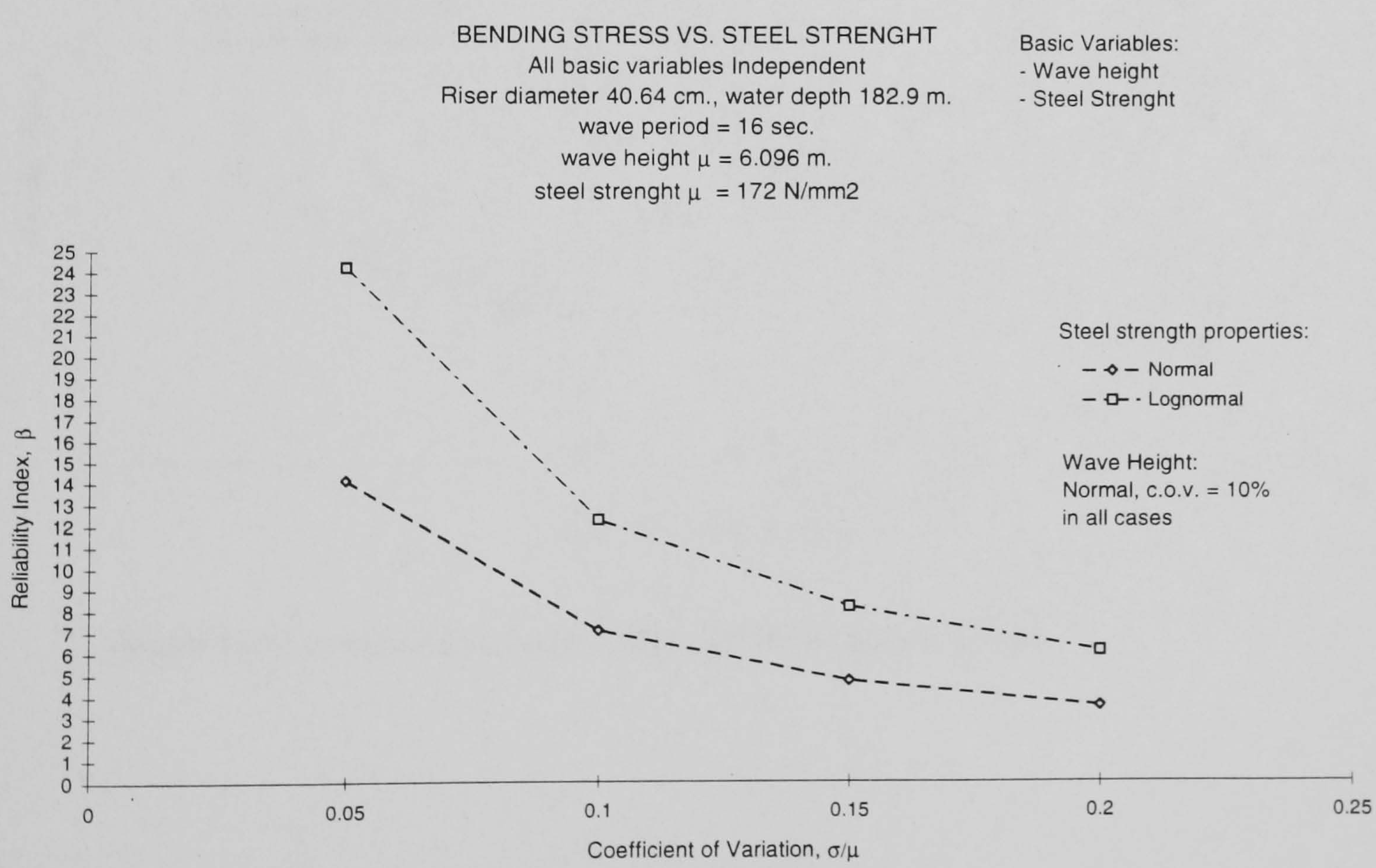

Figure 5.3c. Variation of reliability index with material strength standard deviation. **Case1**.

Case 2.

The following case is the comparison of the reliability index as a function of the wave period, again under the consideration of mutual independence. **Figure 5.4a** shows the variations of the reliability for different PDF's and standard deviations assigned to the wave period. The behaviour displayed this time appears more as expected. The influence of standard deviation on the reliability index is in someway more sensible, as well as the different PDF's. This situation can be more clearly appreciated in **Figures 5.4b** and **5.4c**. However, in the region of 10 to 12 seconds the reliability index is nearly constant, see **Figure 5.4a**, regardless of PDF or standard deviation, this region coincides with the first natural period, where the hydrodynamic damping is larger.

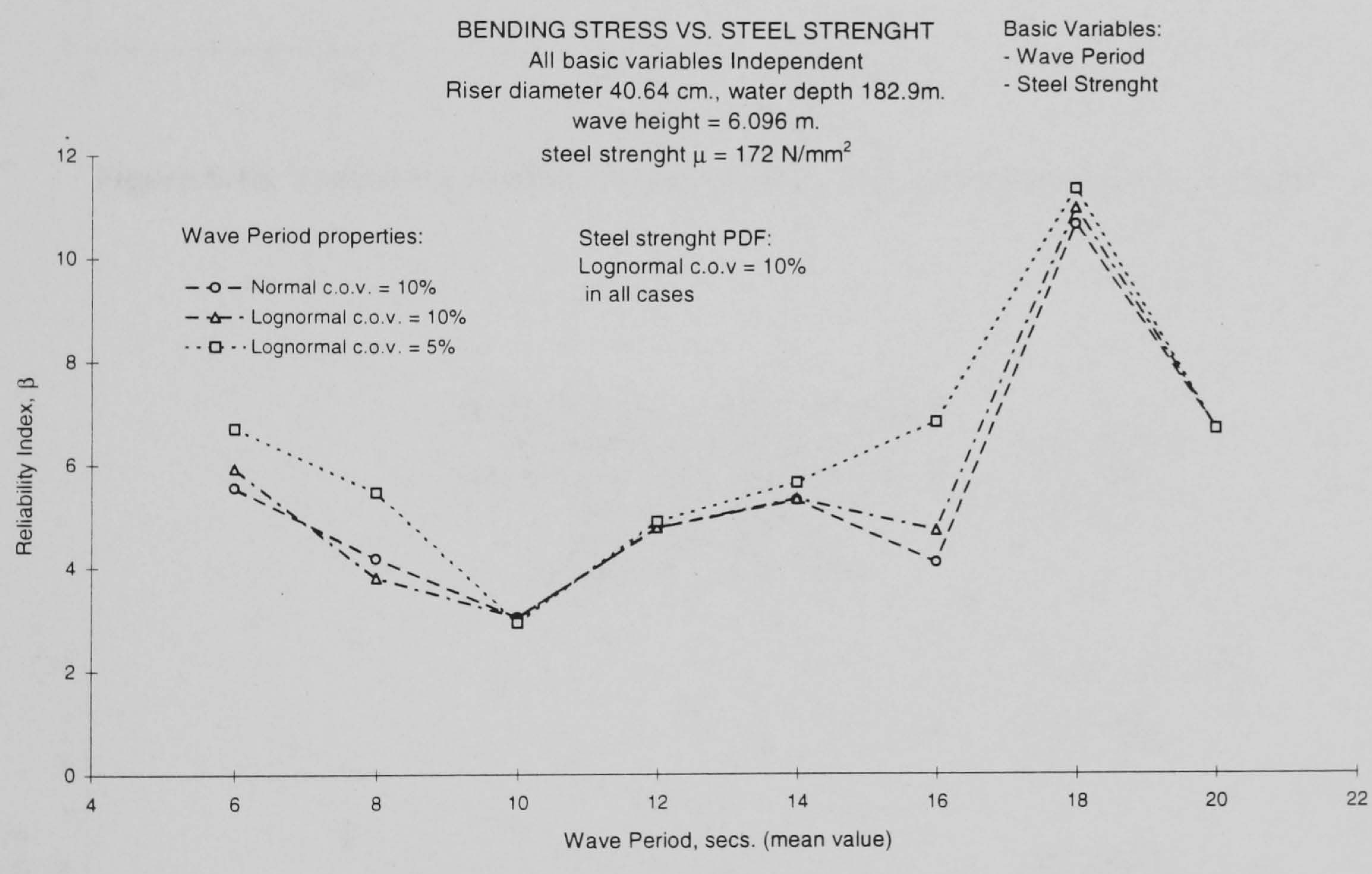

Figure 5.4a. Variation of reliability index with wave period, **Case2**.

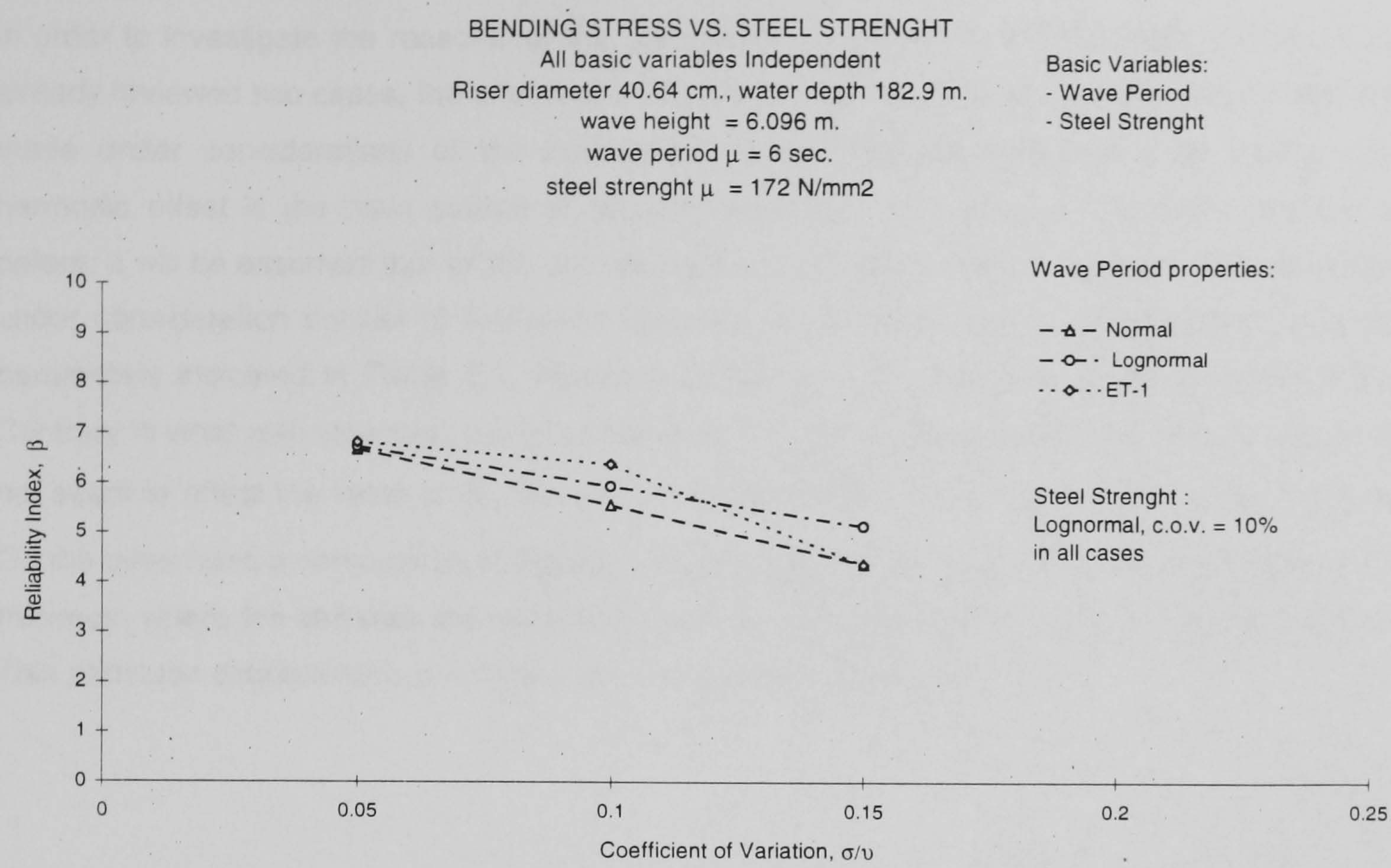

Figure 5.4b. Variation of reliability index with wave period standard deviation, **Case2**.

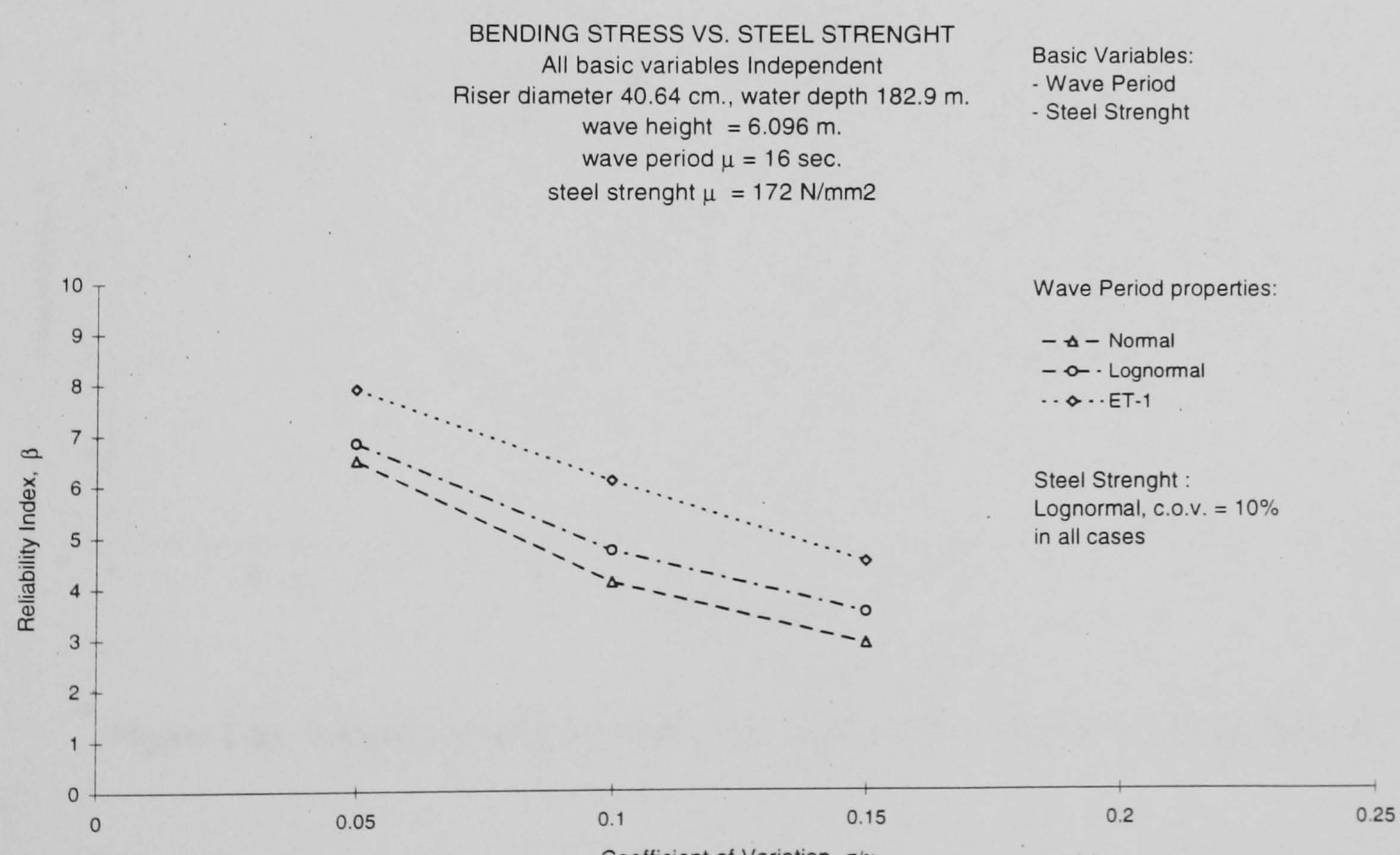

Figure 5.4c. Variation of reliability index with wave period standard deviation, **Case2**.

Case 3.

In order to investigate the reasons for the unexpected performance of the reliability index in the already reviewed two cases, the effects of the harmonic offset will be introduced. This selection is made under considerations of the mechanical model. **Figures 5.1a** and **5.1b** confirm that harmonic offset is the main source of dynamic excitation. Therefore, in the same fashion as before, it will be assumed that all the considered basic variables are independent. The next case under consideration consist of two basic variables, wave height and harmonic offset, with the parameters indicated in **Table 5.1**. **Figure 5.5a** presents the variations of the reliability index. Contrary to what was expected, the influence of PDF's and standard deviations of wave height do not seem to affect the value of β, this can be more distinctly noticed in **Figures 5.5b** and **5.5c**. On the other hand a comparison of **Figure 5.5a** and **Figure 5.1b** shows that the reliability index is minimum where the stresses are maximum, see the region between 10 and 12 seconds periods. This particular characteristic is a consistent and expected behaviour.

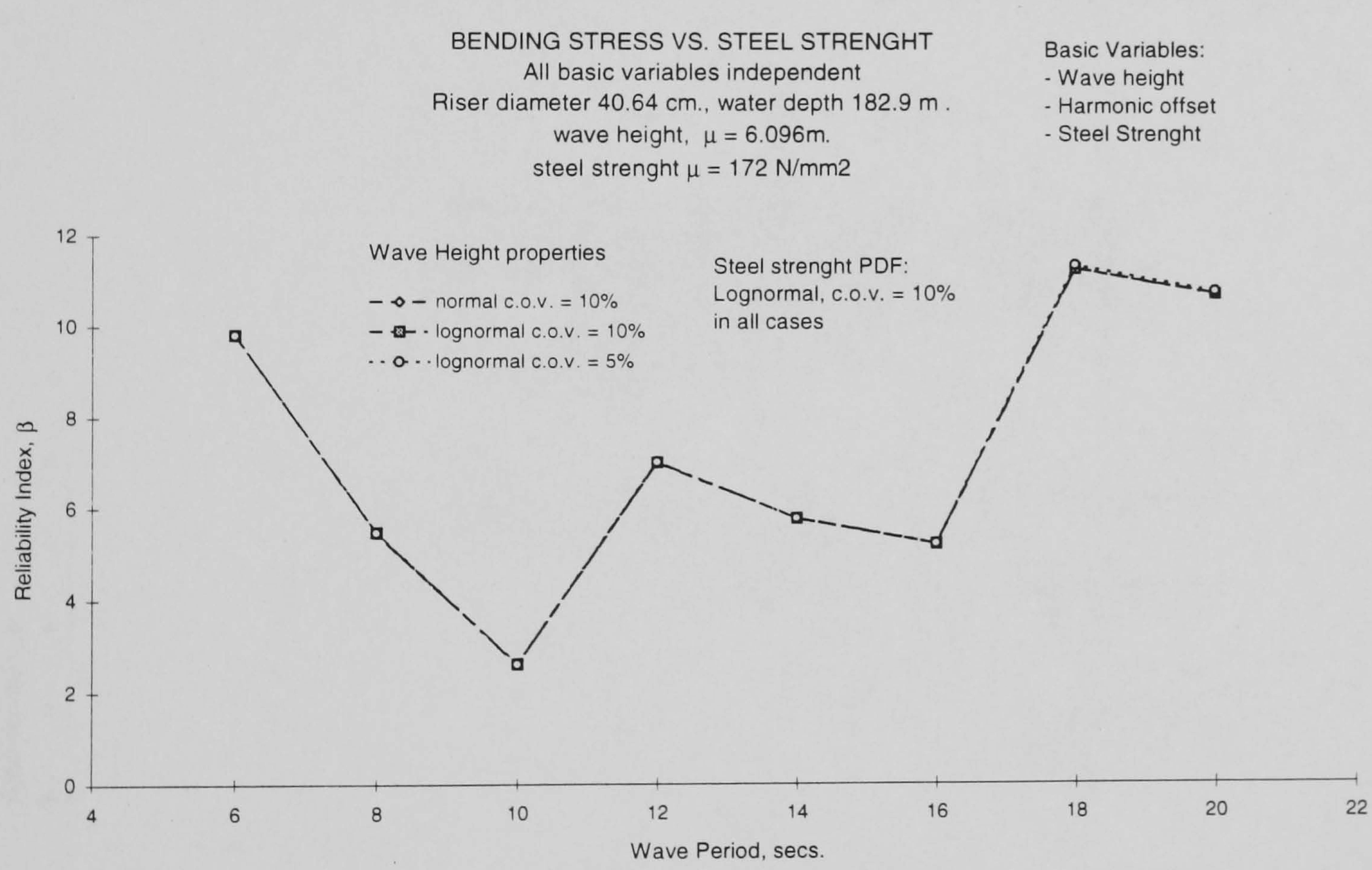

Figure 5.5a. Variation of reliability index with wave height and harmonic offset, **Case 3**.

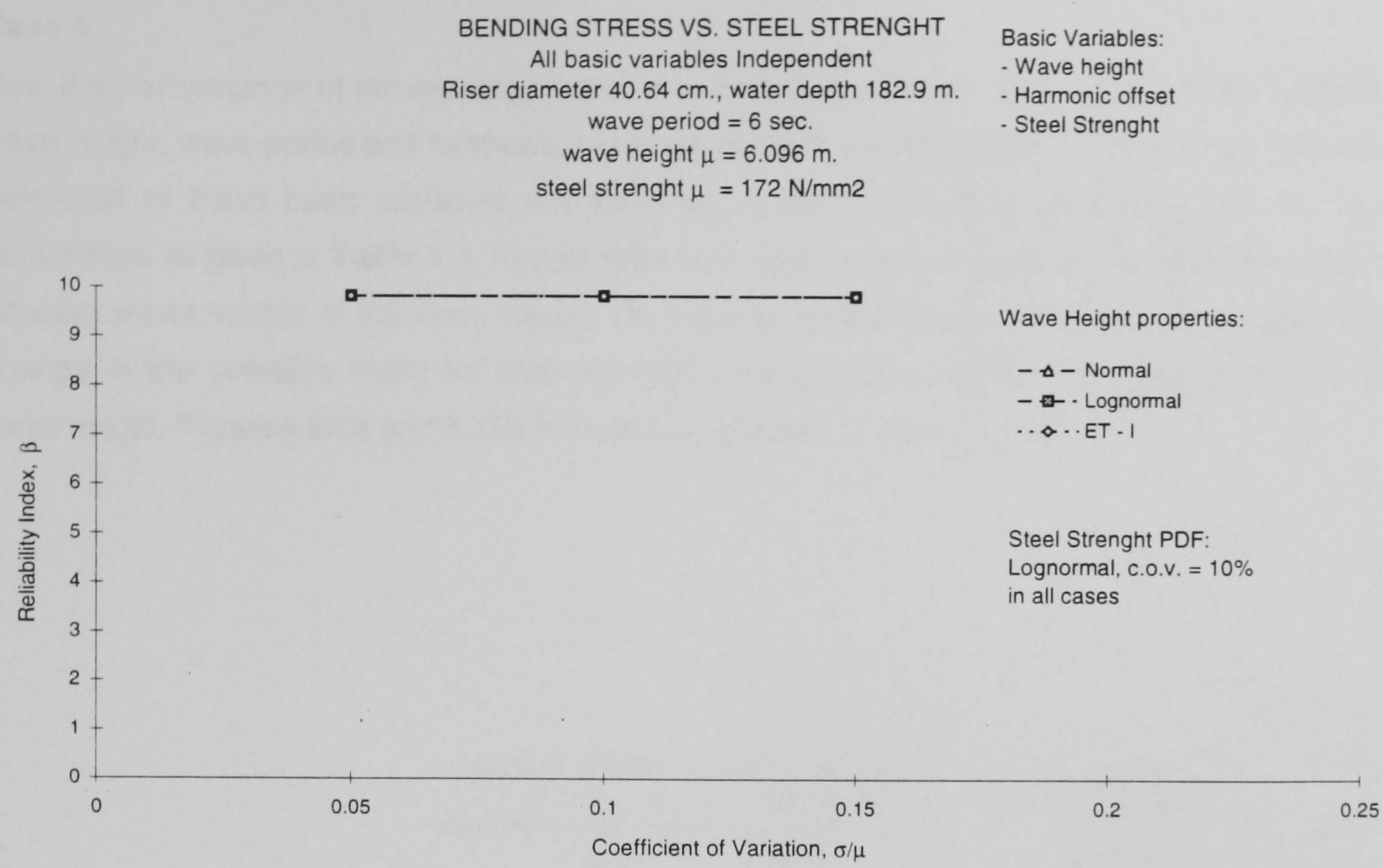

Figure 5.5b. Variation of reliability index with wave height standard deviation, **Case 3**.

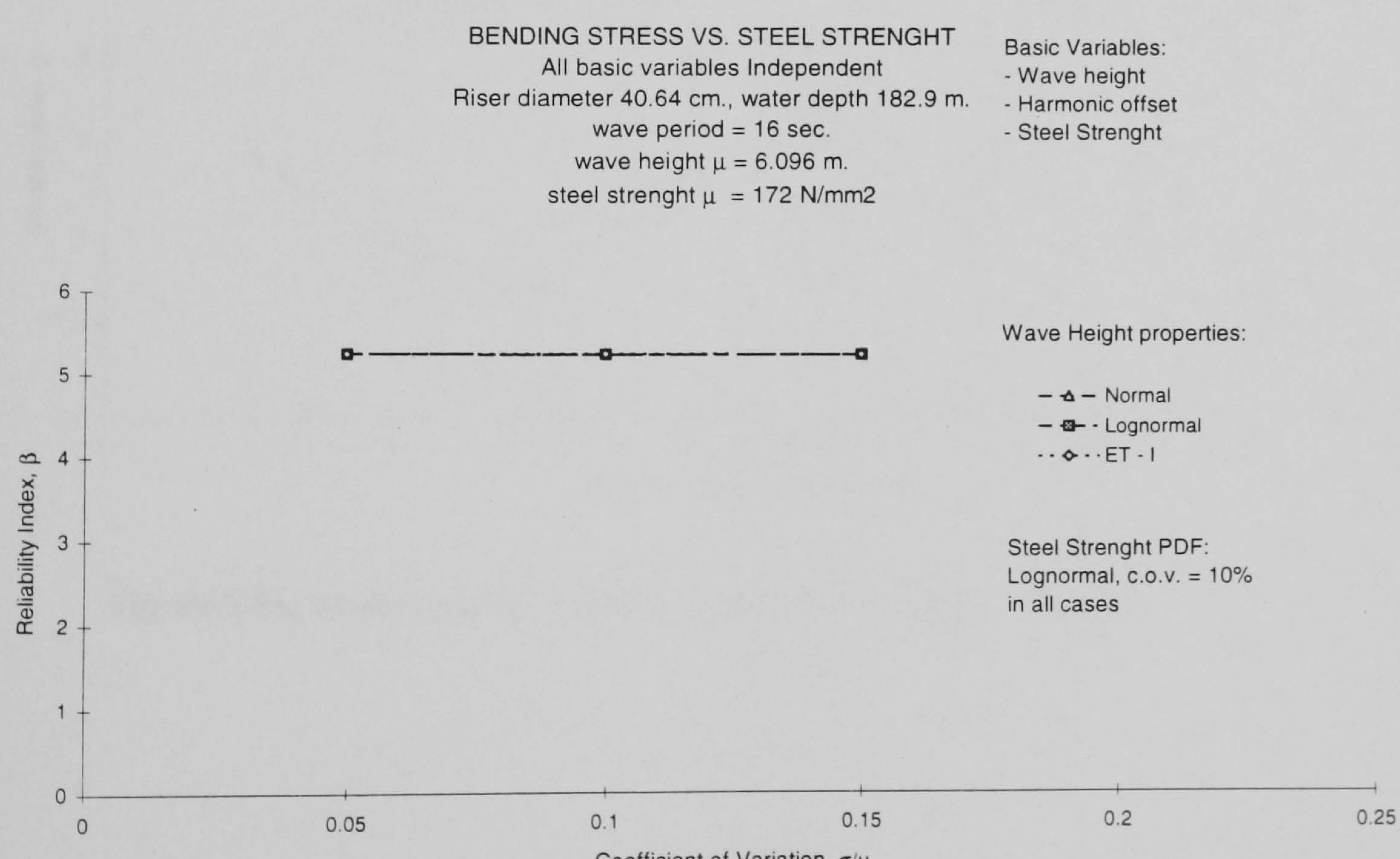

Figure 5.5c. Variation of reliability index with wave height standard deviation, **Case 3**.

Case 4.

Now the performance of the reliability index is to be reviewed when all the three basic variables wave height, wave period and harmonic offset are considered collectively. In the same manner as before all of these basic variables are assumed to be independent, keeping all of the other parameters as given in **Table 5.1**. **Figure 5.6a** illustrates the fluctuations of the reliability index at different mean values of the wave period. Contrary to what was expected there is no significant change in the reliability index for different PDF's and standard deviations associated with the wave height. **Figures 5.6b** and **5.16c** present this situation with more detail.

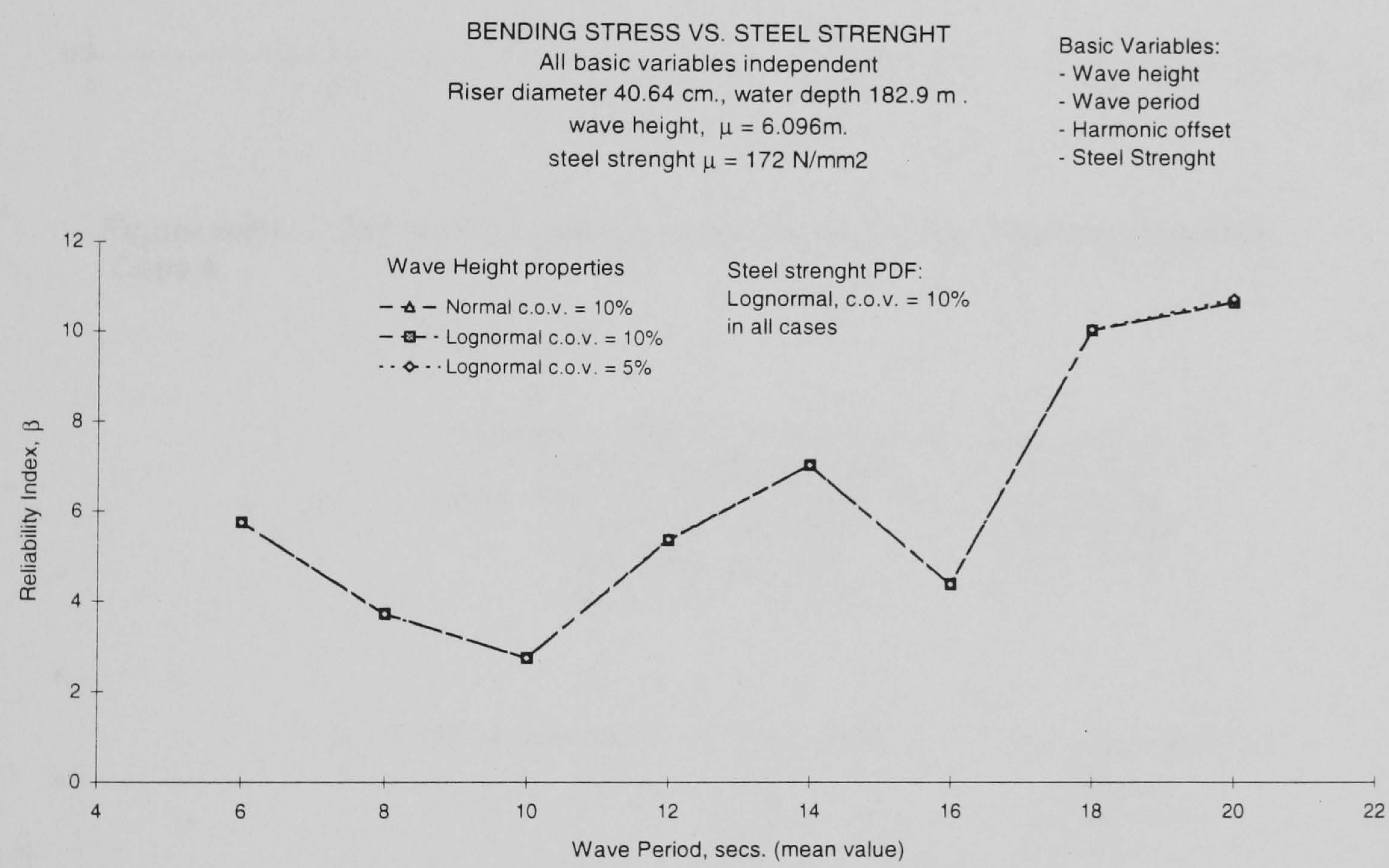

Figure 5.6a. Variation of the reliability index with wave height, **Case 4**.

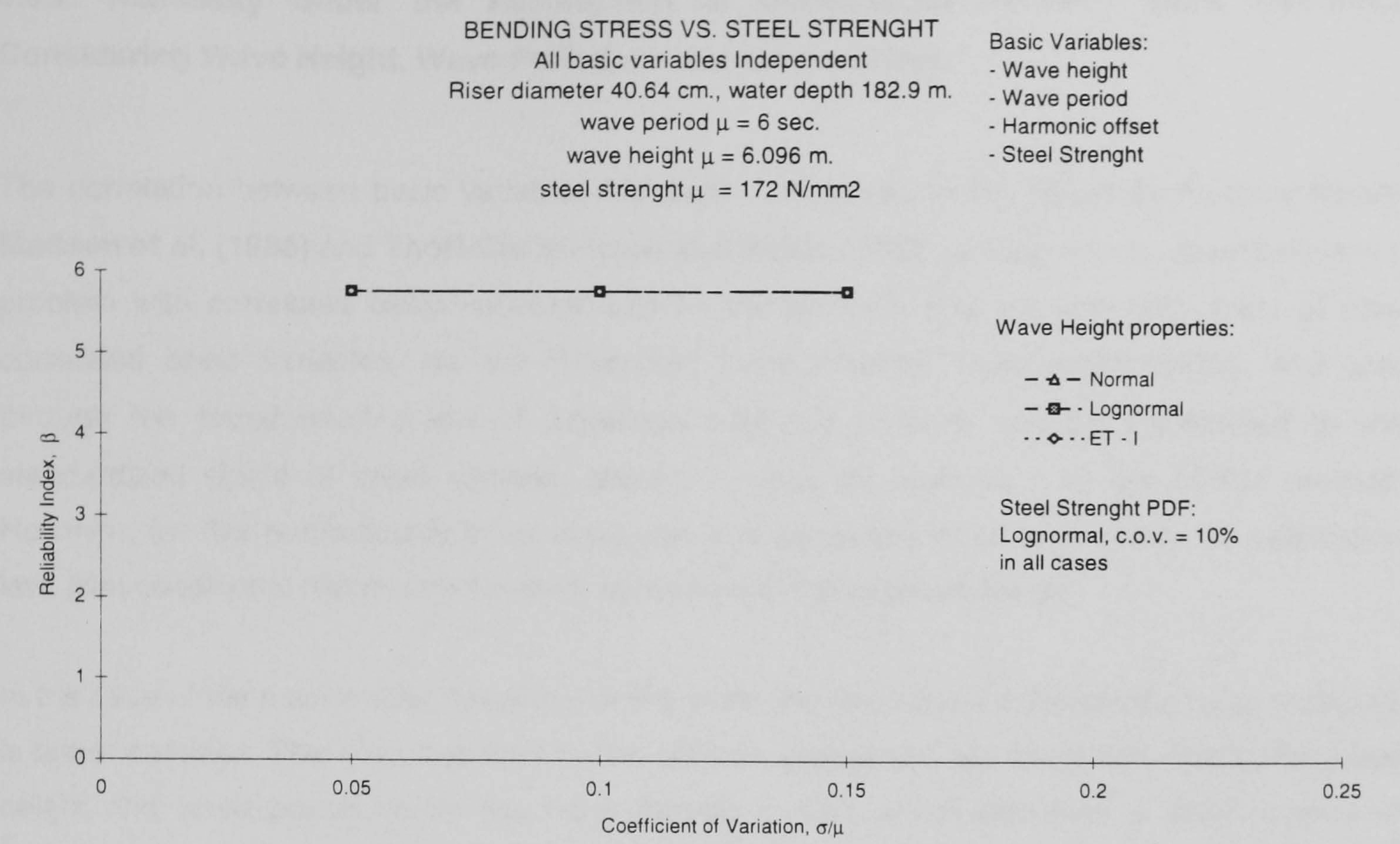

Figure 5.6b. Variation of the reliability index with wave height standard deviation, **Case 4**.

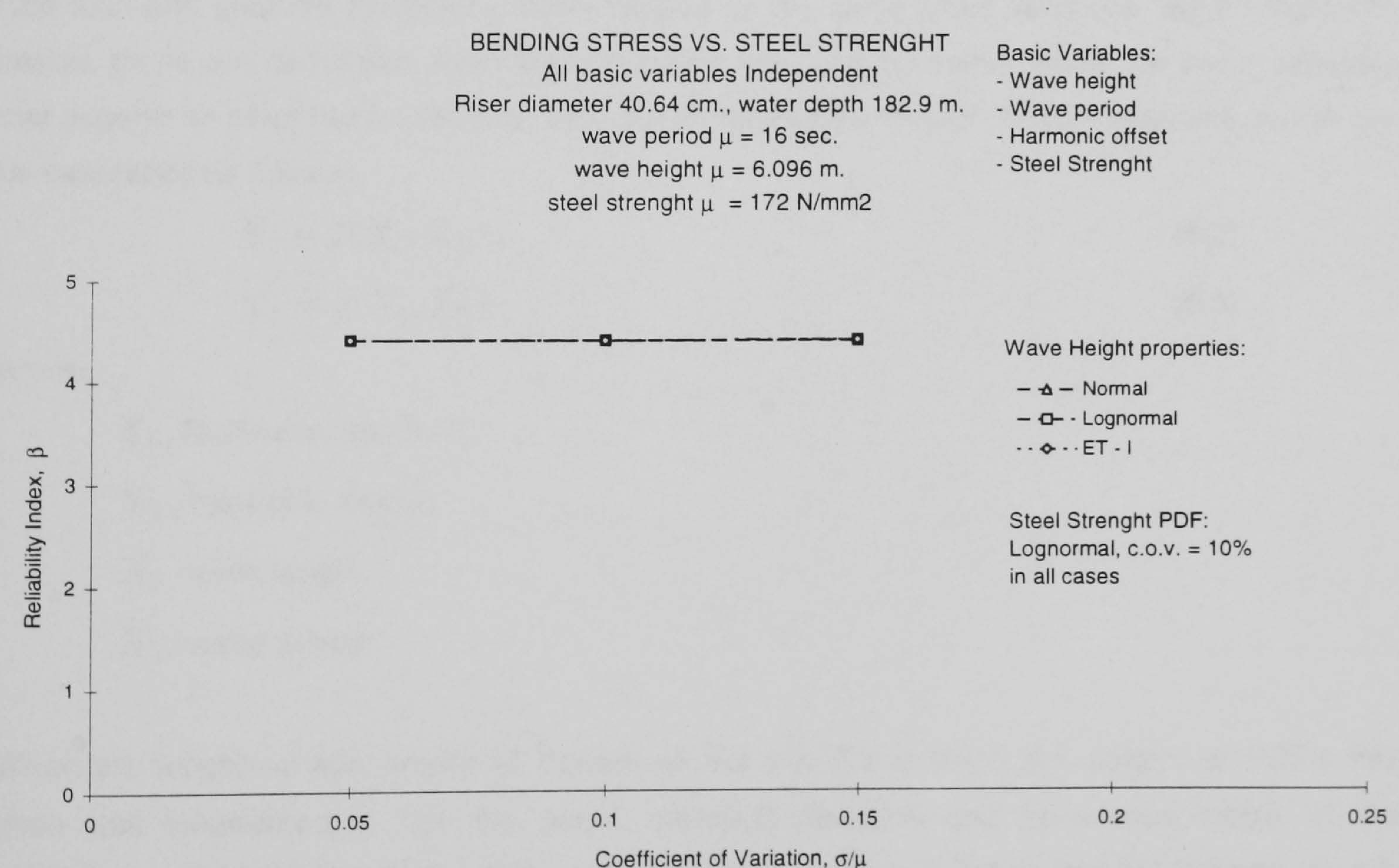

Figure 5.6c. Variation of the reliability index with wave height standard deviation, **Case 4**.

5.3.2. Reliability Under the Assumption of Dependence Between Basic Variables, Considering Wave Height, Wave Period and Harmonic Offset.

The correlation between basic variables has been considered in the Reliability Analysis theory. **Madsen et al. (1986)** and **Thoft-Christensen and Baker (1982)**, among others, described how a problem with correlated basic variables can be transformed, first into one with a set of non-correlated basic variables, via the Rosenblatt transformation, **Rosenblatt (1952)**, and later through the transformation law of **Equation 1.26** the problem can be transported to the standardized space of basic variable, leaving it ready for application of the FORM method. However, for this methodology to be applicable it is necessary to know explicitly the correlation law, joint conditional distribution function, between the implicated variables.

In the case of the marine riser described in this work, the relationship between the basic variables is rather complex. The riser is excited by two different processes, but correlated. Firstly, the wave height and wave period define the wave particle motion, which becomes a direct source of excitation for the riser, the so called Morison type load, see **Equation 4.29**. On the other hand, the wave particle motion induces platform surge and sway, here generically called harmonic offset, which can be found by means of the diffraction theory. This platform motion is the most important source of dynamic excitation, see **Figure 5.1**. Since the two load processes, Morison's type load and platform harmonic motion depend on the same basic variables, wave height and period, these are correlated. Both Morison's type load and harmonic offset are basic variables that depend on other basic variables, they are therefore functions of random variables, which can be expressed as follows:

$$\mathbf{Y}_1 = f(X_1, X_2) \tag{5.2}$$

$$\mathbf{Y}_2 = f(X_1, X_2) \tag{5.3}$$

where:

$\mathbf{Y}_1$, Morison's type load,

$\mathbf{Y}_2$, harmonic motion,

X_1, wave height,

X_2, wave period.

When the functional relationship of **Equations 5.2** and **5.3** is linear the algebra of PDF's has been well established to find the mean, standard deviation and covariance matrix of the correlated variable. If the relationship is non-linear the problem is not as straight forward. As it is possible to observe in **Figure 4.5** the harmonic offset is a non-linear function of wave height and wave period and **Equation 4.29** shows that Morison's type load is also a non-linear function of wave particle kinematics. Therefore, determination of the statistical properties of the harmonic offset and Morison's type load require an application of the algebra of random variables which is not readily available.

As was mentioned at the beginning of the previous section, the approach of **Bucher and Bourgund (1990)** for the construction of the response surface proposed the initial assumption of statistical independence between the basic variables. This approach was followed in **Section 5.3.1**, however, the results demonstrated that the behaviour of the reliability index follows some unexpected performance. This is happening because the response of the platform, in the form of sway or surge, can not be assumed to occur as an independent random variable, but the dependence on wave height and wave period must be taken into account. Nevertheless, if the uncertainty associated with the harmonic offset is to be introduced in the reliability analysis, then it is necessary to know its functional relationship with wave height and wave period. The best method to include the uncertainty of platform response as a function of the uncertainty in wave height and period, and possibly other variables, would be to determine the platform response by means of diffraction theory, or another applicable one, for each different combination of wave height and period, as required for construction of the riser response surface. If the platform response can be given as a more simple functional relationship, as in **Figure 4.5**, the problem would be, as mentioned before, to fit a joint probability distribution for the harmonic offset as a function of wave height and period; but, this perspective poses some complexities, the solution of which within the analytic frame of the algebra of PDF's may prove intricate. Therefore, some approaches to attempt the introduction of the dependence of harmonic offset on wave height and period, as presented in **Figure 4.5**, are proposed and applied in the following.

Two possible procedures to construct the response surface are proposed here. The first approach is to construct the response surface in the usual form, however, the harmonic offset is not introduced as an explicit variable in the equivalent function, $\bar{g}(\mathbf{x}) = 0$, but its specific value is to be found as a function of the particular combination of wave height and period and used in the mechanical model for determination of the riser response. In this way the correlation of harmonic offset with the other two variables is taken into account in an implicit manner. Since the harmonic offset is not an explicit variable in $\bar{g}(\mathbf{x}) = 0$, it will not be possible to review its statistical properties with the response surface. This approach will be referred from now on as **Type I**. In order to apply this approach a rational polynomial was fitted to the curve giving the harmonic motion as a function of wave height and period, **Figure 4.5**. The algorithm contributed by **Graves-Morris and Hopkins (1981)** was used here. The corresponding polynomial is introduced as the load process feeding the mechanical model. With this method it is assumed that the only variables influencing the platform response are wave height and period, consequently, the uncertainty in platform response is a function of the uncertainty in wave height and period.

In the second approach the response surface is built in the usual manner, as well, but a large standard deviation is allowed in order to consider for an ample range of harmonic offset values. One characteristic of this second approach is that harmonic offset is an explicit variable in $\bar{g}(\mathbf{x}) = 0$ and it is, in principle, possible to study different PDF's and standard deviations assigned to it. Such operation will not be executed at this stage, because the joint probability distribution of the variables of interest is needed in an explicit form for the application of the FORM method or for the generation of the random variates in the Monte Carlo simulation, AIS algorithm; that is, the assumption of independence will still be holding. This second approach will be referred to as **Type II**. One additional point should be mentioned, if the standard deviation selected at the stage of construction of the response surface is not sufficiently large, there is a risk of not accounting for some values of harmonic offset, therefore incurring in some unknown degree of error in the response surface. Furthermore, the standard deviation given depend on the judgement of the analyst and some degree of arbitrariness is unavoidable.

After the foregoing discussion it may be appropriate to mention at this point that, though wave height and wave period are two correlated variables, see for instance **Longuet-Higgins (1952)**, the cases presented in this chapter attempt to show the behaviour of the reliability index for a wide range of possible combinations of such variables, and hence these two variables are considered as independent.

Before presenting the results of the sensitivity studies performed in this section, the characteristics of the cases to be discussed are given in **Table 5.3**.

Correlation with Harmonic Offset considered

	Basic variables	PDF type	Mean value	cov.	Response Surface Type
Case 1a	wave height (implicit harmonic offset)	several	6.096 m.	several	Type I
Case2a	wave period (implicit harmonic offset)	several	6 to 20 secs. (several)	several	Type I
Case3a	wave height, harmonic offset	several Lognormal	6.096 m. as in **Fig.4.5**.	several 30%	Type II
Case4a	wave height wave period harmonic offset	several Lognormal Lognormal	6.096 m. 6 - 20 secs. as in **Fig.4.5**.	several 10% 30%	Type II
Case4b	wave height wave period harmonic offset (implicit)	several Lognormal	6.096 m. 6 - 20 secs. as in **Fig.4.5**.	several 10%	Type I

Type I, dependence of harmonic offset considered implicitly.
Type II, all basic variables independent, harmonic offset with a large standard deviation.

Table 5.3. Cases for sensitivity analysis, dependent basic variables.

Case 1a.

Using approach **Type I**, the wave height and steel strength will be considered the two random basic variables and the remaining conditions will be kept as in **Table 5.1**. The reliability index is presented in **Figure 5.7a**, as usual, for a range of wave periods in the interval of 6 to 20 seconds. It can be appreciated that this time the influence of different PDF's and standard deviations seem to be more sound, that is, the higher the uncertainty the lower the reliability index, this can be more clearly distinguished in **Figure 5.7b** and **5.7c**.

It can be noticed that the variation of reliability index at the wave period of 6 seconds is very small. Since the variation of platform offset is a function of wave height and period, **Figure 4.5**, it is observed that for an standard deviation of 0.6096 m., for the wave height, it is possible that events with a wave height between 4.084 m. to 8.107 m. happen, that is a range of 4.023 m. This means that the platform offset can acquire values between 1.225 m. to 2.405 m. While for the period of 16 seconds the harmonic offset can vary from 2.185 up to 4.289 m. This explains why the variation of the reliability index is less sensitive at low wave periods than at large ones, except for the case of 14 seconds. It can be observed in **Figure 5.2** that precisely at that period the stresses for two different wave heights, 6.096 m. and 9.144 m. coincide, as an effect to its closeness to the first natural period, therefore small variations of wave height around 6.096 m. do not significantly affect the reliability index.

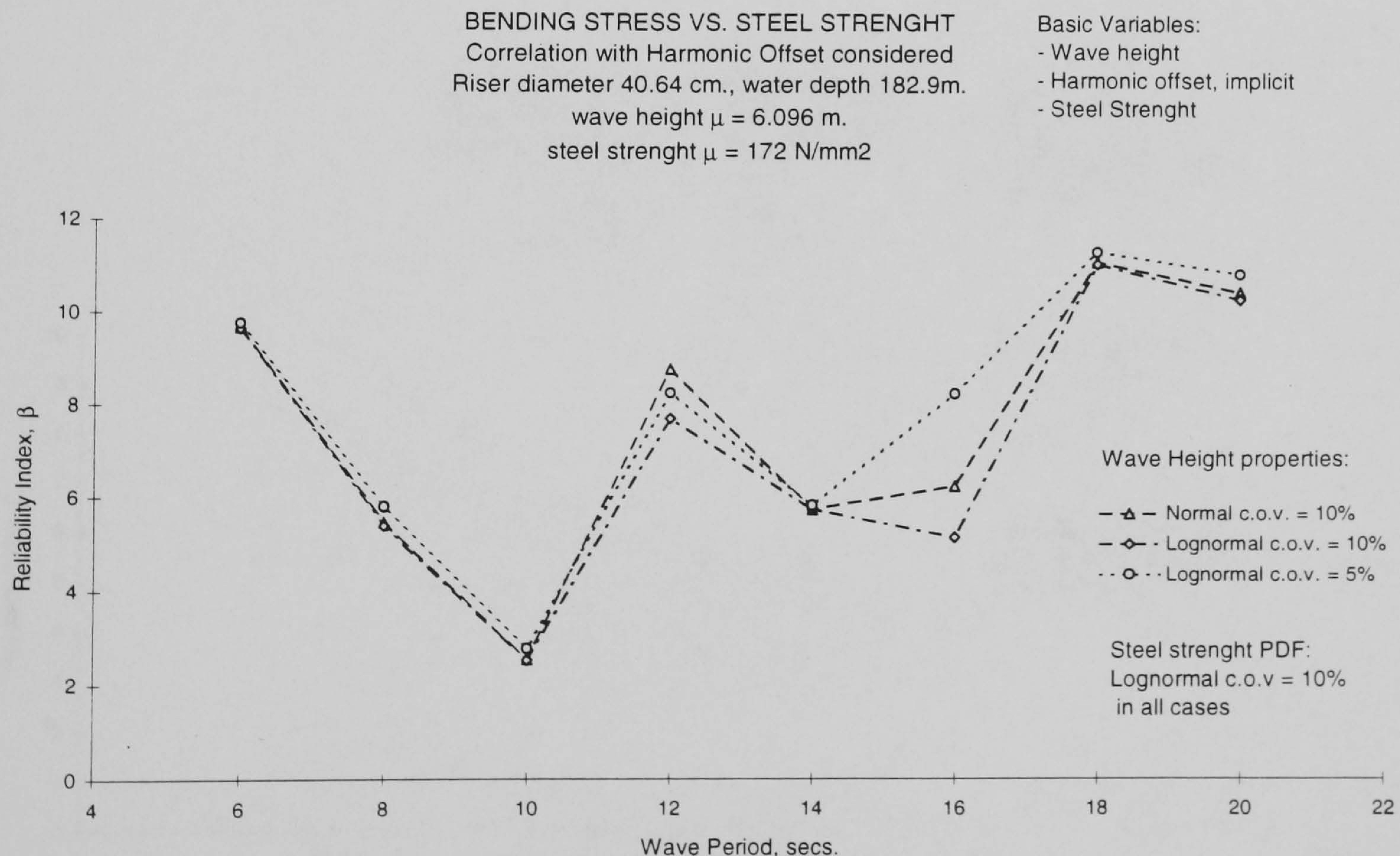

Figure 5.7a. Variation of reliability index with wave height and implicit harmonic offset, **Case 1a**.

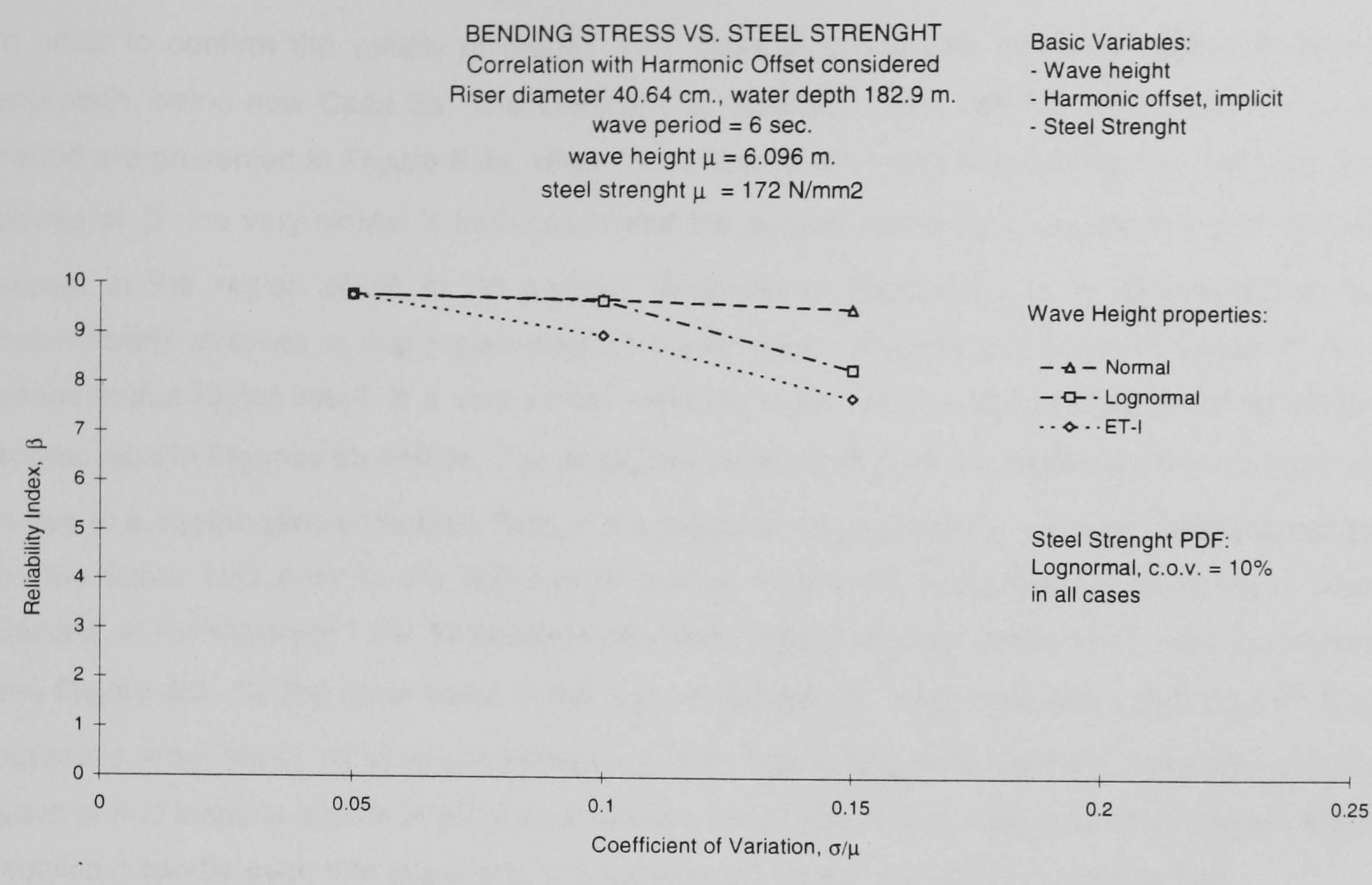

Figure 5.7b. Variation of reliability index with wave height standard deviation, implicit harmonic offset, **Case 1a**.

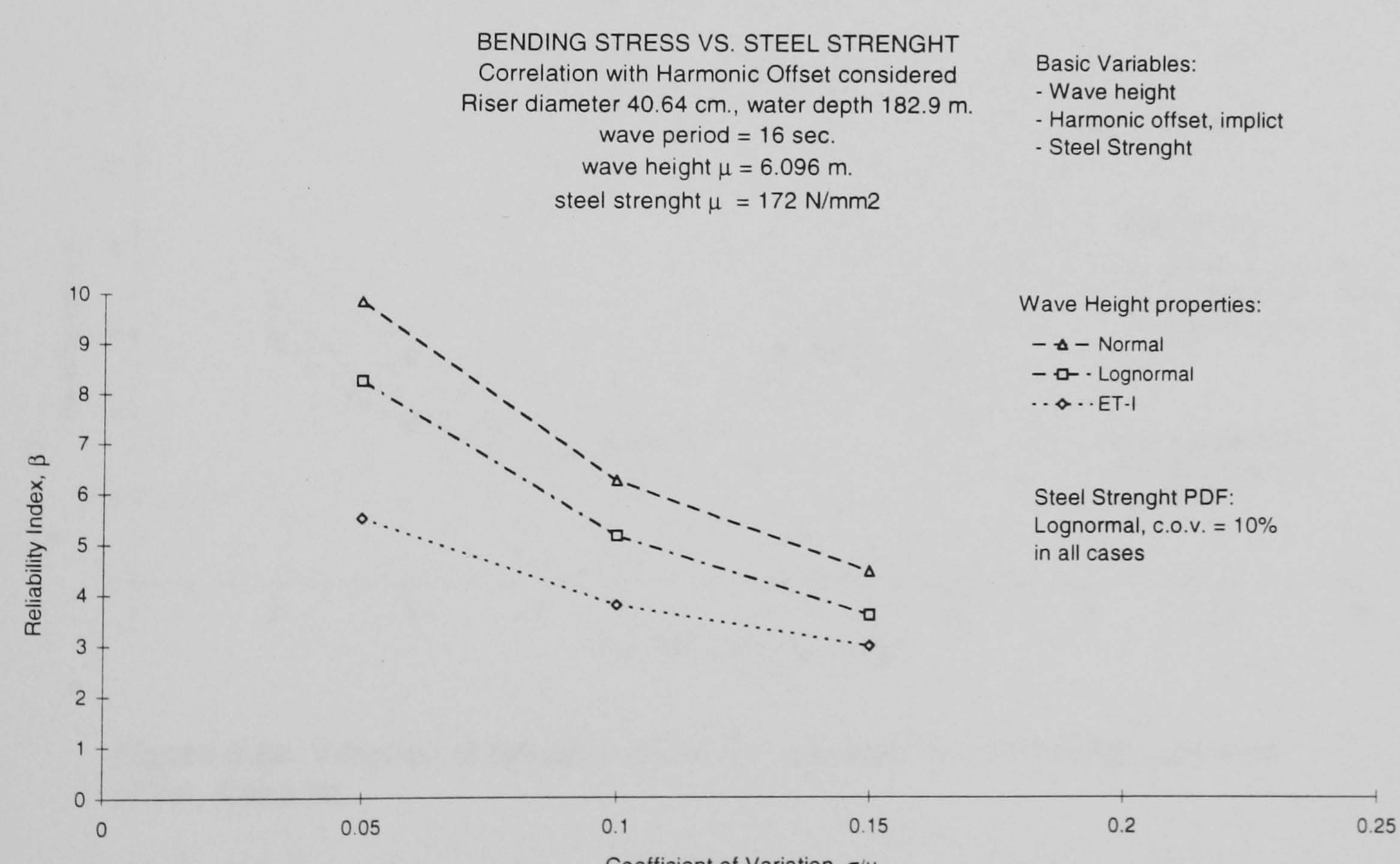

Figure 5.7c. Variation of reliability index with wave height standard deviation, implicit harmonic offset, **Case 1a**.

Case 2a.

In order to confirm the validity of results from **Case 2**, this will be reviewed using the **Type I** approach, being now **Case 2a**. The variations of reliability index with the mean value of wave period are presented in **Figure 5.8a**, where a number of important features can be followed. The values of β are very similar in both cases and the general tendency of variation is also related, except in the region of 18 to 20 second. Referring to **Figure 5.1**, it is perceived that the deterministic stresses in that region present a very weak variation, therefore variations of wave period in that region result in a very similar reliability index. This tendencies can be more clearly appreciated in **Figures 8b** and **8c**. The negligible variation of β in the region of 10 to 14 seconds is due to a combination of factors. First, in the region of 10 seconds the wave period takes values on the upper limit near to the first natural period, where the hydrodynamic damping is high. Second, in the region of 13 to 15 seconds the deterministic stresses present very little fluctuation, see **Figure 5.1**. On the other hand, in the zone of 6 seconds a very important reduction of β is observed, from about 10 to values between 8 to 6. This is due to the fact that uncertainty in the wave period leads to events in which this variable may be as low as 4 second and if **Figure 4.5** is recalled it can be seen that at periods of 3 seconds and lower the platform remains still.

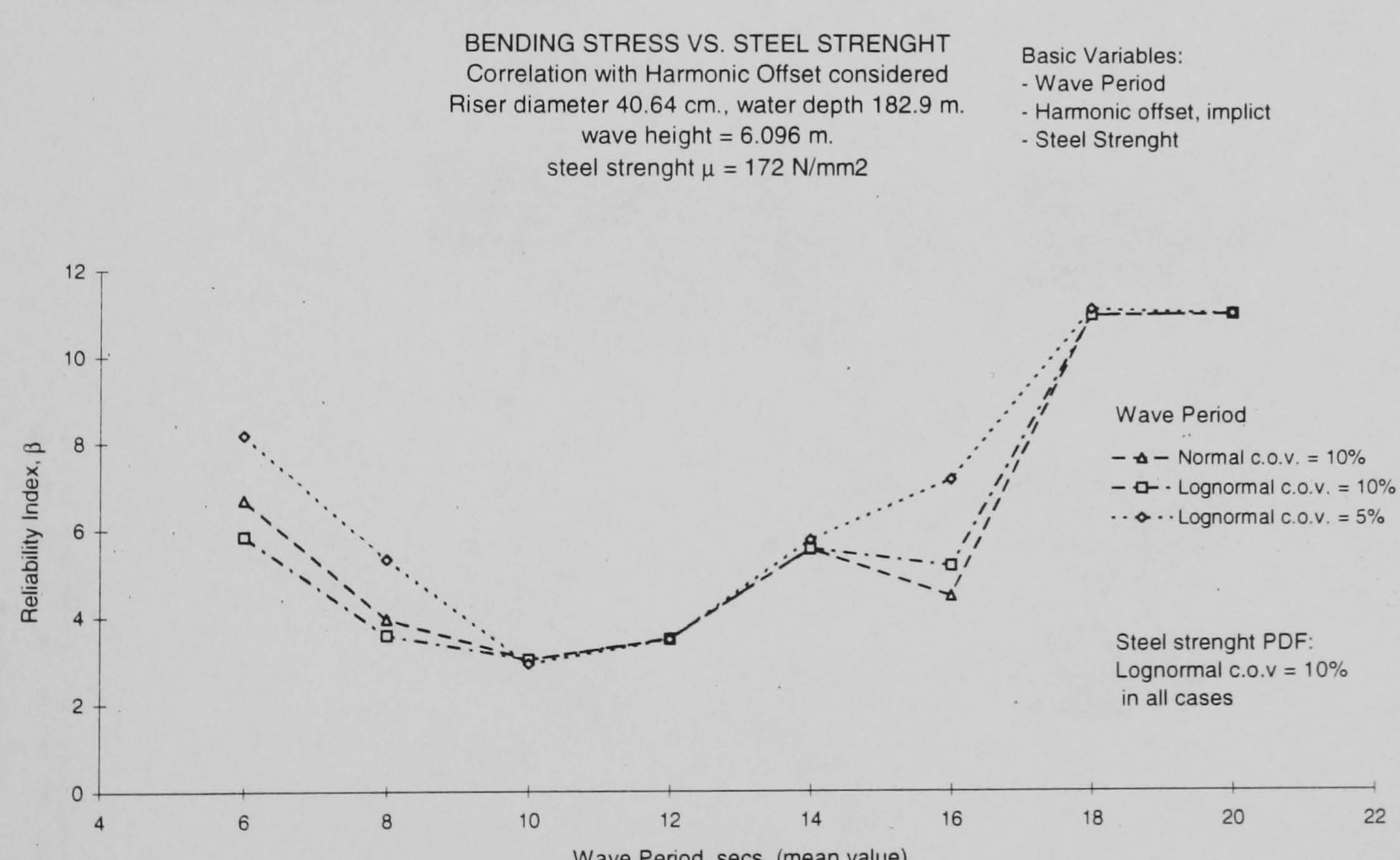

Figure 5.8a. Variation of reliability index with wave period and implicit harmonic offset, **Case 2a**.

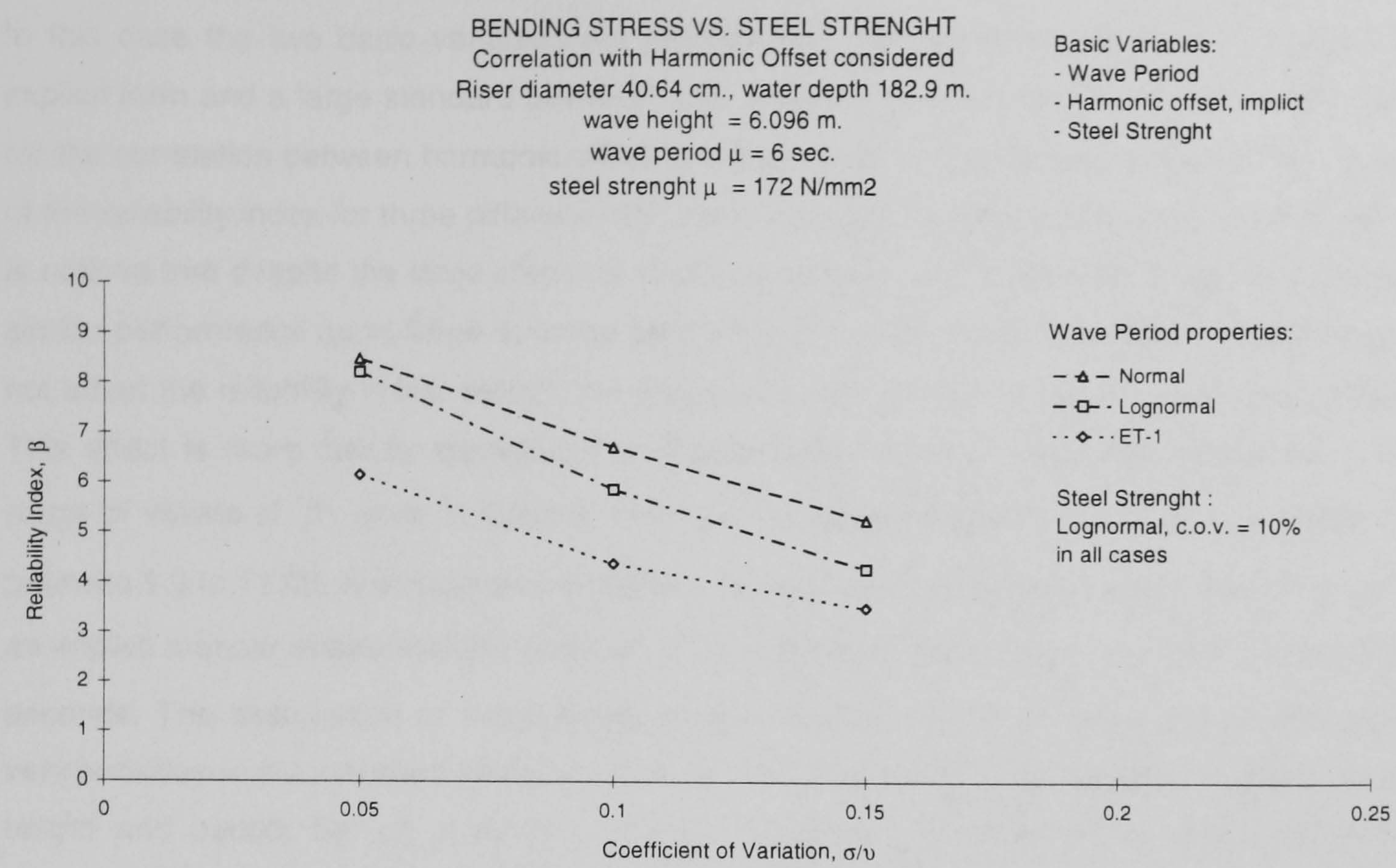

Figure 5.8b. Variation of reliability index with wave period standard deviation, implicit harmonic offset, **Case 2a**.

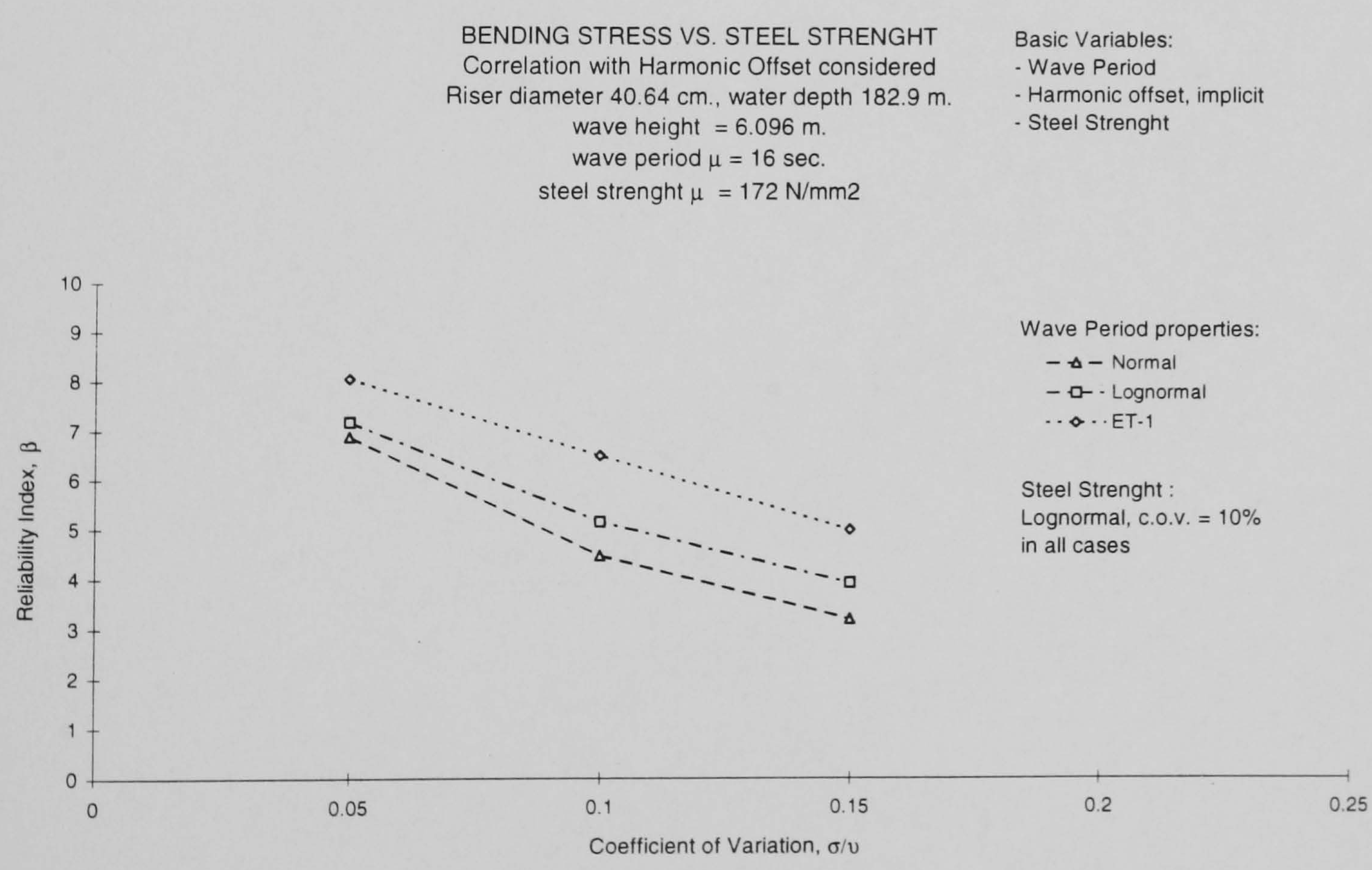

Figure 5.8c. Variation of reliability index with wave period standard deviation, implicit harmonic offset, **Case 2a**.

Case 3a.

In this case the two basic variables are independent, the harmonic offset is introduced in an explicit form and a large standard deviation was assigned to it in order to attempt to compensate for the correlation between harmonic offset and wave height. **Figure 5.9a** presents the variations of the reliability index for three different PDF's and standard deviations assigned to wave height. It is noticed that despite the large standard deviation of harmonic motion the reliability index has a similar performance as in **Case 1**, in the sense that changes in the properties of wave height do not affect the reliability index, though the distribution with respect to the wave period is different. This effect is more clearly appreciated in **Figure 5.9b**. Another noticeable difference is in the range of values of β, while in **Case 1** there is a fluctuation between 2.9 to 12.4, in **Case 3** it is between 1.9 to 11.06. A comparison with **Case 1a**, in which the harmonic offset was introduced in an implicit manner shows that the levels of β are dissimilar, especially in the interval from 6 to 10 seconds. The assumption of independence between these basic variables makes the problem very sensitive to the standard deviation of harmonic offset, which in turn depend not only on wave height and period, but on a number of other variables. Therefore, it is concluded that the assumption of independence between harmonic offset, wave height and wave period is not valid for the riser problem under consideration.

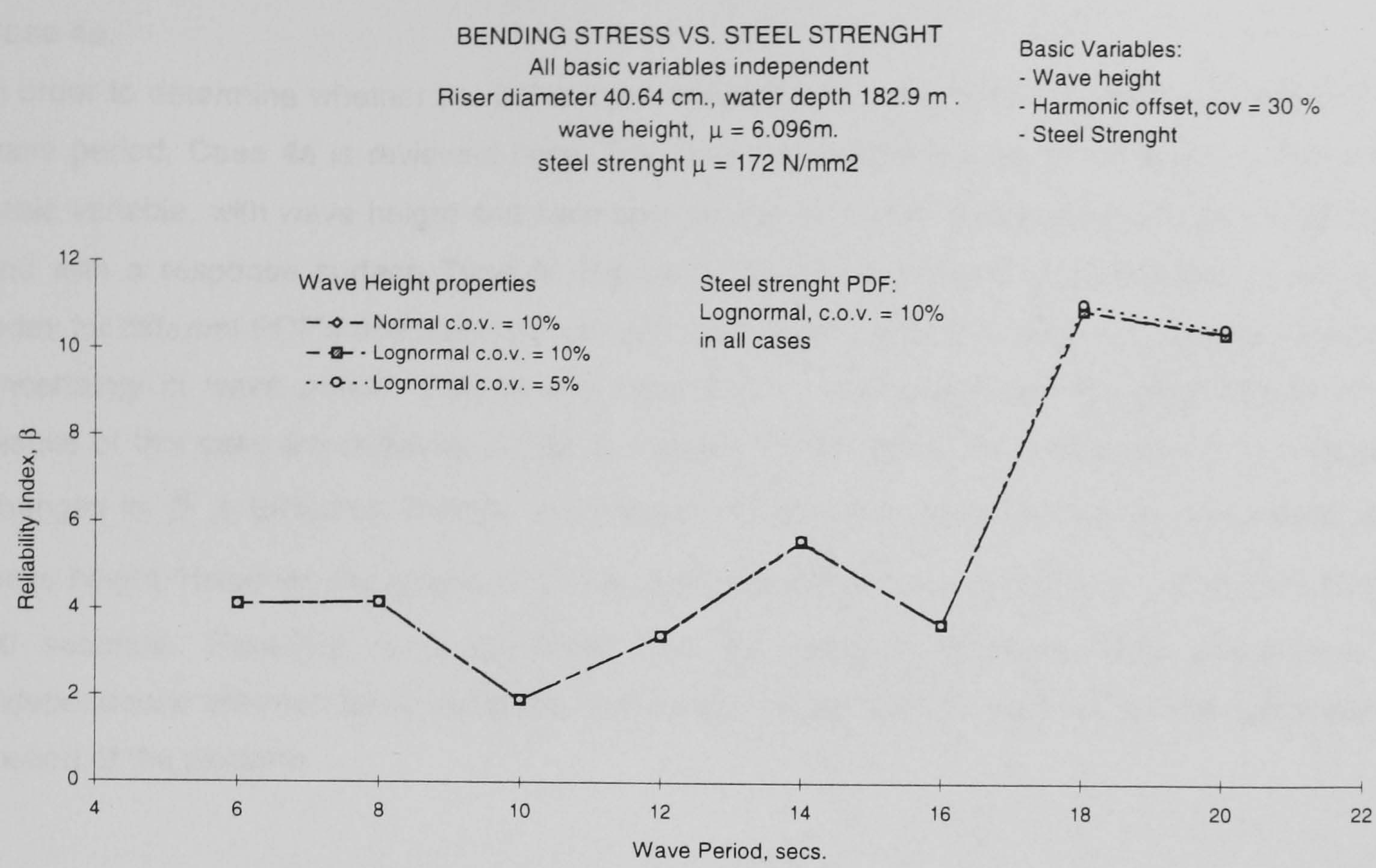

Figure 5.9a. Variation of reliability index with wave period and harmonic offset with large standard deviation, **Case 3a**.

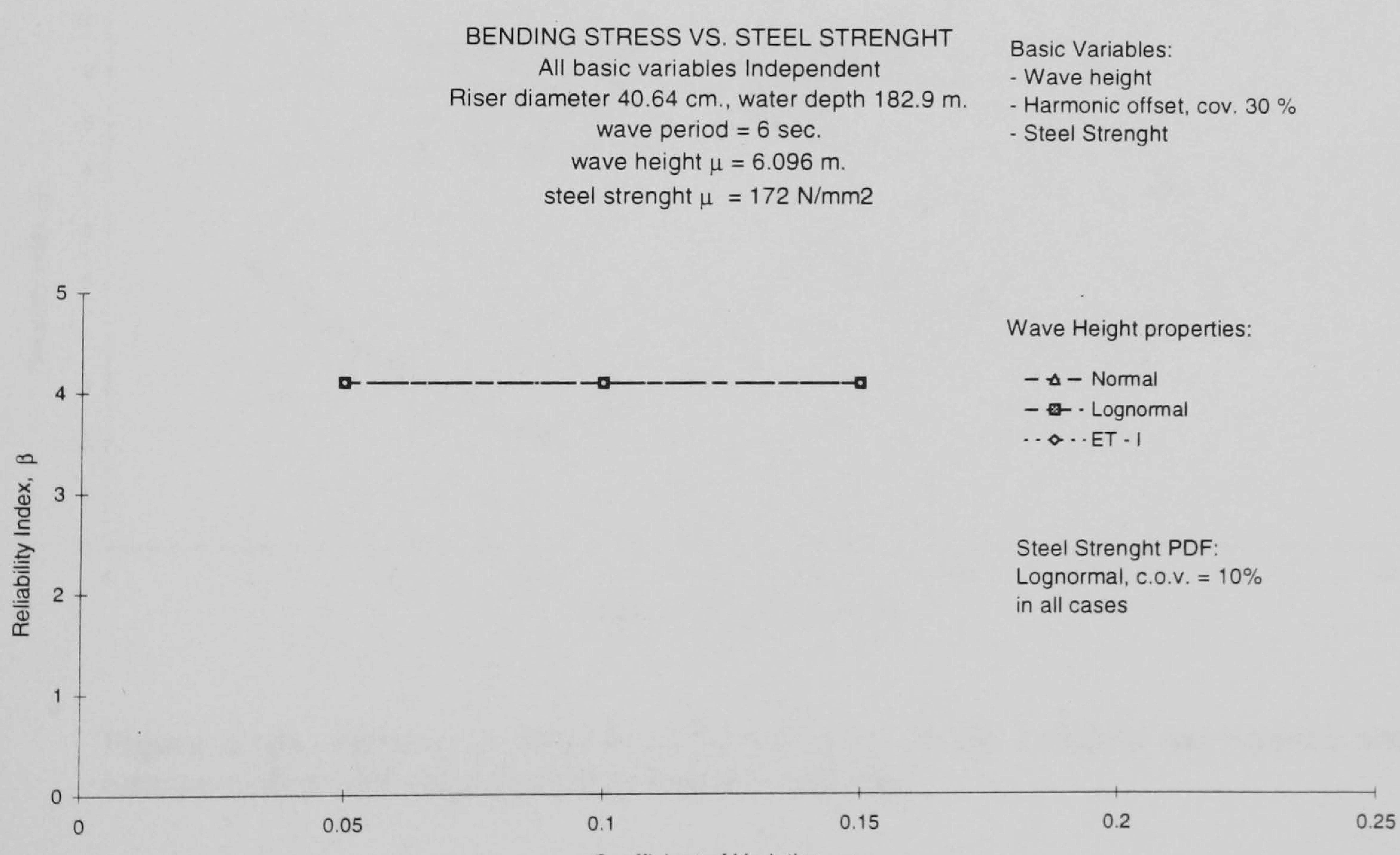

Figure 5.9b. Variation of reliability index with wave height standard deviation, harmonic offset with large variance, **Case 3a**.

Case 4a.

In order to determine whether the behaviour observed previously was due of the influence of the wave period, **Case 4a** is reviewed here. This time the wave period is considered as an explicit basic variable, with wave height and harmonic offset having the same properties as in **Case 3a**, and with a response surface **Type II**. **Figure 5.10a** presents again the variations of reliability index for different PDF's and standard deviations of wave height, this time including the effects of uncertainty in wave period. Despite the increment in harmonic offset standard deviation the results of this case are relatively similar to **Case 4**, in the sense that the tendency of negligible changes in β is exhibited, despite variations on PDF and standard deviations associated with wave height. However, the values of β are noticeably different, particularly in the region of 10 to 20 seconds. Therefore, it is confirmed that the previous statement, the assumption of independence between basic variables is not valid for the case of the marine riser subjected to motion of the platform.

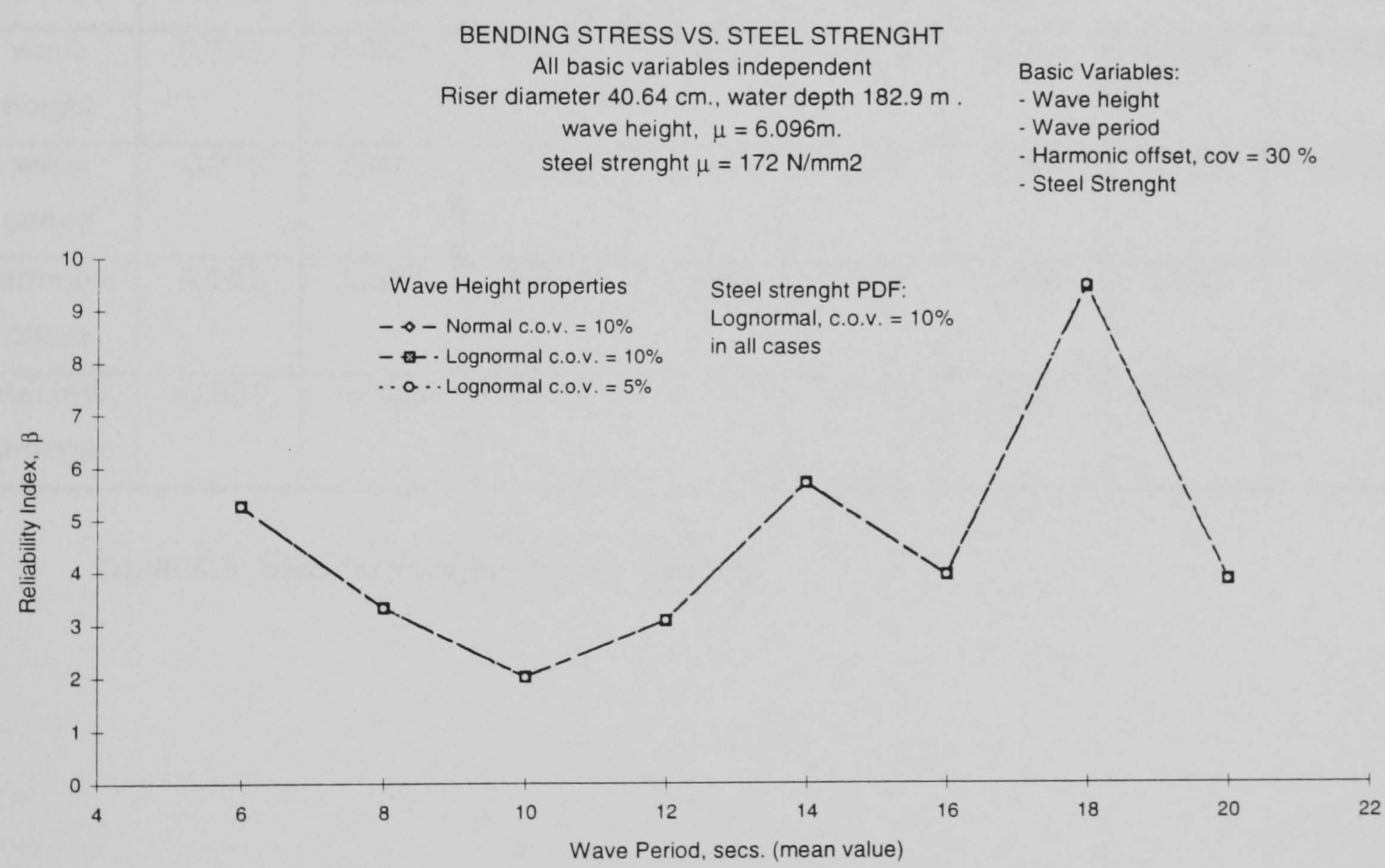

Figure 5.10a. Variation of reliability index with wave height, including wave period and harmonic offset with large standard deviation, **Case 4a**.

This performance is confirmed by the sensitivity coefficients, presented in **Table 5.4**, the wave height is the variable with the smallest sensitivity coefficient values, for all the periods considered. For that reason variations on PDF or standard deviation induce insignificant fluctuation of the β value. The performance of the reliability index for a number of different values of the standard deviation associated with the harmonic offset is given in **Figure 5.10b**. It is possible to observe that at some periods the influence of harmonic offset on the value of β is very low, at the regions around 14 and 18 seconds, while at others it seems to have significant influence, this is also a consequence of the sensitivity coefficients. However, considering that values assigned to the standard deviation are extremely large the fluctuation of β is not as expected. This situation is believed to happen on account of the assumption of independence between these three variables

Basic Variable	6 secs. Period	8 secs. Period	10 secs. Period	12 secs. Period	14 secs. Period	16 secs. Period	18 secs. Period	20 secs. Period
wave height	0.223	0.0031	0.012	0.006	-0.118	0.016	0.074	0.004
wave period	-0.716	0.648	0.038	-0.107	-0.373	-0.643	0.025	-0.093
harmonic offset	0.043	0.527	0.762	0.976	0.124	0.562	0.367	0.972
material strength	-0.661	-0.550	-0.646	-0.192	-0.912	-0.521	-0.927	-0.216

Table 5.4. Sensitivity coefficients for **Case 4a**.

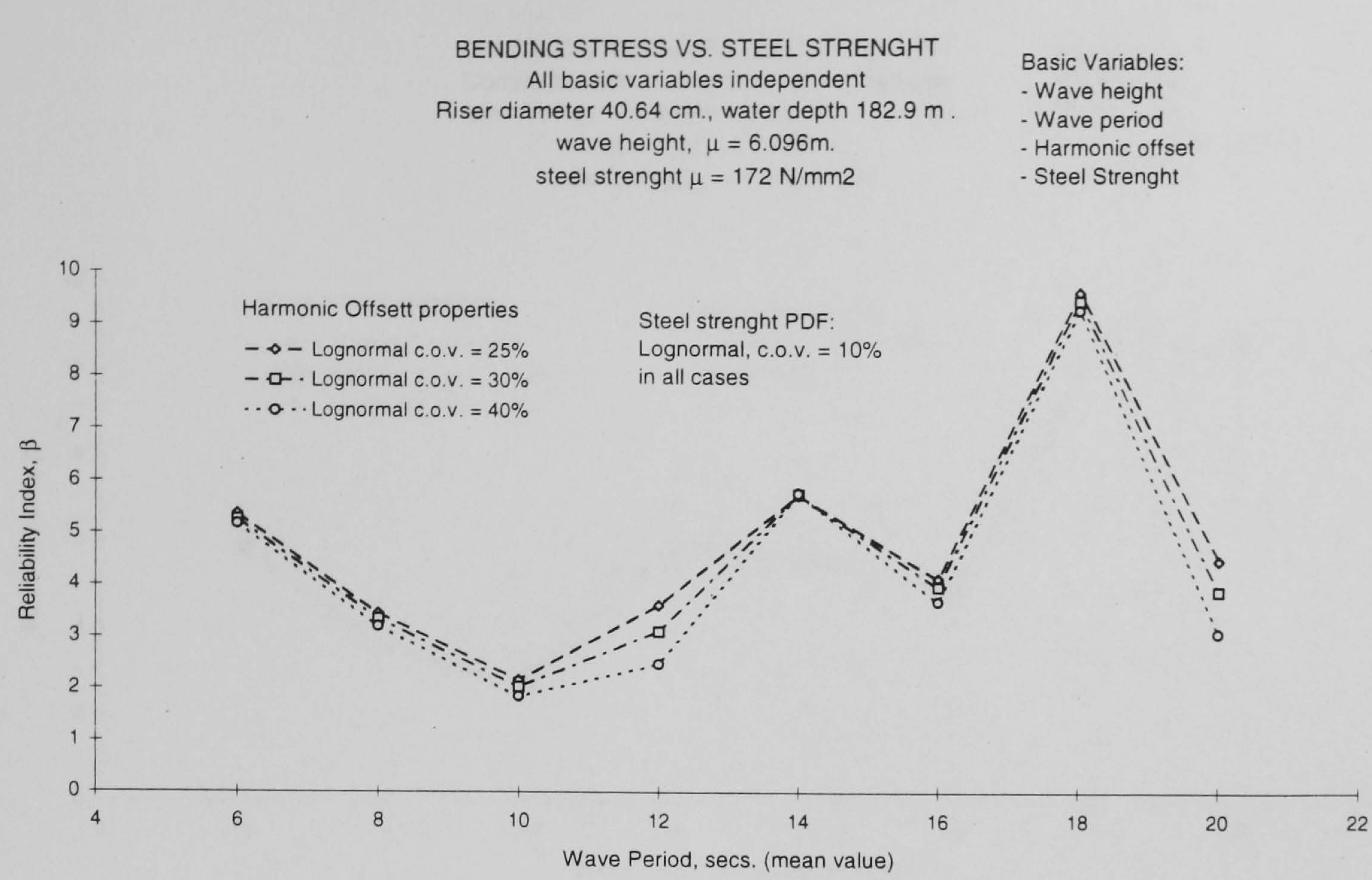

Figure 5.10b. Variation of reliability index for harmonic offset with large standard deviation, including wave period.

Case 4b.

In this case the influence of the harmonic offset is introduced in an implicit manner, **Type I** approach. The variations of β are presented in **Figure 5.11a**. It is possible to appreciate that variations in PDF and standard deviation attached to wave height yield changes in the reliability index, for most of the wave periods, this is presented with more detail in **Figure 5.11b**. In the region of 6 to 8 seconds the wave height uncertainty does not create significant changes in β; moreover, a comparison with **Case 1a** reveals the same decrement in the reliability index already mentioned in **Case 2a**. In other words, a combination of the effects exhibited in **Cases 1a** and **2a** is observed in this case, for the whole range of periods. A comparison with **Cases 4** and **4a** show that values of β are different in each of the three cases, especially in the region from 12 to 20 seconds, though the case of independent basic variables with harmonic offset having 10% standard deviation approaches more sensibly the case when dependence of harmonic offset is taken into consideration. This can be easily appreciated in **Figure 5.12**, where these three cases are compared.

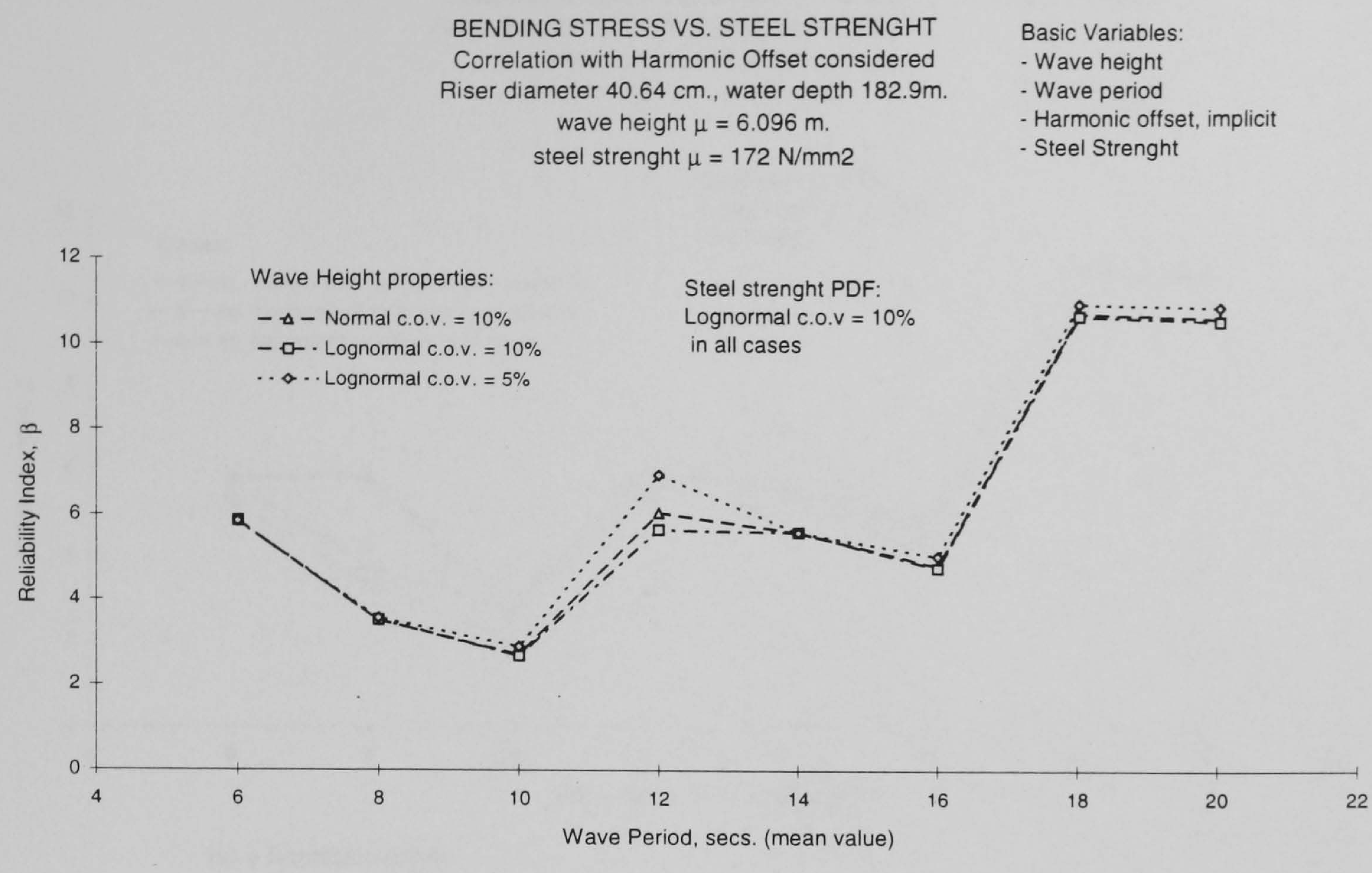

Figure 5.11a. Variation of reliability index with wave height, wave period and harmonic offset included implicitly, **Case 4b**.

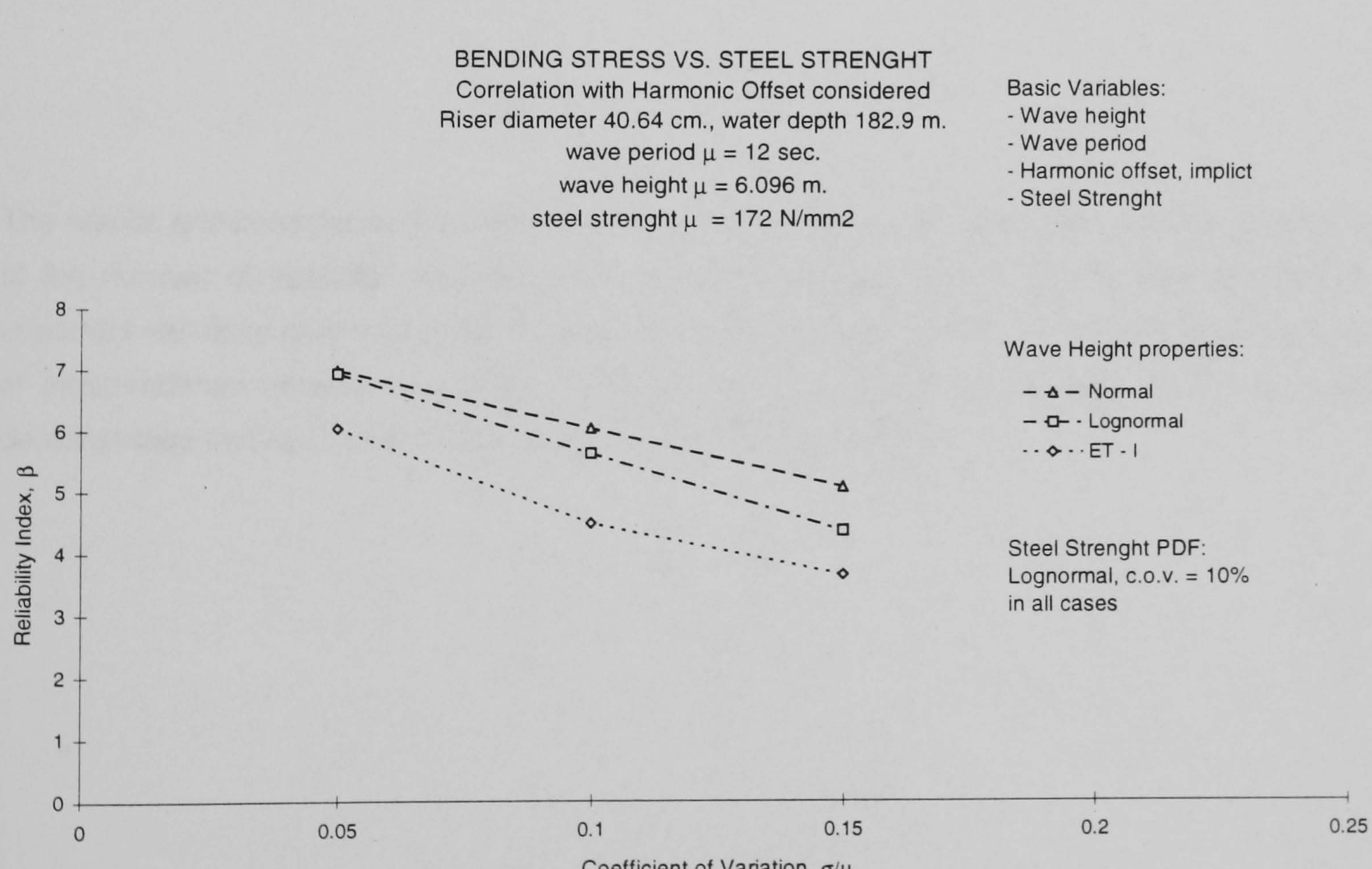

Figure 5.11b. Variation of reliability index with wave height standard deviation, harmonic offset included implicitly, **Case 4b**.

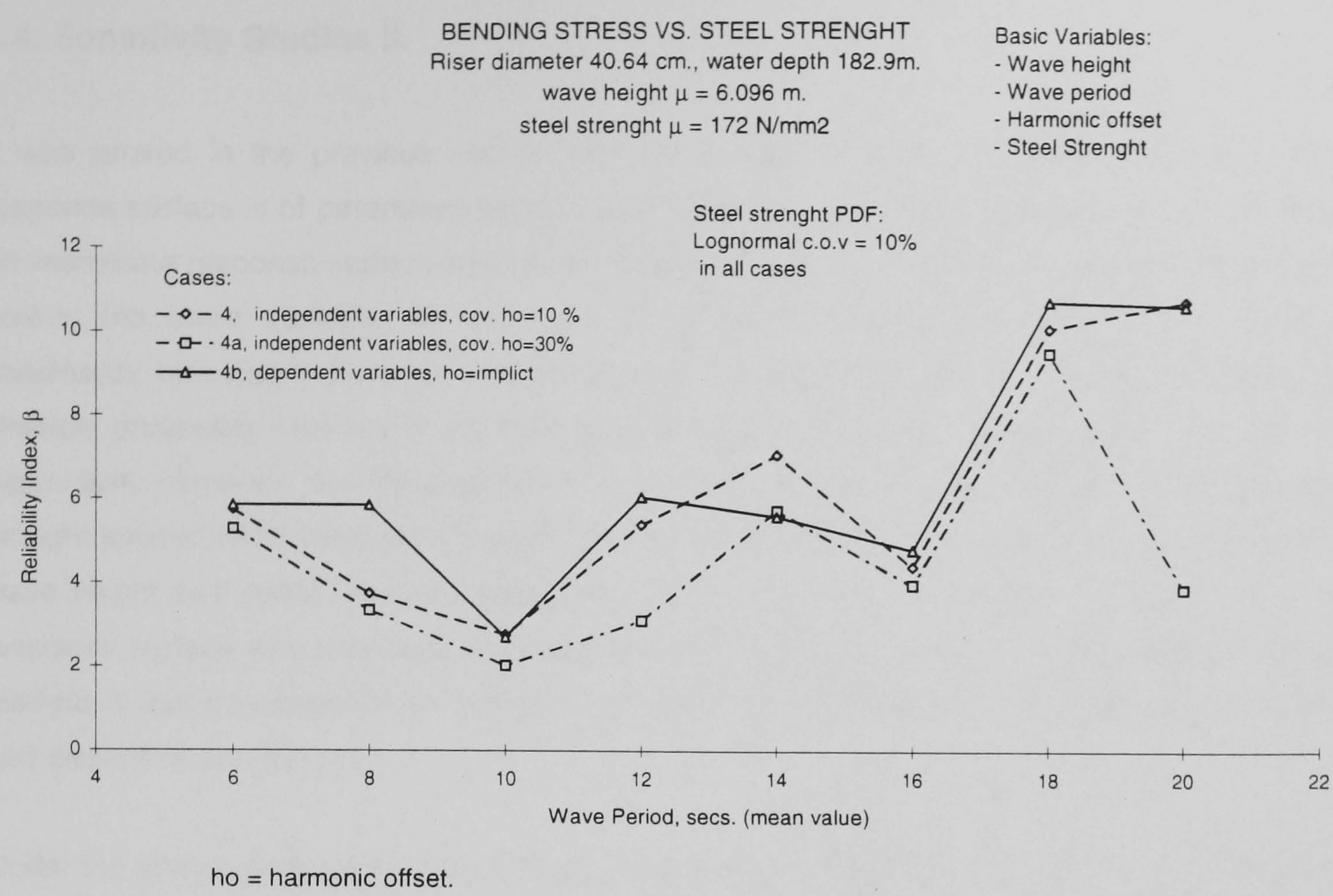

Figure 5.12. Comparison of reliability index for **Cases 4**, **4a** and **4b**.

The results and behaviours observed in the cases analysed in this section reveal the significance of the number of variables included in the response surface model, namely that omission of important variables may lead to dubious reliability index results, in the same fashion assumptions of independence between the basic variables must be considered carefully, as it has been demonstrated that such assumption is not valid for this type of riser.

5.4. Sensitivity Studies II.

It was proved in the previous section that the number of basic variables considered in the response surface is of paramount importance, omission of important basic variables may render an inaccurate response surface and therefore reliability indices. The assumption of independence among the basic variables at the level of construction of the response surface must be considered with due care, since this assumption cannot be applied as a rule. A review of the physical processes involved in the mechanical model may help to assess which variables are dependent. However, the introduction of correlation among the basic variable is not always a straight forward procedure. An approach in which harmonic offset, a basic variable dependent on wave height and period, is introduced in an implicit manner at the stage of construction of the response surface was proposed and demonstrated in **Section 5.3.2**. The disadvantage of such method is that no possibility for further considerations with respect to the probability distribution and dispersion can be given.

Under the above mentioned considerations the next step in the sensitivity studies is to review the reliability of the marine riser taking into account a larger number of basic variables, while harmonic offset is considered implicitly at the level of the mechanical model. The basic variables to be introduced in the response surface, their associated PDF's and standard deviations are presented in **Table 5.5**.

Basic Variable	Probability Distribution Function	Mean Value (units)	Coefficient of Variation
(1) Wave Height	Normal	6.096 m.	10 %
(2) Wave Period	Lognormal	6 to 20 secs.	10 %
(3) Top Tension	Lognormal	721480.3 N (1.2 riser wight)	8 %
(4) Static Offset	Normal	5.486 m. (3% of depth)	10 %
(5) Ocean Current	Lognormal	1.028 m./sec.	10 %
(6) Drag Coefficient	Lognormal	0.5 non-dimensional	10 %
(7) Inertia Coefficient	Lognormal	0.7 non-dimensional	10 %
(8) Material Strength	Lognormal	172 N/mm^2	10 %

Table 5.5. Basic variables and data for riser reliability analysis.

After the estimation of the response surface and the calculation of the reliability index by means of adaptive importance sampling the sensitivity coefficients show which basic variables exert larger influence on the final value of the reliability index. **Table 5.6** exhibits that the tension applied at the top of the riser is by far the most important of all basic variables, in all cases, except for the 8 seconds period where the wave period plays a important roll. This is congruent with physical considerations, the top tension is necessary to provide enough stiffness for the riser to be stable. The reason for the deviation observed at 8 seconds period is attributed to the slope showed by the plot of harmonic offset as a function of wave height and period, see **Figure 4.5**. In this region the rate of change is larger than in any other ones, this means that slight changes in period yield important variations in harmonic offset.

Basic Variable	6 secs. Period	8 secs. Period	10 secs. Period	12 secs. Period	14 secs. Period	16 secs. Period	18 secs. Period	20 secs. Period
1	0.0486	0.0689	0.1206	0.0634	0.0247	0.0734	0.0152	0.0196
2	0.1943	0.6907	0.0002	-0.101	-0.163	-0.367	0.0650	0.0206
3	-0.906	-0.496	-0.829	-0.850	-0.841	-0.836	-0.927	-0.938
4	0.0183	0.0269	0.0285	0.0214	0.0248	0.0179	0.0191	0.0190
5	0.0431	0.0641	0.0674	0.0505	0.0583	0.0419	0.0426	0.0431
6	0.0225	-0.038	0.0298	0.0279	-0.129	0.1073	0.0427	-0.003
7	0.1024	0.0084	-0.086	0.2874	0.0099	0.1309	0.0032	0.0044
8	-0.356	-0.516	-0.534	-0.422	-0.494	-0.362	-0.366	-0.342

Table 5.6. Sensitivity coefficients for a marine riser with eight basic variables.

In order to show the significance of the most important variables a study of the reliability index performance for top tension, material strength, wave period and wave height is presented in the following. It is important to mention that the standard deviations assigned to the basic variables in this study may be somehow larger than the ones usually found in the published literature, however, this was necessary in order to facilitate the visualization of the effects on the reliability index due to changes in such variables.

5.4.1. Top Tension.

The base case, given by **Table 5.5**, is used to study the effects on reliability index caused by variations in top tension PDF and standard deviation. **Figure 5.13a** presents the variations of the reliability index with a number of PDF's and standard deviations given to the top tension. It is possible to observe that β is slightly higher when a lognormal PDF is used instead of the normal, having both of them the same standard deviation. A reduction of the standard deviation, however, causes an important increment of β. Such effect can be further examined in **Figure 5.13b**. It can be concluded that careful consideration to the statistical properties attributed to this variable must be exercised, because of the impact it has in the overall performance of the system. Since the tension at the top of the riser is applied by a dedicated machinery, this variable can be controlled, if the riser is intended for long term operations, then the individual reliability of such component, including design, periodical inspection and maintenance, becomes a crucial step.

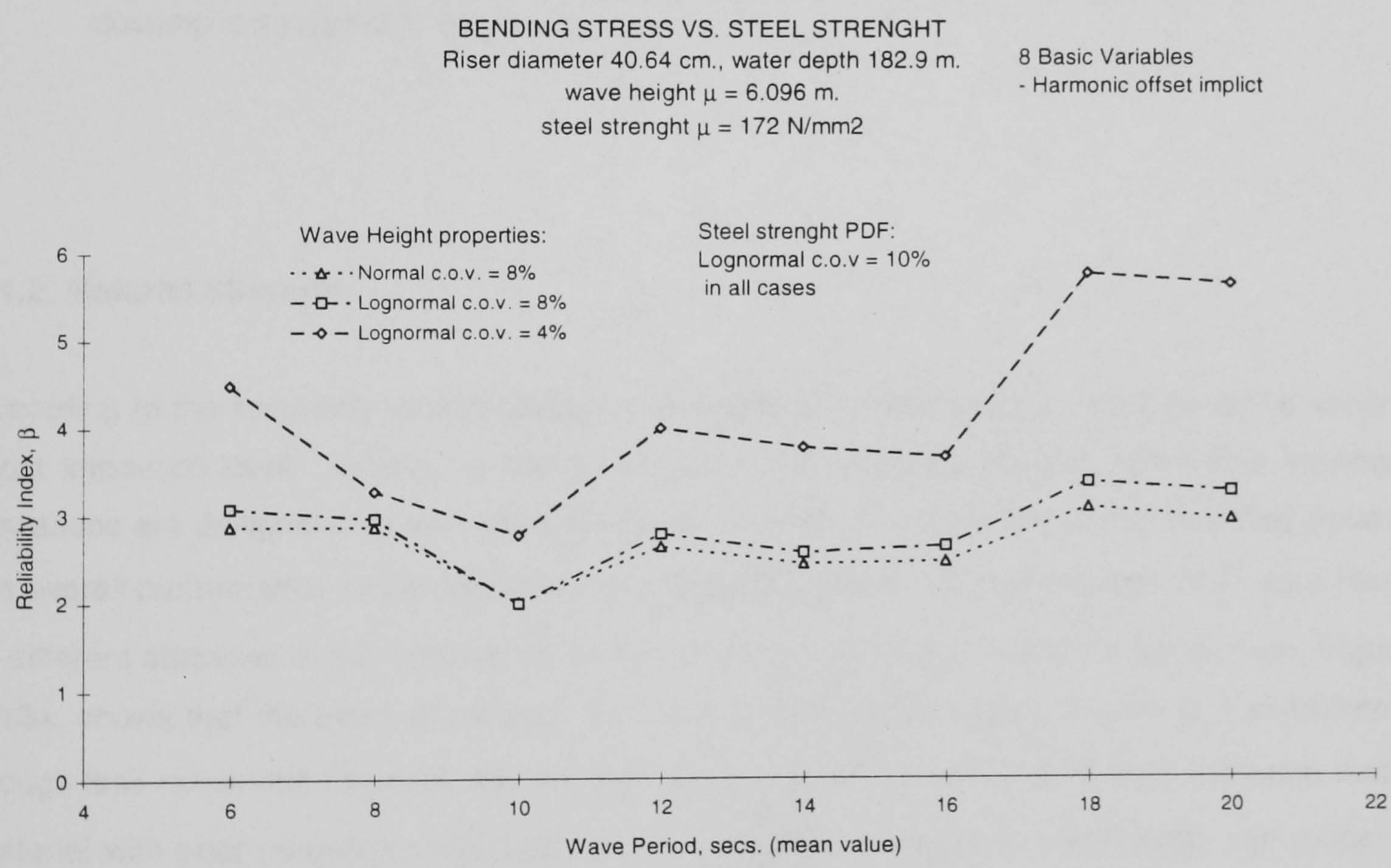

Figure 5.13a. Effects on the reliability index due to different PDF's and standard deviations assigned to top tension.

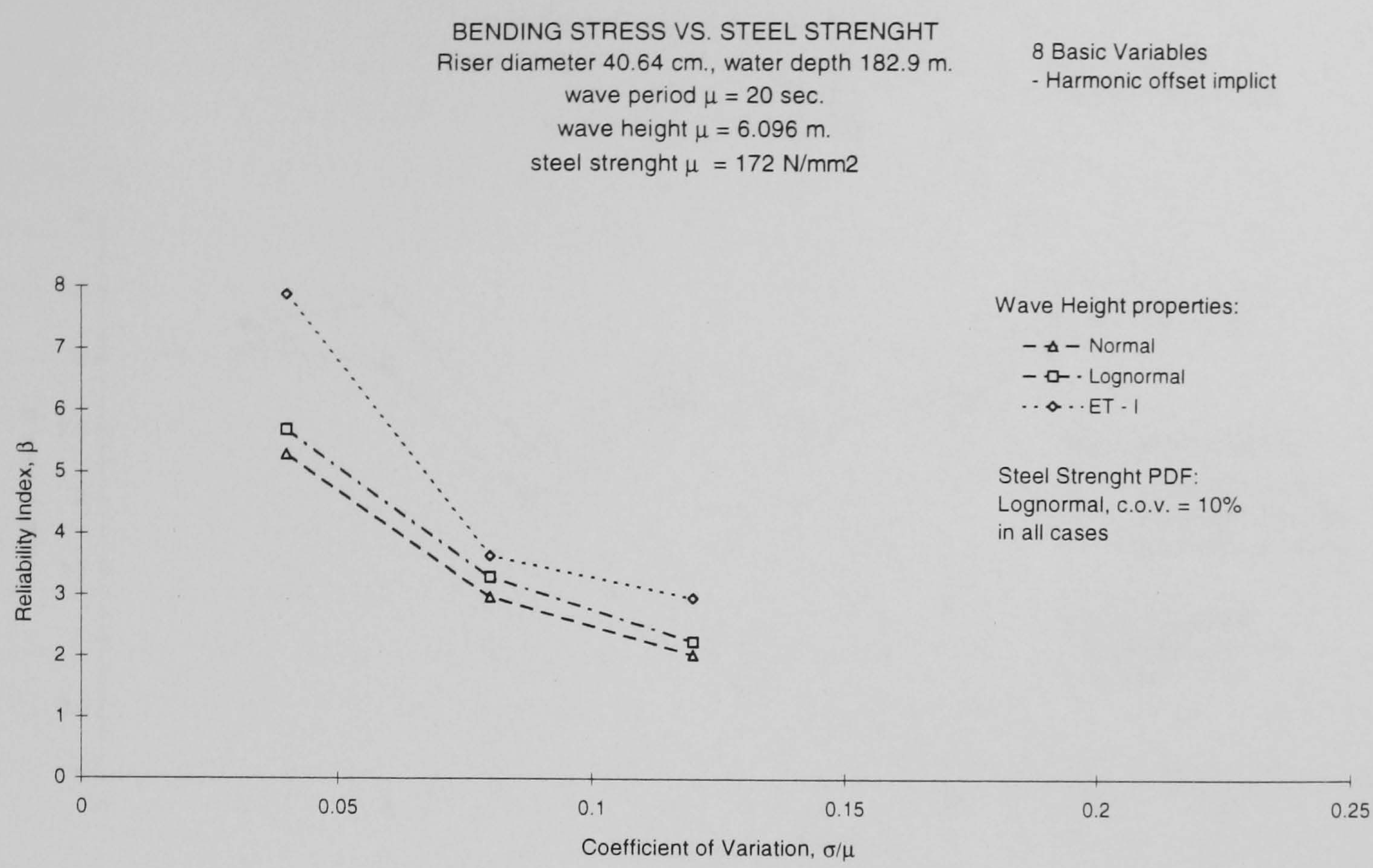

Figure 5.13b. Effects on the reliability index due to different PDF's and standard deviations assigned to top tension.

5.4.2. Material Strength.

According to the sensitivity factors presented in **Table 5.5** the strength of the pipe is the second most important basic variable. In the same fashion as before, different PDF's and standard deviations are designated to the material strength, in order to review the impact that they have in the overall performance of the reliability index. **Figure 5.14a** shows the changes of β as a result of different attributes of the material properties. A comparison with the plot for top tension, **Figure 5.13a**, shows that the trend of variation with wave period holds a good degree of resemblance, though less remarked; however, the levels of β are sensibly lower. These facts evidence that a material with poor properties, characterized by a significant degree of uncertainty, can render a system with reliability levels below the acceptable ones; but, on the other hand they suggest that, particularly in the case of a marine riser, an strict quality management at pipe mill can provide a high level of reliability through a material strength with well clustered strength, as evidenced by **Figure 5.14b**. Therefore, the material strength can be considered as a controllable variable. For a riser intended for long term usage the reductions in strength, such as those due to general corrosion, become another important factor.

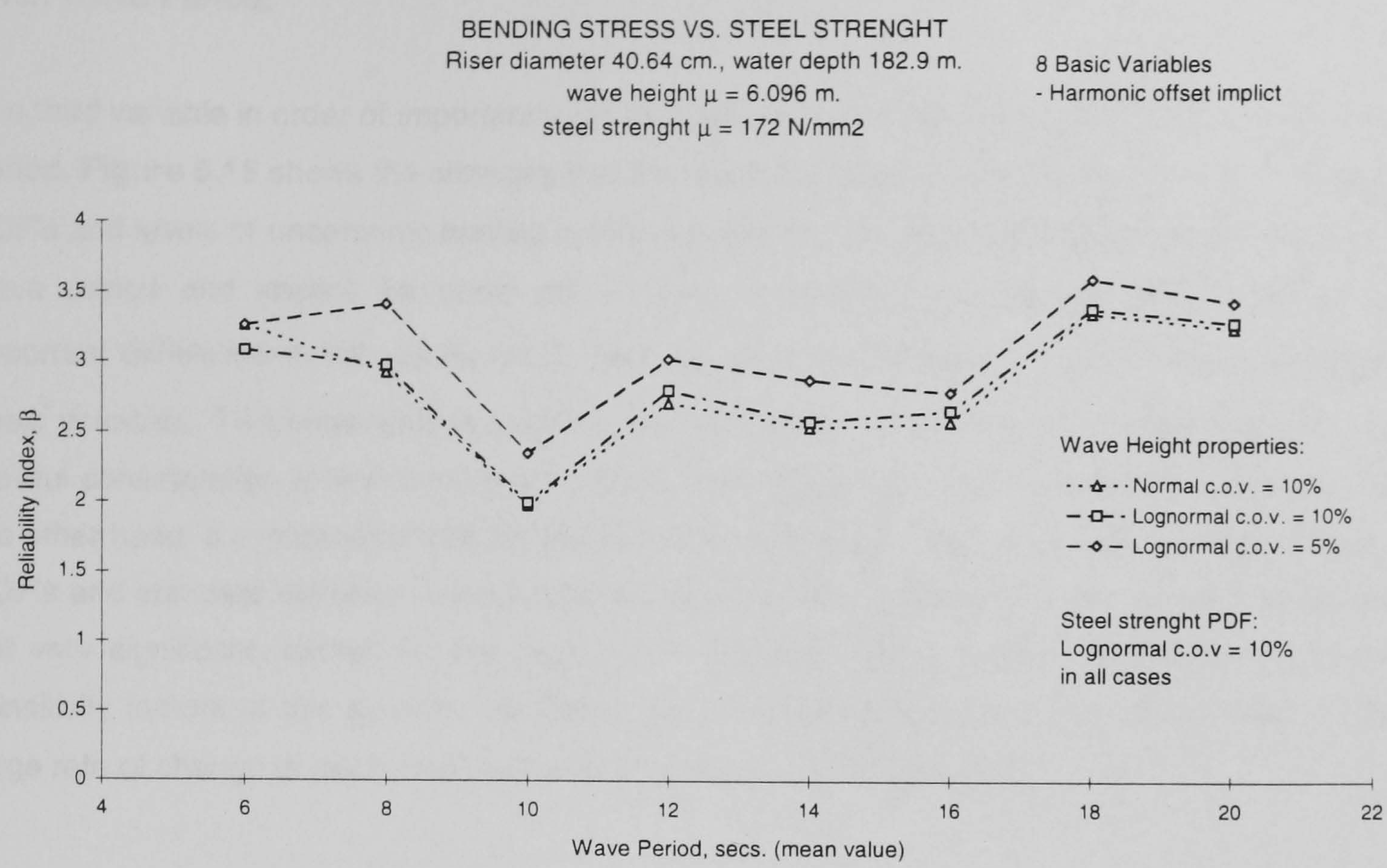

Figure 5.14a. Effects on the reliability index due to different PDF's and standard deviations assigned to material strength.

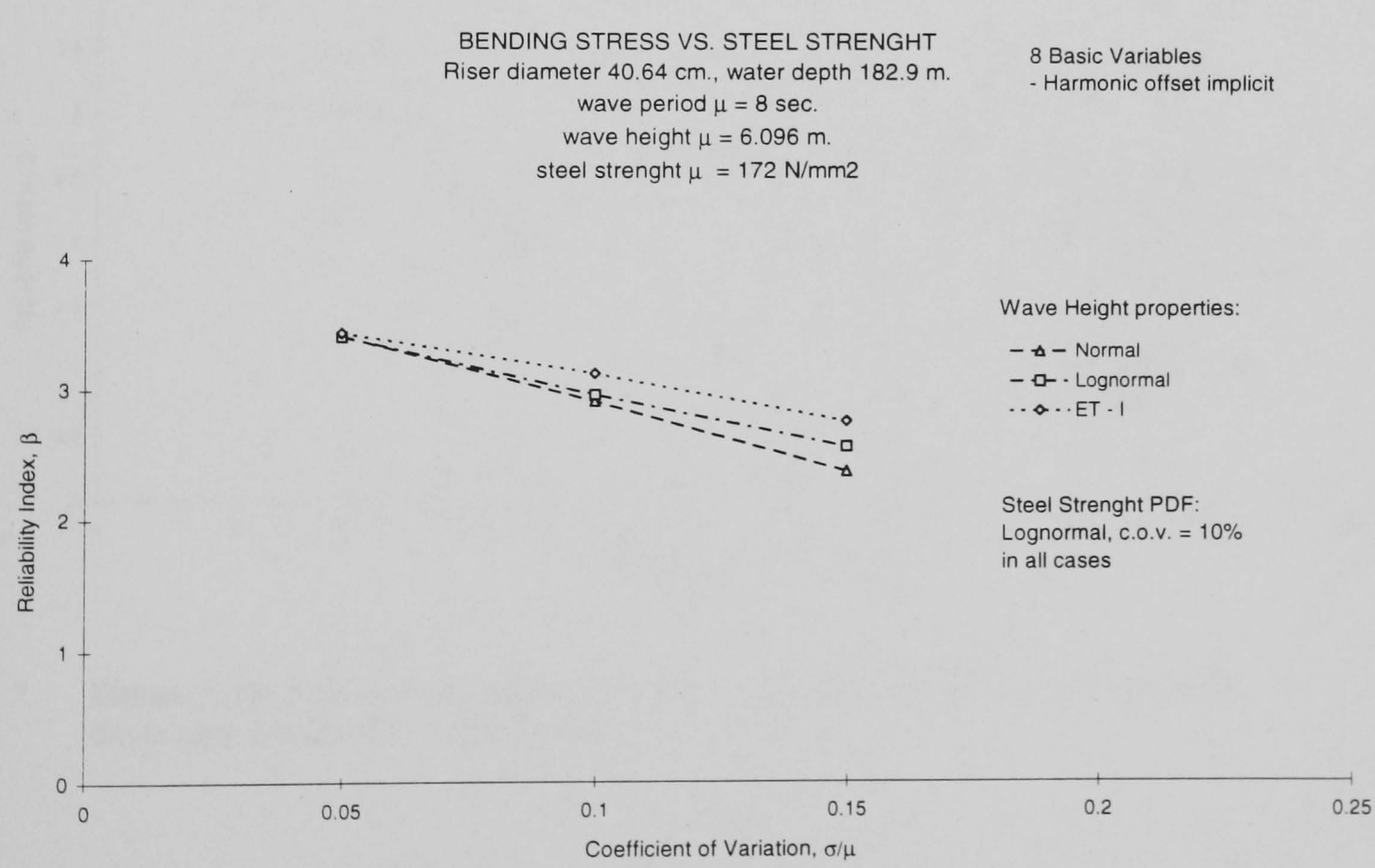

Figure 5.14b. Effects on the reliability index due to different PDF's and standard deviations assigned to material strength.

5.4.3. Wave Period.

The third variable in order of importance, as established by the sensitivity coefficients, is the wave period. **Figure 5.15** shows the changes that the reliability index undergoes as a result of different PDF's and levels of uncertainty applied to this variable. A comparison with **Case 2a**, in which only wave period and implicit harmonic offset were considered, see **Figure 5.8a**, manifest an important difference in the values of β, as a result of the inclusion of a number of significant basic variables. This comparisons confirms the statements at the beginning of **Section 5.4**, that careful consideration to the number of variables defining the response surface is necessary. On the other hand, a comparison with the previous two cases presented, shows that despite different PDF's and standard deviation assigned to this variable, the fluctuations of the reliability index are not very significant, except for the region of 8 seconds. This is a direct consequence of the sensitivity factors of this system, see **Table 5.5**, and, as mentioned before, as an effect of the large rate of change in platform response in that region, see **Figure 4.5**.

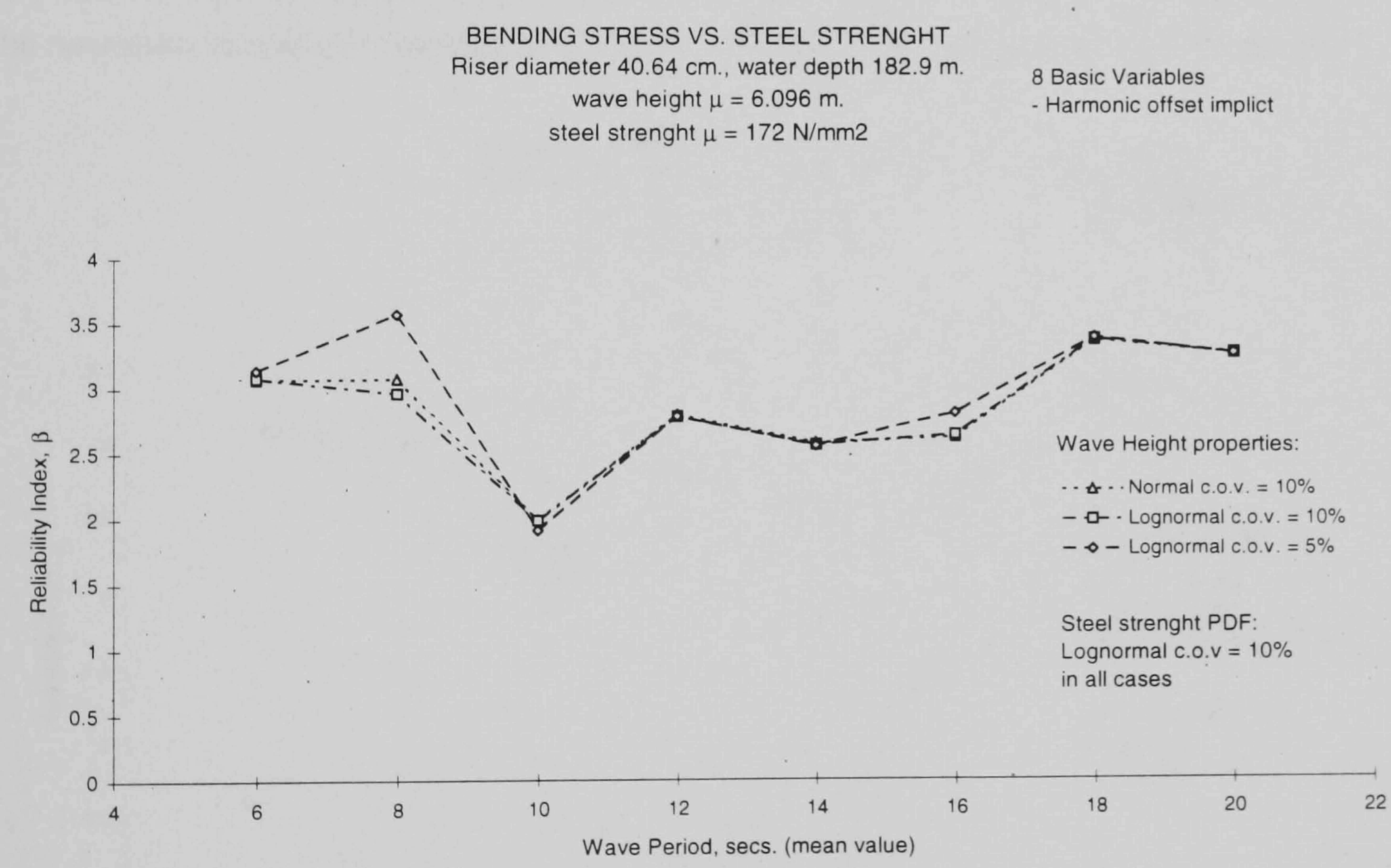

Figure 5.15. Effects on the reliability index due to different PDF's and standard deviations assigned to wave period.

5.4.4. Wave Height.

The fourth variable in descending magnitude of the sensitivity coefficients is the wave height. In the same fashion as in the previous cases this basic variable will be subjected to a number of PDF's and values of standard deviation, so as to asses the impact they have on the overall performance of the reliability index. **Figure 5.16** displays the reliability index for the range of periods usually analysed here. It can be appreciated that there are small changes in the value of β for the different PDF's and standard deviations. A comparison with cases previously considered shows, as expected, that the level of fluctuation of the reliability index decreases as the sensitivity coefficient of the variable analysed diminishes. However, it is possible to observe that the larger fluctuation for wave period is in the range of around 10 seconds, which is around the first natural period of the riser. This tendency continues to the lower periods, where the second natural period is found, and the changes in β are minimal at the regions of higher periods, away from the natural ones. It is important to note that changes in wave height appear to produce changes in the regions of the first (11.6 secs.) and second (5.20 secs.) natural periods of the riser. It must be recalled, however, that in order to confirm the bahaviour of wave height it will be necessary to consider the correlation of this variable with wave period and harmonic offset.

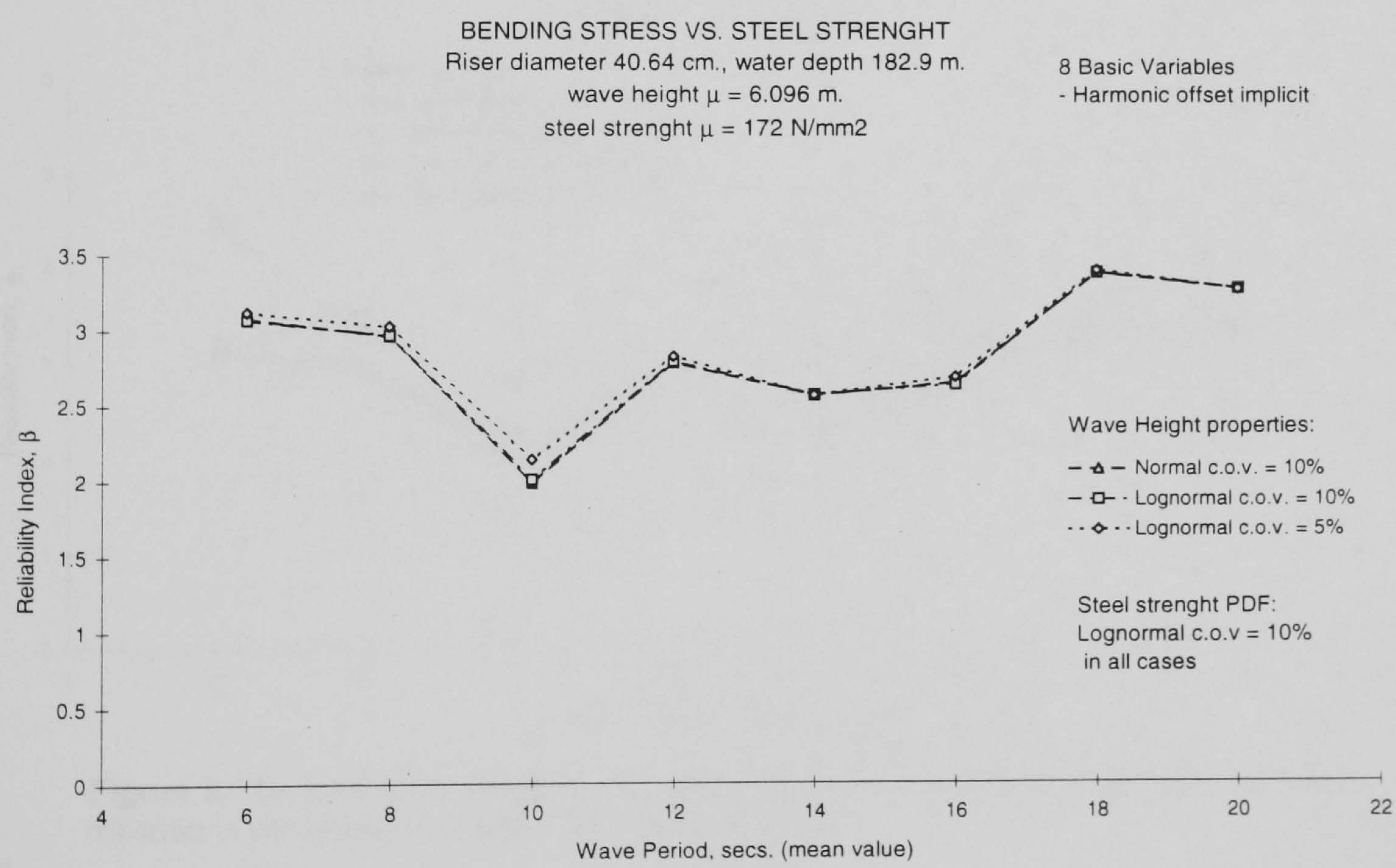

Figure 5.16. Effects on the reliability index due to different PDF's and standard deviations assigned to wave height.

5.4.5. Comparison of the Four Cases.

In order to appreciate the different levels of significance for each of the variables reviewed in the previous five sections, the plots of **Figures 17a** and **17b** present the maximum and minimum values of β respectively, for the PDF's and standard deviations used in those cases and are compared against the base case, see **Table 5.5**. These plots show that according to the sensitivity factors given in **Table 5.6** the variables with large sensitivity coefficient present the larger interval of values for the reliability index. This characteristic may help in the design process to determine which variables require more careful consideration, since a wrongly fitted PDF's and standard deviation can produce erroneous reliability values. On the other hand, this kind of analyses can assist in the assessment of stringent quality procedures to be applied to the controllable variables, and to the determination of more detailed studies in the case uncontrollable variables, such as the environmental ones.

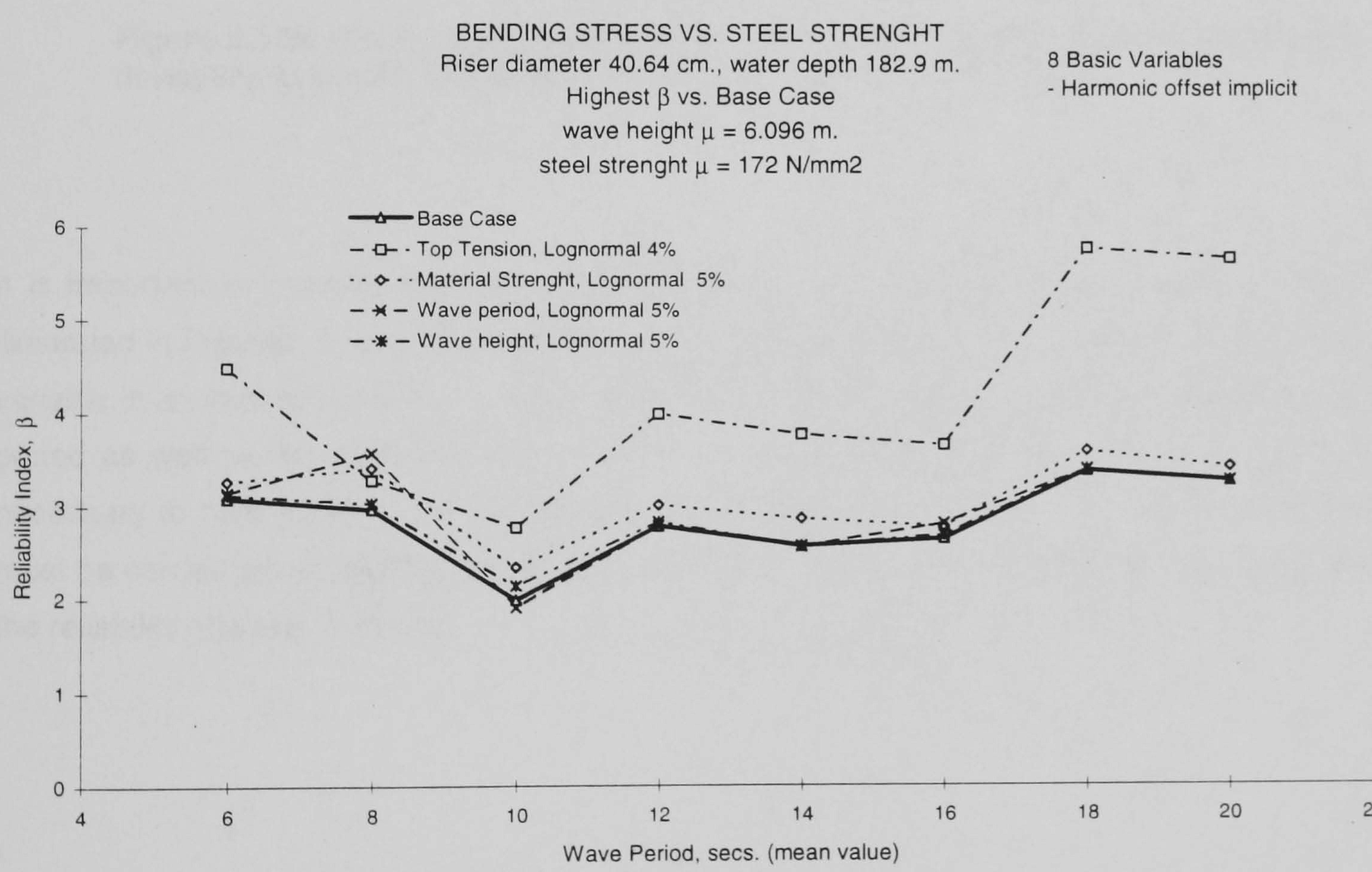

Figure 5.17a. Maximum values of reliability index due to different PDF's and standard deviations assigned, four cases vs. the base case.

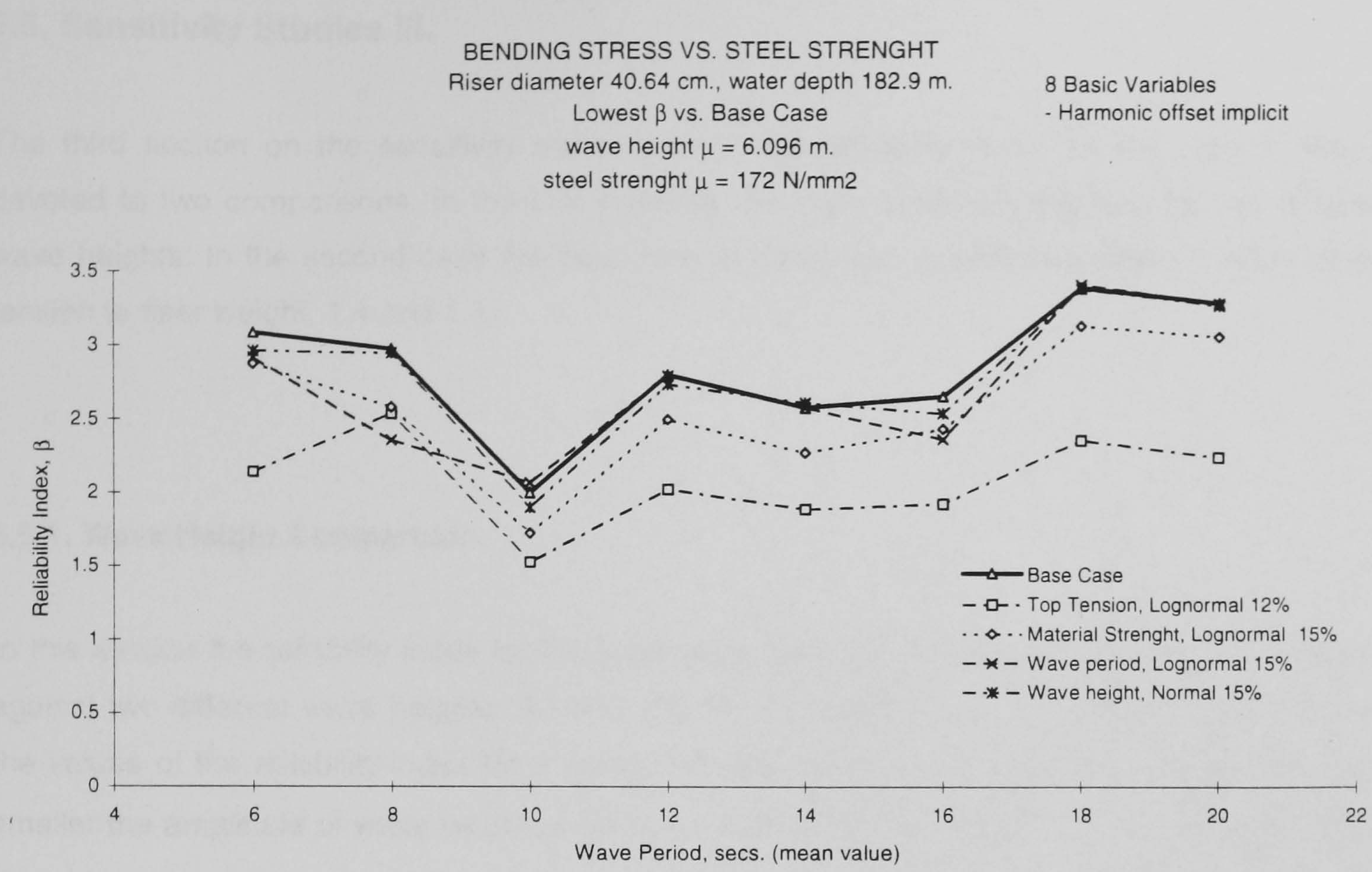

Figure 5.17b. Minimum values of reliability index due to different PDF's and standard deviations assigned, four cases vs. the base case.

It is important to mention that one of the most important variables is the harmonic offset; as illustrated in **Figures 1a** and **1b**; however, all the studies performed in this section considered this variable in an implicit form only. In order to further investigate the significance of wave height and period as well as the harmonic offset itself in the overall performance of the riser system it is necessary to take explicitly into consideration the effects of correlation among them. Such task must be carried out at the stage of construction of the response surface and during application of the reliability analysis methods.

5.5. Sensitivity Studies III.

The third section on the sensitivity comparison of the reliability index for the marine riser is devoted to two comparisons. In the first instance, the base case is compared for two different wave heights. In the second case the base riser is compared against two different ratios of top tension to riser weight, 1.4 and 1.1.

5.5.1. Wave Height Comparison.

In this section the reliability index for the base case riser, see **Tables 4.3** and **5.1**, is compared against two different wave heights, 9.144m. (30 ft.) and 3.048 m. (10 ft.). **Figure 5.18** presents the values of the reliability index for a range of wave periods. It is possible to observe that the smaller the amplitude of wave height larger the values of β, this tendency is as expected, since the lower the wave height the lower the bending stress amplitude. For the case of the lowest wave height the reliability index has a smooth progression through the range of wave periods. This is congruent with the behaviour observed in **Figure 5.1b**. Considering that the main source of riser dynamic excitation is the platform harmonic motion it is convenient to observe, referring again to **Figure 5.1b**, that the smaller wave height the smoother the variation of the stress is, across the range of periods considered. This tendency is confirmed noting that the increment of the platform amplitude of motion is steeper for the higher values of wave height, see **Figure 5.19**. On the other hand, it is worth noting that as the wave period mean value increases there is an increment in the range of values covered by the PDF associated with such variable, as a consequence of the fixed coefficient of variation assigned to every case. This means that at the lower wave periods the assumed dispersion is smaller and results in a more smooth variation of the reliability index at such periods. On the other hand, the effect of larger dispersion at larger values of wave period results in more abrupt changes of the β values.

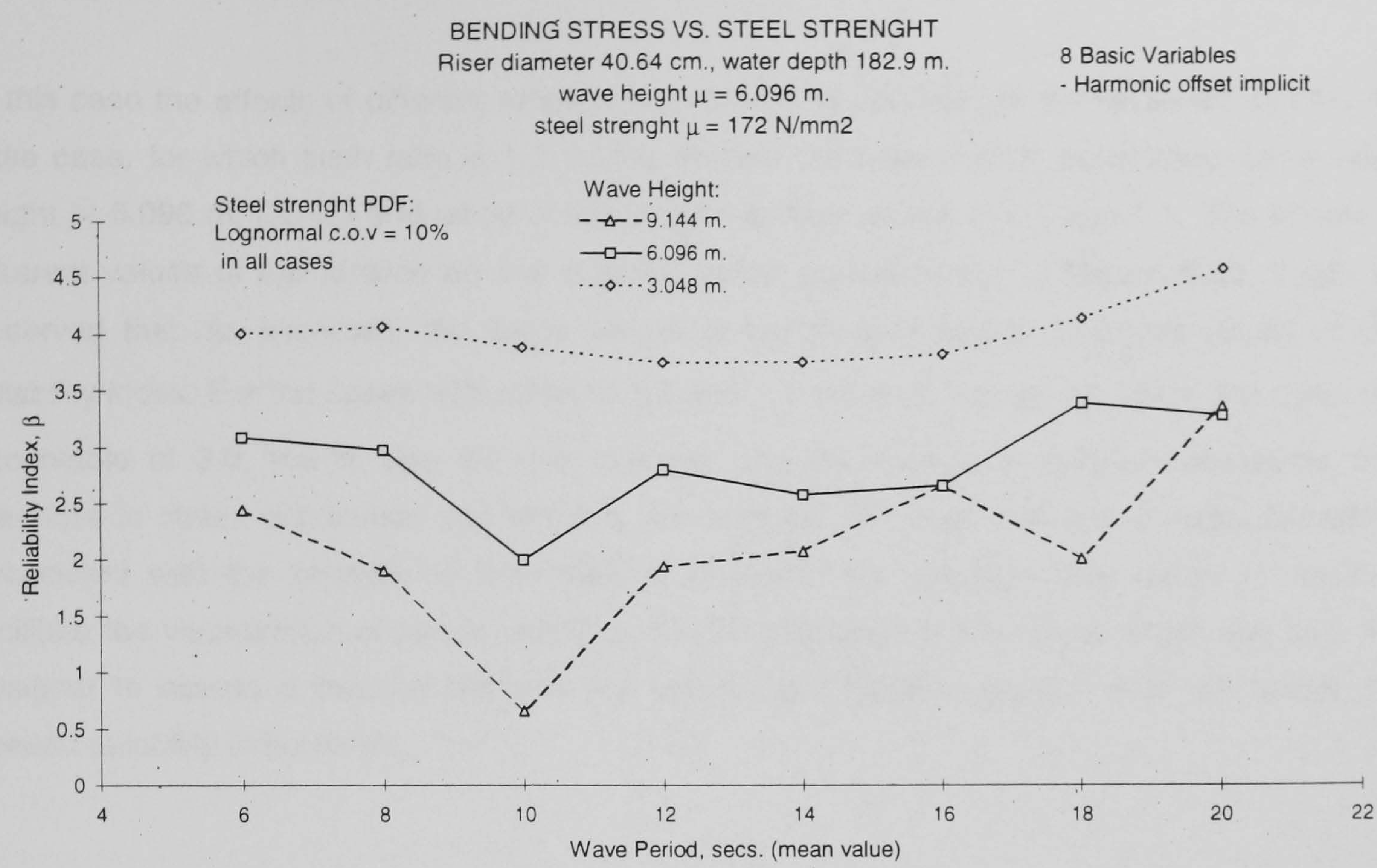

Figure 5.18. Reliability index for three different wave heights.

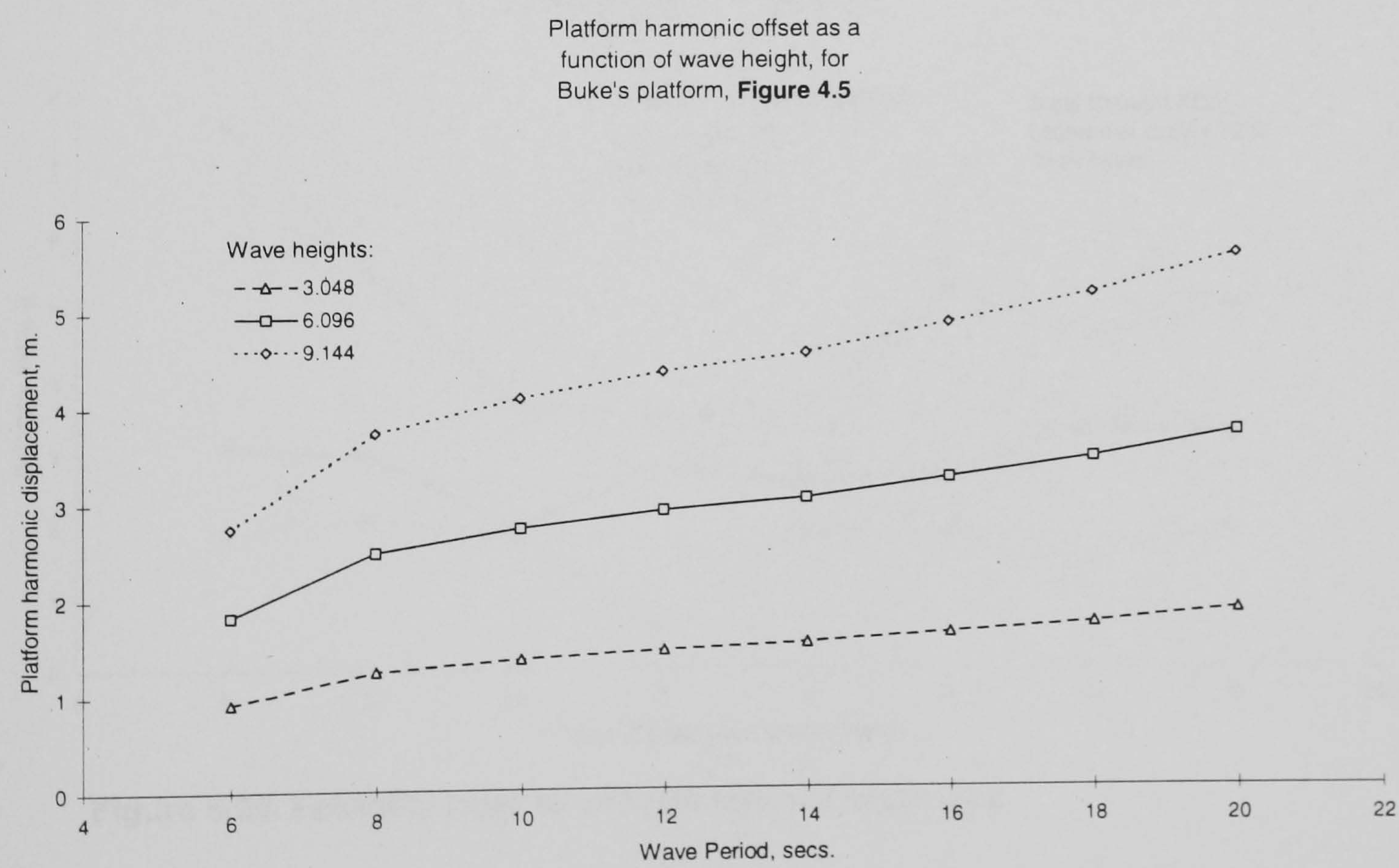

Figure 5.19. Platform harmonic displacements for three different wave heights.

5.5.2.Top Tension Comparison.

In this case the effects of different ratios of top tension to riser weight are reviewed against the base case, for which such ratio is 1.2. In this section the base riser is considered, for a wave height of 6.096 m. (20 ft.) and ratios of top tension to riser weight of 1.4 and 1.1. The effects of different values of top tension on the reliability index are presented in **Figure 5.20**. It can be observed that, as expected, the larger values of top tension results in higher values of the reliability index. For the cases with ratios of 1.2 and 1.1 some β values are below the minimum acceptable of 3.0, this is due the two reasons, one the change in natural frequencies and therefore in stress distribution and second, the relatively low mean value and large dispersion associated with the strength of the material; however, this selection was made in order to facilitate the visualization of trends, such as the one displayed in this figure, which can help the designer to assess a balance between top tension and material strength that will render the desired reliability index levels.

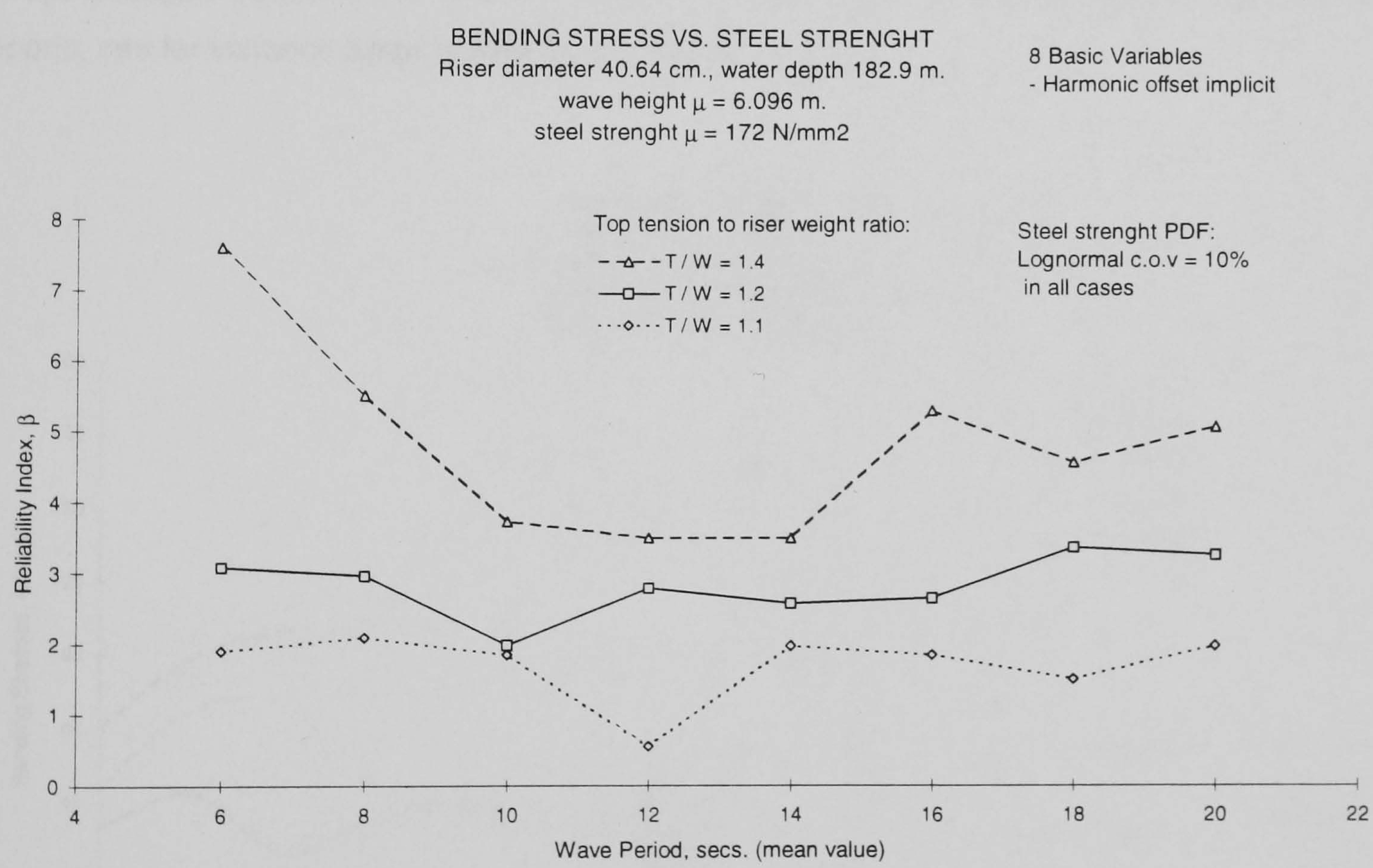

Figure 5.20. Reliability index for different levels of top tension.

5.6. Sensitivity Studies IV.

The last section of sensitivity studies is devoted to the comparison of the reliability index for the base case riser with three different lengths. The particulars of the riser to be reviewed in this section are the same as given in **Tables 4.3** and **5.1**, with the exceptions that in addition to the depth of 182.9 m. (600 ft.) the following two are to be included, 367.76 m (1200 ft.) and 609.6 m (2000 ft.); furthermore, in order to consider an actual value of the material strength standard deviation the value suggested by **Bouma, et al. (1979)**, 7%, is to be adopted in this section.

5.6.1. Deterministic Stresses for Three Riser Lengths.

Before proceeding with the revision of the reliability index for the three riser lengths to be analysed here, it is convenient to observe the deterministic stresses. **Figure 5.21**. shows, for a range of periods, the fluctuation of the bending stresses on a riser with three different lengths. It can be appreciated that the stresses are the lowest and follow the more smooth path for the longer riser. The shorter riser is the one that presents the larger bending stresses with the more abrupt changes between the different period intervals. Such behaviour agrees with previous reports, see for instance **Spanos and Chen (1980)**.

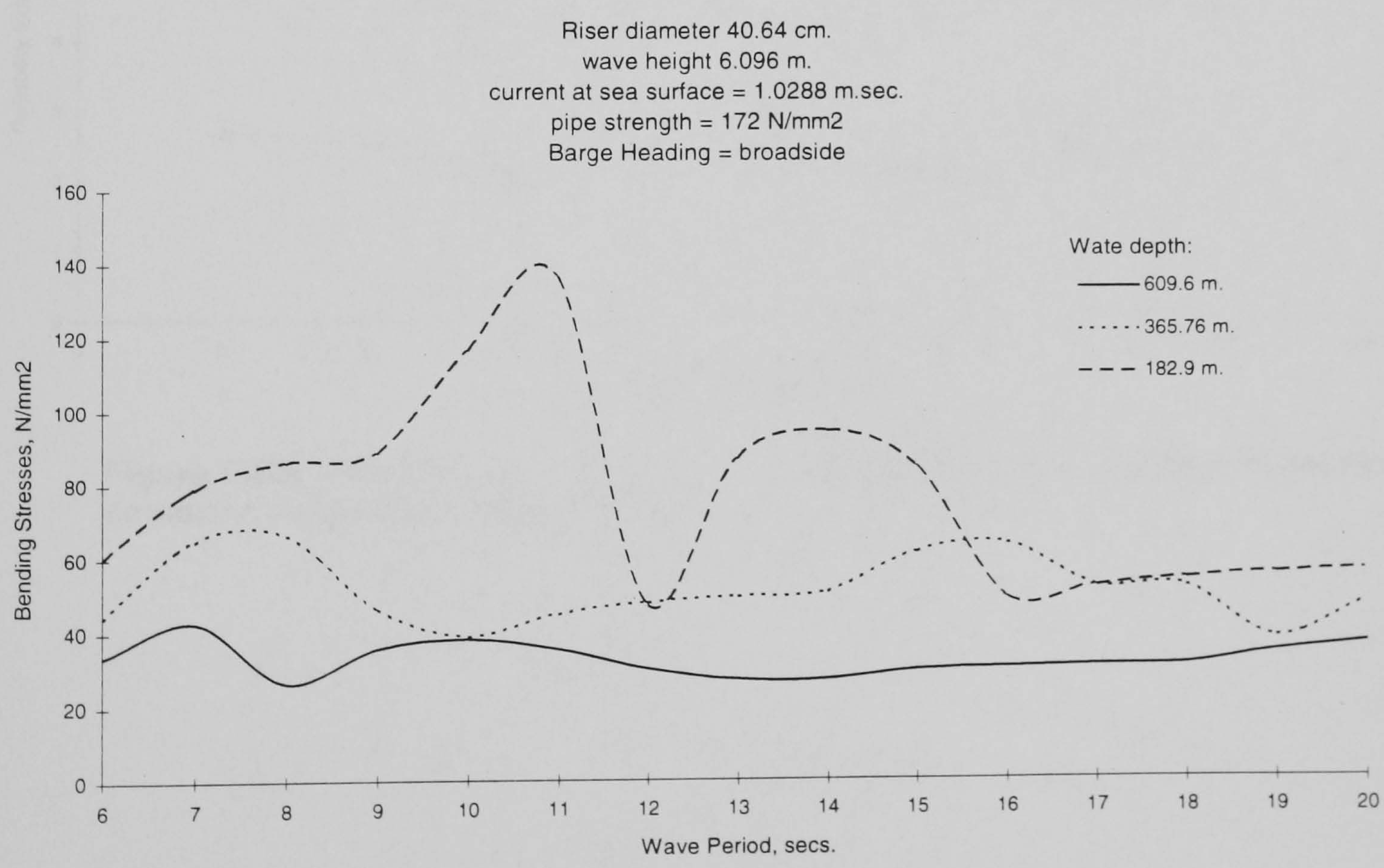

Figure 5.21. Deterministic stresses for three riser lengths.

5.6.2.Top Tension Effects.

As was evidenced in the **Section 5.4.1**, the top tension is the most sensitive variable in this riser problem, therefore, it is convenient to review the effects of different considerations on its standard deviation. **Figures 5.22a**, **5.22b** and **5.22c** present the fluctuations of the reliability index for the three different riser lengths. It can be perceived that for the longer riser, **Figures 5.22a**, the reliability index follows a smooth transition from one period to another, a behaviour expected as a result of the smooth fluctuation of the deterministic stresses. However, it can also be observed that as the standard deviation of the top tension reduces its magnitude the β values increase and the smoothness of the curves tend to diminish. On the other hand, such effects become magnified as the length of the riser is reduced, **Figures 5.22b** and **5.22c**.

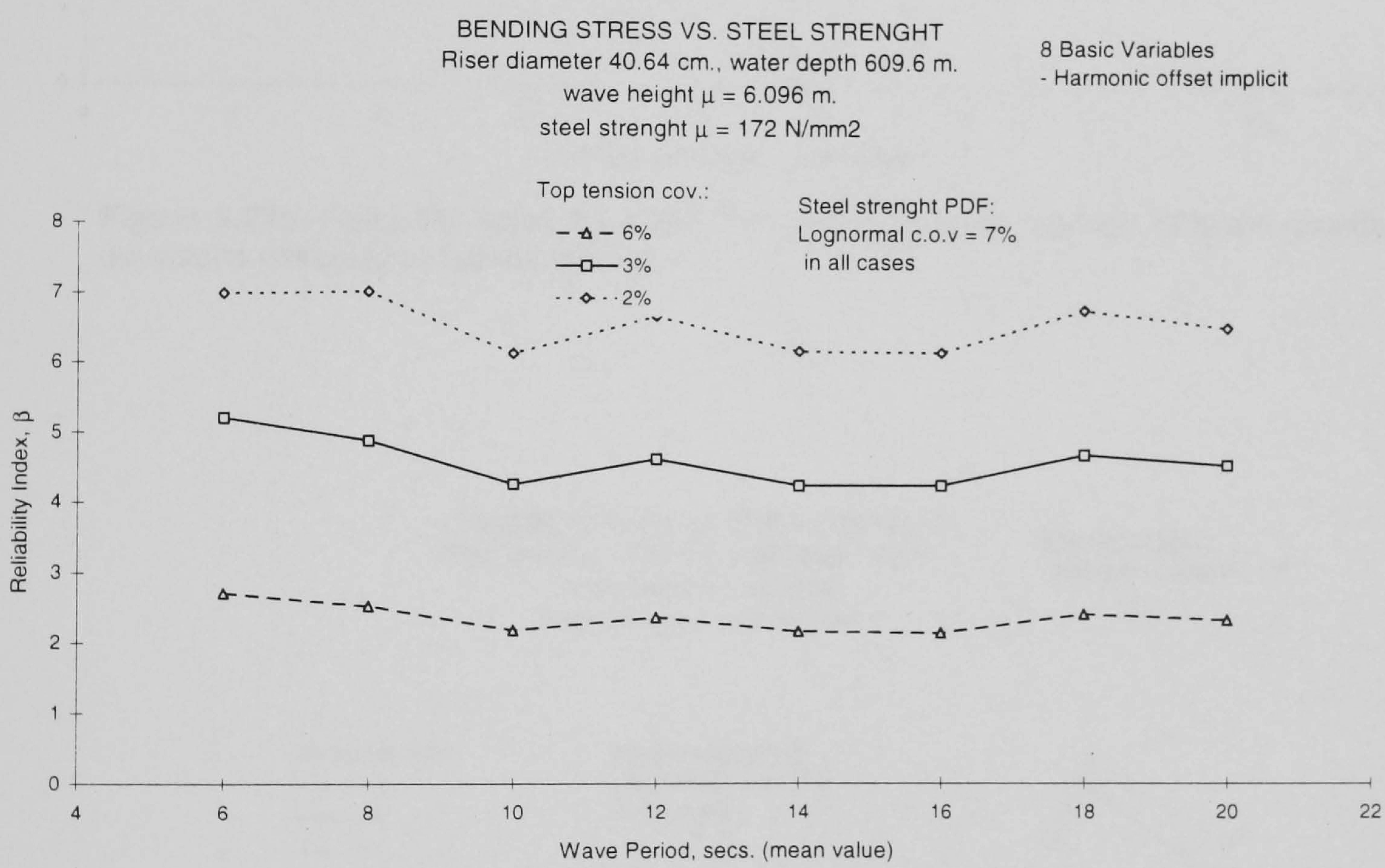

Figure 5.22a. Reliability index for a 609.6 m. (2000 ft) long riser and different standard deviations assigned to the top tension.

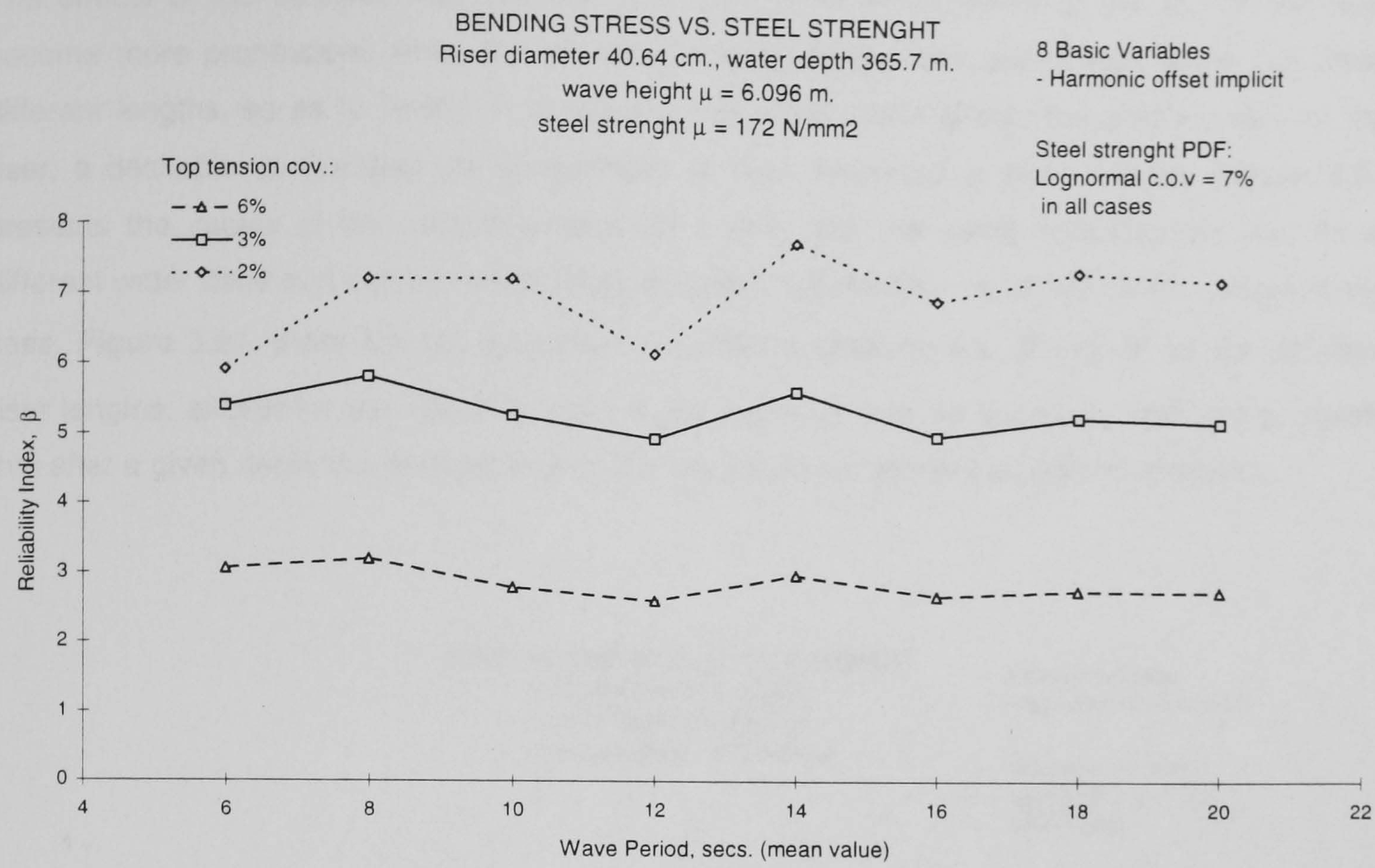

Figure 5.22b. Reliability index for a 365.7 m. (1200 ft) long riser and different standard deviations assigned to the top tension.

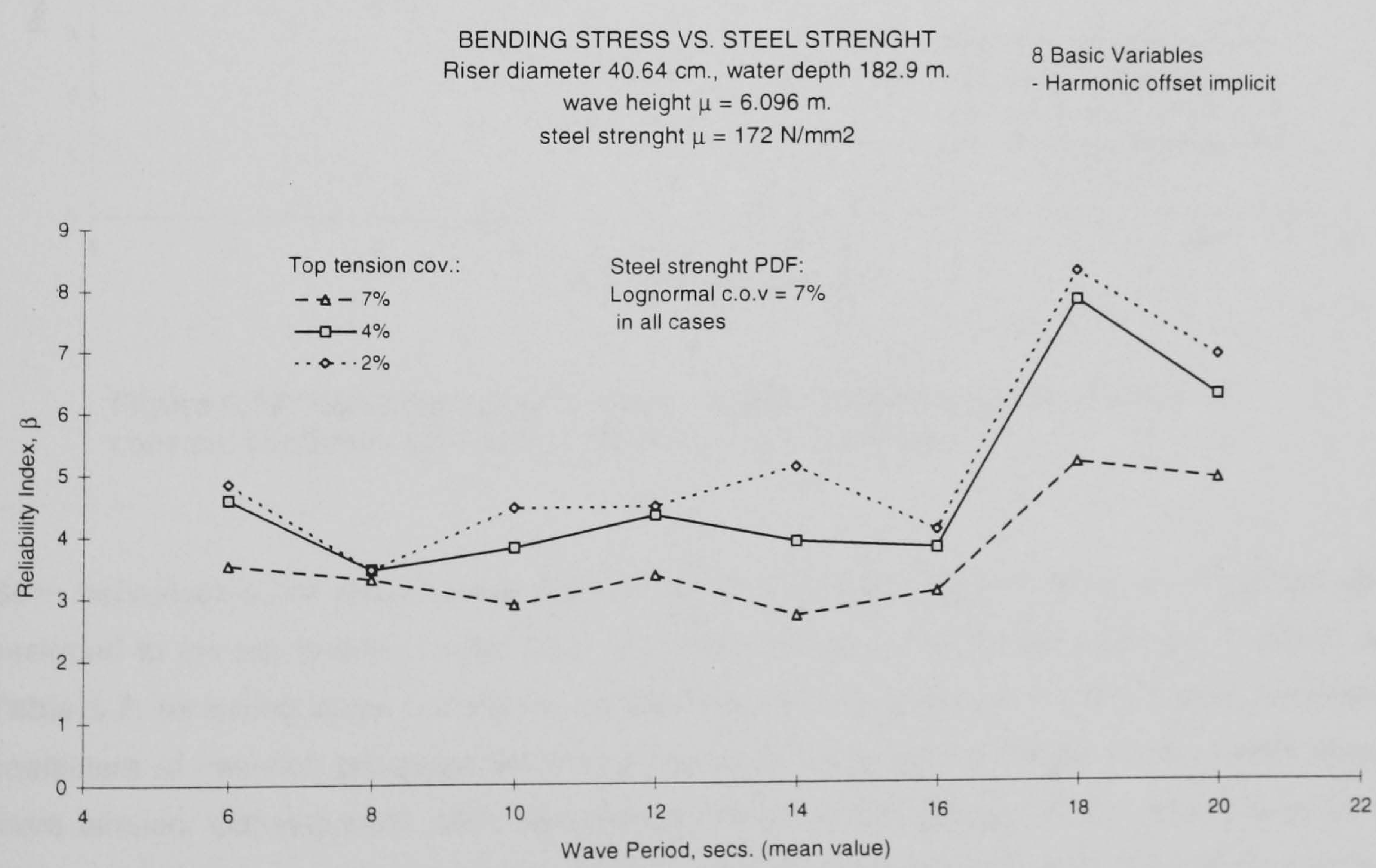

Figure 5.22c. Reliability index for a 182.9 m. (600 ft) long riser and different standard deviations assigned to the top tension.

The effects of the selected standard deviation for the tension applied at the top of the riser become more pronounced when the values of the reliability index are compared for the three different lengths, so as to review in which way the water depth affects the performance of the riser, a desirable comparison for assessment of riser behaviour in deep waters. **Figure 5.23** presents the values of the reliability index for a riser with the same characteristic and three different water depths. It can be noticed that, despite the behaviour observed for the deterministic case, **Figure 5.21**, there are not distinctive separations between the β values for the different riser lengths, except for the 182.9 m. riser in the region of 6 to 16 seconds. This plot suggests that after a given depth the performance of the riser does not present significant changes.

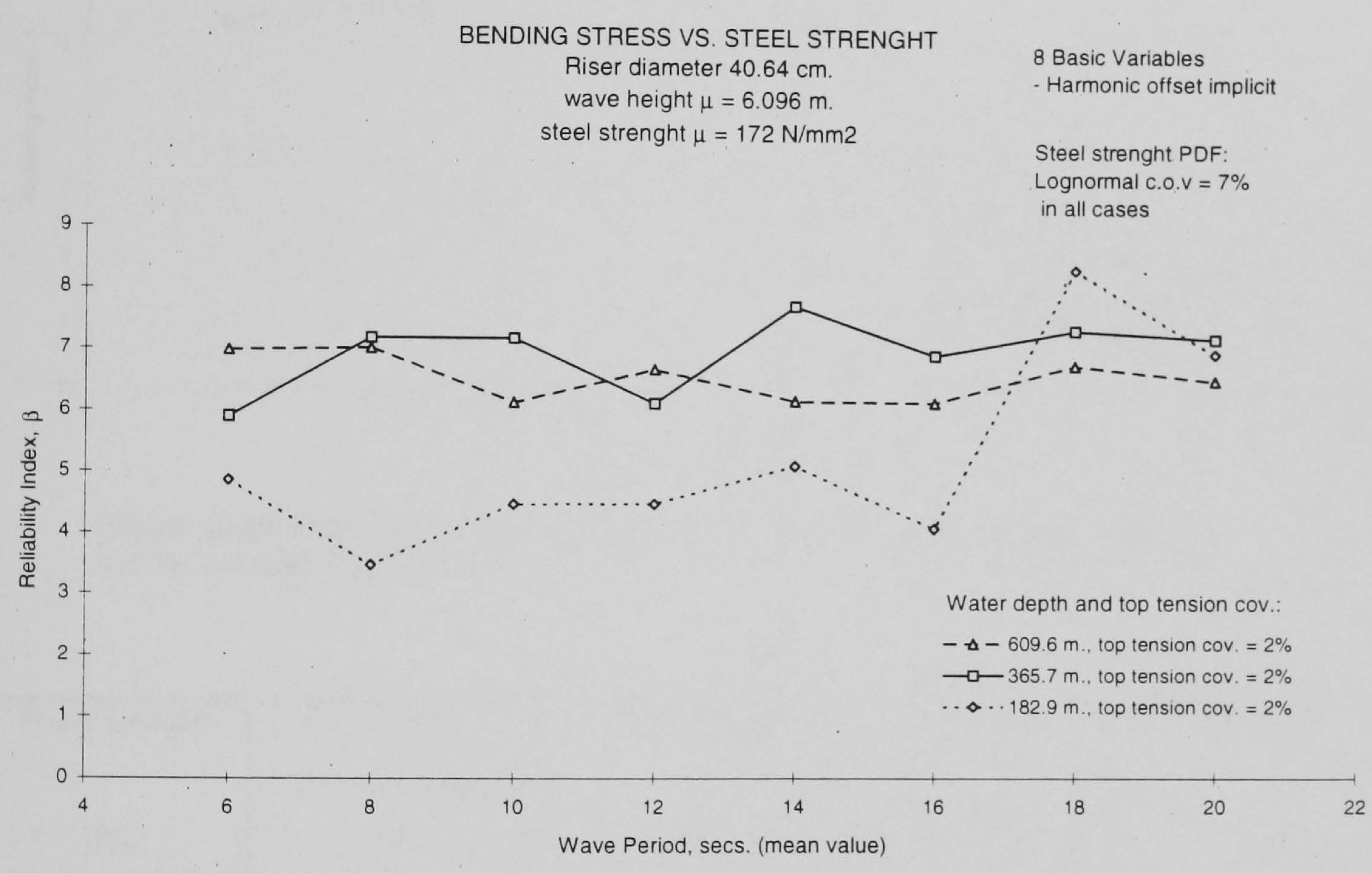

Figure 5.23. Reliability index for a riser in three different water depths and constant coefficient of variation assigned to the top tension.

Such behaviour is the result of the considerations made with regards to the standard deviation assigned to the top tension, in this case the coefficient of variation was taken as constant, see **Table 5.7**, rendering larger uncertainty as the mean value increases. In other words, a constant coefficient of variation produces larger standard deviations for the longer risers, which require more tension. Consequently, such assumption produces lower values of the reliability index for the longer risers, since they are given larger levels of uncertainty. This evident performance is magnified by the large sensitivity coefficient that the top tension holds, see **Table 5.6**.

On the other hand, when the coefficient of variation is selected in such a manner that the standard deviation value, σ, tends to produce similar proportions for the PDF's of the three different values of top tension, see **Table 5.7**, then the reliability index presents a performance more congruent with the behaviour observed in the deterministic case, described in **Figure 5.24**.

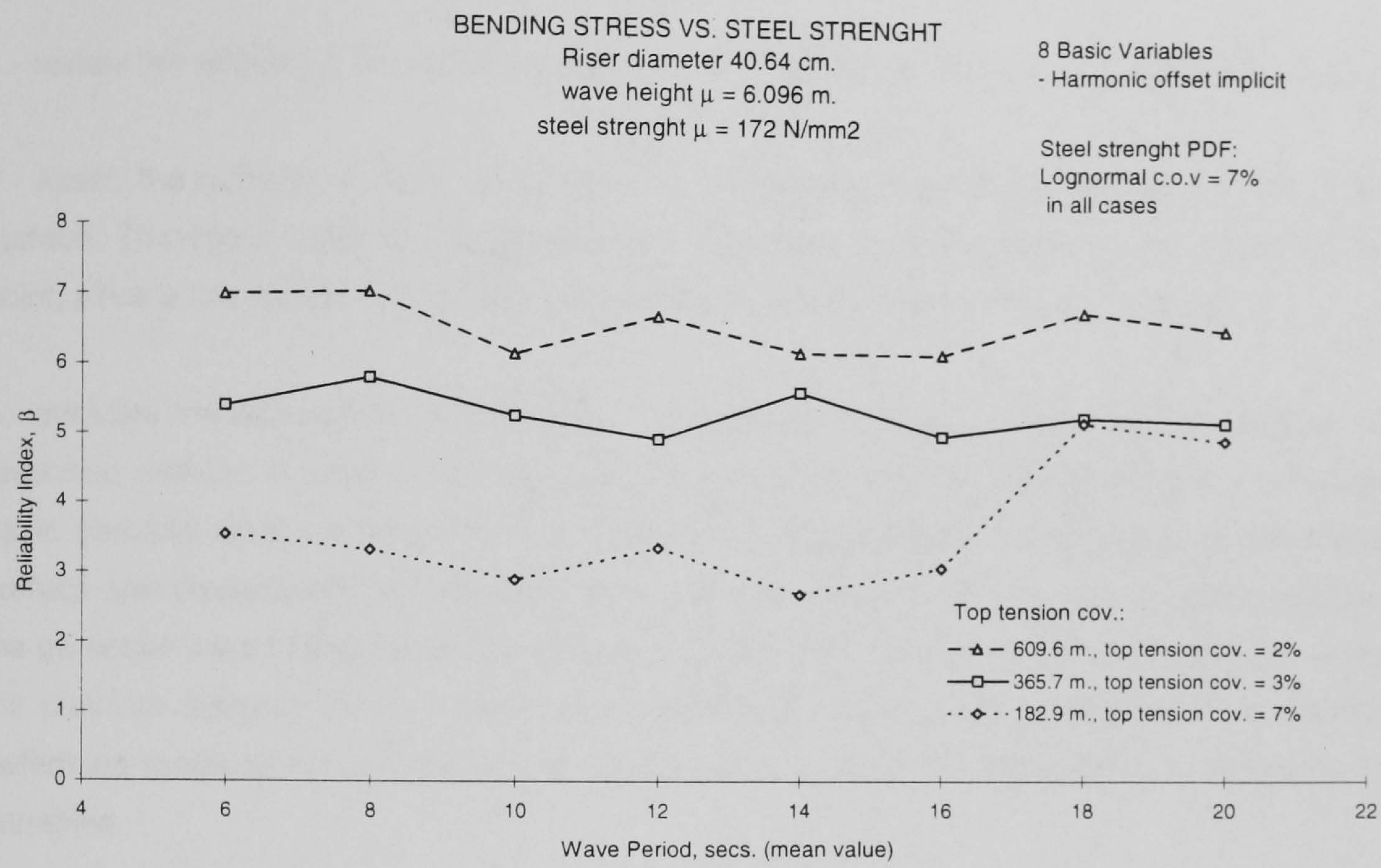

Figure 5.24. Reliability index for a riser in three different water depths and similar standard deviations.

Riser Length (m.)	Top Tension 1.2 × riser weight (N)	cov. = 2% (N)	cov = 3% (N)	cov = 7% (N)
182.9	721 480.27	σ = 14 429.61	σ = 21 644.41	σ = 50 503.62
365.7	1 442 960.53	σ = 28 859.21	σ = 43 288.82	σ = 101 007.24
609.6	2 404 934.22	σ = 48 098.68	σ = 72 180.03	σ = 168 345.40

Table 5.7. Coefficients of variation and standard deviations for top tension values of a riser in three different water depths.

It is concluded, therefore, that very careful consideration must be exercised concerning the appropriate standard deviations values assigned to the basic variables, but this carefulness must be intensified when addressing the variables with larger sensitivity coefficients. The studies performed in this chapter heighten the merits of the response surface approach in the assessment and selection of adequate Probability Distribution Functions and its associated parameters.

SUMMARY, Chapter 5.

A number of sensitivity studies were performed in this chapter making use of the Reliability Analysis Based on Response Surface, RABRS, algorithm. This methodology proved helpful to:

1.- review the effects on the reliability index due of different characteristic of specific variables.

2.- asses the number of basic variables to be considered for the construction of the response surface. Through a number of studies it was found that careful consideration is required in this point, since a low number of basic variables may lead to erroneous reliability indices.

3.- evaluate the assumption of independence between the basic variable for construction of the response surface. It was found that there are instances in which the dependence between the basic variable must be taken into consideration at both stages, construction of the response surface and determination of the reliability index, otherwise the results may be questionable. For the particular case of the marine riser it was possible to introduce one of the dependent variables, the platform dynamic offset, in an implicit manner; however, further investigation is required to determine methods for construction of the response surface in the presence of correlated basic variables.

4.- demonstrate the usefulness of the RABRS method for assessment of the statistical properties assigned to the different basic variables. It was demonstrated that the variables with larger sensitivity coefficients, such as the top tension, require a very careful consideration.

5.- identify controllable variables, for which quality management can help to maintain the required levels of reliability and non-controllable variables, in which case more detailed studies to define their appropriate statistical properties can be justified.

6.- demonstrate that the rigid marine riser is highly dependent on the externally applied tension at its top and that a very careful treatment of the statistical properties of this variable is required for an appropriate definition of the reliability index.

CHAPTER 6. RISER FATIGUE RELIABILITY ANALYSIS.

6.0. Introduction.

In **Section 1.3** the major approaches to fatigue analysis were described, including the fatigue reliability. The most important characteristic of all the reliability approaches to fatigue found in the literature review performed for this work is that the structural model used to determine the stress range is invariably deterministic, even when the spectral approach is used. This can be more clearly appreciated as follows, the behaviour of any structure or structural system can be represented in a general form as:

$$\text{Response} = \mathcal{M}\,\text{Excitation} \tag{6.1}$$

where the response, i.e. stress, etc., is obtained as a function of the excitation , i.e. wave load, transformed by the operator $\mathcal{M}$. This operator represents the structural system and its constitutive properties, i.e. stiffness, damping, etc. $\mathcal{M}$ can be of a simple form or a complex one, such as a finite element model. If the constitutive properties of the system are assumed to be deterministic, then the form of the response is the same as that of the excitation, i.e. deterministic or random, and exclusively as a consequence of the type of such excitation.

As it was mentioned before, in the present reliability approaches to fatigue analysis the stress range is obtained from a structural deterministic operator $\mathcal{M}$, while, the only variables assumed to be random are those related to the fatigue model employed, either S-N curves or Fracture Mechanics method. Therefore, an approach to fatigue reliability is here proposed in which the uncertainty of the system constitutive variables is explicitly taken into consideration. Such approach is to be implemented by means of the response surface methodology, in **Section 6.3**. In order to observe the characteristics of the proposed approach, the fatigue reliability of a marine riser in two different water depths is determined first with the deterministic approach, **Section 6.1**, and secondly with the most common approach in use to fatigue reliability, in **Section 6.2**.

6.1. Deterministic Approach to Fatigue Life.

The fatigue life of a marine riser in two different water depths, 365.7 m. (1200 ft.) and 609.6 m. (2000 ft.), is estimated at the point of maximum bending stresses by the deterministic approach, for several periods of service life. The riser selected for the analyses of this chapter is the one reported by **Spanos and Chen (1980)**, details of which were already given in **Table 4.3**.

The estimation of fatigue life is performed by means of the Miner's damage accumulation rule, **Equation 1.72**, namely:

$$D = \sum_{i=1}^{n} Di = \Delta = 1 \tag{6.2}$$

where, D the total damage equals Δ, critical cumulative damage, at failure. The environmental load considered in this case is a long term sea state which is divided in a number of short term stationary sea states, each of which can be described by a significant wave height, H_Z, an average wave period T_Z, and a probability of occurrence during the long term considered. In view of this description of the environment and Miner's rule, the total damage, D, is composed by the summation of a number of partial damages, D_i, for each of the short term sea states:

$$D_i = \frac{N_T}{N_F} = \frac{N_T}{K} S_i^m \tag{6.3}$$

where:

N_T, number of cycles in time T at the constant stress range, S_i,

N_F, number of cycles to failure, given by the equation of the S-N curve, namely:

$$N_F S^m = K \tag{6.4}$$

with m, K, empirical constants from the relevant S-N curve.

The environmental condition employed in this study was adopted from **Souza and Goncalves (1997)**, and is presented in **Table 6.1**.

SEA STATES	SIGNIFICANT WAVE HEIGHT (m.)	AVERAGE WAVE PERIOD (secs.)	PROBABILITY OF OCCURRENCE
1	0.78	5.24	0.0229
2	1.25	5.27	0.2561
3	1.75	5.77	0.3852
4	2.25	6.26	0.1962
5	2.75	6.89	0.0880
6	3.25	7.72	0.0328
7	3.75	7.89	0.0100
8	4.25	8.20	0.0068
9	4.75	9.00	0.0020
			1.0000

Table 6.1. Environmental condition data for riser fatigue reliability analysis, after **Souza and Goncalves (1997)**.

The S-N data for this analysis is also taken from **Souza and Goncalves (1997)**, the details are presented in **Table 6.2**.

K	m	Δ
9.6762×10^{14}	4.38	1.00

Table 6.2. S-N data for deterministic fatigue analysis, after **Souza and Goncalves (1997)**.

The total damage found for the same riser in two different water depths is plotted against service life, in **Figure 6.1**. The riser in deeper water is less sensitive to fatigue damage, on account of a lower level of stresses, as it was demonstrated in **Section 5.6**, see **Figure 5.21**. The riser in 365.8 m. (1200 ft.) exhausted completely its fatigue strength at 20 years of service, while the riser in 609.6 m. (2000 ft.) has a predicted service life of 94 years.

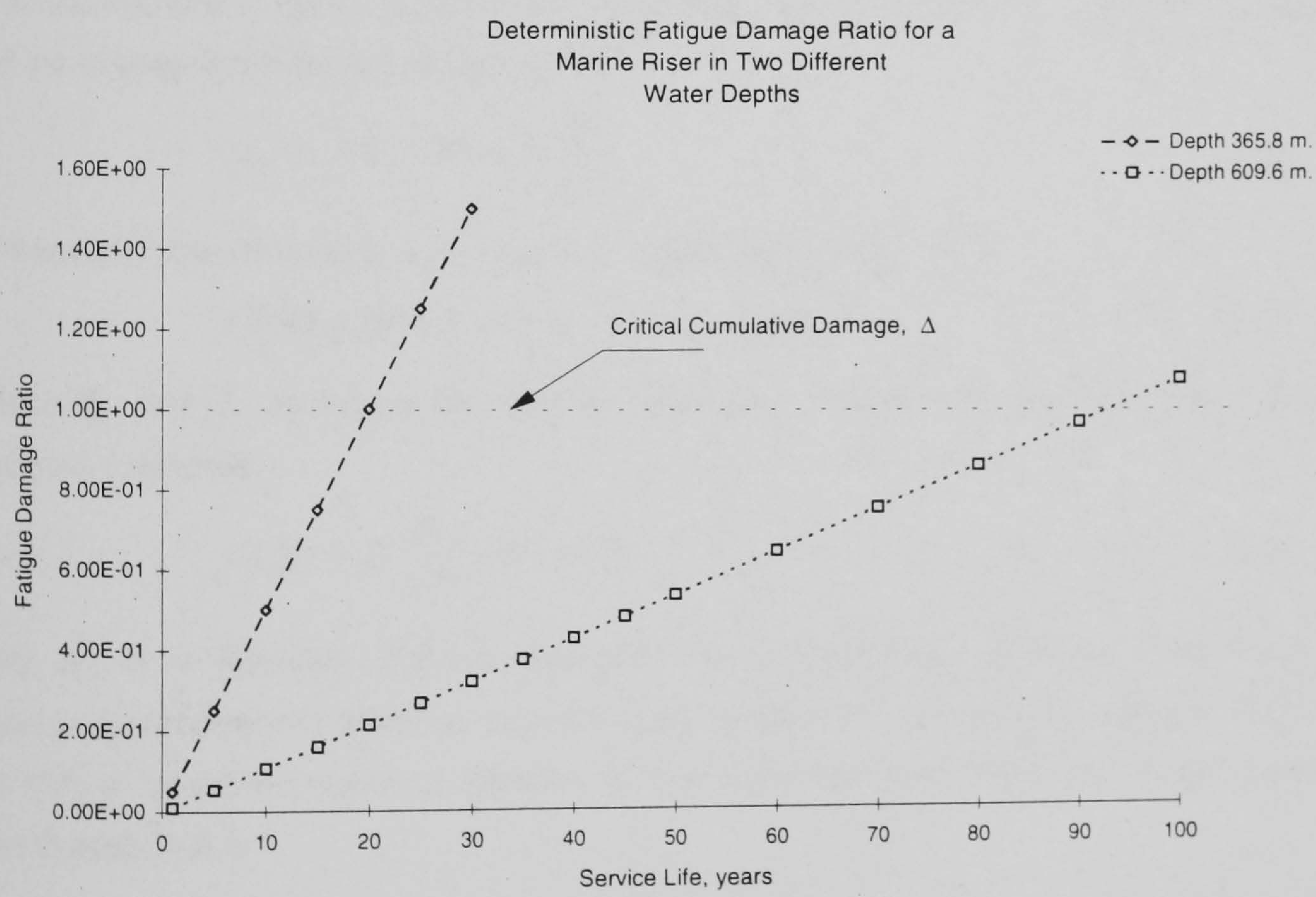

Figure 6.1. Deterministic fatigue damage ratio for a riser in two different water depths.

6.2. Fatigue Reliability Analysis of a Riser I.

As explained in **Section 1.3.3**, the most extended approach to fatigue reliability analysis is that due to **Wirsching (1984)**, where the variables assumed random are those defining the S-N curve, the critical damage ratio, Δ, and the constant K, while all the uncertainties associated with stress quantification are modelled with the introduction of a new random variable, B.

In order to derive the limit state equation for the fatigue reliability analysis the equation defining the S-N curve is considered:

$$N_F S^m = K \tag{6.5}$$

Miner's rule, given by **Equations 6.2** and **6.3**, states that:

$$D = \frac{N_T}{N_F(X)} = \Delta \tag{6.6}$$

where:

$N_F(X)$, number of cycles to failure, function of a number of random variables, and

N_T, number of cycles occurring in service life T,

With the number of cycles to failure from **Equation 6.5**, substituted in Miner's rule, **Equation 6.6**, can be expressed in the following manner:

$$N_T = \Delta N_F(X) = \Delta \frac{K}{S^m} \tag{6.7}$$

and applying the difference state equation, **Equation 1.86**, namely:

$$G(\boldsymbol{X}) = \boldsymbol{M} = \boldsymbol{S} - \boldsymbol{L} = S(\boldsymbol{X}_A) - L(\boldsymbol{X}_B) \tag{6.8}$$

where $\boldsymbol{S}$ and $\boldsymbol{L}$ represent the strength and load variables respectively, then the limit state equation becomes:

$$G(X) = \Delta \frac{K}{S^m} - N_T \leq 0 \tag{6.9}$$

Only K, Δ in **Equation 6.9** are assumed to be random basic variables. The stress range S may be deterministic or spectral, depending on the form in which the load is expressed, however, the model for determination of stresses is most commonly assumed deterministic, as explained with **Equation 6.1**.

Using the limit state of **Equation 6.9**, **Wirsching (1995)** proposed a closed form solution for determination of the reliability index, and proposed at the same time the introduction of the random variable B to account for uncertainties in stress determination, therefore:

$$\beta = \frac{\ln\left(\tilde{N}_F / N_T\right)}{\sigma_{\ln N_F}} \tag{6.10}$$

where: $\tilde{N}_F$, the median value of N_F is given by:

$$\tilde{N}_F = \frac{\tilde{\Delta}\tilde{K}}{\tilde{B}^m S^m} \tag{6.11}$$

and the standard deviation of N_F is

$$\sigma_{\ln N_F} = \ln\left[\left(1 + C_\Delta^2\right)\left(1 + C_K^2\right)\left(1 + C_B\right)^2\right]^{1/2} \tag{6.12}$$

The variable B is assumed to contain the uncertainties due to several sources, as described in **Section 1.3.3** by **Equation 1.96**, namely:

$$B = B_M \cdot B_S \cdot B_F \cdot B_N \cdot B_H \tag{6.13}$$

where the uncertainties considered are due to:

B_M, fabrication and assembly operations,

B_S, sea state description,

B_F, wave load predictions,

B_N, nominal member loads and

B_H, estimation of hot spot stress concentration factors.

Wirsching (1984) assumed that each of the random variables defining B follow a lognormal distribution, therefore the median is given by:

$$\tilde{B} = \prod_i \tilde{B}_i \qquad \text{for } i = M, S, F, N, H \tag{6.14}$$

and the coefficient of variation by:

$$C_B = \left[\prod_i \left(1 + C_i^2\right) - 1\right]^{1/2} \tag{6.15}$$

The statistical values of each of the random variables in **Equation 6.13** was given by **Wirsching (1984)**, based on the opinion of groups of experts. The assignation of specific values for B is, therefore, subjected to some degree of judgement or even arbitrariness. Nevertheless, Wirsching's approach will be applied for determination of the reliability index of the riser for which the deterministic fatigue life was presented in the previous section. However, regardless of the availability of an explicit form for determination of the reliability index, namely **Equation 6.10**, the response surface method combined with the adaptive importance sampling algorithm will be used in this work in order to find the values of β. The statistical properties to be used in the determination of the reliability index are given in **Table 6.3**. In **Case 1**, only K and Δ are used, and in **Case 2** the variable accounting for uncertainty in stress, B, will be introduced.

The parameters defining the S-N curve are considered as follows: m is deterministic in both cases, the constant K is assumed random, and as suggested by **Wirsching (1984)**, accounts for all the data scatter in the S-N curve. The relevant properties of both variables are adopted from **Souza and Goncalves (1997)**, see **Table 6.2**. On the other hand the values of the critical cumulative damage, Δ, which according to **Wirsching (1984)**, accounts for modelling errors in the description of the fatigue strength, and the random variable accounting for uncertainties in stress, B, are both taken from that author, who also indicated that, K, Δ and B, conform to a lognormal distribution function. Their properties are exhibited in **Table 6.3**.

K	9.6762×10^{14}	Lognormal	Ref. 1
σ_K	1.0233		Ref. 1
m	4.38	deterministic	Ref. 1
Δ	1.00	Lognormal	Ref. 2
σ_Δ	0.3		Ref. 2
$\tilde{B}$	0.7	Lognormal	Ref. 2
σ_B	0.5		Ref. 2

Ref. 1, **Souza and Goncalves (1997)**.
Ref. 2, **Wirsching (1984)**.

Table 6.3. Statistical properties of random variables in the S-N model for riser reliability fatigue analysis.

Case 1.

The values of the reliability index, for **Case 1**, in which the uncertainty variable B is not taken into consideration are presented in **Figure 6.2**. A number of years of service life is contemplated for the two riser depths analysed. The most commonly accepted adequate value of the reliability index was inserted in the such figure so as to facilitate appreciation of the levels of reliability. For the deeper riser, 609.6 m. (2000 ft.) the fatigue reliability can be considered appropriate, after a service life of 20 years, when the riser is probably near the end of its intended useful life, β values of less that three may become acceptable, depending on the conditions of the structure at that moment, see **Table 1.8**. For the riser in 365.8 m. (1200 ft.) the fatigue strength properties of the material selected are not adequate for an intended service life of more than five years. On the other hand, from the sensitivity coefficients displayed in **Table 6.4** it can be observed that the most important variable, in this case is the critical cumulative damage. On the other hand, the standard practice of deterministic design, determination of the damage for one year and then conversion into service life, is not applicable in fatigue reliability. As **Figure 6.2** demonstrates, an acceptable reliability index for the first year does not guarantee an appropriate reliability for the intended service life.

	1 year	5 years	10 years	15 years	20 years	25 years	30 years
Δ, 365.8 m.	0.9988	0.9988	0.9988	0.9988			
K, 365.8 m.	0.0489	0.0489	0.0489	0.0489			
Δ, 609.6 m.	0.9988	0.9988	0.9988	0.9988	0.9988	0.9988	0.9988
K, 609.6 m.	0.0489	0.0489	0.0489	0.0489	0.0489	0.0489	0.0489

Table 6.4. Sensitivity coefficients for **Case 1**, no uncertainty in stress determination is assumed.

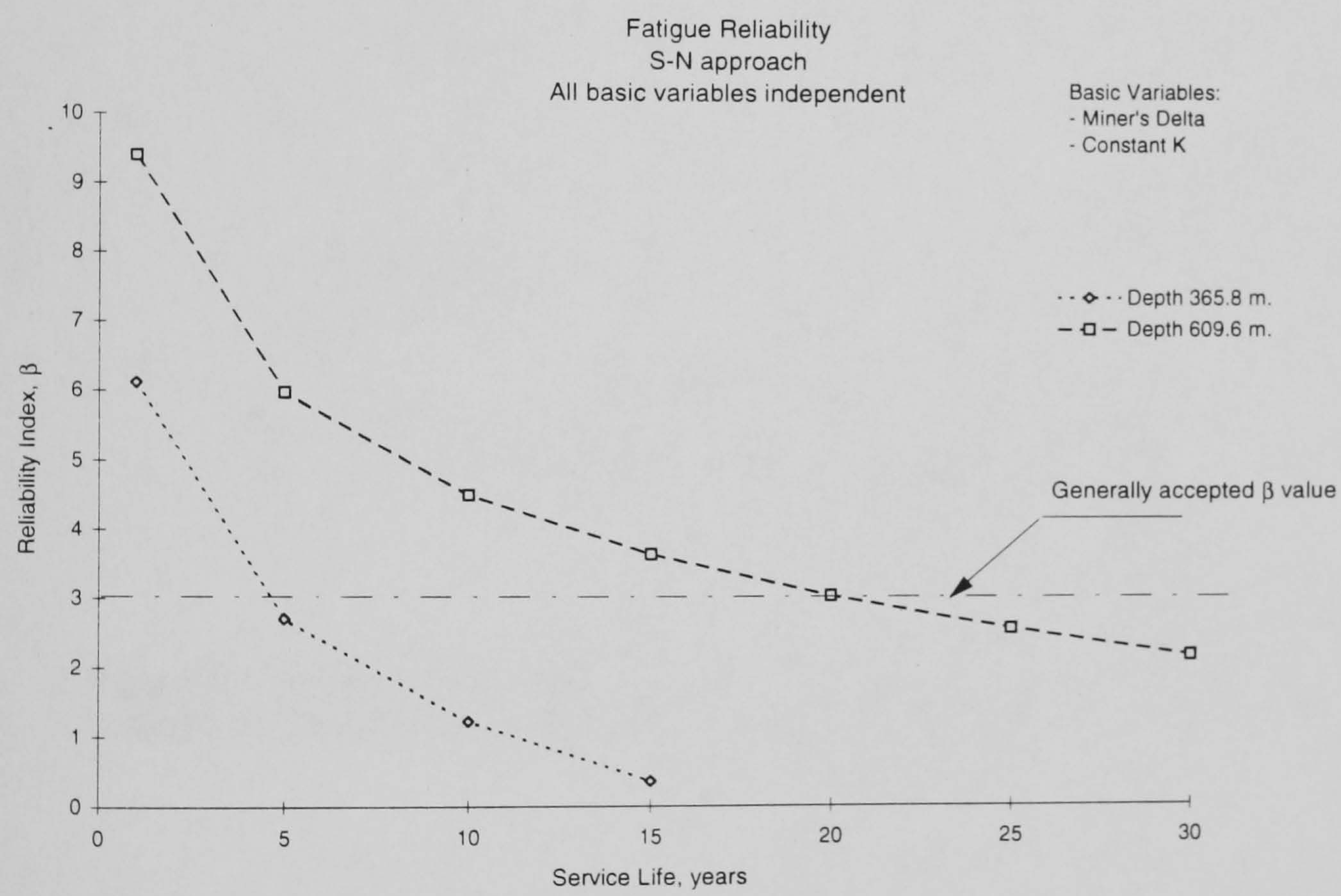

Figure 6.2. Reliability index for a riser in two different water depth, no uncertainty is associated with stress values, **Case 1**.

Case 2.

In this case it is assumed that, as suggested by **Wirsching (1984)**, all the uncertainties associated with stress determination can be concentrated in one random variable, B, that is introduced in the limit state equation, namely **Equation 6.9**. The values of the reliability index were found for such limit state, by means of the response surface methodology and the adaptive importance sampling method, using the parameters indicated in **Table 5.1**, except for the limit state. **Figure 6.3** presents the values of β plotted for a number of years of service life. It can be observed that the influence of the stress uncertainty variable, B, becomes the most important one, as the sensitive coefficients demonstrate in **Table 6.5**. The impact on β due to the introduction of uncertainty in stress is very clear, the reliability index experiences significant changes in comparison with the case where stress uncertainty is not considered. It can also be appreciated that as the age of the structure grows the sensitivity of stress uncertainty becomes more significant, which explains why the slope of reliability index reduces as the service life increases. This fact heightens the importance of the uncertainty associated with stress determination.

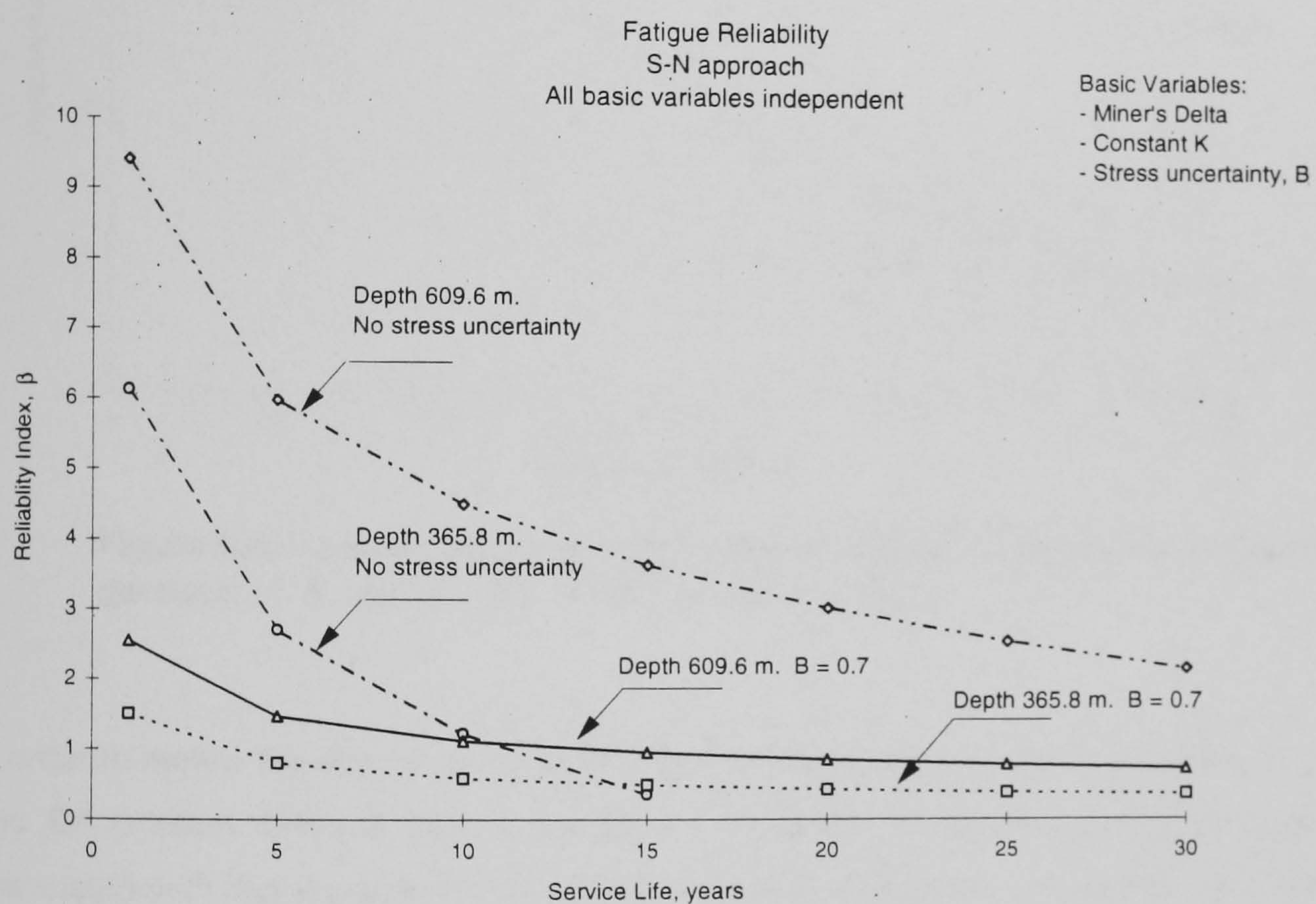

Figure 6.3. Reliability index for a riser in two different water depths, uncertainty in stress values is introduced by means of variable B, **Case 2**.

	1 year	5 years	10 years	15 years	20 years	25 years	30 years
B, 365.8 m.	0.9626	0.9897	0.9953	0.9972	0.9982	0.9987	0.9990
Δ, 365.8 m.	-0.271	-0.143	-0.096	-0.074	-0.060	-0.051	-0.044
K, 365.8m.	-0.001	-0.001	-0.001	-0.001	-0.001	-0.001	-0.001
B, 609.6 m.	0.9382	0.9640	0.9774	0.9841	0.9879	0.9904	0.9921
Δ, 609.6 m.	-0.346	-0.266	-0.211	-0.178	-0.155	-0.138	-0.125
K, 609.6m.	-0.000	-0.001	-0.001	-0.001	-0.001	-0.001	-0.001

Table 6.5. Sensitivity coefficients for **Case 2**, uncertainty in stress determination is introduced by means of variable B.

The sensitivity of B and Δ, relative to each other can be more easily appreciated in **Figure 6.4**, when the riser in 609.6 m. (2000 ft.) depth is considered for a service life of 5 years.

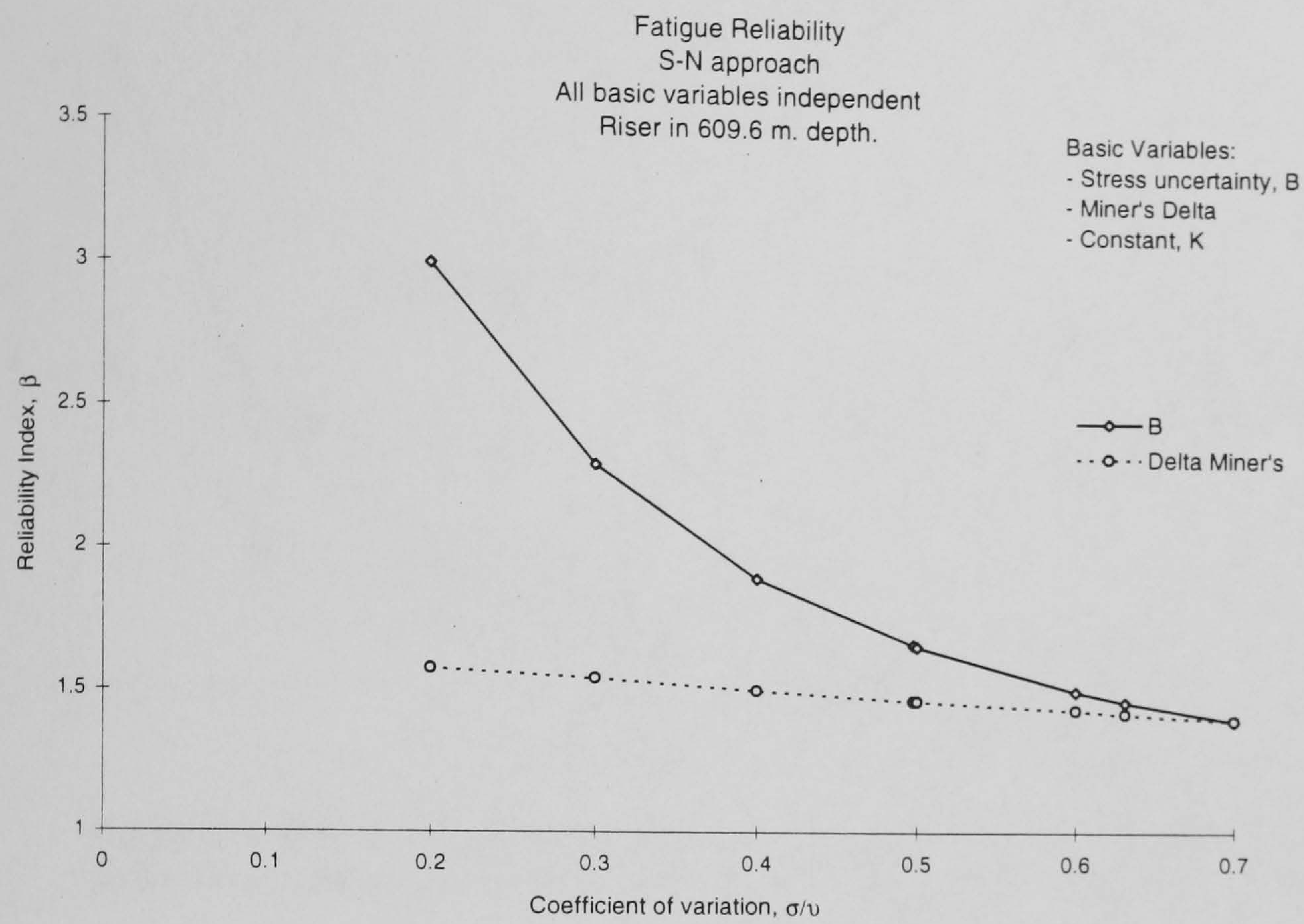

Figure 6.4. Variation of the reliability index for different values of the standard deviation of B and Δ, at a service period of 5 years.

In order to review the effects of the introduction of the uncertainty stress variable, B, **Figures 6.5** and **6.6** present **Case 2** with a number of variations in the mean and standard deviations associated with this variable. So as to facilitate the comparisons, the results from **Case 1**, where no stress uncertainty, B, is assumed, are included in these two figures. **Figure 6.5** corresponds to the riser in 365.8 m. (1200 ft.) depth and **Figure 6.6** for the riser in 609.6 m. (2000 ft.) of water.

As can be observed from **Figure 6.5**, the riser in 365.8 m. (1200 ft.) depth, the influence of variable B in the variation of the reliability index is higher than for the deeper riser, particularly for the longer periods of service life, as it is confirmed by the sensitivity coefficients of **Table 6.5**. This behaviour indicates that the statistical properties of the stress uncertainty variable must be assigned with particular caution. If the riser considered is the one in 609.6 m. (2000 ft.) of water, the influence of B makes the riser reach unacceptable values of the reliability index at a much earlier service life than those predicted without uncertainty in the stress levels. However, if the riser considered is the one in 365.8 m. (1200 ft.) depth, the influence of B could create an appearance that despite the low values of β there could be still be some fatigue strength beyond the service life presented by the same case but without stress uncertainty. Therefore, further consideration of the uncertainty in stress determination is required, this task is accomplished in the following section.

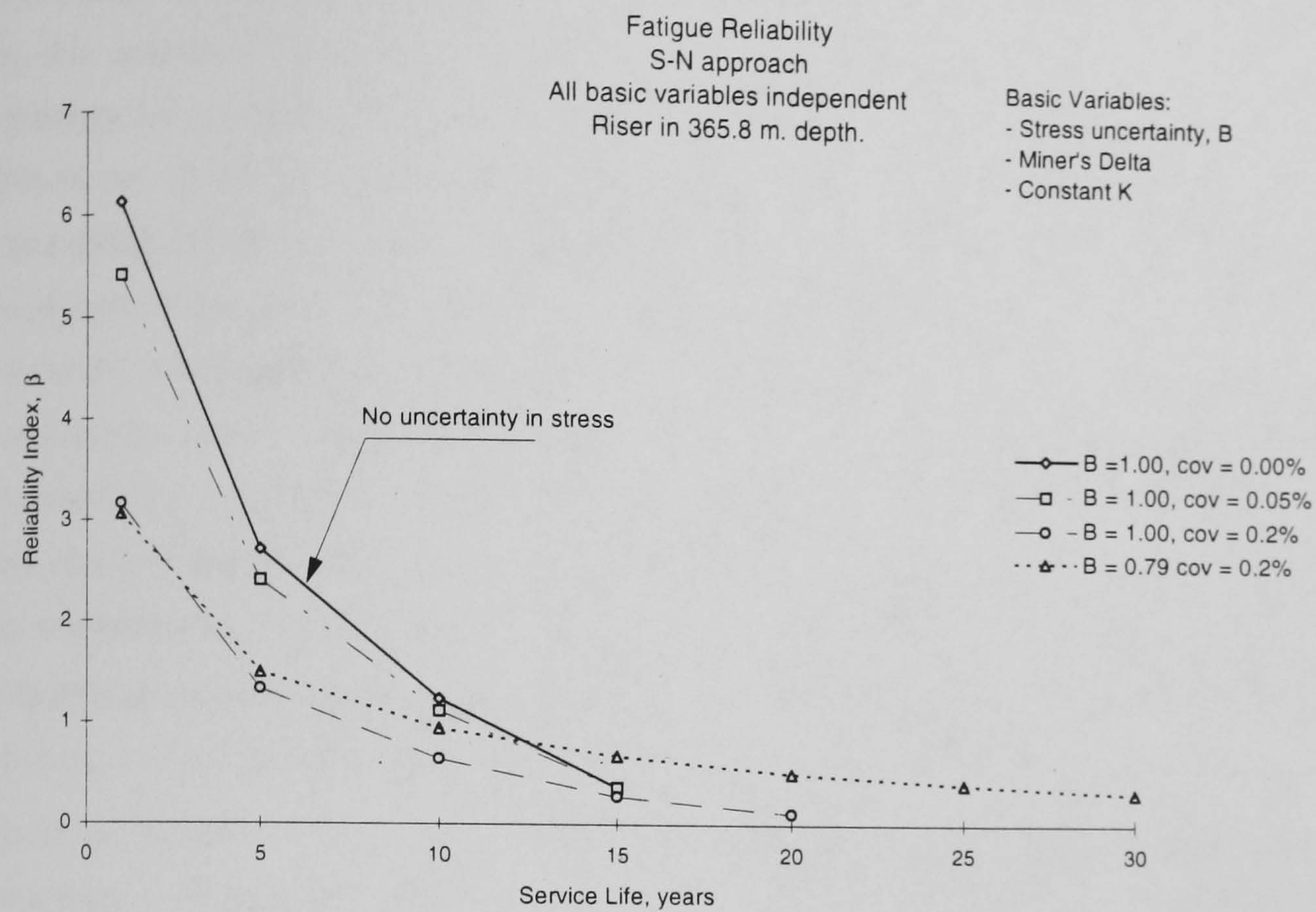

Figure 6.5. Reliability index as a function of different mean and coefficients of variation of the stress uncertainty variable, B , for a riser in 365.8 m.

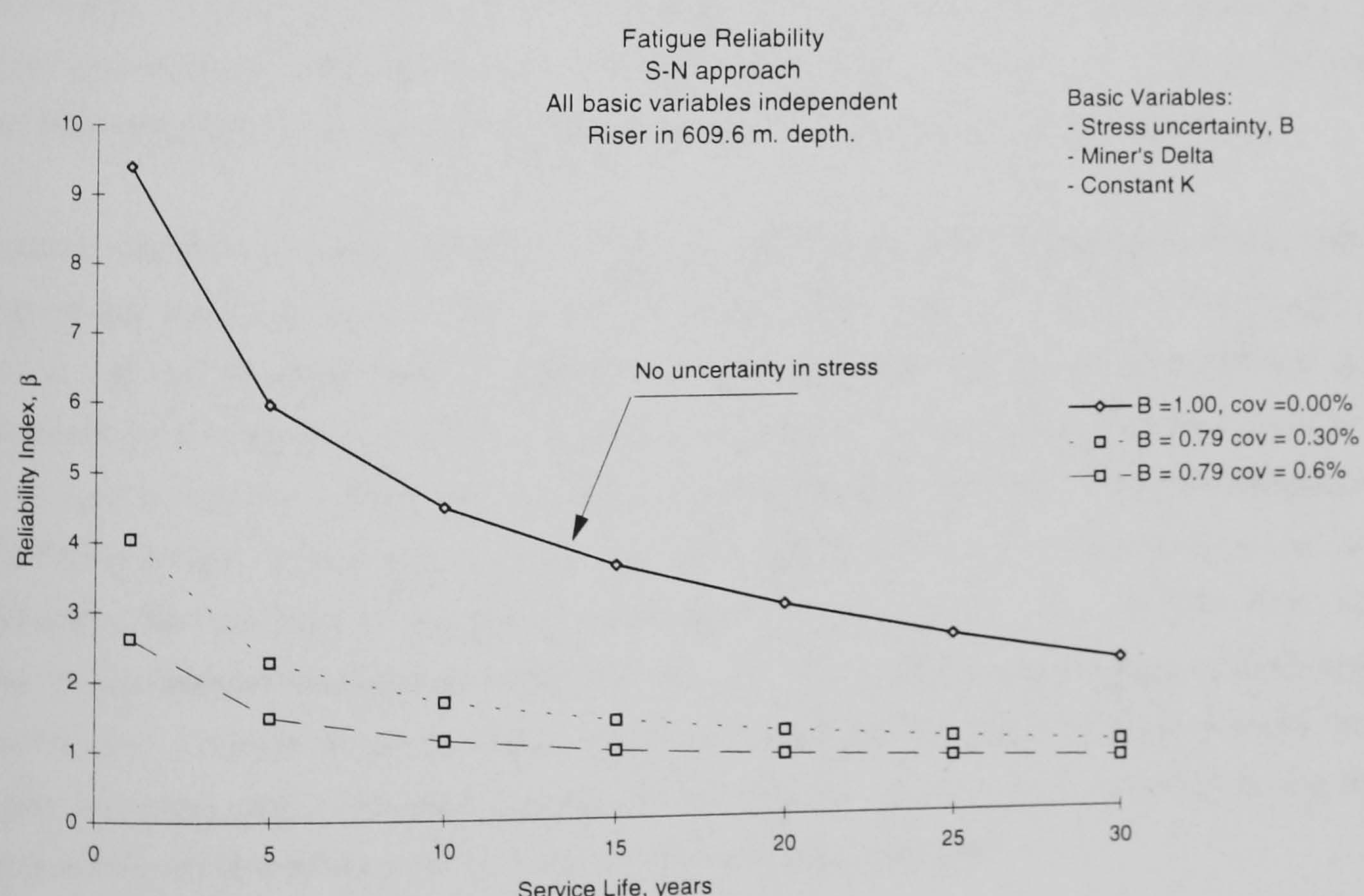

Figure 6.6. Reliability index as a function of different mean and coefficients of variation of the stress uncertainty variable, B , for a riser in 609.6 m.

A comparison with the only riser fatigue reliability analysis found in the literature review performed by this author is convenient. **Souza and Goncalves (1997)** presented an study of fatigue reliability for a vertical rigid riser, similar to the one presented in this work, but for a depth of 914.40 m. (3000 ft.). Their approach to fatigue reliability is similar to the one proposed by **Wirsching (1984)**, but they suggested that the uncertainty in stress could be more accurately modelled by the use of time series, in order to account for the effects of a wide band spectrum. However, as **Figure 6.3** shows they did not compare their results against cases where the uncertainty stress variable, B, and its standard deviation assumed significant values. Furthermore, as mentioned at the beginning of **Section 6.0** their riser model is deterministic, in the sense of **Equation 6.1**; therefore, the only type of uncertainty considered by them is that due to environmental modelling and the variables from the S-N model. On the other hand, it is interesting to note that when the probability distribution functions of Δ and K are considered as Normal, the curves describing the variation of β versus service life become linear, **Figure 6.7**, which is the form of the curves presented by **Souza and Goncalves (1997)**, showed here for reference in **Figure 6.8.** The consideration of probability density function assigned to a particular variable is very important, as a comparison of **Figures 6.2**, lognormal variables, and **Figure 6.7**, normal variables, demonstrate; therefore, assumptions with regard to any particular probability function must be supported. Concerning this point, **Wirsching (1984)**, indicated that the selection of lognormal type distribution function obeys to previous studies, namely **Wirsching (1983)**, physical considerations reinforce that point of view. The numerical values of Miner's critical cumulative damage depend on number of cycles to failure and number of cycles occurring in a given period, since the lowest possible value of any number of cycles is zero, these variables may not take negative values and then a lognormal distribution is more representative.

It can be observed that the reliability index, as presented by **Souza and Goncalves (1997)**, see **Figure 6.8**, for a riser in 914.40 m. (3000 ft.) water depth varies from nearly 2.0 at the first year of life to 1.65 at 30 years, for their Case 3. In order to compare those values with the approach proposed in this section, a riser of the same length was analysed, the resulting reliability indices vary from 2.0013 to 1.7584 and are plotted in **Figure 6.7**. The riser of **Souza and Goncalves (1997)** is similar to the one used in this work, as they are of the same diameter and wall thickness, but the riser of this work is not buoyed, and the weight in air is 3287 N/m^2 while the riser of **Souza and Goncalves (1997)** is 2745 N/m^2; furthermore, details such as drag and inertia coefficients, Young's modulus, floater responses, etc. were not given by those authors. However, it can be reasonably concluded that the use of time domain or frequency analysis one does not produce significant differences in the final fatigue reliability results.

Finally, it is worth mentioning that the comparisons presented above regarding the influence of each variable and its assessment in view of the sensitivity coefficients could have not been carried out if Wirsching's explicit formula, **Equation 6.10**, for determination of the reliability index would have been used.

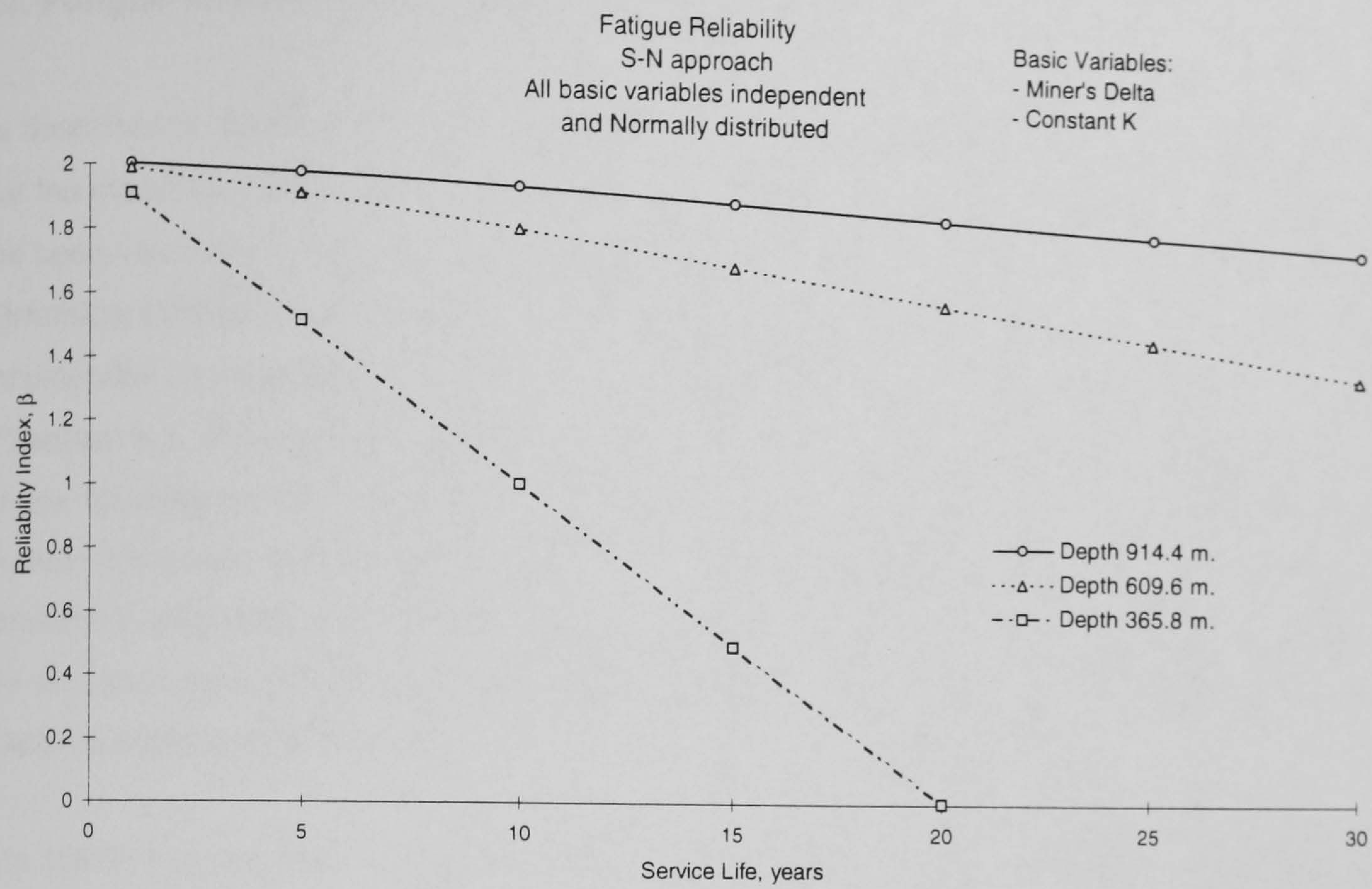

Figure 6.7. Reliability index for a riser in three different water depths, no uncertainty is associated with stress values, **Case 1**. The two basic variables considered are assumed to be Normally distributed.

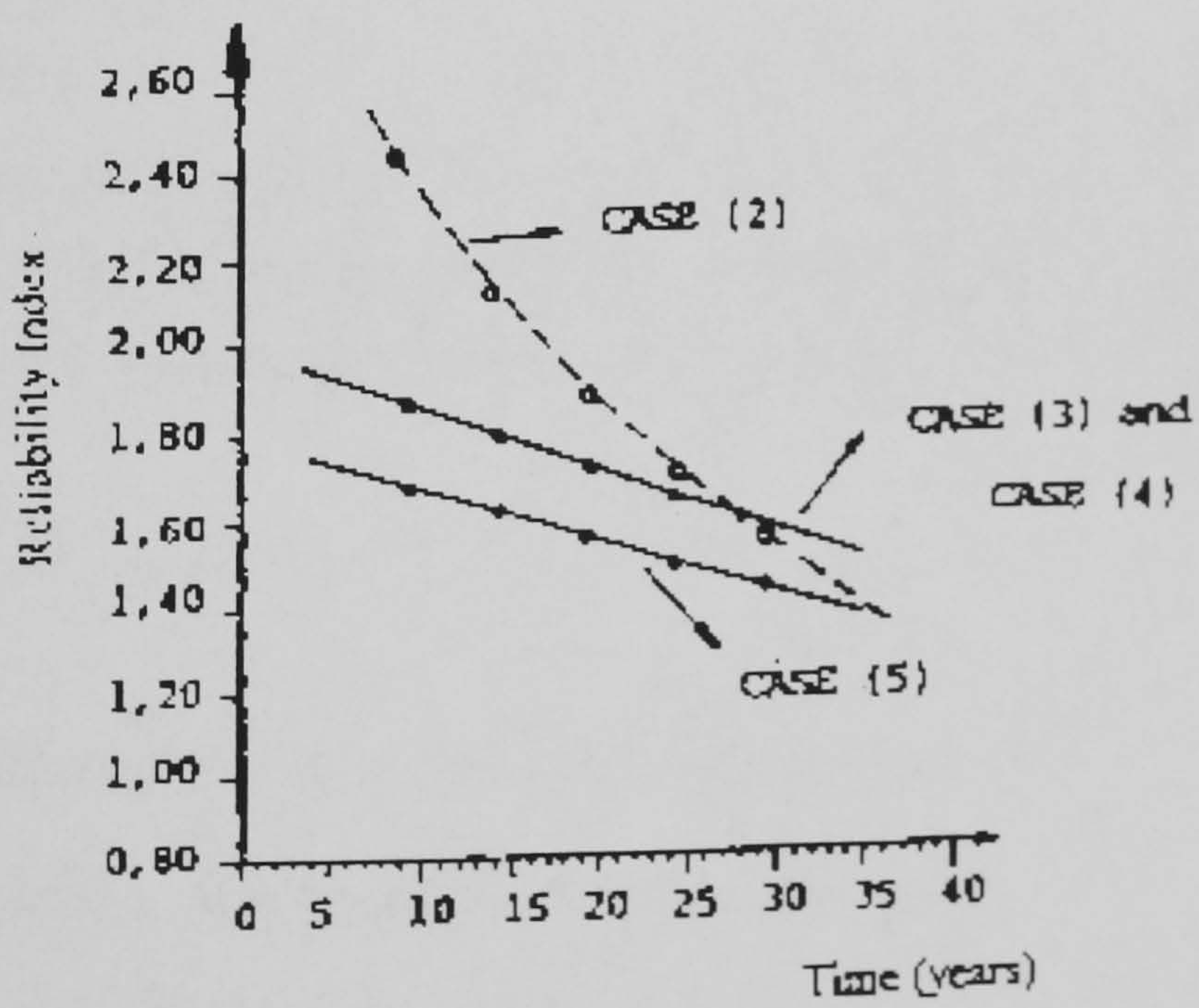

Figure 6.8. Riser reliability index as a function of operational life, for a riser in 914.4m. (3000 ft.) water depth, after **Souza and Goncalves (1997)**. Case 2 here contains the stress uncertainty variable B.

6.3. Fatigue Reliability Analysis of a Riser II.

As described in **Section 6.1** all the presently published approaches to fatigue reliability assume that the model for stress determination is deterministic, in the sense of **Equation 6.1**, uncertainty has been treated in several way but invariable only for environmental and fatigue model variables. **Wirsching (1984)** proposed the introduction of a random variable in order to account for all the uncertainties associated with stress, namely **Equation 6.10** and **6.11**. However, as demonstrated in **Section 6.1**, the values assigned to such variable, B, must be carefully assessed, since in the fatigue reliability model this variable becomes the most significant one, and small changes in it produce important variations in the final value of the reliability index. Therefore, in this section an approach is proposed in which the stress uncertainty due to randomness of the basic variables in the structural or mechanical model, **Equation 6.1**, is explicitly taken into consideration, via the response surface methodology.

If in the limit state which Wirsching used to derive his approach to fatigue reliability, namely **Equation 6.9**:

$$G(X) = \Delta \frac{K}{S^m} - N_T \leq 0 \tag{6.16}$$

the stress range, S^m, is considered a random variable, which is a function of other basic variables, the limit state can be expressed in a general form:

$$G(X) = (\Delta, K, N_T, S^m) \tag{6.17}$$

where Δ, K, N_T, and S are random variables. Furthermore, the stress variable S is a function of a number of variables, if we consider the same seven basic variables used in the exercises of **Section 5.4, Table 5.5**, except for material strength and recall that in this case the long term environment is described by nine short term pairs of wave heights and periods, **Table 6.1**, then:

$$S(H_{Z_{1,\dots,9}}, T_{Z_{1,\dots,9}}, T_T, S_O, O_C, D_C, I_C) \tag{6.18}$$

where:

$H_{Z_{1,\dots,9}}$, significant wave height for the short terms 1 to 9,

$T_{Z_{1,\dots,9}}$, average wave period for the short terms 1 to 9,

T_T, applied tension at the top of the riser,

S_O, floater static offset,

O_C, ocean current,

D_C, drag coefficient,

I_C, inertia coefficient.

The number of cycles that occur in a given period, N_T, become a random variable since this depends on the wave period, which is in this case a random variable, then:

$$N_{T_{1,\ldots,9}}(T_{Z_{1,\ldots,9}}) \tag{6.19}$$

Therefore, the limit state of **Equation 6.16** can be expressed as follows:

$$G(X) = \Delta \frac{K}{S^m} - N_T \leq 0 \tag{6.20}$$

with S and N_T given by **Equations 6.18** and **6.19**.

It was attempted to construct the required response surfaces using the above mentioned limit state, **Equation 6.20**, and the method proposed here in chapter 2 for such purposes; however, in this case the method failed to produce the necessary response surface, on account that the system of equations generated rendered close to singular. As it was mentioned in **Section 2.4**, the method for construction of the response surface used in the present work is not always guaranteed to deliver the expected response surface. Consequently, other approaches to construction of the response surface, such as linear regression techniques, must be tested for the riser fatigue reliability problem proposed in this work. Therefore, the comparison and testing of different methods for construction of the required response surface for the limit state of **Equation 6.20** is left as a matter for further research.

SUMMARY, Chapter 6.

The fatigue life reliability of the marine riser was reviewed. The deterministic fatigue life was found first, for comparison purposes. The reliability of the marine riser was then determined using the commonly accepted approach, in which uncertainty is considered only on the material and environmental variables. In a second stage the uncertainty in stress range was introduced as suggested by **Wirsching (1984)**, where the sources of uncertainty in stress are considered by the introduction of a new variable. A number of parametric studies reveal that this variable is the most significant for the fatigue reliability problem. Therefore, an approach for a more detailed consideration of the uncertainty in stress range is proposed, based on the response surface, was proposed. The improvement that this approach would contribute is that the explicit treatment of the uncertainty in the constitutive variables of the mechanical model. Finally, the reliability levels of the marine riser used for the present studies were compared with those obtained by **Souza and Goncalves (1997)** for a similar riser. The results compare well. Furthermore, the agreement between the two cases reveals that the frequency domain approach of this work produces accurate results, as compared to the time domain analysis followed by the above mentioned researchers.

CHAPTER 7. CONCLUSIONS.

The methods of Structural Reliability lacked a technique for the reliability analysis of structures modelled by the state of the art techniques, such as the finite element method. Therefore, the objective of this work was to determine the applicability of the response surface approach as a method for obtaining an explicit surrogate for the limit state surface which is given only in an implicit manner in any structure modelled by the finite element method. Counting with an explicit form of the limit state surface, it is then possible to apply the well established methods of the structural reliability. The structure selected for this task was a marine riser, in the frequency domain , its reliability levels were analysed for a wide range of environmental conditions, through a number of parametric studies. The reliability assessment of the fatigue life was also undertaken. Therefore, the main conclusions form this study are given below.

1.- The response surface methodology is a powerful technique able to construct an explicit surrogate of the limit state function, in the majority of the cases. It is also demonstrated that, despite the low number of experiments required with the finite element model, the surrogate limit state function provided by this technique is capable of producing accurate values of the reliability index.

2.- The technique for construction of the response surface, due to **Bucher and Bourgund (1990)**, and used in this work, is very systematic, and therefore the lack of fit error is considered small and consistent, a characteristic that makes it very convenient for parametric studies. Moreover, applications of this technique had not been previously reported, in the publicly available literature, in problems of large magnitude, such as the marine riser.

3.- **Bucher and Bourgund (1990)** indicated that the assumption of statistical independence between the basic variables is applicable with their technique for construction of the response surface. It was found, however, in this work that there are instances in which this assumption is not valid. The behaviour of the marine riser is actually the result of two structures connected together, the riser and the floating platform to which this is attached. The wave actions result in a load process acting on each of the structures, but in addition to this, the response of the platform to waves becomes a second and the main source of excitation for the riser. This complex interaction is translated into statistical correlation between the basic variables involved in the problem. Therefore, an approach was proposed here to consider this correlation in an implicit manner, at the level of the mechanical model, which rendered sensible results, as presented in **Figure 5.12**.

4.- The studies conducted in this work show that the Adaptive Importance Sampling simulation technique is able to refine the reliability index values provided by the First Order Reliability Method, depending on the degree of non-linearity of the limit state surface.

5.- The results of the parametric studies of the marine riser reliability indicate that careful consideration is due to the selection of the number of basic variables and its statistical properties, since the validity of the reliability index value depends on such factors, as can be observed in **Figures 5.17a** and **5.17b**. One of the advantages of the response surface approach is that the selection of basic variables can be accomplished with the use of this methodology, since the low computing time required allows a large number of studies to be conducted. Furthermore, similar reliability analyses for the type of marine riser studied here, were not found reported in the public literature. In this case, the externally applied top tension is the most significant basic variable.

6.- The introduction of uncertainty in the fatigue life estimation, by means of the S-N approach, proved that acceptable levels of deterministic fatigue life may render unacceptable levels of reliability. Moreover, most of the models for fatigue reliability analysis only consider uncertainty in the variables associated with the material behaviour, the S-N curve, and in the load process, that is the model for determination of the stress range is considered deterministic.

7.- **Wirsching (1984)** proposed a model in which all the sources of uncertainty in stress range determination are nested in one single variable. Parametric studies conducted with the uncertainty model proposed by that author demonstrated that the uncertainty associated with the stress range is the most significant parameter in the fatigue reliability problem. Furthermore, this kind of studies were not found in the published literature. As can be observed from **Figure 6.3** fatigue reliability index values acceptable when no uncertainty in stress range is considered can become unacceptable after the introduction of that type of uncertainty.

8.- The reliability levels of the riser investigated here compare well with those published by **Souza and Goncalves (1997)**. Furthermore, the agreement between the two cases reveals that the frequency domain approach used in this work produces accurate results, as compared to the time domain procedure followed by the above mentioned researchers.

9.- On account of the significance of the uncertainty associated with stress range determination it is sensible to attempt a more detailed consideration. Therefore, an approach is suggested in which, by means of the response surface, the uncertainty in the constitutive variables of the system, i.e. stiffness, can be taken into explicit consideration. However, the algorithm used here for construction of the response surface was unable to produce the required surface.

CHAPTER 8. RECOMMENDATIONS FOR FURTHER WORK.

This study shows that the response surface methodology is a technique able to produce, in most cases, a surrogate for the limit state function of structures modelled by the finite element method, with which it is then possible to find the reliability index. However, in some instances of the fatigue reliability problem the response algorithm failed. On the other hand it was fund that the model uncertainty associated with the riser problem is significant. Therefore some work can be recommended as a matter of further research, as follows:

1.- It is recommended that different algorithms for construction of the response surface, other than the one used here, have to be tested for the reliability fatigue approach suggested here, namely **Equation 6.20**, with which the uncertainty in the constitutive variables of the system, i.e. stiffness, can be taken into explicit consideration.

2.- The construction of the response surface with the algorithm proposed by **Bucher and Bourgund (1990)** is based on the assumption of statistical independence between the basic variables; however, as this work shows there are instances in which is necessary to take into consideration the correlation of the basic variables. Therefore, the modification of this technique to introduce the correlation between the variables or the development of a new one are the subject of further research.

3.- The error due to lack of fit was not quantitatively determined, mainly because the techniques proposed have not been completely validated. This type of error is thought not to be very significant in the case of parametric studies; however , in the case of a final design it is considered convenient, if not necessary, to measure this kind of error and assess it impact on the final value of the reliability index. Therefore, more research work is needed in order to find adequate techniques for measuring the error due lack of fit and ultimately to define if corrections are necessary in order to improve the reliability index values obtained with the response surface methodology.

4.- The model uncertainty associated with the riser analytical models is important, as it is confirmed in chapter 4. A number of topics dealing with the riser behaviour are opened for further research, mainly the vortex shedding effects and its interaction with the in-line dynamic displacements.

References.

ASCE (American Society of Civil Engineers), (1982): Committee on Fatigue and Fracture Reliability. "Fatigue and Fracture Reliability: A State-of-the-Art Review", *Journal of the Structural Division of American Society of Civil Engineers*. Vol. 108, pp. 3 - 104.

API (American Petroleum Institute), (1993): *Recommended Practice for Planning, Designing and Constructing Fixed Offshore Platforms - Load and Resistance Factor Design, RP2A - LRFD*, Dallas Texas, American Petroleum Institute.

Baker, M. J. and Wyatt, T. A., (1979): "Methods of Reliability Analysis for Jacket Platforms", *Proceedings of the Second International Conference on Behaviour of Offshore Structures, BOSS'79*, London, paper 84, pp. 499 - 520.

Basu, A. K., (1995): "Iterative Frequency Domain Solutions for Nonlinear Riser Response", *Proceedings of the 5th International Offshore and Polar Engineering Conference*, The Hague, Netherlands, June 16, Vol. II, pp. 219 - 216.

Bea, R. G., (1990): "Reliability Criteria for New and Existing Platforms", *Proceedings of the 22nd Annual Offshore Technology Conference*, Houston, OTC paper 6312, pp. 393 - 408.

Beyko, E., and Bernitsas, M., (1992): " Large Admissible Perturbations Approach to Reliability: Global Failure Equations For Elastic/Plastic Material Behaviour", in *Proceedings of the Sixth International Conference on Behaviour Offshore Structures, BOSS'92*, Supplement, London, UK.

Bjerager, P., (1989): "Probability Computation Methods in Structural and Mechanical Reliability", in *Computational Mechanics of Probabilistic and Reliability Analysis*, Eds. Liu, W. K. and Belyschko, T., Elempress Int. Lausanne, Switzerland.

Böhm, F. and Brückner-Foit, A., (1991): "On Criteria for Accepting a Response Surface Model", *Probabilistic Engineering Mechanics*, Vol. 7, pp. 183 - 190.

Boubenider, R., (1992): "Nonlinear Dynamic Behaviour of Deep Water Risers, Tendons and Cables", PhD. Dissertation The University of Texas, at Austin.

Bouma, A. L., Monnier, Th., and Vrouwenvelder, A., (1979): "Probabilistic Reliability Analysis", *Proceedings of the Second International Conference on Behaviour of Off-Shore Structures, BOSS'79.*, paper 85, pp. 521 - 542.

Box, G. E. P., (1954): "The Exploration and Exploitation of Response Surface: Some General Considerations and Examples", *Biometrics*, Vol. 10, pp. 16 - 60.

Breitung, K., (1984): "Asymptotic Approximation for Multinormal Integrals", *Journal of Engineering Mechanics*, American Society of Civil Engineering, Vol. 110, No. 3, pp. 357 - 366.

Bucher, C. G., (1988): " Adaptive Sampling - An Iterative Fast Monte Carlo Procedure", *Structural Safety*, Vol. 5, pp. 119 - 125.

Bucher, C. G., and Bourgund, U., (1990): "A Fast and Efficient Response Surface Approach for Structural Reliability Problems", *Structural Safety*, Vol. 7, pp. 57 - 66.

Burke, B. G., (1974) "An Analysis of Marine Risers For Deep Water", *Journal of Petroleum Technology*, April, pp. 455 - 465.

Chakrabarti, S. K. and Frampton, R. E., (1982): "Review of riser Analysis Techniques" *Applied Ocean Research*, Vol. 4, No. 2, pp. 73 - 90.

Chakrabarti, S. K., (1990): *Nonlinear Methods in Offshore Engineering*. Elsevier, Amsterdam, The Netherlands.

Chang, P.Y., (1990): "A State-of-the-Art Review of the Reliability Approach and Methodology for the Design of Aerospace and Ocean Systems", *Marine Technology*, Vol. 27, No. 5, Sept., pp. 300 - 320.

Chen, X., and Lind, N.C., (1983):"Fast Probability Integration by Three Parameter Normal Tail Approximation", *Structural Safety*, Vol. 1, pp. 269 - 276.

Chiu, H., (1992): "Offshore Production Systems for Ultra-Deep Water in the Gulf of Mexico - Part I: Well Systems", *International Journal of Offshore and Polar Engineering*, Vol. 2, No., 4, December, pp. 241 - 249.

Chryssostomidis, C. and Patrikalakis, N. M., (1992): "An Experimental Procedure for the Prediction of Dynamic Behaviour of Riser Type Systems", *Proceedings of the Third International Conference on Behaviour of Offshore Structures, BOSS 82*, August 2-5, Vol. I, pp. 565 - 598.

Clauss, G., Lehmann, E., and Ostergaard, C., (1992): *Offshore Structures, Vol. II, Strength and Safety For Structural Design*, Springer-Verlag, London, UK.

Clough, R. W. and Penzien, J., (1993): *Dynamics of Structures*, McGraw Hill, International Editions.

Cook, M. F. and Gardner, T.F., (1985): "Riser and Vessel Motion Data From Deep Water Drilling Operation", *17th Annual Offshore Technology Conference,* Houston, Texas, May 6-9, OTC paper 5004, pp. 385 - 394.

Cornell, C. A., (1969): "A Probability-Based Structural Code", *Journal of American Concrete Institute*, Vol. 66, No. 12, pp. 974 - 985.

Crandall, S. H., (1958): *Random Vibration*, John Wiley and Sons, New York.

Cronin, D. J., Godfrey, P. S., Hook, P. M. and Wyatt, T. A.., (1978): "Spectral Fatigue Analysis for Offshore Structures", in *Numerical Methods in Offshore Engineering*, Eds. Zienkiewicz, O. C., Lewis, R. W. and Stagg, K. C., John Wiley and Sons, Bristol.

Cruse, T. A., Burnside, O. H., Wu, Y.-T., Polch, E. Z., and Dias, J. B., (1988): "Probabilistic Structural Analysis Methods for Select Space Propulsion Systems Structural Components", (PSAM), *Computers and Structures*, Vol. 29, No. 5, pp. 891 - 901.

Daering, D. W. and Huang, T., (1976): "Natural Frequencies of Marine Drilling Risers", *Journal of Petroleum Technology*, July, pp. 813 - 818.

Daering, D. W. and Huang, T., (1979): "Marine Riser Vibration Response Determine by Modal Analysis", *Transactions of the ASME, Journal of Energy Resources Technology*, September Vol. 101, pp.159 - 166.

Der Kiureghian, A., Liu, P. L., (1986): "Structural Reliability Under Incomplete Probability Information", *Journal Engineering Mechanics*, American Society of Civil Engineers, Vol. 112, No. 54, pp. 85 - 104.

Der Kiureghian, A., Lin, H. Z., and Hwang, S. F., (1987): "Second-Order Reliability Approximations", *Journal of Engineering Mechanics*, American Society of Civil Engineers, Vol. 113, No. 8, pp. 1208 - 1225.

Der Kiureghian, A., De Stefano, M., and Trombetti, T., (1991): "An Efficient Second Order Reliability Method", in *Proceedings of the 10th, International Conference on Offshore Mechanics and Arctic Engineering*, OMAE, Vol. II, Safety and Reliability, pp. 151 - 156.

Ditlevsen, O., (1979a): "Generalised Second Moment Reliability Index", *Journal of Structural Mechanics*, American Society of Civil Engineers, Vol. 7, No. 4, pp. 435 - 451.

Ditlevsen, O., (1979b): "Narrow Reliability Bounds for Structural Systems", *Journal of Structural Mechanics*, American Society of Civil Engineers. Vol. 7, No. 4, pp. 453 - 472.

Ditlevsen, O., (1981): "Principle of Normal Tail Approximation", *Journal Engineering Mechanics Division*, American Society of Civil Engineers, Vol. 107, No. 4, pp. 453 - 472.

Ditlevsen, O., (1983): "Fundamental Postulate in Structural Safety", *Journal of Engineering Mechanics Division*, American Society of Civil Engineers, Vol. 109, No. 4, pp 1096 - 1102.

DNV (Det Norske Veritas), (1977): *Rules for the Design, Construction and Inspection of Offshore Structures, Appendix C, Steel Structures*, Hovik, Norway.

DOE (Department of Energy), (1984): *Offshore Installation: Guidance on Design and Construction*. London, Her Majesty's Stationery Office.

Egeland, O. and Solli, L. P., (1980): "Some Approaches to the Comparison of Riser Analysis Methods Against Full-Scale Data", *Proceedings of 12th Annual Offshore Technology Conference*, Houston, Texas, USA, May 5-8, Vol. II, OTC paper 3778, pp. 355 - 361.

Ellingwood, B., Galambos, T. V., MacGregor, J. C. and Cornell, C. A., (1980): "Development of a Probability-Based Load Criterion for American National Standard A 58. *National Bureau of Standards Publication 577*, Washington, D. C.

Eurocode No. 3, (1989): Design of Steel Structures, Part 1 - General Rules and Rules for Buildings.

Fang, H. and Xu, F., (1995): "Fatigue Reliability Calculation for Structure Members of Offshore Fixed Platform", Proceedings of the Fifth International Offshore and Polar Engineering Conference, Vol. IV, pp. 394 - 398.

Fiessler, B., Newman, H.J., and Rackwitz, R., (1979) "Quadratic Limit States in Structural Reliability", *Journal of Engineering Mechanics Division*, American Society of Civil Engineers, Vol. 105, No. EM4, August, pp. 661 - 676.

Fischer, W. and Ludwing, M., (1966): "Design of Floating Vessel Drilling Risers", *Journal of Petroleum Technology*, March, pp. 272 - 280.

Flint, A. R., Baker, M. J., Beckman, P., Potter, I. M. D. and Feneron, S., (1977): *Rationalisation of Safety and Serviceability Factors in Structural Codes*, Report 63, Construction Industry Research and Information Association, London, UK, reprint 1984.

Frangopol, D. M., Itzuka, M., and Yoshida, K., (1991): "Redundancy measures and Evaluation of Structural Systems", *Proceedings of the 10th International Conference on Offshore Mechanics and Arctic Engineering, OMAE'91*, Vol. II.

Freudenthal, A. M., (1956): "Safety and the Probability of Structural Failure", *Transactions of the American Society of Civil Engineers*, 121, pp. 1337 - 1397.

Gardner, T. N. and Kotch, M. A., (1976): "Dynamic Analysis of Riser and Caissons by the Element Method", *Proceedings of the 8th Offshore Technology Conference*, Houston, Texas, USA, May 3 - 6, OTC paper 2651, pp 405 - 421.

Graves-Morris, P. R. and Hopkins, T. R. (1981): "Reliable Rational Interpolations", *Numer. Math.*, Vol. 36, pp. 111 - 128.

Haldar, A., and Mahadevan, S., (1995): "First-Order and Second-Order Reliability Methods", in *Probabilistic and Structural Mechanics Handbook, Theory and Industrial Applications*, Ed. Sundararajan, C., Chapman and Hall, New York, USA.

Hamersley, J. M., and Handscomb, D. C., (1964): *Monte Carlo Methods*, Printed by Spottiswoode, Ballantyne and Co. Ltd., London and Colchester.

Hanson, T. D. and Nielsen, A. U., (1994): "Assessment of a Probabilistic Approach for Design of Dynamic Flexible Risers", *Proceedings of the 4th International Offshore and Polar Engineering Conference*, Osaka, Japan, April 10 - 15, Vol. II, pp. 238 - 245.

Harbitz, A., (1986): "An Efficient Sampling Method For Probability of Failure Calculation", *Structural Safety*, Vol. 3, pp. 109-115.

Hasofer, A. M. and Lind, N. C., (1974):"Exact and Invariant Second-Moment Code Format", *Journal of Engineering Mechanics*, American Society of Civil Engineers, Vol. 100, No. EM1, pp.111 - 121.

Hohenbichler, M. and Rackwitz, R., (1981): "Non-normal Dependent Vectors in Structural Reliability", *Journal of Engineering Mechanics Division*, American Society of Civil Engineers, Vol. 107, No. EM6, December, pp. 1227 - 1238.

Hu, Y. and Chen, B., (1993): "A First Order Second Moment Approach to Systems Fatigue Reliability of Offshore Structures", Proceedings of the Offshore Mechanics and Arctic Engineering Conference, OMAE, Vol. II, pp. 327 - 334.

Huang, T. and Chucheepsakul, S., (1985): "Large Displacement Analysis of a Marine Riser", *Transaction of the ASME, Journal of Energy Resources Technology*, March, Vol. 107, pp. 54 - 59.

Jiao, G., (1992): "Limit State Design for Flexible Pipes", *Marine Structures*, Vol. 5, pp.431 - 454.

Jiao, G. and Moan, T., (1992): "Reliability Based Fatigue and Fracture Design Criteria for Welded Offshore Structures", *Engineering Fracture Mechanics*. Vol. 41, No. 2, pp. 271 - 282.

Khuri, A. F., and Cornell, J. A., (1987): *Response Surfaces, Design and Analysis*. Marcel Decker Inc. New York, USA.

Kim, S. H., and Na, S. W., (1997): "Response Surface Method Using Vector Projected Sampling Points", *Structural Safety*, Vol. 19, No. 1, pp. 3 -19.

Kirk, C. L.., (1985): "Dynamic Response of Marine Risers by Single Wave and Spectral Analysis Methods", *Applied Ocean Research*, Vol. 7, No. 1, pp. 1 - 13.

Kokarakis, J. E. and Bernitas, M. M., (1987): "Nonlinear Three Dimensional Dynamic Analysis of Marine Riser", *Transactions of the ASME, Journal of Energy Resources Technology*, September 1987, Vol. 109, pp. 105 - 111.

Kreyszig, E., (1993): *Advanced Engineering Mathematics*. 7th Edition John Wiley and Sons, Inc. USA.

Krolikowski, L. P. and Gay, T. A., (1980): "An Improved Linearization Technique for Frequency Domain Riser Analysis", *Proceedings of 12th Annual Offshore Technology Conference*, Houston, Texas, USA, May 2-5, OTC paper 3777, pp. 341 - 353.

Labeyrie, J. and Schoefs, F., (1996): "Matrix Response Surfaces for Describing Environmental Loads", in *Proceedings of the 15th International Offshore Mechanics and Arctic Engineering Conference, OMAE'96*, Vol. II, Safety and Reliability, pp.119 - 126.

Laurie Kennedy, D. J., (1984): "Limit States Design of Steel Structures in Canada". *Journal of Structural Engineering*, American Society of Civil Engineers, Vol. 110, No. 2, February, pp. 275 - 290.

Lebas, G., Lacasse, S., and Cornell, C. A., (1992): "Response Surfaces For Reliability Analysis of Jacket Structures", in *Proceedings of the 11th International Offshore Mechanics and Arctic Engineering Conference, OMAE'92*, Vol. II, Safety and Reliability, pp. 403 - 409.

Lee, J.-S., Krakovski, M. B., and Yakubovich, A. N., (1993): "Investigation of Response Surface For Reliability Analysis of Structural System", in *Proceedings of the 12th International Offshore Mechanics and Arctic Engineering Conference, OMAE'93*, Vol. II, Safety and Reliability, pp. 323 - 326.

Liu, P.-L., and Der Kiureghian, A., (1988): " Optimisation Algorithms for Structural Reliability", in *Computational Probabilistic Methods*, AMD Publications ASME, Vol. 93, Ed. by Belytschko, Lawrence and Cruse, pp. 185 - 196.

Liu, Y. W., and Moses, F., (1991): "Bridge Design with Reserve and Residual Reliability Constraints", *Structural Safety*, Vol. II, pp. 29 - 42.

Longuet-Higgins, M. S., (1952): "On the Statistical Distribution of the Height of Sea Waves", *Journal or Marine Sci.*, II, pp. 245 - 266.

Madsen, H. O., Krenk, S. and Lind, N. C., (1986): *Methods of Structural Safety*, Prentice-Hall, Inc., Englewood Cliffs, N.J.

Mann, N. R., Schafer, R. E., and Singpurwalla, N. D., (1974): " *Methods For Statistical Analysis of Reliability and Life Data*", John Wiley, New York, USA.

Mansour, A. E. and Wirsching, P. H., (1996): "Safety Assessment and Target Reliabilities for Floating Structures", *International Workshop on Very Large Floating Structures*, Hayama, Japan, November, pp. 283 - 291.

McIver, D. B. and Olson, R. J., (1981): "Riser Effective Tension - Now You See It, Now You Don't", ASME, *37th Petroleum Mechanical Engineering Workshop & Conference*, Dallas Texas, September 13 - 15.

McIver, D. B. and Lunn, T. S., (1983): "Improvements to Frequency-Domain Riser Analysis Programs", *Proceedings of 15th Annual Offshore Technology Conference*, Houston, Texas, USA, May 2 - 5, OTC paper 4559, pp. 395 - 406.

Melchers, R. E., (1987): *Structural Reliability Analysis and Prediction*, Ellis Horwood, Ltd., Chichter, England.

Melchers, R. E., (1989): "Importance Sampling in Structural Systems", *Structural Safety*, Vol. 6, pp. 3 - 10.

Melchers, R. E., (1990): "Search-Based Importance Sampling", *Structural Safety*, Vol. 9, pp. 117 - 128.

Miner, M. A., (1945): "Cumulative Damage in Fatigue", Journal of Applied Mechanics, Vol. 12, pp. 156 - 164.

Modi, V. J. and Calisal, S. M., Atadan, A. S. and Guo, Y., (1994) : "Dynamic Analysis of a Marine Riser", *Proceedings of the Fourth International Offshore and Polar Engineering Conference*, Osaka, Japan, April 10 - 15, Vol. II, pp. 224 - 230.

Moses, F., (1995): "Probabilistic Analysis of Structural Systems", in *Probabilistic and Structural Mechanics Handbook, Theory and industrial Applications*, Ed. Sundararajan, C., Chapman and Hall, New York, USA.

Murotsu, Y., Okada, H., Matsuda, A., Niho, O., Kobayashi, M., and Kaminaga, H., (1992): "Application of the Structural Reliability Analysis System (STRELAS) to a Semisubmersible Platform", in *Proceedings of the 11th International Conference on Offshore Mechanics and Arctic Engineering, OMAE'91*, Vol. II, pp. 209 - 217.

Muzeau, J.-P., Lemaire, M., Besse, P. and Locci, J-M., (1993): "Evaluation of Reliability in Case of Complex Mechanical Behaviour", *Proceedings of Offshore Mechanics and Arctic Engineering, OMAE'93*, Vol. II, Safety and Reliability, ASME, pp. 47 - 56.

Nakanishi, S., and Nakayasu, H., (1996): "Review of Standardised Transformation Methods for Structural Reliability", *in Proceedings of Offshore Mechanics and Arctic Engineering, OMAE*, Vol. II, Safety and Reliability, ASME, pp. 95 - 102.

Nielsen, A. U. and Hanson, T. D., (1995): "Reliability Based Design of 15" Dynamic Flexible Gas Export Riser", *Proceedings of the 5th International Offshore and Polar Engineering Conference*, The Hauge, Netherlands, June 11 - 16, Vol. II, pp. 373 - 382.

Nordgren, R. P., (1982): "Dynamic Analysis of Marine Risers with Vortex Excitation", *Transactions of ASME, Journal of Energy Resources Technology*, September, Vol. 104, pp.14 - 19.

Paris, P. C. and Erdogan, F., (1963): "A Critical Analysis of Crack Propagation Laws", *Transactions*, American Society of Mechanical Engineers, *Journal of Basic Engineering*, Series D, Dec. pp 528 - 534.

Parkinson, D. B., (1980): "Computer Solution for the Reliability Index", *Eng. Struct.*, Vol. 2, January, pp. 57 - 62.

Patel, M. H. and Goeffrey, J. L., (1990); "Marine Risers and Pipelines", in *Marine Technology Reference Book.*, Ed. Morgan, N., Butterworths.

Patel, M. H. and Sarohia, S., (1982): "On the Dynamics of Production Risers", *Proceedings of the Third International Conference on Behaviour of Offshore Structures, BOSS'82*, August 2-5, Vol. I, pp. 599 - 617.

Patel, M. H. and Sarohia, S., (1984): "Finite Element Analysis of the Marine Riser", *Engng. Struct.*, Vol. 6, July, pp. 175 - 184.

Petyt, M., (1990): *Introduction to Finite Element Vibration Analysis*, Cambridge University Press, Cambridge, UK.

Rackwits, R., and Fiessler, B., (1978): "Structural Reliability Under Combined Random Load Sequences", *Computers and Structures*, No. 9, pp. 489 - 494.

Ravindra, M. K. and Galambos, T. V., (1978): "Load and Resistance Factor Design for Steel", *Journal of the Structural Division, Proceedings of the American Society of Civil Engineers*, Vol. 4, No. ST9, September, pp. 1337 - 1353.

Reed, D. A. and Brown, C. B., (1992): "Reliability in the Context of Design", *Structural Safety*, Vol. 11, pp. 109 - 119.

Rosenblatt, M., (1952): "Remarks on a Multivariate Transformation", *The Annals of Mathematical Statistics*, Vol. 23, pp. 470 - 472.

Rosenblueth, E., and Esteva, L., (1972): "Reliability Basis For Some Mexican Codes", in: American Concrete Institute, Spec. SP-31. Detroit, MI.

Salmon, C. G., and Johnson, J. E., (1990): *Steel Structures, Design and Behaviour, Emphasising Load and Resistance Factor Design*, Haper Collins, Publishers. New York, USA.

Schitkowsky, K., (1985): "NLPQL: A FORTRAN Subroutine Solving Constrained Nonlinear Programming Problems", *Annals of Operation Research*. Vol. 5, No.6, pp. 486 - 500.

Schüeller, G. I., and Stix, R., (1987): "A Critical Appraisal of Methods to Determine Failure Probabilities", *Structural Safety*, Vol. 4, pp. 293 - 309.

Schüeller, G. I., Bucher, C. G., Bourgund, U., and Ouypornprasert, W., (1989): " On Efficient Computational Schemes to Calculate Structural Failure Probabilities", *Probabilistic Engineering Mechanics*, Vol. 4, No. 1, pp. 10 - 18.

Schüeller, G. I., Bucher, C. G., and Pradlwarter, H. J., (1991): "On Procedures to Calculate the Reliability of Structural Systems Under Stochastic Loading", *Proceedings of the First International Conference on Computational Stochastic Mechanics*, Eds. Spanos, P. D. and Brebbia, C. A. pp. 59 - 69.

Sheffield, R., (1980): *Floating Drilling: Equipment and Its Use*, Gulf Publishing Company Houston, Texas.

Shetty, N. K., (1993): "Selective Enumeration Methods For Identification of Dominant Failure Paths of Large Structures", in *Proceedings of the 12th International Conference on Offshore Mechanics and Arctic Engineering*, Vol. II, Safety and Reliability, ASME.

Shinosuka, M., (1983): "Basic Analysis of Structural Safety", *Journal of Structural Engineering* American Society of Civil Engineers, Vol. 109, No. 3, pp. 721 - 740.

Skjong, R., (1995): "Applications in Offshore Structures", in *Probabilistic Structural Mechanics Handbook*, Ed. Sundararajan, C., Chapman and Hall.

Souza, G. F. M. and Goncalves, E., (1997): "Fatigue Performance of Deep Water Rigid Marine Risers", *Proceedings of the Seventh International Offshore and Polar Engineering Conference*, Vol. II, pp. 144 - 151.

Spanos, P-T. D., and Chen, T. W., (1980): "Vibration of Marine Riser System", *Transactions of ASME, Journal of Energy Resources Technology*, Vol. 102, December, pp. 203 - 213.

Spanos, P. D., Tein, W. Y. and Ghanem, R., (1990): "Frequency Domain Analysis of Marine Risers with Time Dependent Tension", *Applied Ocean Research*, Vol. 12, No. 4, pp. 200 - 210.

Sparks, C. P. , (1984): "The Influence of Tension, Pressure and Weight on Pipe and Riser Deformations and Stresses.", *Transactions of ASME, Journal of Energy Resources Technology*, Vol. 106, March , pp. 46 - 54.

Stahl, B., (1986):"Reliability Engineering and Risk Analysis", in *Planning and Design of Fixed Offshore Platforms*, Eds. McClelland, B. and Reifel, M. D., Van Nostrand Reinhold Co.

Thacker, B. H. and Wu, Y. -T., (1992): "A New Response Surface Approach for Structural Reliability Analysis", AIAA - 92 - 2408 - CP, American Institute of Aeronautics and Astronautics. pp. 586 - 593.

Thayamballi, A. K., Kutt, L. and Chen, Y. N., (1987): "Deterministic and Reliability-Based Retrospective Strength Assessment of Ocean Going Vessels", *Transactions of the Society of Naval Architects and Marine Engineers.*

Thoft-Christensen, P., and Baker M. J., (1982): *Structural Reliability Theory and Its Applications* Springer-Verlag, Berlin, Germany.

Tucker, T. C. and Murtha, J. P., (1973): "Nondeterministic Analysis of a Marine Riser System", *Proceedings of the 5th Offshore Technology Conference*, Houston, Texas, USA, paper 1770, pp. 439 - 448.

Turk, G., Ramirez, M. R. and Corotis, B., (1994): "Structural Reliability Analysis of Nonlinear Systems", *Structural Safety and Reliability*, Eds. Schüeller, Shinozuka and Yao. Pp. 1345 - 1352.

Tvedt, L., (1988): "Second Order Reliability by an Exact Integral", *Proceedings of the 2nd IFIP, Working Conference on Reliability and Optimisation of Structural System*, Ed. Thoft-Christensen, P. Springer-Verlag, pp. 376 - 384.

Veneziano, D., (1979): "New Index of Reliability", *Journal of Engineering Mechanics Division*, American Society of Civil Engineers, Vol. 105, (EM5), pp. 277 - 296.

Verbeek, P. H. J., (1983): "Analysis of Riser Measurements in the North Sea", *Proceedings of 15th Annual Offshore Technology Conference*, Houston, Texas, USA, May 5 - 8, Vol. II, OTC paper 4562, pp. 425 - 437.

Westin, L. H., (1983): "Random Analysis of Riser for a Floating Production System, (FPS)", in a Northern North Sea Environmental, *Proceedings of 15th Annual Offshore Technology Conference*, Houston, Texas, USA, May 2-5, OTC paper 4560, pp. 407 - 416.

Wirsching, P. H., (1983): "Probability Based Fatigue Design Criteria For Offshore Structures", *Final Report*, American Petroleum Institute, PRAC Project 81-15.

Wirsching, P. H., (1984): "Fatigue Reliability for Offshore Structures", Journal of Structural Engineering, American Society of Civil Engineers, Vol. 110, No. 10, pp.2340 - 2356.

Wirsching, P. H., (1995): "Probabilistic Fatigue Analysis", in *Probabilistic Structural Mechanics Handbook*, Ed. Sundararajan, C., Chapman and Hall.

Ximenes, M. C. C., (1991): "Fatigue Reliability and Inspection of TLP Tendon System", Marine Technology, Vol. 28, No. 2, March, pp. 99 - 110.

Young, R. D., Fowler, J. R., Fisher, E. A., and Luke, R. R., (1978):"Dynamic Analysis as an Aid to the Design of Marine Risers", *Transactions of ASME, Journal of Pressure Vessel Technology*, Vol. 100, May, pp. 200 - 205.

Zimmermann, J. J. and Banon, H., (1994): "System Fatigue Reliability and Inspection Planning for Offshore Platforms", Proceedings of the Offshore Mechanics and Arctic Engineering Conference, OMAE, Vol. II pp.151- 160.

APPENDIX 1.

Determination of the Probability of Failure for the Case of Two Independent Basic Variables.

A mathematical expression for the probability of failure is that given by **Equation 1.10**, namely:

$$P_f = \int_{G(\mathbf{X})\leq 0} f_{\mathbf{X}}(\mathbf{x})d\mathbf{x} \qquad \text{(A1.1)}$$

where:

$\mathbf{X}$, vector of n basic random variables,

$f_{\mathbf{X}}(\mathbf{x})$,joint probability density function,

$G(\mathbf{X})$, limit state function.

For the case of two basic variables, resistance S , and load L the limit state condition given as $G(\mathbf{X}) = S - L \leq 0$ represents the failure domain and **Equation A.1** becomes

$$P_f = \int_{G(\mathbf{X})\leq 0} f_{S.L}(s,l)dsdl \qquad \text{(A.1.2)}$$

If S and L are statistically independent we have

$$f_{S.L} = f_S(s)f_L(l) \qquad \text{(A1.3)}$$

This situation is graphically represented in **Figure 1.2**. The overlapping area of the probability distribution functions of S and L represents the failure domain. **Figure A.1**, which is adopted from **Haugen (1980)**, provides an amplified view of this area for detailed analysis.

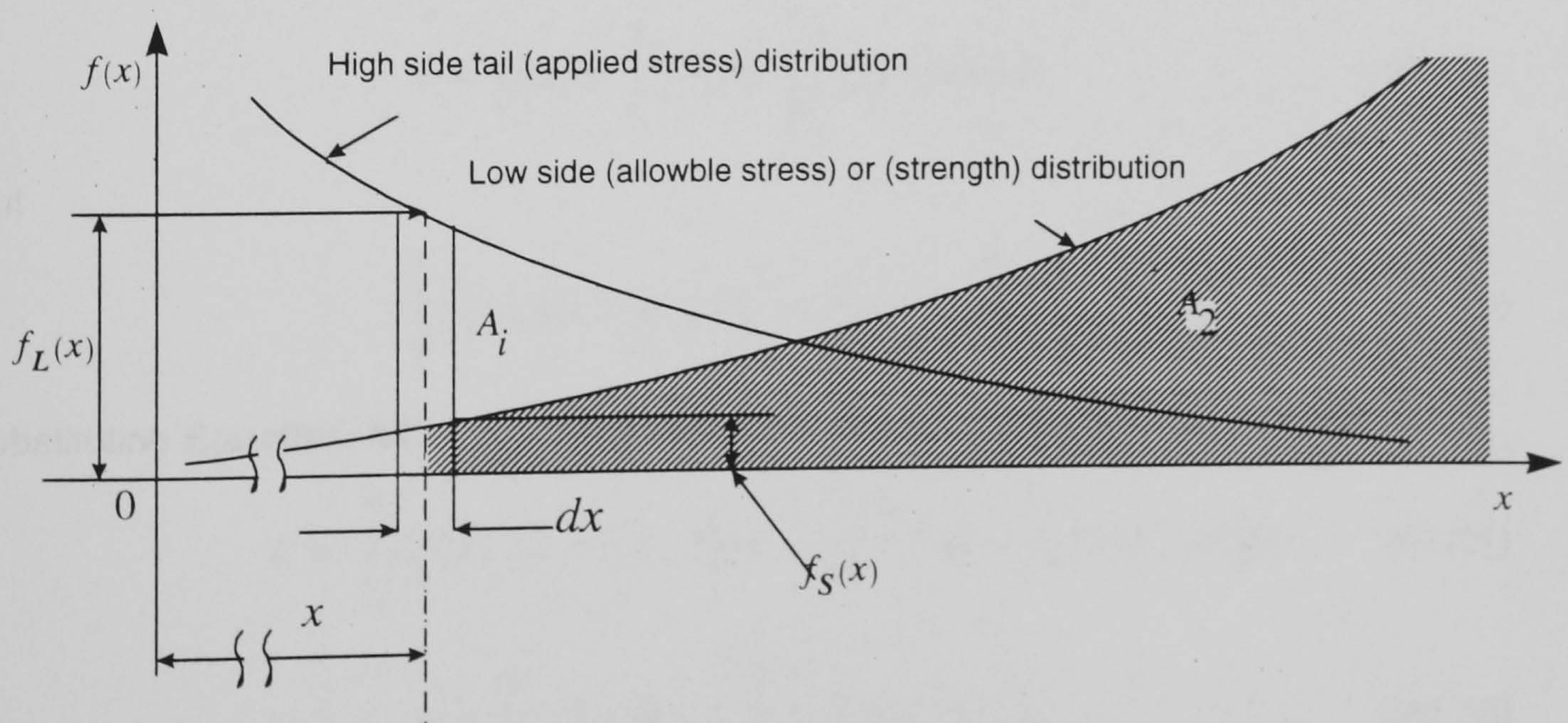

Figure A.1. Probability of failure, allowable vs. applied stress, after **Haugen (1980)**.

The cumulative probability that an applied stress undertakes a value of x_i is numerically equivalent to the area of the element dl or A_i .

$$P\left\{x_i - \frac{dx}{2} \leq x \leq x_i + \frac{dx}{2}\right\} = f_L(x_i)dx = A_i \qquad \text{(A1.4)}$$

since S and L are given by their PDF's. On the other, the probability that $S \geq x_i$ is numerically equivalent to the area A_2 , Thus.

$$P\{S \geq x_i\} = \int_{x_i}^{\infty} f_S(x)dx = A_2 \qquad \text{(A1.5)}$$

Now, the structure will be in a safe condition if the events of the load falling in the interval dx and the resistance being equal or exceeding such value of l occur simultaneously, that is:

$$R = P(A_2 \cap A_i) = A_2 \cdot A_i \qquad \text{(A1.6)}$$

because the load and resistance are assumed to be independent the multiplication rule applied.

Substituting **Equation A1.5** and **Equation A1.4** into **Equation A1.6**, the reliability becomes:

$$R = P\left\{x_i - \frac{dx}{2} \leq x \leq x_i + \frac{dx}{2}\right\} \cdot P\{S > x_i\} \qquad \text{(A1.7)}$$

Since reliability in **Equation A1.7** is given in terms of the probability of the elemental area A_i the reliability is also elemental, that is:

$$dR = f_L(x)dx \cdot \int_{x}^{\infty} f_S(x)dx \qquad \text{(A1.8)}$$

In order that the structure is safe the strength needs to be equal or exceed the load in all possible realisations of L, that is:

$$R = \int dR = \int_{-\infty}^{\infty} f_L(x) \cdot \left[\int_{x}^{\infty} f_S(x)dx\right]dx \qquad \text{(A1.9)}$$

but

$$\int_{x}^{\infty} f_S(x)dx = F_S(x)\Big|_{x}^{\infty} = F_S(\infty) - F_S(x) = 1 - F_S(x) \qquad \text{(A1.10)}$$

substituting **Equation A1.10** into **Equation A1.9**:

$$R = \int_{-\infty}^{\infty} f_L(x) \cdot [1 - F_S(x)]dx = \int_{-\infty}^{\infty} [f_L(x) - f_L(x)F_S(x)]dx \qquad \text{(A1.11)}$$

$$R = \int_{-\infty}^{\infty} f_L(x)dx - \left[\int_{-\infty}^{\infty} f_L(x)F_S(x)\right]dx \qquad \text{(A1.12)}$$

$$R = 1 - \int_{-\infty}^{\infty} f_L(x) - F_S(x)dx \qquad \text{(A1.13)}$$

since $R = 1 - P_f$,

$$P_F = \int_{-\infty}^{\infty} f_L(x) F_S(x)\,dx \tag{A1.14}$$

References:

Haugen, E. B., (1980): *Probabilistic Mechanical Design*, John Willey and Sons, New York, USA.

APPENDIX 2.

Deduction of the Reliability Index for a Linear Limit State Function Using the Geometry of Surfaces.

Given a linear limit state function:

$$g(\mathbf{u}) = b_0 + \sum_{i=1}^{n} b_i u_i = 0 \tag{A2.1}$$

the components of the outward normal vector of a hyperplane given by $g(\mathbf{u}) = 0$ are given by the geometry of surfaces, **Sokolnikoff and Redheffer (1958)**, as:

$$c_i = \lambda \frac{\partial g}{\partial u_i} \tag{A2.2a}$$

where λ is an arbitrary constant. The length of the outward normal is:

$$\ell = \left(\sum_{i=1}^{n} c_i^2 \right)^{1/2} \tag{A2.2b}$$

and its corresponding directions cosines

$$\alpha_i = \frac{c_i}{\ell} \tag{A2.2c}$$

If α_i is known, then the coordinates of the design point are:

$$u_i^* = -\alpha_i \beta \tag{A2.3}$$

Where β is the shortest distance from the hyperplane to the origin, see **Figure A2.1**, which satisfies the condition that:

$$\beta = \min\left(\sum_{i=1}^{n} u_i^2 \right)^{1/2} = \min\left(u^T \cdot u\right)^{1/2} \tag{A2.4}$$

Therefore, the problem becomes the one of finding a set of coordinates u_i^* that satisfies both **Equation A2.3** and **A2.4**. Indeed, substituting the direction cosines of the outward normal in **Equation A2.5**

$$u_i^* = -\frac{c_i}{\ell} \beta \tag{A2.5}$$

and since u_i^* must satisfy that $g(u_i^*) = 0$:

$$g(u_i^*) = b_0 + \sum_{i=1}^{n} -b_i \frac{c_i}{\ell} \beta = 0 \tag{A2.6}$$

which is equivalent to:

$$\beta \sum_{i=1}^{n} -\frac{b_i}{\ell} c_i = -b_0 \tag{A2.7}$$

therefore:

$$\beta = \frac{b_0}{\sum_{i=1}^{n} \frac{b_i}{\ell} c_i} \tag{A2.8}$$

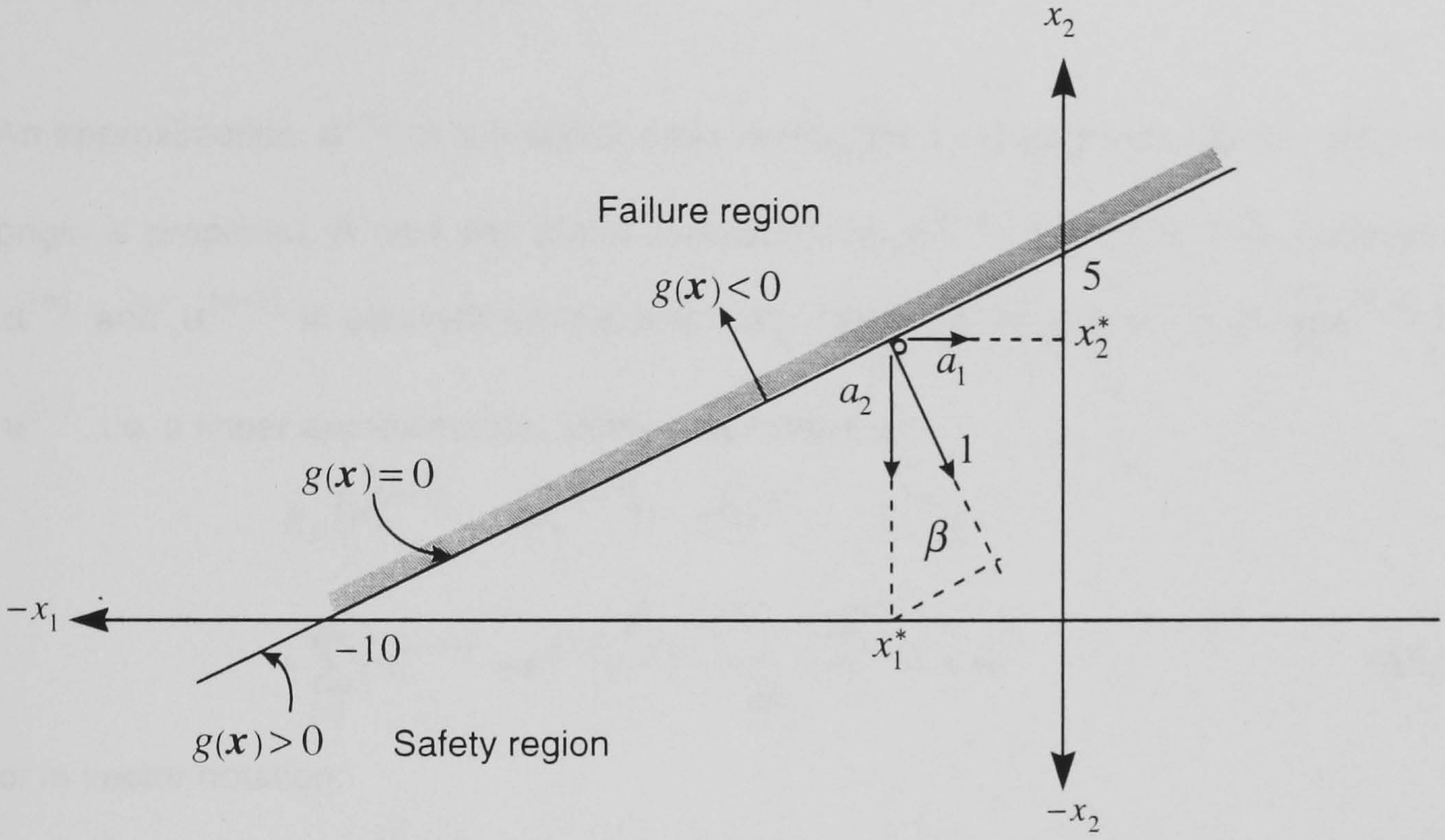

Figure A2.1. Location of the design point by geometry of surfaces, for a linear limit state surface, after **Melchers (1997)**.

References:

Melchers, R. E., (1987): *Structural Reliability Analysis and Prediction*, Ellis Horwood, Ltd., Chichter, England.

Sokolnikoff, I.S. and Redheffer, R.M., (1958): *Mathematics of Physics and Modern Engineering*. McGraw Hill, New York. USA..

APPENDIX 3.

Iterative Algorithm for Finding the Reliability Index for a Non-linear Limit State Function (First Order Reliability Method).

The algorithm was originally proposed by **Hasofer and Lind (1974)** and the following description was given by **Melchers (1987)**.

An approximation $\mathbf{u}^{(m)}$ of the vector representing the local perpendicular to $g(\mathbf{u}) = 0$ from the origin is proposed. A new and better approximation $\mathbf{u}^{(m+1)}$ is sought. The relationship between $\mathbf{u}^{(m)}$ and $\mathbf{u}^{(m+1)}$ is obtained from a first order Taylor series expansion of $g\left(\mathbf{u}^{(m+1)}\right) = 0$ about $\mathbf{u}^{(m)}$, i.e. a linear approximation. Using index notation:

$$g_L\left(u_1^{(m+1)}, \dots, u_n^{(m+1)}\right) \approx g\left(u_1^{(m)}, \dots, u_n^{(m)}\right) +$$

$$+\sum_{i=1}^{n}\left(u_i^{(m+1)} - u_i^{(m)}\right)\frac{\partial_g\left(u_1^{(m)}, \dots, u_n^{(m)}\right)}{\partial u_i} = 0 \qquad \text{(A3.1)}$$

or in vector notation:

$$g_L\left(\mathbf{u}^{(m+1)}\right) \approx g\left(\mathbf{u}^{(m)}\right) + \left(\mathbf{u}^{(m+1)} - \mathbf{u}^{(m)}\right)^T \cdot \Delta g\left(\mathbf{u}^{(m)}\right) = 0 \qquad \text{(A3.2)}$$

This expression presents a hyperplane $g_L(\mathbf{u}) = 0$ approximating a hypersurface $g(\mathbf{u}) = 0$. The linearized limit state function must be satisfied at $\mathbf{u}^{(m+1)}$, that is $g_L\left(\mathbf{u}^{(m+1)}\right) = 0$. However, it is possible to find the direction cosines for the previous trial point, using the proposed trial value of β, by means of **Equation A2.3**:

$$\mathbf{u}^{(m)} = -\alpha^{(m)}\beta^{(m)} \qquad \text{(A3.3)}$$

from where the coordinates of the unit outward normal:

$$\alpha^{(m)} = \frac{\mathbf{u}^{(m)}}{\beta} = \frac{\mathbf{u}^{(m)}}{\ell} \qquad \text{(A3.4)}$$

$\mathbf{u}^{(m)}$ are the components of an outward normal vector, which are given by **Equation A2.2a**. Thus substituting such equation in **Equation A3.4** and using vector notation:

$$\alpha^{(m)} = \frac{\nabla g\left(\mathbf{u}^{(m)}\right)}{\ell} \qquad \text{(A.3.5)}$$

The length, ℓ, is given by **Equation A2.2b** and using again vector notation:

$$\ell = \left(\nabla g\left(\mathbf{u}^{(m)}\right)^{T} \cdot \nabla g\left(\mathbf{u}^{(m)}\right) \right)^{1/2} = \left| \nabla g\left(\mathbf{u}^{(m)}\right) \right| \tag{A3.6}$$

substituting **Equation A3.5** and **A3.6** into **A3.3**

$$\mathbf{u}^{(m)} = -\frac{\nabla g\left(\mathbf{u}^{(m)}\right)}{\left|\nabla g\left(\mathbf{u}^{(m)}\right)\right|}\beta^{(m)} = -\alpha^{(m)} \tag{A3.7}$$

Now substituting in **Equation A3.7** into **Equation A3.2**:

$$g\left(\mathbf{u}^{(m)}\right) + \left(\mathbf{u}^{(m+1)} + \alpha^{(m)}\beta^{(m)}\right) \cdot \nabla g\left(\mathbf{u}^{(m)}\right) = 0 \tag{A3.8}$$

performing the dot product and rearranging the terms:

$$\mathbf{u}^{(m+1)} \cdot \nabla g\left(\mathbf{u}^{(m)}\right) = -g\left(\mathbf{u}^{(m)}\right) - \alpha^{(m)}\beta^{(m)} \cdot \nabla g\left(\mathbf{u}^{(m)}\right) \tag{A3.9}$$

now multiplying each term by the inverse of ℓ, **Equation A3.6**, and using vector notation:

$$\mathbf{u}^{(m+1)} \cdot \frac{\nabla g\left(\mathbf{u}^{(m)}\right)}{\left|\nabla g\left(\mathbf{u}^{(m)}\right)\right|} = -\frac{g\left(\mathbf{u}^{(m)}\right)}{\left|\nabla g\left(\mathbf{u}^{(m)}\right)\right|} - \alpha^{(m)}\beta^{(m)} \cdot \frac{\nabla g\left(\mathbf{u}^{(m)}\right)}{\left|\nabla g\left(\mathbf{u}^{(m)}\right)\right|} \tag{A3.10}$$

Knowing from **Equation A3.7** that:

$$\alpha^{(m)} = \frac{\nabla g\left(\mathbf{u}^{(m)}\right)}{\left|\nabla g\left(\mathbf{u}^{(m)}\right)\right|} \tag{A3.11}$$

Equation A3.10 becomes:

$$\mathbf{u}^{(m+1)} \cdot \alpha^{(m)} = \frac{-g\left(\mathbf{u}^{(m)}\right)}{\ell} - \alpha^{(m)}\beta^{(m)} \cdot \alpha^{(m)} \tag{A3.12}$$

finally, multiplying each term by $\alpha^{(m)}$ and knowing that $\alpha^{(m)} \cdot \alpha^{(m)} = 1$, the coordinates for the following iteration are found to be:

$$\mathbf{u}^{[m+1]} = \frac{-\alpha^{(m)} g\left(\mathbf{u}^{(m)}\right)}{\ell} - \alpha^{(m)}\beta^{(m)} \tag{A3.13}$$

Comparing **Equation A3.13** with **Figure 1.7** we find that the point for the following iteration, $\mathbf{u}^{(m+1)}$, is the sum of the projection of $\beta^{(m)}$ in the direction of $\alpha^{(m)}$ plus the term introduced to account for the fact that $g\left(\mathbf{u}^{(m)}\right)$ may be different from zero, that is $-\alpha^{(m)} \cdot g\left(\mathbf{u}^{(m)} / \ell\right)$.

The steps followed for implementation of this algorithm, as used in the present work, are given below. It should be noted that the basic variables must be of the normal type and uncorrelated, if a transformation is required in order to conform with this requisite, **Rosenblatt (1959)** transformation has to be performed before this algorithm can be applied.

Steps necessary for implementation of this algorithm:

(a) Standardize basic random variables $\mathbf{X}$ into $\mathbf{U}$ (space of normal, standardized variables):

$$\mathbf{U} = \frac{\mathbf{X} - \mu_{\mathrm{X}}}{\sigma_{\mathrm{X}}}$$

(b) transform $G(\mathbf{X}) = 0$ into $g(\mathbf{U}) = 0$

(c) select initial design point, in this case $\mathbf{u}^{(1)} = 0$

(d) compute $\beta^{(1)} = \left(\mathbf{u}^{(1)^T} \cdot \mathbf{u}^{(1)}\right)^{1/2}$

(e) compute directions cosines, **Equation A2.3**

(f) compute $g\left(\mathbf{u}^{(m)}\right)$

(g) compute $\mathbf{u}^{(m+1)}$ using **Equation A3.13**

(h) compute $\beta^{(m)} = \left(\mathbf{u}^{(m+1)^T} \cdot \mathbf{u}^{(m+1)}\right)^{1/2}$

(I) check whether $\mathbf{u}^{(m+1)}$ and/or $\beta^{(m+1)^T}$ have stabilised, or else go to (e) and repeat until stabilisation is gained.

References:

Hasofer, A.M., and Lind, N. C., (1994): "An exact and Invariant First Order Reliability Format", *Journal of Engineering Mechanics*, American Society of Civil Engineers, Vol. 100, No. EM, pp. 111 - 121.

Melchers, R. E., (1987): *Structural Reliability Analysis and Prediction*, Ellis Horword Ltd., Chichester England.

Rosenblatt, M., (1952): "Remarks on a Multivariate Transformation", *The Annals of Mathematical Statistics*, Vol. 23, pp. 470 - 472.

APPENDIX 4.

Socio-economic Criterion to Set a Target Probability of Failure.

In order to apply structural reliability analysis at the design stage it is necessary first to set a target probability of failure.

One approach to establish the value of this probability of failure was proposed by **Stahl (1986)**, based on a criterion previously suggested by **Flint, et al. (1979)**. This approach takes into consideration the economic as well as the social constraints. It is represented as follows:

$$P_a = \frac{C}{[EQCF + (v\eta_r^2/K_S)]PVF} \qquad \text{(A4.1)}$$

where:

P_a is the annual probability of failure. This can be converted to the probability of failure for a certain reference period, t, i.e. the useful life of the facility, by

$$P_f = P_a \cdot t \qquad \text{(A4.2)}$$

This is necessary in order to account for the fact that the representation of load processes is based on the probability that a certain threshold value of load, i.e. wave height, will be equalled or exceeded, on average, once during the reference period, say,100 years. The load is then customarily expressed as the 100 year design condition.

C, is a constant that represents the increment of the initial cost required to reduce P_a by a factor of $e \approx 2.71$. C is obtained from:

$$CI = C_O - C\ln P_a \qquad \text{(A4.3)}$$

where CI is the initial cost of the facility and C_O is a constant. **Equation A4.3** was obtained by designing the facility for several different "design waves" in order to observe the variation of initial cost with the design wave.

$EQCF$ is the equivalent cost of failure, which is the result of adding different quantities that have an impact in the total cost of failure, they are:

• if in the event of failure the facility will not be replaced:

The cost of lost revenue:

$$EQCF_{lr} = Ri^{-1}\left\{\exp(-iT^*) - \left[1 + i(T - T^*)\right]\exp(-iT)\right\} / [1 - \exp(-iT)] \qquad \text{(A4.4)}$$

in order to consider for the revenue stream that would be lost in the event of collapse of the facility.

The cost of restoration after the event of failure of the facility:

$$EQCF_a = CF_a \tag{A4.5}$$

• if in the event of failure the facility will be replaced:

The cost of the deferred stream:

$$EQCF_{dr} = R[1-\exp(-i\Delta T)]i^{-1}[1-\exp(-iT^*)-iT^*\exp(-iT)]/$$
$$/[1-\exp(-iT)] \tag{A4.6}$$

The cost of replacement of the facility:

$$EQCF_b = CF_b[1-\exp(-iT^*)]/[1-\exp(-iT)] \tag{A4.7}$$

R, the uniform revenue of the stream per year, i, the annual discount rate is given by:

$$i = j - r \tag{A4.8}$$

where j is the annual discount rate used to convert future payments to present values and r is the annual rate of inflation, usually 12 to 16%.

T is the project life, T^* is some point in time, $T^* < T$ at which replacement is not economical, CF_a and CF_b are the cost of restoration for the cases of no-replacement and replacement, respectively.

The $EQCF$ was selected for introduction in Equation A4.1 because in a realistic case it will not be possible to find a hard boundary between the replacement and non-replacement assumptions. If failure of the facility occurs in its early projected life, it should be feasible to replace the platform and continue the extraction operations. If failure occurs at some point T^*, $T^* < T$ a replacement will not be economical. Therefore $EQCF$ in a combined model is equal to

$$EQCF = EQCF_{dr} + EQCF_{lr} + EQCF_a + EQCF_b \tag{A4.9}$$

PVF is the present value of a unit annual cost uniformly distributed over T years, given by:

$$PVF = \frac{1-\exp(-iT)}{i} \tag{A4.10}$$

The social issues are circumscribed by:

v, constant, suggested by **Flint, et. al. (1977)** at $50,000.

η_r, number of personnel manning the facility.

K_S, social criteria constant suggested by **Flint, et. al. (1977)** as 5.0 for offshore structures.

References:

Flint, A. R., Baker, M. J., Beckman, P., Potter, I. M. D. and Feneron, S., (1977): *Rationalisation of Safety and Serviceability Factors in Structural Codes: Supplementary Report on Offshore Installations.*, Report 63 Supplement, Construction Industry Research and Information Association, London, UK, reprint 1984.

Stahl, B., (1986): "Reliability Engineering and Risk Analysis", in *Planning and Design of Fixed Offshore Platforms.* Eds. McClelland, B. and Reifel, M. D., Van Nostrand Reinhold Co. USA.

APPENDIX 5.

Approximation of the Response Function.

The algorithm utilized in this work to construct the response function is based on the methodology proposed by **Bucher and Bourgund (1990)**. It is based on a polynomial approximation of the true limit state surface. The algorithm is described as follows:

a).- define the n basic random variables of the problem and their second order statistical properties, e.g. $x_i \sim (\bar{x}_i, \sigma_i)$.

b).- derive $2n+1$ sets of realisations of x_i, using the vector of means as the centre of the interpolation, e.g. $x_i = \bar{x}_i \pm f_i \sigma_i$, as indicated in **Figure 2.1**.

c).- derive $2n+1$ sets of values of the true response of the system, $G(\mathbf{x}_i)$, with the finite element model, for the $2n+1$ sets of realisations obtained in b).

d).- formulate the linear system of equations, **Equation 2.5**, and solve them for the vector of unknown coefficients of the equivalent polynomial, $\bar{g}(\mathbf{X})$, of **Equation 2.3**.

e).- with the coefficients found in d) construct the first approximation of the response surface $\bar{g}_1(\mathbf{X})$, **Equation 2.3**, and determine the design point $\mathbf{x}_1^*$. FORM algorithm as given in **Appendix 4** is employed here; however, if such algorithm does not converge the design point will be found by means of the Adaptive Importance Sampling algorithm, described in **Appendix 6.**

f).- determine the new centre for interpolation, $\mathbf{x}_M$, using **Equation 2.7**. This requires the determination of the true response of the system at $\mathbf{x}_M$, that is: $G(\mathbf{x}_M)$.

g).- repeat steps b) to d), this time using as centre for interpolation $\mathbf{x}_M$, as showed in **Figure 2.2**.

h).- with the second approximation of the response function, $\bar{g}(\mathbf{X})$, continue the reliability analysis , i.e. find the probability of failure. Any suitable algorithm of reliability analysis can be used, FORM, SORM, etc. In this work the adaptive importance sampling method is used, as described in **Appendix 6**.

References:
Bucher, C. G., and Bourgund, U., (1990): "A Fast and Efficient Response Surface Approach for Structural Reliability Problems". *Structural Safety*, Vol. 7, pp. 57-66.

APPENDIX 6.

The Adaptive Importance Sampling Method.

The determination of the probability of failure in this work is accomplished by means of the adaptive importance sampling method. The algorithm followed here to implement the computer code is the one suggested by **Melchers (1990)**, which is given below:

a).- select a starting point: $\mathbf{x}^{(k)}$, $k = 1$. The starting point, in this case, is the design point as given by FORM, if FORM fails the point of mean values can be used.

b).- select an importance sampling function: ${}_k h_{\mathbf{V}}(\mathbf{v})$, with appropriate large variances, and centred at $\mathbf{x}^{(k)}$.

c).- obtain a sample ${}_k\mathbf{v}_j$ from ${}_k h_{\mathbf{V}}(\mathbf{v})$ and check if it falls in the failure domain.

d).- determine $f_{\mathbf{X}}\left({}_k\mathbf{v}_j\right)$ for each sample point ${}_k\mathbf{v}_j$ falling in the failure domain D, then apply **Equation 2.15**. Find the point with maximum $f_{\mathbf{X}}\left({}_k\mathbf{v}_j\right)$ and record its coordinates as being the design point $\mathbf{x}^*$.

e).- for each sample point that does not belong to the failure domain, D, find the minimum value of $\bar{g}(\mathbf{v}_j)$. Denote this as $\bar{g}_m(\cdot)$ and record the corresponding coordinates as $\mathbf{x}^{**}$.

f).- repeat steps c) to e) for the number of sample points in the *kth* importance sampling function, ${}_k h_{\mathbf{V}}(\mathbf{v})$.

g).- If none of the samples fall in the failure domain relocate the next sampling function, ${}_k h_{\mathbf{V}}(\cdot)$ at $\mathbf{x}^{**}$. If some samples do fall in the failure domain, check for every sample if $f_{\mathbf{X}} > \gamma f_{\mathbf{X}}(\mathbf{x}^*)$, if it is so, relocate the next sampling function ${}_k h_{\mathbf{V}}(\cdot)$ at $\mathbf{x}^*$. γ is a selected sensitivity factor, say $\gamma = 1.02$ to prevent excessive oscillation between successive locations of the importance sampling function.

References:

Melchers, R. E., (1990): "Search-Based Importance Sampling", *Structural Safety*, Vol. 9, pp. 117 - 128.

Appendix 7.

Derivation of the Statically Equivalent Force Due to Hydrostatic Pressures on the Riser.

In order to derive expressions for the statically equivalent forces that arise from the effects of external and internal pressures acting on the marine riser, the physical approach contributed by **Sparks (1984)** is summarised here.

The first step is to review Archimedes principle. **Figure A7.1** shows that the hydrostatic upthrust is equivalent to the weight of fluid displaced. However, it is important to note that Archimedes principle can only be applied to closed pressure fields, such as the one presented on **Figure A7.1**, and that such principle is unable to predict internal forces in submerged bodies (or bodies of fluid, as in this case), as those acting on the dashed line a-a.

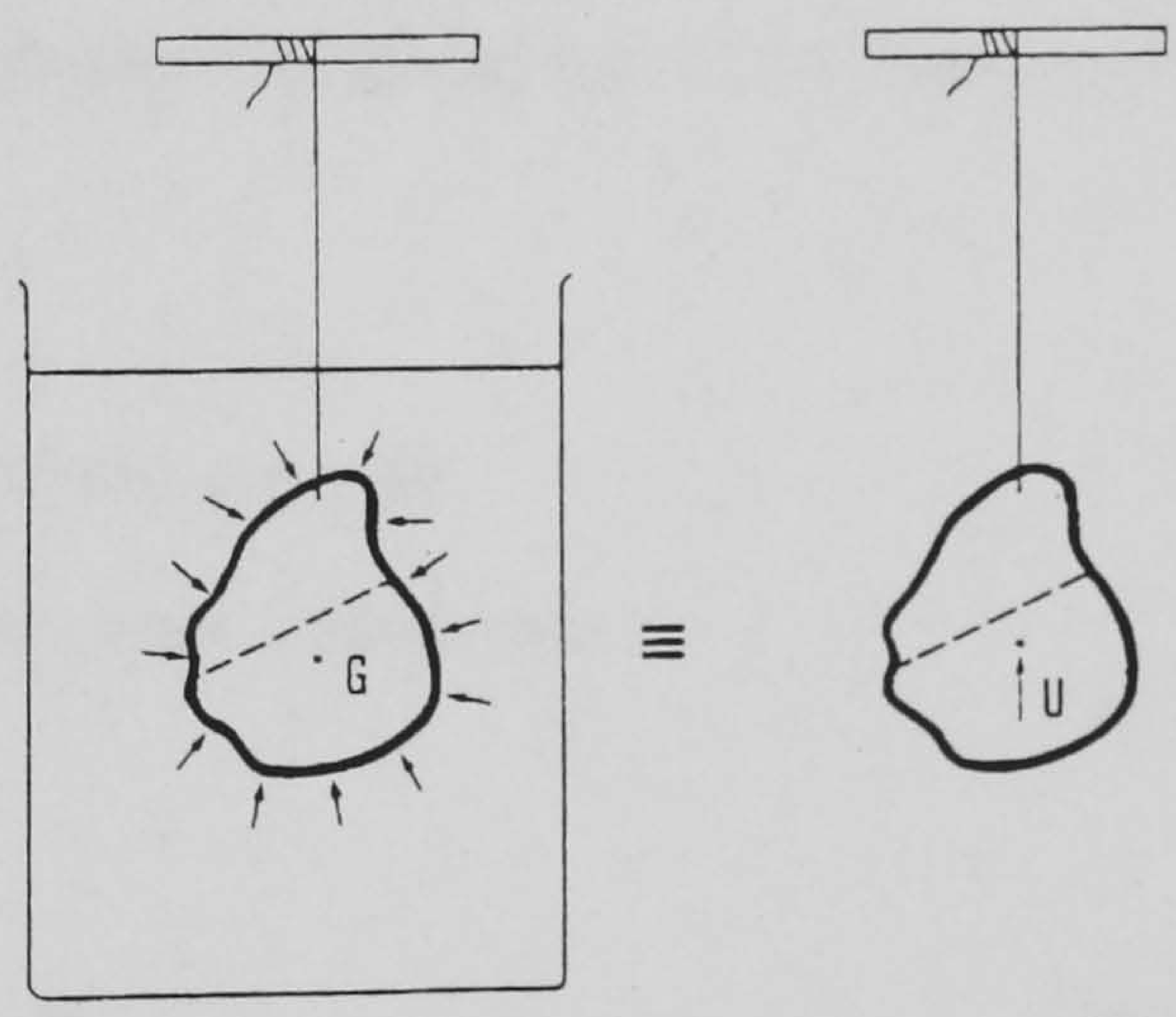

U = upthrust = weight of fluid displaced

Figure A7.1. Archimedes' Law, after **Sparks (1984)**.

The physical proof that this principle is true can be observed from the fact that the resolution of forces from pressure and weight is in equilibrium, otherwise the fluid within an enclosed pressure field would rise or fall, see **Figure A7.2**. Therefore, the following corollary (A) is valid: "the combined effects of the enclosing pressure field and the self weight of the enclosed fluid can produce no resultant force (in any direction), so their combined effect can produce no resultant moment anywhere in the fluid".

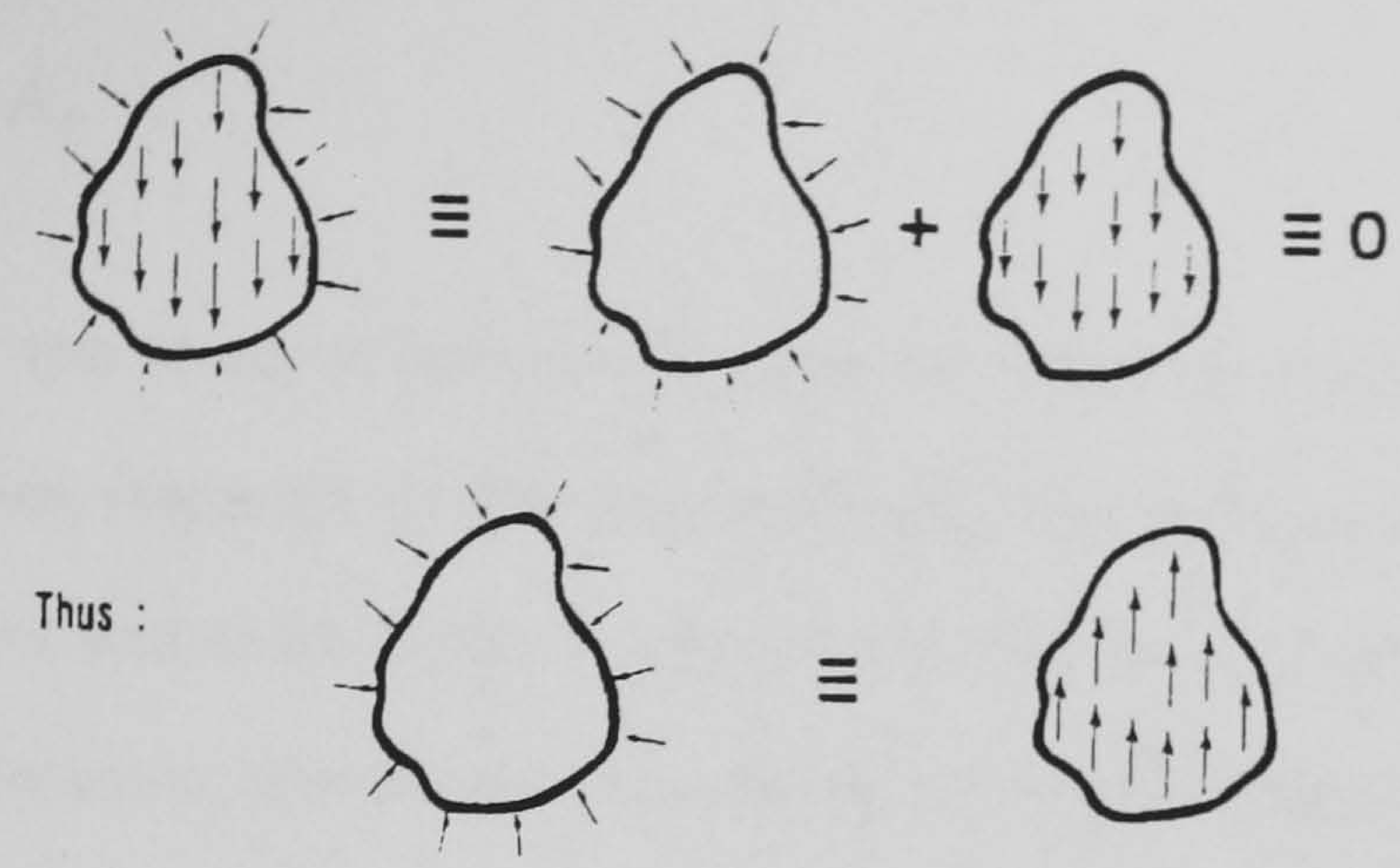

Figure A7.2.Pressure and weight acting in a fluid. Equivalence resulting from resolution of forces, in any direction (or moments about any point), after **Sparks (1984)**.

The second step is to analyse the internal forces on the submerged body of **Figure A7.1**. Notice that the pressure field is not closed. In order to apply Archimedes principle, **Sparks (1984)** closed the pressure field by adding a "missing pressure", which acts on the cross section surface of the body, section a-a, see **Figure A7.3**, giving rise to the following force:

$$F_{P_E} = P_E A_E \qquad \text{(A7.1)}$$

where:

P_E , external hydrostatic pressure, and

A_E , external cross section area, section a-a.

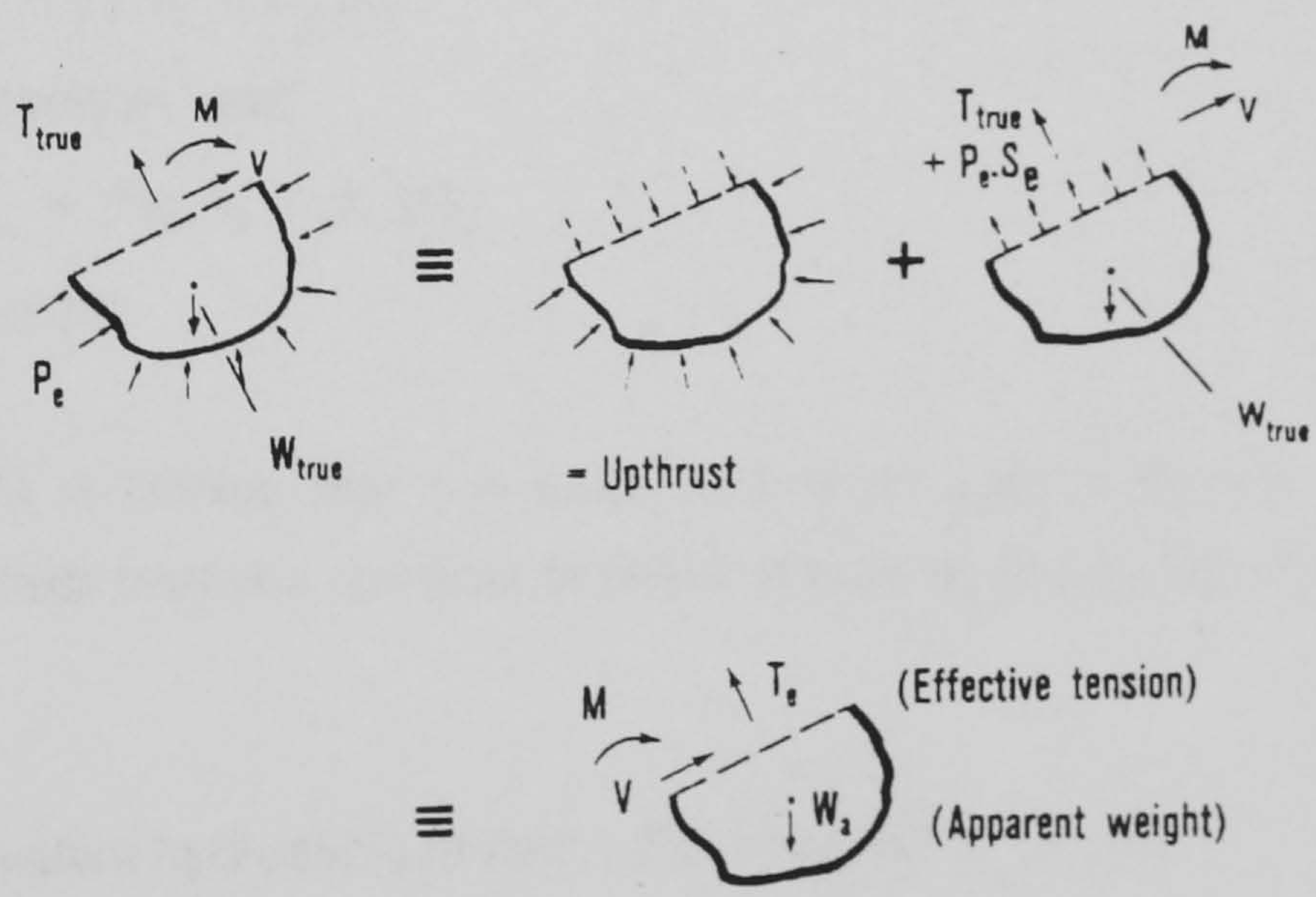

Figure A7.3.Equivalent force systems acting on part of a submerged body. after **Sparks (1984)**.

Equilibrium laws require that a force equal to and opposite to the one created by addition of the "missing pressure" has to be introduced and therefore added to the externally applied true tension, T_{true} , to which the body is subjected, then ,by force summation of the true tension and the statically equivalent one given by **Equation A7.1**, the following expression for the ***equivalent tension*** is obtained:

$$T_e = T_{true} + P_E A_E \tag{A7.2}$$

Figure A7.3 shows that the effective tension, T_e, can be found by resolution of forces normal to section a-a and that it only depends on the apparent weight of the segment, W_a. On account of corollary (A), the moment and shear force in agreement with the true tension, T_{true}, true weight, W_{true}, and hydrostatic pressure are the same as those compatible with the apparent weight, W_a, and effective tension,. T_e.

Now, application of the "missing pressure" scheme to a differential segment of riser pipe will lead to and expression for the equivalent tension, this time, however, the effect of the internal pressure has to be considered as well. **Figure A7.4** shows a differential element of riser where the "missing pressures" have been introduced separately so as to enclose the external and internal pressure fields, respectively. Afterwards, they are replaced by the Archimedes upthrusts, that is:

$$\rho_E g A_E \delta L \tag{A7.3}$$

$$\rho_I g A_I \delta L \tag{A7.4}$$

As before, the required forces to maintain equilibrium after application of the "missing pressures" must be introduced and added to the true tension, in the same fashion the Archimedian weight is added to the true weight, as presented in **Figure A7.4**. The resultant expressions are:

$$T_e = T_{true} - P_I A_I + P_E A_E \tag{A7.5}$$

for the equivalent tension, and

$$W_a = W_{true} + \rho_I g A_I - \rho_E g A_E \tag{A7.6}$$

for the apparent weight.

From corollary (A) it follows that the equivalent force system due to effective tension and apparent weight must produce identical bending effects as the system of true tension and true weight.

The statically equivalent hydrostatic forces in **Equation A7.5**, namely:

$$F_{P_E} = P_E A_E \tag{A7.7}$$

$$F_{P_I} = P_I A_I \tag{A7.8}$$

are used in **Section 4.1** for derivation of the riser differential equation of motion.

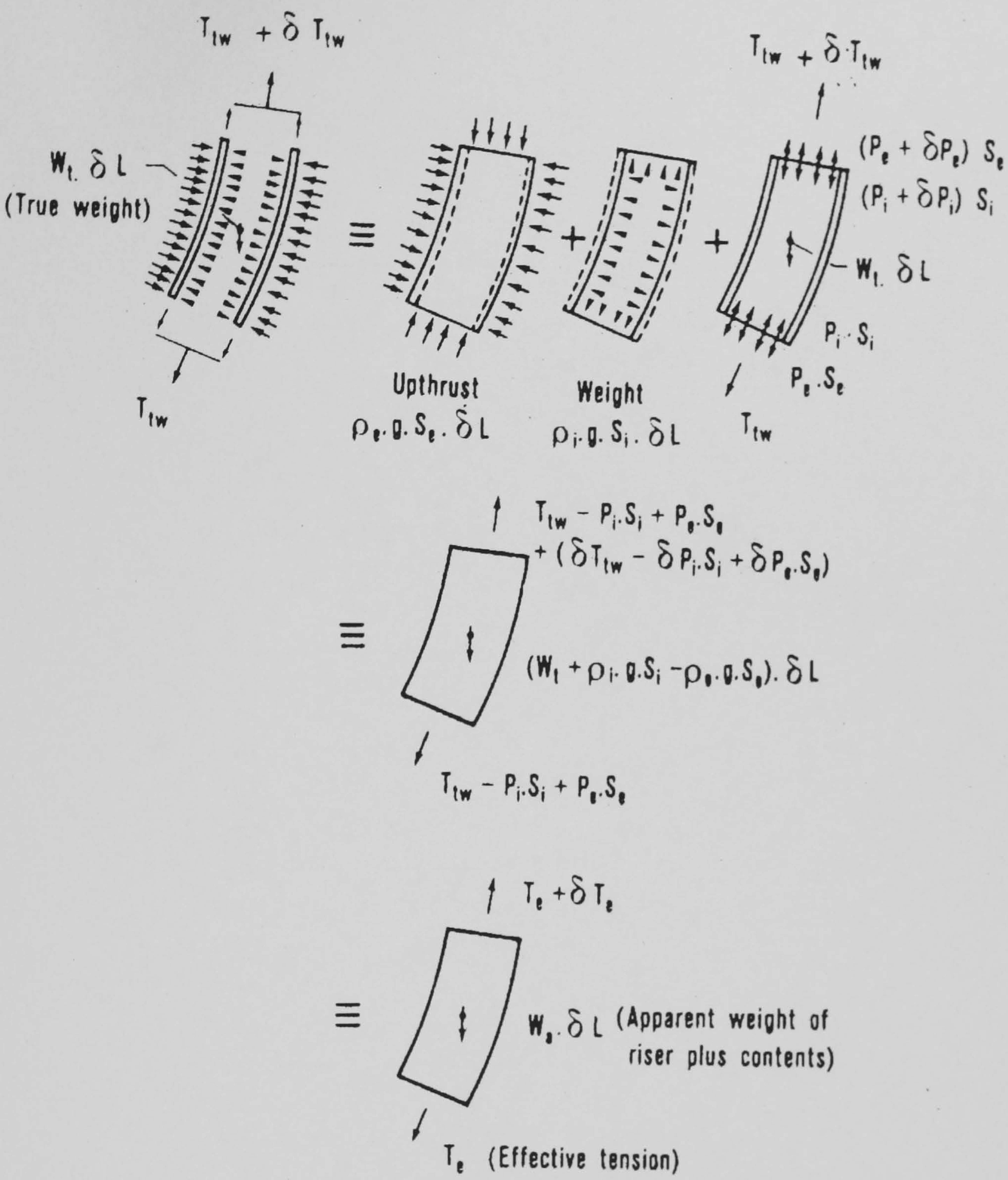

Figure A7.4. Equivalent force system acting on a segment (δL) of pipe or riser, after **Sparks (1984)**.

References:

Sparks, C. P. , (1984): "The Influence of Tension, Pressure and Weight on Pipe and Riser Deformations and Stresses.", *Transactions of ASME, Journal of Energy Resources Technology*, Vol. 106, March , pp. 46 - 54.